MULTIFUNCTIONAL DENDRIMERS FOR ANTIBACTERIAL APPLICATIONS

Emma Leire, MSc

Thesis submitted to the School of Pharmacy,

University of Nottingham for the degree of Doctor of Philosophy

July 2016

ABSTRACT

In this thesis gallic acid-triethylene glycol (GATG) dendrimers were synthesised and efficiently functionalized with hydroxyl groups, phenylboronic acids and primary amines. The interactions of the dendrimers with bacteria and the potential for development of new antimicrobials were evaluated in this study. Specifically, the ability of the dendrimers to induce bacterial clustering and interfere with small molecule autoinducer-2 (AI-2) in the Quorum Sensing (QS) pathway of the marine bacteria *V. harveyi* was studied with the use of Coulter Counter aggregation assays and detection of QS–controlled luminescence. Novel alkynylated ligands with diol-, tetraol-, glucose- and mannose- moieties were synthesised and successfully functionalized to GATG dendrimers of generation G1 and G3 through catalyst-free azide-alkyne cycloaddition (AAC). The results of luminescence experiments reveled that the dendrimers functionalized with hydroxyl groups decreased AI-2-induced luminescence of *V. harveyi* MM32 at the at early time points (4 h) while a dose-dependent increase of luminescence and increased bacterial growth was observed at later time points.

GATG dendrimers of generation G1 and G3 were decorated with 9 and 81 phenylboronic acid in the periphery. These dendrimers had an inhibitory effect on growth and luminescence as observed by luminescence, aggregation and colony forming unit-counting assays. Although the mechanism is not yet fully understood, these promising results should be further explored.

Cationic GATG dendrimers of generation G1, G2 and G3 with 9, 27 and 81 primary amines in the periphery induced formation of clusters in *V. harveyi* in a generation dependent manner, an improved ability to induce cluster formation when compared with poly(N-[2-(dimethylamino)propyl]methacrylamide), a cationic linear polymer previously shown to cluster bacteria. Viability of the bacteria within the formed clusters and the evaluation of the QS controlled luminescence suggests that the GATG dendrimers may be activating microbial responses by maintaining a high concentration of QS signals inside the clusters while increasing permeability of the microbial outer membrane. Thus, a generation-dependent effect in bacterial luminescence production and membrane permeability was induced by the cationic dendrimers. The inhibition of growth and increased membrane permeability in combination with cell clustering may be promising antibacterial features of these dendrimers.

These results highlight the potential of the GATG dendritic platform to develop new antimicrobials aimed to target microbial viability and/or virulence (e.g. adhesion) and encourage further investigations on the importance of polymeric architecture and multivalency in the antimicrobial field.

ACKNOWLEDGEMENTS

Firstly I would like to express my sincere gratitude to my supervisors Prof. Cameron Alexander, Prof. Eduardo Fernandez-Megia and Dr. Francisco Fernandez-Trillo for their guidance, motivation and continuous support during my PhD studies. I would also like to thank Dr. Klaus Winzer for his helpful discussions and assistance in the microbiology work and together with Dr. Steve Diggle giving me access to microbiology research facilities. I am deeply grateful to Dr. Juan F. Correa, Sandra P. Amaral and Marcos Fernandez-Villamarin for all their encouragement, helpful discussions and endless support both in and out of the lab in Santiago. Many thanks to Dr. Iria Louzao for her insightful comments and advice. I would like to thank Samuel Parcero for continuing the work on the dendrimer synthesis. Thanks to Prof. Victor Nizet and Dr. Sascha Kristian who provided me with the opportunity to join the Altermune team as an intern. Many thanks to my fellow labmates at the University of Santiago de Compostela and the University of Nottingham for their helpful discussions and company. I acknowledge Dr. Tim Overton and Dr. David Onion for their guidance with regards to the flow cytometry work. I also thank Bonnie Bassler (Princeton University) for providing *V. harveyi* and Cheng Sui (University of Nottingham) for P1. I thank the European Commission (EACEA) for an Erasmus Mundus grant under the NanoFar Joint Doctoral Program.

I am very grateful to my family and friends, especially the Kitxi girls, for all their love and support. Most important, I want to thank my partner Tim Arnold for always believing in me and for his love and encouragement.

CONTRIBUTIONS

I would like to acknowledge the use of material presented in this thesis that were not synthesized by me but by my colleagues at University of Nottingham (UNot) and University of Santiago de Compostela (USdC). The following compounds were synthesized by others:

GATG repeating unit (**21**)	Sandra P. Amaral (USdC)
GATG core (**34**)	Sandra P. Amaral (USdC)
Model system compounds (**33, 34**)	Juan F. Correa (USdC)
Compound **5**	Juan F. Correa (USdC)
G3-Mannose	Samuel Parcero (USdC)
G3-Glucose	Samuel Parcero (USdC)
G3-NH_2-MCCA	Iria Louzao (UNot)
P1 polymer DP49 and DP99	Cheng Sui (UNot)

TABLE OF CONTENTS

LIST OF ABBREVIATIONS

AMP	Antimicrobial peptide
AAC	Azide-Alkyne cycloaddition
AB	Autoinducer Bioassay
AHL	Acylated homoserine lactones
AI	Autoinducer
AI-2	Autoinducer-2
AIP	Autoinducer peptides
AMC	Activated methyl cycle
CAI-1	Cholera autoinducer -1
CFU	Colony Forming Units
DLS	Dynamic Light Scattering
DMSO	Dimethyl sulfoxide
DP	Degree of polymerization
DSC	N,N'-disuccinimidyl carbonate
DSF	Diffusible signal factor
DPD	4,5-dihydroxy 2,3 pentanedione
ESI	Electrospray ionization
FIA	Flow injection analysis
FT-IR	Fourier Transformed Infrared Spectroscopy
GATG	Gallic-acid triethyelene glycol
IA	Itaconic acid
IQS	Integrated quorum sensing systems
LB	Lysogeny broth

LPS	Lipopolysaccharides
MCCA	7-methoxy coumarin-3- carboxylic acid
MPLC	Medium Pressure Liquid Chromatography
NHS	N-hydroxysuccinimide
NMR	Nuclear magnetic resonance
OD	Opical Density
PAMAM	Poly(amidoamine)
PBP	Penicillin-binding protein
PBS	Phosphate-buffered saline
PEG	Polyethylene glycol
PI	Propodium iodine
PPI	Poly(propylenimine)
PQS	Pseudomonas Quinolone Signal
PSS	Polymer Standard Service
PVA	Polyvinyl alcohol
QS	Quorum sensing
QQ	Quorum quenching
RF	Retention factor
RU	Repeating Unit
SAH	S-adenosylhomocysteine
SAM	S-adenosylmethionin
SEC	Size Exclusion Chromatography
SRH	S-ribosylhomocysteine
TLC	Thin-layer chromatography
TOF	Time-of-flight

Bacterial strain abbreviations

E. coli	*Escherichia coli*
P. aeruginosa	*Pseudomonas aeruginosa*
S. aureus	*Staphylococcus aureus*
S. typhimurium	*Salmonella typhimurium*
V. cholera	*Vibrio cholera*
V. fisheri	*Vibrio fisheri*
V. harveyi	*Vibrio harveyi*

1. Introduction

1.1 Need for new antibacterial materials

It has been estimated that 50 000 people die each year from infections by antibiotic resistant bacteria across Europe and the US alone, numbers that are predicted to grow to 10 million deaths worldwide each year according to a recent report on antibiotic resistance in 2014 for the UK government [1]. Antibiotic resistance is recognized as one of the greatest threats to human health worldwide [2]. Microorganisms are becoming extremely resistant to existing antibiotics, reaching up to 25% of pathogenic bacteria in many European countries [3]. At the same time only two new classes of antibacterial drugs have been discovered in the last 40 years and an increasing number of bacteria strains are becoming resistant to the antibiotics available. A strain of *Escherichia coli* (*E. coli*) resistance to polymyxins, often the last resort of antibiotics used to treat serious infectious of multi-drug-resistant bacteria, was discovered in November 2015 [4]. These are very concerning findings, as the resistance gene was found on a plasmid, and could be transferred easily to other bacteria, including bacteria with previous multiple drug resistance. The rise in antibiotic resistant strains makes the treatment of microbial infectious diseases more challenging and there is a need for new anti-infectious materials capable of interfering with bacterial infections through different mechanisms than those of traditional antibiotics. It is clear that there is a need not only to take control over the overuse of antibiotics and to find new bactericides, but it is also crucial to look at alternative antibacterial materials that are less likely to cause resistance in the future.

To overcome the increased antimicrobial resistance, significant efforts have been made both in development of novel classes of antibiotics, but also in exploration of novel antimicrobial strategies. Anti-virulence strategies that try to minimize the impact of infection without targeting microbial viability have been proposed as an alternative to current antibiotics [5]. Non-lethal anti-virulence agents that target key stages in infection such as the ability of bacteria to attach and infect host cells [6, 7] and bacterial signalling to coordinate expression of virulence factors [8, 9] are promising new approaches. Because these strategies do not compromise microbial viability and survival, the evolutionary pressure on bacteria is lower than that of conventional antibiotics, and resistance is less likely to develop [10]. Moreover, these anti-virulence strategies can be combined with other antimicrobial treatments to obtain addition benefits [11].

1.2 Thesis Objectives

The aim of this work was to develop a library of materials that could interfere with bacterial communication systems and/or bacterial adhesion, using dendrimers as a platform for novel antibacterial material. The objectives were a) to develop an efficient and catalyst-free method to conjugate functional groups able to interact with bacterial cell surfaces or Quorum sensing (QS) communication molecules to the dendrimer structures, and b) to study the effect of dendrimer size and number of functional groups on the interactions with bacteria and cell signals. Accordingly, some key concepts relating to bacterial communication systems and adhesion will be covered in this

introduction chapter. In addition, polymeric materials as antibacterial platforms and dendrimer synthesis and conjugation will be reviewed.

1.3 Quorum Sensing – Bacterial Communication

Bacteria communicate with each other to regulate community behaviour in a process, which is now termed "quorum sensing" (QS). Quorum sensing involves the production, detection and response to extracellular chemical signal molecules [12]. These small hormone-like molecules are called auto inducers (AI) and are used by bacteria to regulate and synchronize gene expression in response to changes in cell population density [13]. When bacterial populations grow, the concentrations of AI increase and reach a threshold where gene transcription alters. By these mechanisms, the bacterial population can induce transcription of certain virulence factors only when living in a large enough "community", enabling the bacteria to work as a multicellular organism [12, 14]. Various QS systems have been identified in both Gram-positive and Gram-negative bacteria and involve, among others, control over genes responsible for secretion of virulence factors, formation of biofilms conjugation, sporulation and bioluminescence [13, 15, 16].

Several different QS signal molecules have been identified and bacteria generally respond to different extracellular molecules, restricting the communication to be within one species. Typically, Gram-negative bacteria use acylated homoserine lactones (AHLs), while Gram-positive bacteria use oligopeptides (autoinducer peptides, AIP) often with side chain modifications such as isoprenyl groups (*Bacillus subtilis*) or thio-lactone *(Staphylococcus*

aureus) (*Figure 1.1*) [13]. However, other autoinducer molecules have been identified, including 2-alkyl-4-quinolones, γ-butyrolactones fatty acids, and AI-3 γ-butyrolactones and derived fatty acids [17-19]. Autoinducer-2 (AI-2) has been found in both Gram-negative and Gram-positive bacteria and has been described as a universal QS molecule for interspecies communication [13, 20, 21].

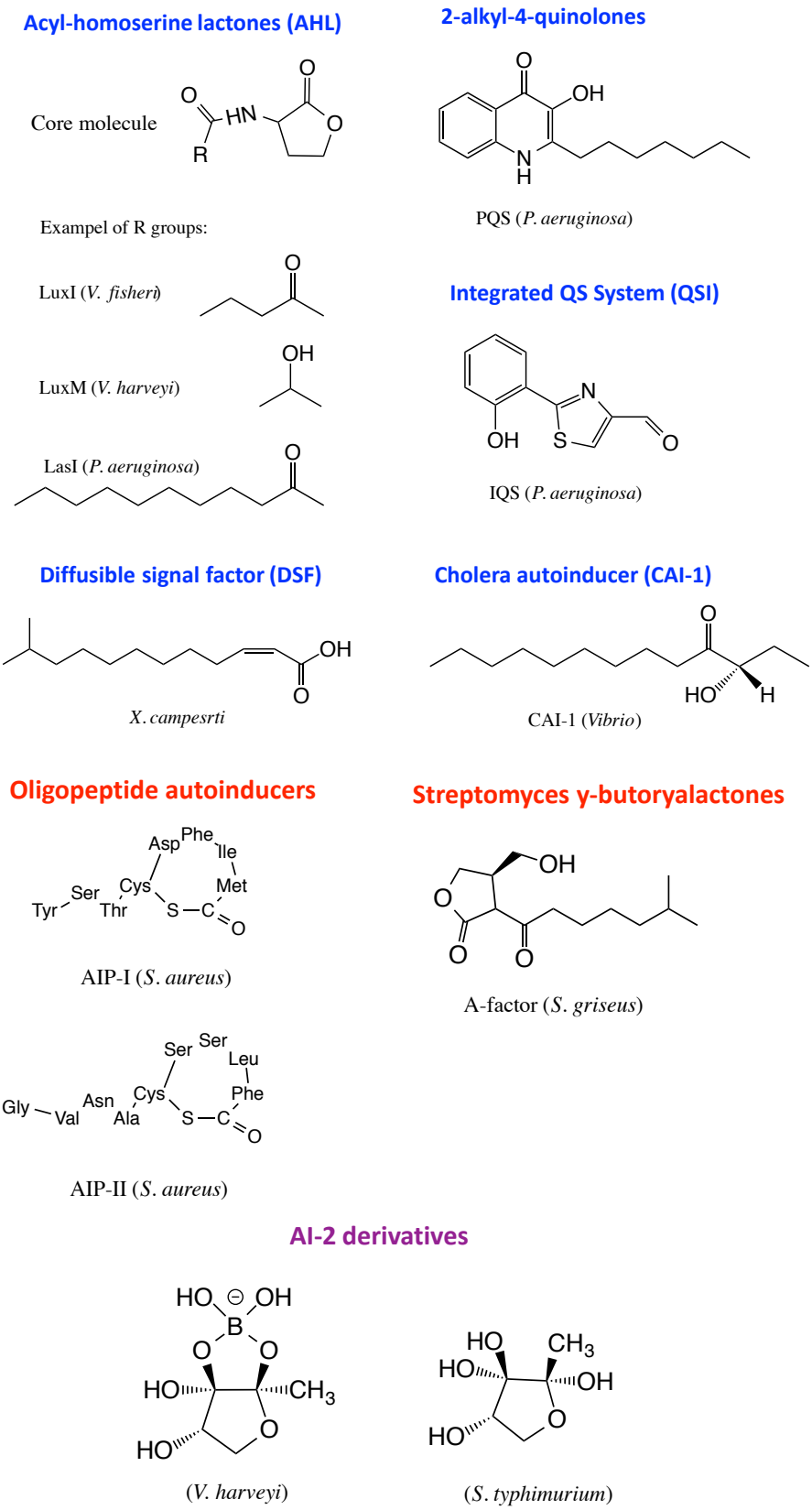

Figure 1.1 Various autoinducers in Gram-negative (blue) and Gram-positive (red) bacteria. AI-2 (purple) is found in both Gram-negative and Gram-positive bacteria. Figure adapted from references [12, 17, 18].

1.3.1 Multiple QS Systems in *V. harveyi*

The observation that bacteria can communicate with multiple quorum-sensing systems was first discovered in *Vibrio harveyi (V. harveyi)* [22], a bioluminescent Gram-negative marine bacterium. *V. harveyi* is a pathogen of fish and invertebrates and is a leading cause of death among commercially farmed shrimp [23].

V. harveyi produce and respond to three different AI that all regulate the QS pathway. Similar to many other Gram-negative bacteria, *V. harveyi* produces an AHL molecule (3OHC4HSL), recognized by a membrane-bound sensor histidine kinase (LuxN) (*Figure 1.2*) [24, 25]. *V. harveyi* also uses the AI-2 QS signal, found in both Gram-negative and Gram-negative bacteria. AI-2 is recognized by the periplasmatic LuxP receptor and the complex interacts with the membrane-bound histidine sensor kinase LuxQ [22]. The third QS signal is the cholera autoinducer-1 (CAI-1) recognized by another membrane-bound sensor histidine kinase, CqsS [26].

At low cell density, in the absence of a critical concentration of AI, LuxN, LuxQ and CqsS, act as kinases, transferring the phosphorylation downstream to the LuxO (*Figure 1.2*). This activates a downstream phosphorylation cascade, which leads to the inhibition of *luxR* genes important for high density-gene transcription such as luminescence and also activation of Alpha-A expression, a regulator of low-density gene transcription [26]. At high cell density, the accumulated AIs bind to its corresponding sensor and the sensor shifts from

being a kinase to phosphatase. The un-phosphorylated LuxO allows production of LuxR that regulates the high cell density phenotype.

Simultaneous activation/deactivation of LuxO by the three autoinducers is needed for the maximal impact on gene transcription [26]. However the signal strength is not equal between the autoinducers and the relative kinase/phosphorylation input from each signal can change depending on the environment.

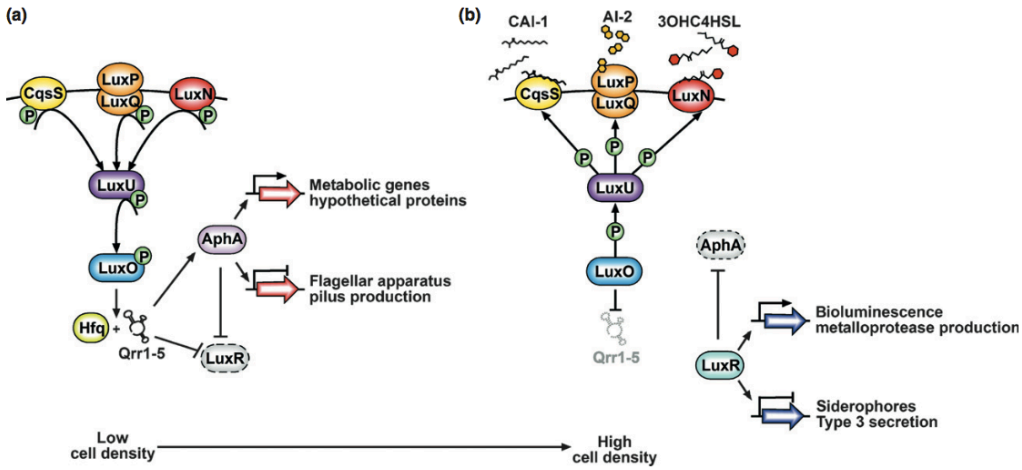

Figure 1.2 Multiple QS system in *V. harveyi.* (a) At low cell density, at sub-threshold concentrations of AI, LuxN, LuxQ and CqsS. Phosphorylated LuxO destabilizes *luxR* mRNA, the high cell density regulator, through five Quorum regulatory-RNA (Qrr). LuxR is the regulator of high cell density phenotypes. In addition Qrr 1-5 activates AphA, initiating transcription of over 100 genes important in low cell density conditions. (b) At high cell density, the accumulated autoinducers bind to its corresponding sensor, promoting phosphatase activity, moving the phosphate flow upstream. The un-phosphorylated LuxO will not initiate transcription of Qrr 1-5 and therefore there is no inhibition of LuxR. When *luxR* is produced high cell density genes are transcribed, including genes responsible for luminescence. Figure from reference [16].

1.3.2 AI-2 Signalling

AI-2, the product from the LuxS enzyme, is a QS signal molecule broadly conserved in the bacterial world [16, 26, 27]. Homologues of the *luxS* gene have been discovered in roughly half of all bacterial genomes sequenced, and AI-2 production has been verified in a large number of these bacteria [16]. AI-2 controls gene expression in a wide range of both Gram-negative and Gram-positive bacteria, including biofilm formation, cell attachment, motility, antibiotic susceptibility and other important virulence factors [16]. The LuxS gene *in E. coli* has been described to have a central role for the transition to the pathogenic existence inside the host [28] where it controls virulence factors such as biofilm formation, motility or gene expression [29-32]. These findings suggest that AI-2 is an inter-community signal molecule, enabling communication between different bacterial species [13, 20, 21].

However, LuxS is also important in the activated methyl cycle (AMC), an important metabolic pathway for recycling the most important methyl donor in the cell, S-adenosylmethionine (SAM) (*Figure 1.3*) [33, 34]. The transfer of methyl group from SAM to an acceptor molecule gives rise to the toxic intermediate, S-adenosylhomocysteine (SAH) that is converted to S-ribosylhomocysteine (SRH) by Pfs. LuxS catalyses the cleavage of SRH to homocysteine, adenine and the communication molecule AI-2 [35]. In non-LuxS containing organisms the SAhH enzyme converts SAH directly to homocysteine and adenosine.

Because the role of LuxS, not only in the synthesis of 4,5-dihydroxy 2,3 pentanedione (DPD) — the linear form of AI-2 (*Figure 1.4*), but also as a crucial component of the AMC metabolic pathway, it is suggested that AI-2 is only a metabolic by-product in some species [35]. This is important to consider when studying the effect of inactivation of LuxS and demonstration of the role of AI-2 as a quorum sensing molecule [16] as a lack of LuxS will have substantial metabolic effects. Interestingly, SAM is also the substrate for the synthesis of the two other QS molecules, AHLs and CAI-I, suggesting a link between metabolism and quorum sensing [16].

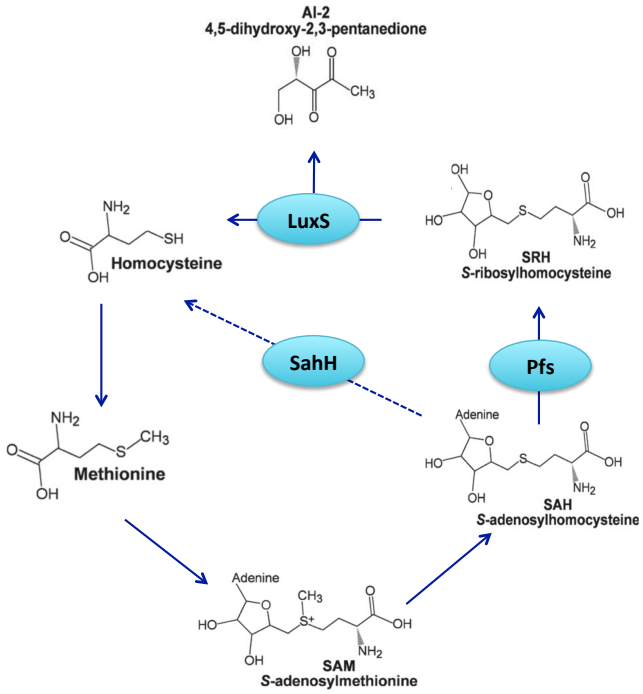

Figure 1.3 The transfer of methyl group from SAM to an acceptor molecule gives rise to the toxic intermediate, S-adenosylhomocysteine (SAH) that is converted to S-ribosylhomocysteine (SRH) by Pfs. LuxS catalyzes the cleavage of SRH to homocysteine, adenine and communication molecule DPD. In non-LuxS containing organisms the SAhH enzyme convert SAH directly to homocysteine and adenosine. Figure adapted from reference [16].

In the extracellular environment, the DPD molecule itself is very unstable and undergoes spontaneous rearrangements to several furones in water and different bacteria recognize different DPD derivatives (*Figure 1.4*) [21, 36]. While *V. harveyi* recognizes the S-THMF-borate complex formed of DPD and the boric acid present naturally in their environment (0.4 mM concentration), *Salmonella typhimurium* (*S. typhimurium)* and *E. coli* recognize a different form of the DPD, the R-THMF (*Figure 1.4*) [37, 38]. AI-2 is hydrophilic in nature with a low affinity for lipid binding, suggesting a transport pathway across the cell membrane is required, although this is still unclear [16].

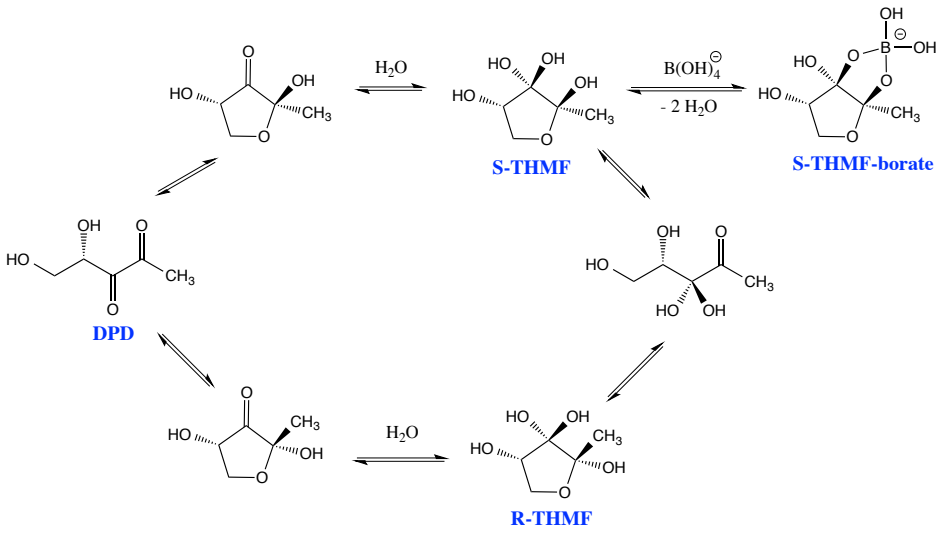

Figure 1.4 Structures of DPD and derivatives. Figure adapted from reference [39].

Two classes of AI-2 receptors have been well characterized; the LsrB, first identified in *S. typhimurium* [36], and the LuxP family from *V. harveyi* [21]. While the overall folding of the protein is similar (*Figure 1.5*), they share very low sequence homology (11%) [21, 36, 40]. A member of the ribosome-binding protein (RbsB) may also act as AI-2 receptor in Gram-negative

Aggregatibacter actinomycetemcomitans and *Haemophilus influenza* bacteria [41, 42]. In addition, AI-2 response has been observed in bacteria lacking any of the known receptors, suggesting there are alternative AI-2 receptors not yet discovered [16].

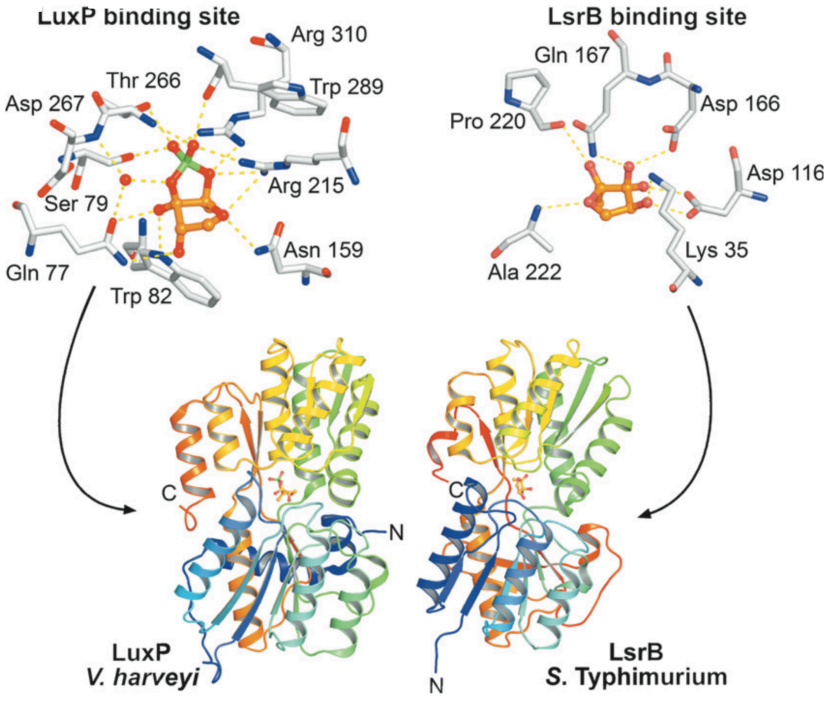

Figure 1.5 Structure and binding site of AI-2 receptors LuxP (S-THMF-borate) and LsrB (R-THFM). The structure of the receptors, shown by ribbon diagrams, are coloured in rainbow order from N- (blue) to C-terminus (red). Figure taken from reference [16].

1.3.3 Quorum quenching molecules

Discovery of the AI-2 signalling system in over 70 species of both Gram-negative and Gram-positive bacteria [17] makes DPD a promising target for quorum quenching of a wide range of bacteria species. Research efforts have been concentrated on identifying and designing small molecule QS inhibitors,

including inhibitors of AI-2 synthesis, receptor interaction, degradation of the signal molecule, and several type of AI-2 analogues [17, 43, 44].

Recently a new area using macromolecules for quorum quenching has emerged [45]. The prospects of using three types of proteins for interference with QS; enzymes that can hydrolyse QS molecules, anti-QS molecule antibodies and decoy receptors trapping QS molecules, was recently reviewed [45]. Many of the proteins described can inhibit QS with various levels of potency, however the mechanism is not always clearly understood and several questions have been raised regarding efficiency and rate of protein-mediated hydrolysis of QS molecules and whether the macromolecules can evoke an immune response in humans.

Initial efforts to mimic protein binding to QS molecules using synthetic polymers have been reported. The group of Piletsky has developed polymeric materials containing itaconic acid (IA) for the inhibition of AHL able to inhibit QS phenotypes in *Vibrio fisheri* (*V. fisheri)* and *Pseudomonas aeruginosa (P. aeruginosa*) [46-48]. Monomers were screened using receptor-docking software for affinity towards N-(β-ketocaproyl)-L-homoserine lactone (3-oxo-C6-AHL). A polymer with 5% functional monomer (IA) was able to sequester the AHL signal and prevent up-regulation of luminescence while not affecting cellular growth [46]. A series of molecular-imprinted IA polymers were developed which were able to quench the activity of N-(3-oxodedecanoyl)-L-homoserine lactone (3-oxo-C12-AHL) from *P. aeruginosa*, and were thus able to attenuate the biofilm formation [48]. Recently the Piletsky group developed co-polymers

with itaconic and methacrylic acids as functional monomers inhibiting luminescence in *V. fisheri* and biofilm formation of *Aermonas hydrophila* by absorption of AHL [47]. Addition of exogenous AHL to recover the inhibitory effect on QS phenotypes demonstrated the ability of polymers to sequester AHL.

Conjugation of quorum inhibitors to a polymeric material can increase the multivalency and the inhibitory effect of the quencher [49]. Polymers containing multiple analogues of autoinducing peptide 4 (AIP4') of *S. aureus* were demonstrated to bind to the AgrC receptor, affecting the QS response in a multivalent fashion [49]. Increased loading of AIP-4' on the polymer increased binding to the AgrC receptor and decreased the QS phenotype in *S. aureus* RN9371 (reported by a β-lactamase reporter gene).

A dual-acting synthetic polymer able to both quench QS molecule AI-2 and cause aggregation of *V. harveyi* was previously reported by our group (*Figure 1.6*) [50]. Xue and colleagues investigated the affinity of different diol moieties to boronic acids and designed synthetic polymers decorated with diols for quenching of AI-2 by high affinity binding to the boric acid in the media, thereby preventing the formation of the active form of AI-2 in *V. harveyi* (S-THMF-borate). The synthetic polymers containing carbohydrate and catechol moieties were both able to quench QS signals in *V. harveyi* MM32.
In addition carbohydrates and cationic moieties functioned as anti-adhesive agents causing the bacteria to cluster.

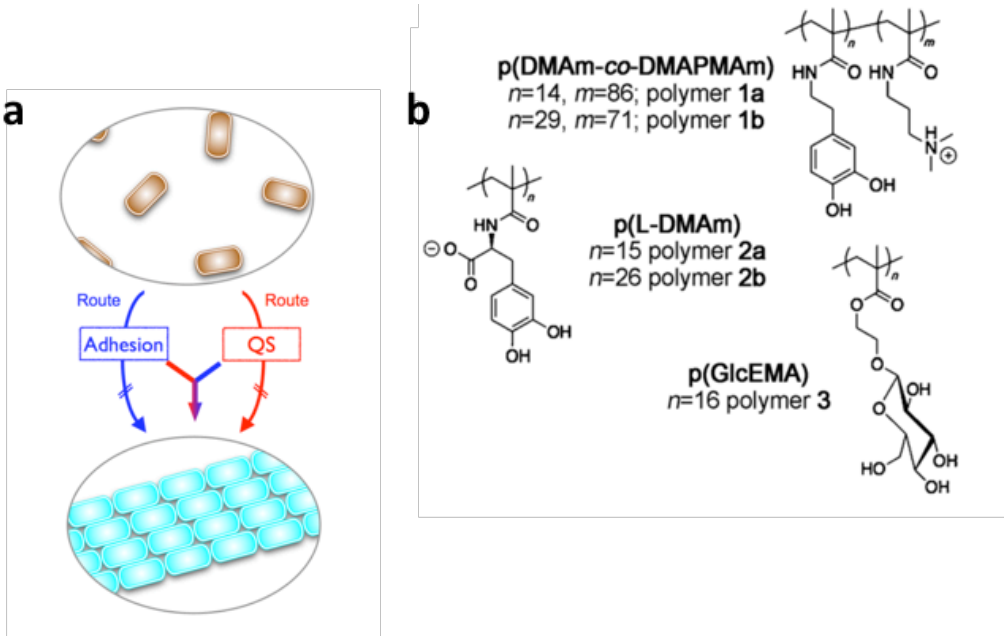

Figure 1.6 Dual-acting polymers interfering with bacterial aggregation and QS signalling (a) Structures of polymers containing catechol and carbohydrate moieties with positive and negative charges (b) Figure taken from reference [50].

1.4 Anti-adhesion

Materials that can prevent bacteria to attach to host cells and cause disease are a promising non-lethal strategy to avoid increased antibiotic resistance. Two main pathways for anti-adhesive therapeutics have been explored, the first using antifouling surfaces to inhibit the adhesion of bacteria directly [51, 52], and the second to target the bacteria with material containing moieties with high affinity for the bacterial surface, thus inducing bacteria clusters and blocking bacteria from host cell carbohydrate recognition [53-55].

The adhesion of bacteria to the host cell surface is often mediated by interaction between proteins (lectins) on the pathogen and carbohydrates on the host cell [56]. Polymeric materials with multivalent sugar moieties have been

recognized as promising anti-adhesive agents [52, 53, 56, 57]. Glycopolymers have been prepared that target the mannose-specific type 1 fimbriae lectin [52, 58], which is strongly associated with *E. coli* urinary tract infections in humans [59].

Cationic polymers, which can cluster bacteria through electrostatic interactions, constitute the basis for another anti-adhesive strategy (as defined by prevention of adhesion to the host rather than to the bacteria). Bacteria generally carry a net negative charge on the surface due to the specific components making up the cell wall. This includes the lipopolysaccharides (LPS) and phospholipids of the Gram-negative outer cell wall and teichoic acids (or lipoteichoic) of the Gram-positive cell wall and the cytoplasmic membrane itself [60]. Polycationic materials can therefore associate with the bacteria through electrostatic interactions and can aggregate bacteria into clusters, thereby preventing bacterial adhesion to host cells [57]. Depending on the design of the material, polycations can also disrupt the cell wall and cytoplasmic membranes, causing cell lysis and death.

Introducing secondary functionalities on the polymer can lead to increased complementary interactions. Catechol moieties have a positive effect on bacterial adhesion, but only in the presence of positive charges [54]. Cationic polymers with catechol moieties were more efficient in binding to both Gram-negative and Gram-positive bacteria, and generated larger clusters compared to polymers with only cationic moieties (*Figure 1.7*) [54].

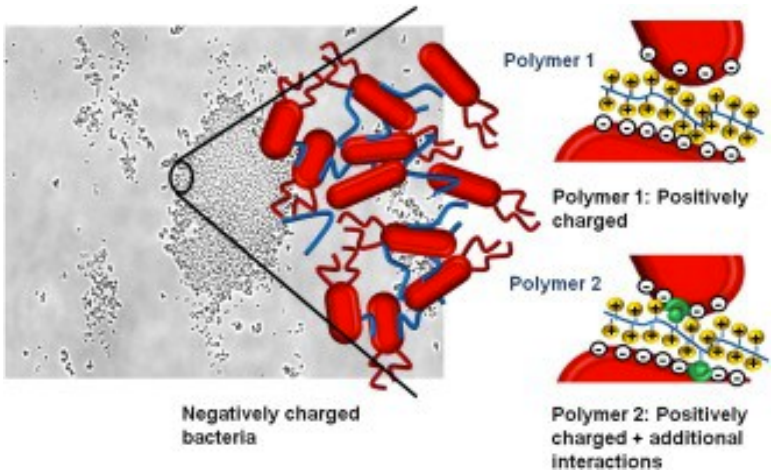

Figure 1.7 Clustering of negatively charged bacteria initiated by polymers with positive charges (Polymer 1). Addition of hydrophobic interactions to the polymer (Polymer 2) reinforces the binding and increased cluster size [54].

1.5 Dendrimers

Synthetic polymers are often prepared by routes that generate a wide range of molecular weights, giving a polydisperse final material. The variation in size can have significant effects on biological interactions. For instance, the binding properties of polymers with otherwise similar chemical structures can vary strongly with molecular weight. With a polydisperse material it is difficult to know which polymer components in terms of size and multivalency are responsible for specific functions or biological activities. Unlike conventional synthetic polymers, dendrimers enable precise control of the number and position of ligands and have been recognized as promising scaffolds in various biomedical applications [61]. Ideal dendrimers are perfectly monodisperse structures (same size, shape and mass) made of branched repeating units from a central core [62]. Starting from the core, the dendrimer branches three-dimensionally, with each generation (usually) in regular shells from inside to

outside (*Figure 1.8*) [63]. With high numbers of functional groups in the periphery to fine-tune their chemical and biological properties, dendrimers can be modulated in activity for many desired applications.

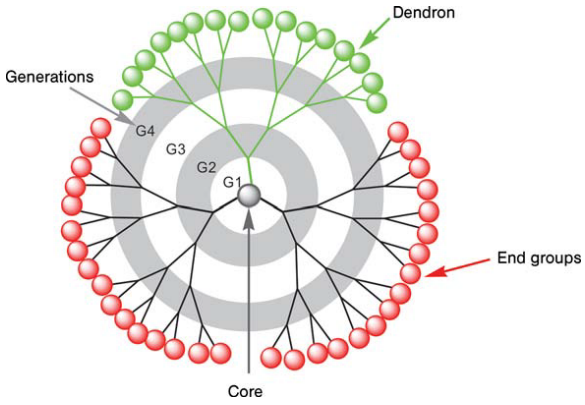

Figure 1.8 General dendrimer structure. Figure taken from reference [63].

An important feature of dendrimers is that they have a lower viscosity in solution compared to corresponding non-branched compounds of the same overall molecular weight and, unlike linear polymers, the intrinsic viscosity of dendrimers does not increase linearly with molecular mass [63]. The viscosity reaches a maximum at a certain generation and will decrease with higher generations after this. This can be explained by the transformation of the open structure of the dendrimers at lower generation to an almost globular structure with higher generations, and this is why dendrimers of higher generation have smaller volumes than corresponding linear polymers as well as showing better solubility in organic solvents. Multiple ligands on the same particle can increase affinity through the effect of multivalency, which has shown to strongly increase activity compared to corresponding monomeric interactions [61]. Multivalency can also increase the specificity of an interaction: this

phenomenon is common in biological systems, where organisms are able to use sequential and cooperative low-affinity binding interactions to ensure that only when multiple copies of receptor-ligand species are present, associations take place. This effect is particularly important for carbohydrate-protein receptor interactions in natural systems [61, 64].

1.5.1. Antibacterial Dendrimers

Dendrimers are promising platforms for antimicrobial applications [65-67]. Starpharma, a world leading company of dendrimer development for pharmaceutical applications, has launched a condom coated with antiviral and antibacterial L-lysine based dendrimer with naphthalene disulfonic acid groups in the periphery (VivaGel®) for prevention of sexually transmitted infections [68]. Various strategies for dendrimers as antibacterial drugs have also been described; dendrimers decorated with antibiotics [69], antimicrobial peptides [70], NO-releasing dendrimers [71] and anionic dendrimers [72]. Glycodendrimers and cationic dendrimers have gained a lot of attention due to their potential to interfere with bacterial adhesion through multivalent display of carbohydrates or positive charges [50, 54-56, 65, 73].

1.5.1.1 Glycodendrimers

Glycodendrimers have been described to block microbal adherence to cell surfaces by targeting the carbohydrate-binding proteins in a multivalent manner [56, 73]. Mannosylated dendrimers targeting *E. coli* mannose-specific type 1 adhesins for anti-adhesive activities therapy have been synthesised [55, 73]. Nagahori and collegues studied the binding of mannose-terminating

dendrimers to type I adhesin of *E. coli* and determined that the factors effecting inhibition most were the alpha-orientation of the hydrophobic groups and the presence of large numbers of mannose units on a flexible structure that could span over distances of 20 nm or longer [74].

Lectins can often be assembled into appendages called pili or fimbriae [75]. The tip of P-fimbriae contains a lectin that recognizes the galactosyl-α-1-4-galactose (galabiose) moieties, and both *E. coli* and *Streptococcus suis* have been described to bind to galabiose [75, 76]. The potency to block *E. coli* binding to human erythrocyte increased per carbohydrate with higher valency of dendrimers decorated with mono- di-tetra- and octavalent galabiose residues [75]. This showed the effect of dendrimer multivalency on inhibition of *E. coli* adhesion to host cells. The same dendrimer generation effect blocking galabiose-specific adhesion was seen in *Streptococcus suis*, a bacteria involved in meningitis. However, when the same dendrimers were functionalised with mannose for targeting type I fimbriae, the multivalent effect was only observed for valencies up to four. The octavalent dendrimer had decreased activity, suggested to be due to that for certain binding domains larger glycodendrimers are not accomodated in the binding site.

The multivalency of glycodendrimers has been shown to inhibit biofilm formation in *P. aeruginosa* by targeting the galactose specific LectinA and fucose-specific LectinB [77, 78]. Screening of dendrimer libraries with alpha-C fucose residues identified a tetravalent glycopeptide dendrimer with high potency against LecB, a surface protein of *P. aeurginosa* important for the

bacterial host-cell attachment [79]. The dendrimer completely inhibited formation of *P. aeurginosa* biofilms with a 50-fold affinity gain compared to a monovalent system (IC_{50} 10μM) [77]. Interestingly, dendrimers were also able to completely disrupt already established biofilms.

Decorating the dendrimer with differently linked galactose instead of fucose, glycodendrimers targeted galactose-dependent LecA instead of LecB from *P. aeurginosa for* inhibtion of biofilms [78]. Affinity for LecA was increased with higher generation dendrimers, demonstrating the importance of multivalency.

In addition several glycodendrimers have been reported able to target and inhibit the binding of bacteria virulence factors known as AB_5 toxins, such as the enterotoxin toxin secreted by *E. coli,* that upon entry into epithelial cells in the intestine, cause traveler's disease [65].

1.5.1.2 Cationic dendrimers

Cationic particles are in general toxic to mammalian cells due to their strong and potentially damaging interactions with the cell membrane [61]. Cationic dendrimers have had their bactericidal properties attributed to binding and disruption of the bacteria cell wall and membrane [65]. Poly(propylenimine) (PPI) dendrimers with quaternary amines in the periphery showed 100-fold higher antimicrobial activity against *E. coli* compared to small molecule counterparts [80]. The toxic effect of the dendrimer was measured as a decrease in luminescence in an assay with a recombinant *E. coli* TV 1048 strain. The

effect of dendrimer generation and its hydrophobic chain length was further investigated and showed the antibacterial effect to be G5 > G4 > G1 > G2 > G3 [81]. This effect was proposed to be a balance between the higher antibacterial effect with increasing number of amines and a decreased cell permeability of larger dendrimers. Interestingly, dendrimers had a higher antimicrobial effect compared with hyper-branched polymers with the same number of functional groups. Nevertheless, dendrimers are not always more bactericidal than their linear polymer analogues. Ammonium functionalized carbosilane dendrimers of generation G1, G2 and G3 showed generation-dependent bactericidal effect against *E.coli* and *S. aureus* [82, 83]. However the largest dendrimer showed lower activity compared to cationic hyper-branched polycarbosilane with a similar molecular weight and activity as the second-generation dendrimer.

Substitution of primary amines to tertiary or quarternary amines reduces the toxicity to human cells while mainting the bactericidal effect [84]. Poly(ethylene glycol) (PEG) chains of various length have been attached to cationic dendrimers to mask their peripheral cationic charge and thereby overcoming some of the toxicity to mammalian cells. Cai and colleagues investigated the antimicrobial activity of poly(amidoamine) (PAMAM) dendrimers with or without PEG coatings. Shielding the positive charges of generation G3 significanly reduced the antimicrobial actvivity of *S. aureus,* whereas coating the dendrimer with 6% of PEG reduced the toxicity against human corneal cells while still maintaining the bactericidal effect against *P. aeurginosa* [85]. PEG-dendrimers have been explored as anti-fouling agents to prevent bacterial colonization [86]. Titanium-based structures coated with PEG-PAMAM

dendrimers of generation G5 inhibited growth of *S. aureus* and *P. aueriginosa* and did not inhibit cell adhesion of human bone mesenchymal stem cells.

1.5.1.3 Quorum Quenching Dendrimers

Dendrimers have been used as multivalent scaffolds for inhibition of quorum sensing receptors in Gram-negative bacteria [87]. QseC is a membrane-bound histidine receptor that responds to QS molecule AI-3 as well as to the host cell stress hormones epinephrine and norepinephrine [88]. PAMAM dendrimers of generation G3 were decorated with LED209, a specific inhibitor of the bacterial receptor QseC [87]. LED209 is a pro-drug, that through allosteric binding to the QseC receptor, prevented activation of virulence factors. The conjugation of LED209 to PAMAM dendrimers lowered the cytotoxicity to mammalian cells, while retaining strong antibacterial activity [87]. The dual effect from the dendrimers came from inhibition of the virulence pathway through inhibition of the QseC cascade and the broad antibacterial function of amine moieties, however no multifunctional effect was explored.

Janda and colleagues have reported a set of alkyl-DPD analogues and compared their inhibitory effect on the AI-2 system in *V. harveyi* and *S. typhimurium* [89]. A hexyl-DPD derivative was identified as the most promising DPD analogue and was used in the decoration of the surface of PAMAM dendrimers. The resulting dendrimer was an antagonist to the QS system in *S. typhimurium* by targeting the Lsr-type receptor (recognizing the R-THMF form of DPD). No quorum quenching activity of the dendrimer was noted in *V. harveyi,* most likely due to the fact that *S. typhimurium* and *V. harveyi* use

different quorum sensing receptors, LsrB and LuxP rescpectively. No multivalent effect of the receptor interaction was observed, suggesting any generation of PAMAM larger than generation 0 (*Figure 1.9*) were cytotoxic, and no multivalent antagonistic effects could be observed.

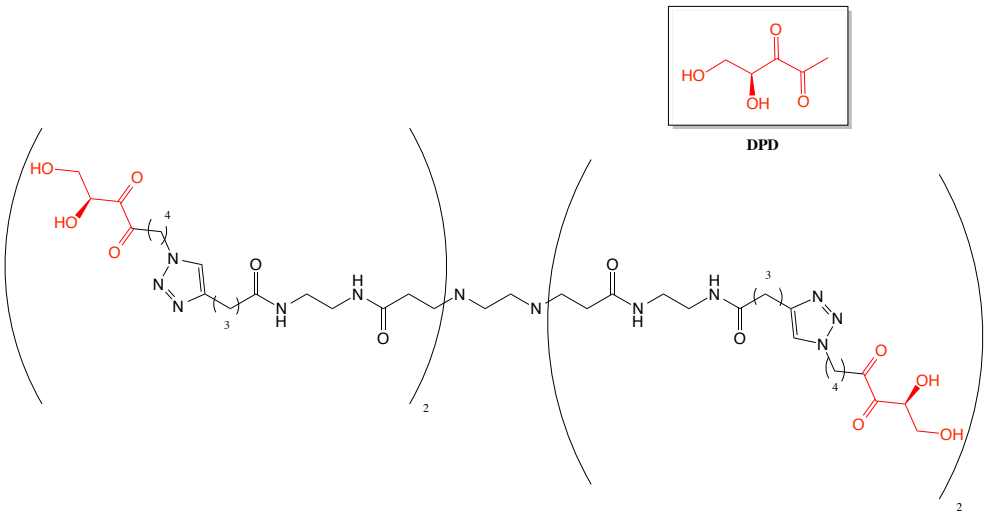

Figure 1.9 PAMAM dendrimers with alkyl-DPD analogues. Figure adapted from reference. [90].

1.6 Project focus

Despite the use of dendrimers as broad-spectrum antibacterial materials, only limited studies have explored their use as quorum sensing quenchers. Cationic dendrimers have emerged as promising antibacterial agents due to their disruption of the bacterial cell membrane. However the effect of dendrimer architecture on clustering of bacteria has not been investigated, and often insufficient data have been obtained to determine a structure-activity relationship [65]. Glycodendrimers are promising anti-adhesive agents, although some reports of increased effect with higher generations have been reported, no clear trend for multivalency to all carbohydrate targets can be defined [65].

The aim of this project was to synthesise dendrimers of different generations and sizes containing various number of ligands for interference with quorum sensing and/or clustering of bacteria. The goals were to 1) synthesise ligands containing hydroxyl moieties with affinity for the boronic acid present in medium needed for the formation of the active AI-2 form in *V. harveyi* and with the possibility to work as anti-adhesive agents, 2) to develop an efficient method for conjugation of diol ligands to GATG dendrimers of different size and multivalency (generations), 3) to synthesise dendrimers functionalized with phenylboronic acids for inhibiting the formation of STHMF-borate molecule, and 4) to synthesise cationic dendrimers as potential anti-adhesive macromolecules. The dendrimers containing hydroxyl, phenylboronic acid, and cationic moieties were evaluated *in vitro*, using *V. harveyi* as model bacteria to study the effect of the dendrimers on AI-2 quenching and bacteria aggregation.

1.6.1 Synthesizing Diol Ligands

The strategy for developing quorum quenching dendrimers was to decorate dendrimers with diol functionalities similar to those with quorum quenching activity reported for linear diols [50] and study the structure-activity relationship for different generations of globular dendrimers. In order to develop efficient functionalization the ligands were conjugated to the dendrimers using azide-alkyne cycloaddition (AAC).

1.6.1.1 Azide-Alkyne Cycloadditions

The concept of "click-chemistry" in the field of drug discovery was introduced by Sharpless and co-workers in 2001 with the view that "all searches for [drug

candidates] must be restricted to molecules that are easy to make" [91]. These reactions should be processes with a high thermodynamic driving force allowing efficient transformation from highly energetic starting materials (preferably from nature or easily manufactured). The reactions should also have wide functional group tolerance, to give the desired product under a broad range of experimental conditions, while using benign solvents, resulting in no or few by-products and with no purification steps needed. These criteria were fulfilled only by a few limited chemical transformations; i.e. additions to carbon-carbon multiple bonds, nucleophilic substitution, carbonyl-chemistry of "non-aldol" type and cycloaddition of unsaturated species such as 1,3-dipolar cycloaddition.

An azide-alkyne cycloaddition reaction (AAC, also referred to as Huisgen AAC) is a 1,3–dipolar cycloaddition between an azide and a terminal or internal alkyne to give a 1,2,3-triazole and can be performed under thermal conditions or catalysed by copper or ruthenium (*Figure 1.10*) [92].

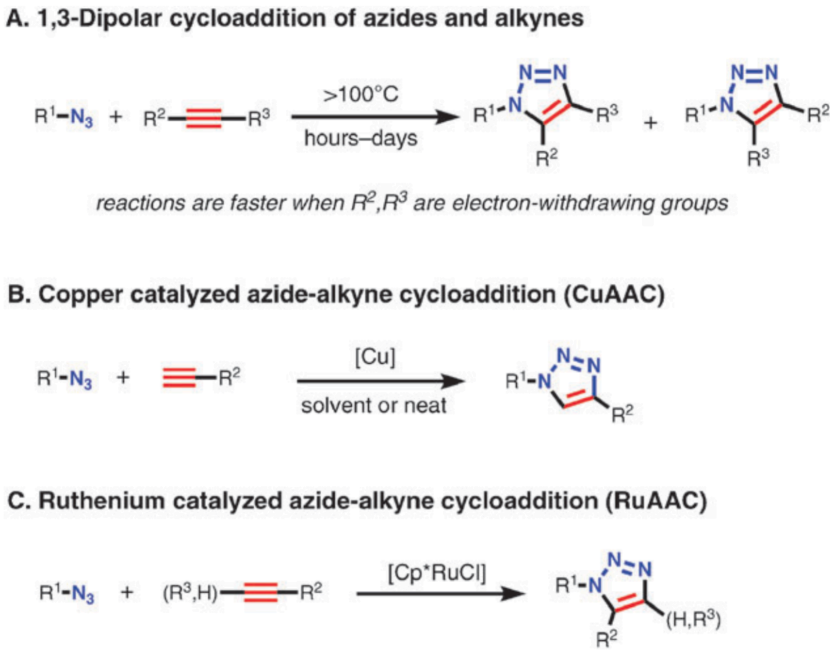

Figure 1.10 Azide-alkyne cycloaddition (AAC) performed at high temperature (a), Cu(I)-catalysed (b) or ruthenium-catalysed (c). Figure taken from reference [92]

1.6.2 Dendrimers for AAC

The second aim of this thesis was to develop an efficient method for conjugation of ligands to the dendrimers using thermal AAC. Dendrimers have to be synthesised with high yield and be stable during the thermal conditions needed for the catalyst-free ligand conjugation.

1.6.2.1 GATG Dendrimers

The dendritic gallic acid-triethylene glycol (GATG) family is composed of a repeating unit with a gallic acid core and hydrophilic triethylene glycol arms (*Figure 1.11*) [93, 94]. GATG dendrimers of various architectures have been

developed in our group and have been reported in a wide range of biomedical applications *(Figure 1.12)* [95].

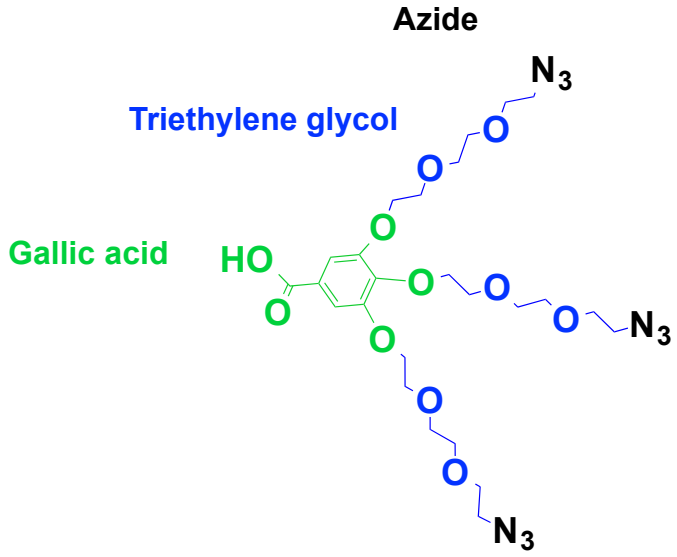

Figure 1.11 GATG repeating unit composed of a gallic acid core (green) and branches of triethylene glycol (blue) with terminal azides (black).

Conjugation of PEG at the dendritic core can increase the solubility or enable formation of micelles and other nanostructures. Our group has developed PEG-GATG block copolymers with G3 with various functional groups such as peptides, carbohydrates and cationic and anionic groups to study their effect on cellular uptake. Cationic GATG dendrimers are easily obtained by reduction of the terminal azide groups. PEG-G3 with terminal amine groups and functionalized with cargo molecules and a fluorescent dye showed high cellular uptake by HeLA cells and was also able to release the cargo to the cytoplasm following lysosomal escape [96]. The high density of peripheral positive charges on PEG-GATG G3 enables condensation and protection of negatively charged nucleic acids to form stable dendriplexes. The PEG chain reduces the cationic

dendrimers cytotoxicity to human cells and aggregation of blood components by masking the excess of positive charges [97]. The dendriplexes were biocompatible and protected the DNA from degradation and were effectively internalized by HEK-293T cells. The terminal azide groups of GATG are advantageous for dendrimer generation growth as well as for the easy functionalization of the dendrimer peripheral through AAC.

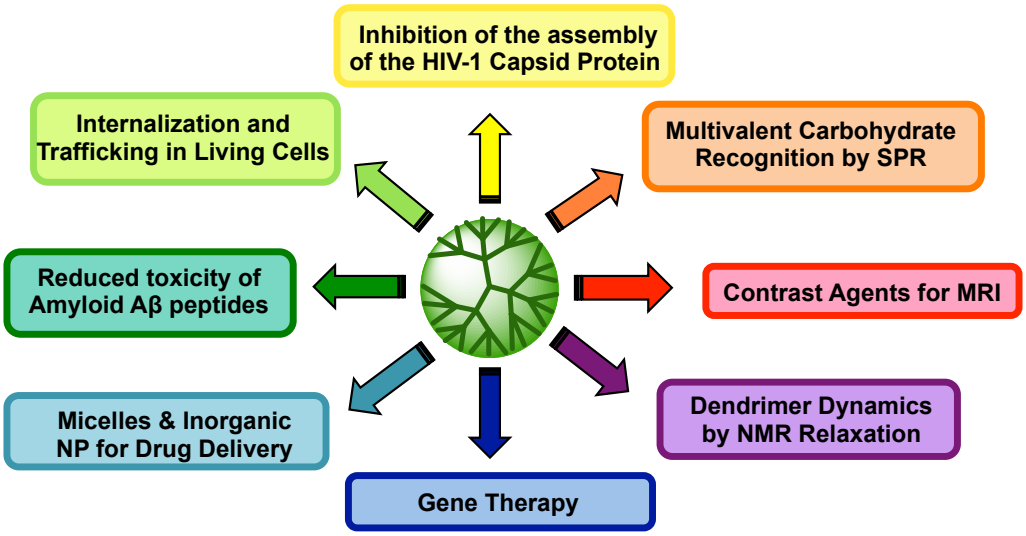

Figure 1.12 Biomedical applications of GATG dendrimers. Figure adapted from reference [95].

1.6.3 Evaluation of Microbiological Activity

Evaluations of synthesised dendrimers were focused on their ability to interfere with quorum sensing and aggregate bacteria. To study the effect of diol-dendrimer on QS inhibition two *V. harveyi* mutant strains of MM32 and BB170 were used. Both mutants lack the LuxN receptor and can therefore not respond to the second QS system, AI-1 (AHL), but only to AI-2 [25]. In addition

MM32 lacks the LuxS enzyme responsible for the synthesis of DPD and is thus unable to produce AI-2 [36]. The ability for dendrimers to cluster bacteria was measured with a Coulter counter, comparing the size of bacteria alone and after incubation with dendrimers (general methods are presented in Chapter 2).

1.7 REFERENCES

[1] O'Neill, J., *Antimicrobial Resistance: Tackling a crisis for the health and wealth of nations*, in *Review on Antimicrobial Resistance*. 2014: The Welcome Trust HM Government.

[2] Spellberg, B., Blaser, M., Guidos, R.J., Boucher, H.W., Bradley, J.S., Eisenstein, B.I., Gerding, D., Lynfield, R., Reller, L.B., Rex, J., Schwartz, D., Septimus, E., Tenover, F.C., and Gilbert, D.N. (**2011**). *"Combating antimicrobial resistance: policy recommendations to save lives."* Clin Infect Dis 52(5).

[3] ECDC/EMEA, *ECDC/EMEA Joint Technical Report: The bacterial challenge: time to reach*. 2009, European Centre for Disease Prevention and Control.

[4] Liu, Y.-Y., Wang, Y., Walsh, T.R., Yi, L.-X., Zhang, R., Spencer, J., Doi, Y., Tian, G., Dong, B., Huang, X., Yu, L.-F., Gu, D., Ren, H., Chen, X., Lv, L., He, D., Zhou, H., Liang, Z., Liu, J.-H., and Shen, J. (**2015**). *"Emergence of plasmid-mediated colistin resistance mechanism MCR-1 in animals and human beings in China: a microbiological and molecular biological study."* Lancet Infect Dis

[5] Rasko, D.A. and Sperandio, V. (**2010**). *"Anti-virulence strategies to combat bacteria-mediated disease."* Nat Rev Drug Discov 9(2): 117-28.

[6] Klemm, P., Vejborg, R.M., and Hancock, V. (**2010**). *"Prevention of bacterial adhesion."* Appl Microbiol Biotechnol 88(2): 451-9.

[7] Krachler, A.M. and Orth, K. (**2013**). *"Targeting the bacteria-host interface: strategies in anti-adhesion therapy."* Virulence 4(4): 284-94.

[8] Praneenararat, T., Palmer, A.G., and Blackwell, H.E. (**2012**). *"Chemical methods to interrogate bacterial quorum sensing pathways."* Org Biomol Chem 10(41): 8189-99.

[9] Singh, R.P. (**2015**). *"Attenuation of quorum sensing-mediated virulence in Gram-negative pathogenic bacteria: implications for the post-antibiotic era."* MedChemComm 6(2): 259-272.

[10] Allen, R.C., Popat, R., Diggle, S.P., and Brown, S.P. (**2014**). *"Targeting virulence: can we make evolution-proof drugs?"* Nat Rev Microbiol 12(4): 300-8.

[11] Gill, E.E., Franco, O.L., and Hancock, R.E. (**2015**). *"Antibiotic adjuvants: diverse strategies for controlling drug-resistant pathogens."* Chem Biol Drug Des 85(1): 56-78.

[12] Waters, C.M. and Bassler, B.L. (**2005**). *"Quorum sensing: cell-to-cell communication in bacteria."* Annu Rev Cell Dev Biol 21: 319-46.

[13] Henke, J.M. and Bassler, B.L. (**2004**). *"Bacterial social engagements."* Trends Cell Biol 14(11): 648-56.

[14] Miller, M.B. and Bassler, B.L. (**2001**). *"Quorum sensing in bacteria."* Annual. Rev. Microbiol 55: 165–99.

[15] Williams, P., Winzer, K., Chan, W.C., and Camara, M. (**2007**). *"Look who's talking: communication and quorum sensing in the bacterial world."* Philos Trans R Soc Lond B Biol Sci 362(1483): 1119-34.

[16] Pereira, C.S., Thompson, J.A., and Xavier, K.B. (**2013**). *"AI-2-mediated signalling in bacteria."* FEMS Microbiol Rev 37(2): 156-81.

[17] Guo, M., Gamby, S., Zheng, Y., and Sintim, H.O. (**2013**). *"Small Molecule Inhibitors of AI-2 Signaling in Bacteria: State-of-the-Art and Future Perspectives for Anti-Quorum Sensing Agents."* Int J of Mol Sci 14(9): 17694-17728.

[18] Atkinson, S. and Williams, P. (**2009**). *"Quorum sensing and social networking in the microbial world."* J R Soc Interface 6(40): 959-78.

[19] Karavolos, M.H., Winzer, K., Williams, P., and Khan, C.M. (**2013**). *"Pathogen espionage: multiple bacterial adrenergic sensors eavesdrop on host communication systems."* Mol Microbiol 87(3): 455-65.

[20] Bassler, B.L., Greenberg, E.P., and Stevens, A.M. (**1997**). *"Cross-species induction of luminescence in the Quorum-sensing bacterium Vibrio harveyi."* J Bacteriol 179(12): 4043.

[21] Chen, X., Schauder, S., Potier, N., Van Dorsselaer, A., Pelczer, I., Bassler, B.L., and Hughson, F.M. (**2002b**). *"Structural identification of a bacterial quorum-sensing signal containing boron."* Nature 415(6871): 545-9.

[22] Bassler, B.L., Wright, M., and Silverman, M.R. (**1994**). *"Multiple signalling systems controlling expression of luminescence in Vibrio harveyi: sequence and function of genes encoding a second sensory pathway."* Mol Microbiol 13(2): 273-86.

[23] Austin, B. and Zhang, X.H. (**2006**). *"Vibrio harveyi: a significant pathogen of marine vertebrates and invertebrates."* Lett Appl Microbiol 43(2): 119-24.

[24] Cao, J.G. and Meighen, E.A. (**1989**). *"Purification and structural identification of an autoinducer for the luminescence system of Vibrio harveyi."* J Biol Chem 264(36): 21670-6.

[25] Bassler, B.L., Wright, M., Showalter, R.E., and Silverman, M.R. (**1993**). *"Intercellular signalling in Vibrio harveyi: sequence and function of genes regulating expression of luminescence."* Mol Microbiol 9(4): 773-86.

[26] Henke, J.M. and Bassler, B.L. (**2004**). *"Three parallel quorum-sensing systems regulate gene expression in Vibrio harveyi."* J Bacteriol 186(20): 6902-14.

[27] Xavier, K.B. and Bassler, B.L. (**2005**). *"Interference with AI-2-mediated bacterial cell-cell communication."* Nature 437(7059): 750-3.

[28] Surette, M.G., Miller, M.B., and Bassler, B.L. (**1999**). *"Quorum sensing in Escherichia coli, Salmonella typhimurium, and Vibrio harveyi: A new family of genes responsible for autoinducer production."* PNAS 96: 1639-44.

[29] Rezzonico, F. and Duffy, B. (**2008**). *"Lack of genomic evidence of AI-2 receptors suggests a non-quorum sensing role for luxS in most bacteria."* BMC Microbiol 8: 154.

[30] Ren, D., Sims, J.J., and Wood, T.K. (**2001**). *"Inhibition of biofilm formation and swarming of Escherichia coli by (5Z)-4-bromo-5-(bromomethylene)-3-butyl-2(5H)-furanone."* Environ Microbiol 3(11): 731-6.

[31] Gonzalez Barrios, A.F., Zuo, R., Hashimoto, Y., Yang, L., Bentley, W.E., and Wood, T.K. (**2006**). *"Autoinducer 2 controls biofilm formation in Escherichia coli through a novel motility quorum-sensing regulator (MqsR, B3022)."* J Bacteriol 188(1): 305-16.

[32] DeLisa, M.P., Wu, C.F., Wang, L., Valdes, J.J., and Bentley, W.E. (**2001**). *"DNA microarray-based identification of genes controlled by autoinducer 2-stimulated quorum sensing in Escherichia coli."* J Bacteriol 183(18): 5239-47.

[33] Schauder, S. and Bassler, B.L. (**2001**). *"The languages of bacteria."* Genes Dev 15(12): 1468-80.

[34] Miller, C.H. and Duerre, J.A. (**1968**). *"S-ribosylhomocysteine cleavage enzyme from Escherichia coli."* J Biol Chem 243(1): 92-7.

[35] Winzer, K., Hardie, K.R., Burgess, N., Doherty, N., Kirke, D., Holden, M.T., Linforth, R., Cornell, K.A., Taylor, A.J., Hill, P.J., and Williams, P. (**2002**). *"LuxS: its role in central metabolism and the in vitro synthesis of 4-hydroxy-5-methyl-3(2H)-furanone."* Microbiology 148(Pt 4): 909-22.

[36] Miller, S.T., Xavier, K.B., Campagna, S.R., Taga, M.E., Semmelhack, M.F., Bassler, B.L., and Hughson, F.M. (**2004**). *"Salmonella typhimurium recognizes a chemically distinct form of the bacterial quorum-sensing signal AI-2."* Mol Cell 15(5): 677-87.

[37] Miller, S.T., Xavier, K.B., Campagna, S.R., Taga, M.E., Semmelhack, M.F., Bassler, B.L., and Hughson, F.M. (**2004**). *"Salmonella typhimurium Recognizes a Chemically Distinct Form of the Bacterial Quorum-Sensing Signal AI-2."* Mol Cell 15(5): 677.

[38] Chen, X., Schauder, S., Potier, N., Van Dorsselaer, A., Pelczer, I., Bassler, B.L., and Hughson, F.M. (**2002**). *"Structural identification of a bacterial quorum-sensing signal containing boron."* Nature 415(6871): 545-9.

[39] Globisch, D., Lowery, C.A., McCague, K.C., and Janda, K.D. (**2012**). *"Uncharacterized 4,5-dihydroxy-2,3-pentanedione (DPD) molecules revealed through NMR spectroscopy: implications for a greater signaling diversity in bacterial species."* Angew Chem Int Ed Engl 51(17): 4204-8.

[40] Taga, M.E., Semmelhack, J.L., and Bassler, B.L. (**2001**). *"The LuxS-dependent autoinducer AI-2 controls the expression of an ABC transporter that functions in AI-2 uptake in Salmonella typhimurium."* Mol Microbiol 42(3): 777-93.

[41] Armbruster, C.E., Hong, W., Pang, B., Dew, K.E., Juneau, R.A., Byrd, M.S., Love, C.F., Kock, N.D., and Swords, W.E. (**2009**). *"LuxS promotes biofilm maturation and persistence of nontypeable haemophilus influenzae in vivo via modulation of lipooligosaccharides on the bacterial surface."* Infect Immun 77(9): 4081-91.

[42] James, D., Shao, H., Lamont, R.J., and Demuth, D.R. (**2006**). *"The Actinobacillus actinomycetemcomitans ribose binding protein RbsB interacts with cognate and heterologous autoinducer 2 signals."* Infect Immun 74(7): 4021-9.

[43] Bhardwaj, A.K., Vinothkumar, K., and Rajpara, N. (**2013**). *"Bacterial quorum sensing inhibitors: attractive alternatives for control of infectious pathogens showing multiple drug resistance."* Recent Pat Antiinfect Drug Discov 8(1): 68-83.

[44] Jiang, T. and Li, M. (**2013**). *"Quorum sensing inhibitors: a patent review."* Expert Opin Ther Pat 23(7): 867-94.

[45] Amara, N., Krom, B.P., Kaufmann, G.F., and Meijler, M.M. (**2011**). *"Macromolecular inhibition of quorum sensing: enzymes, antibodies, and beyond."* Chem Rev 111(1): 195-208.

[46] Piletska, E.V., Stavroulakis, G., Karim, K., Whitcombe, M.J., Chianella, I., Sharma, A., Eboigbodin, K.E., Robinson, G.K., and Piletsky, S.A. (**2010**). *"Attenuation of Vibrio fischeri quorum sensing using rationally designed polymers."* Biomacromolecules 11(4): 975-80.

[47] Cavaleiro, E., Duarte, A.S., Esteves, A.C., Correia, A., Whitcombe, M.J., Piletska, E.V., Piletsky, S.A., and Chianella, I. (**2015**). *"Novel linear polymers able to inhibit bacterial quorum sensing."* Macromol Biosci 15(5): 647-56.

[48] Piletska, E.V., Stavroulakis, G., Larcombe, L.D., Whitcombe, M.J., Sharma, A., Primrose, S., Robinson, G.K., and Piletsky, S.A. (**2011**). *"Passive control of quorum sensing: prevention of Pseudomonas aeruginosa biofilm formation by imprinted polymers."* Biomacromolecules 12(4): 1067-71.

[49] Melamed Yerushalmi, S., Buck, M.E., Lynn, D.M., Lemcoff, N.G., and Meijler, M.M. (**2013**). *"Multivalent alteration of quorum sensing in Staphylococcus aureus."* Chem Commun (Camb) 49(45): 5177-9.

[50] Xue, X., Pasparakis, G., Halliday, N., Winzer, K., Howdle, S.M., Cramphorn, C.J., Cameron, N.R., Gardner, P.M., Davis, B.G., Fernandez-Trillo, F., and Alexander, C. (**2011**). *"Synthetic polymers for simultaneous bacterial sequestration and quorum sense interference."* Angew Chem Int Ed Engl 50(42): 9852-6.

[51] Hook, A.L., Chang, C.Y., Yang, J., Luckett, J., Cockayne, A., Atkinson, S., Mei, Y., Bayston, R., Irvine, D.J., Langer, R., Anderson, D.G., Williams, P., Davies, M.C., and Alexander, M.R. (**2012**). *"Combinatorial discovery of polymers resistant to bacterial attachment."* Nat Biotechnol 30(9): 868-75.

[52] Junter, G.A., Thebault, P., and Lebrun, L. (**2015**). *"Polysaccharide-based antibiofilm surfaces."* Acta Biomater.

[53] Pasparakis, G., Cockayne, A., and Alexander, C. (**2007**). *"Control of bacterial aggregation by thermoresponsive glycopolymers."* J Am Chem Soc 129(36): 11014-5.

[54] Louzao, I., Sui, C., Winzer, K., Fernandez-Trillo, F., and Alexander, C. (**2015**). *"Cationic polymer mediated bacterial clustering: Cell-adhesive properties of homo- and copolymers."* Eur J Pharm Biopharm 95(Pt A): 47-62.

[55] Touaibia, M. and Roy, R. (**2007**). *"Glycodendrimers as anti-adhesion drugs against type 1 fimbriated E. coli uropathogenic infections."* Mini Rev Med Chem 7(12): 1270-83.

[56] Pieters, R.J. (**2007**). *"Intervention with bacterial adhesion by multivalent carbohydrates."* Med Res Rev 27(6): 796-816.

[57] Muñoz-Bonilla, A. and Fernández-García, M. (**2012**). *"Polymeric materials with antimicrobial activity."* Prog Pol Sci 37(2): 281-339.

[58] Appeldoorn, C.C.M., Joosten, J.A.F., Ait el Maate, F., Dobrindt, U., Hacker, J., Liskamp, R.M.J., Khan, A.S., and Pieters, R.J. (**2005**). *"Novel multivalent mannose compounds and their inhibition of the adhesion of type 1 fimbriated uropathogenic E. coli."* Tetrahedron: Asymmetry 16(2): 361-372.

[59] Sharon, N. (**2006**). *"Carbohydrates as future anti-adhesion drugs for infectious diseases."* Biochim Biophys Acta 1760(4): 527-37.

[60] Salton M., K.K. (**1996**). Structure, in S. Baron (Ed) Medical Microbiology. Galveston (TX), University of Texas Medical Branch at Galveston.

[61] Boas, U. and Heegaard, P.M. (**2004**). *"Dendrimers in drug research."* Chem Soc Rev 33(1): 43-63.

[62] Barner-Kowollik, C., Du Prez, F.E., Espeel, P., Hawker, C.J., Junkers, T., Schlaad, H., and Van Camp, W. (**2011**). *""Clicking" polymers or just efficient linking: what is the difference?"* Angew Chem Int Ed Engl 50(1): 60-2.

[63] Vögtle F., R.G., Werner N (**2009**). Dendrimer Chemistry. Weinheim, WILEY-VCH Verlag GmbH & Co.

[64] Munoz, E.M., Correa, J., Fernandez-Megia, E., and Riguera, R. (**2009**). *"Probing the relevance of lectin clustering for the reliable evaluation of multivalent carbohydrate recognition."* J Am Chem Soc 131(49): 17765-7.

[65] Mintzer, M.A., Dane, E.L., O'Toole, G.A., and Grinstaff, M.W. (**2012**). *"Exploiting dendrimer multivalency to combat emerging and re-emerging infectious diseases."* Mol Pharm 9(3): 342-54.

[66] Zhang, L., Pornpattananangku, D., Hu, C.M., and Huang, C.M. (**2010**). *"Development of nanoparticles for antimicrobial drug delivery."* Curr Med Chem 17(6): 585-94.

[67] Heegaard, P.M. and Boas, U. (**2006**). *"Dendrimer based anti-infective and anti-inflammatory drugs."* Recent Pat Antiinfect Drug Discov 1(3): 331-51.

[68] Price, C.F., Tyssen, D., Sonza, S., Davie, A., Evans, S., Lewis, G.R., Xia, S., Spelman, T., Hodsman, P., Moench, T.R., Humberstone, A., Paull, J.R., and Tachedjian, G. (**2011**). *"SPL7013 Gel (VivaGel(R)) retains potent HIV-1 and HSV-2 inhibitory activity following vaginal administration in humans."* PLoS One 6(9): e24095.

[69] Choi, S.K., Myc, A., Silpe, J.E., Sumit, M., Wong, P.T., McCarthy, K., Desai, A.M., Thomas, T.P., Kotlyar, A., Holl, M.M., Orr, B.G., and Baker, J.R., Jr. (**2013**). *"Dendrimer-based multivalent vancomycin nanoplatform for targeting the drug-resistant bacterial surface."* ACS Nano 7(1): 214-28.

[70] Pini, A., Giuliani, A., Falciani, C., Runci, Y., Ricci, C., Lelli, B., Malossi, M., Neri, P., Rossolini, G.M., and Bracci, L. (**2005**). *"Antimicrobial activity of novel dendrimeric peptides obtained by phage display selection and rational modification."* Antimicrob Agents Chemother 49(7): 2665-72.

[71] Sun, B., Slomberg, D.L., Chudasama, S.L., Lu, Y., and Schoenfisch, M.H. (**2012**). *"Nitric oxide-releasing dendrimers as antibacterial agents."* Biomacromolecules 13(10): 3343-54.

[72] Tulu, M., Aghatabay, N.M., Senel, M., Dizman, C., Parali, T., and Dulger, B. (**2009**). *"Synthesis, characterization and antimicrobial activity of water soluble dendritic macromolecules."* Eur J Med Chem 44(3): 1093-9.

[73] Imberty, A., Chabre, Y.M., and Roy, R. (**2008**). *"Glycomimetics and glycodendrimers as high affinity microbial anti-adhesins."* Chemistry 14(25): 7490-9.

[74] Nagahori, N., Lee, R.T., Nishimura, S., Page, D., Roy, R., and Lee, Y.C. (**2002**). *"Inhibition of adhesion of type 1 fimbriated Escherichia coli to highly mannosylated ligands."* Chembiochem 3(9): 836-44.

[75] Salminen, A., Loimaranta, V., Joosten, J.A., Khan, A.S., Hacker, J., Pieters, R.J., and Finne, J. (**2007**). *"Inhibition of P-fimbriated Escherichia coli adhesion by multivalent galabiose derivatives studied by a live-bacteria application of surface plasmon resonance."* J Antimicrob Chemother 60(3): 495-501.

[76] Kouki, A., Pieters, R.J., Nilsson, U.J., Loimaranta, V., Finne, J., and Haataja, S. (**2013**). *"Bacterial Adhesion of Streptococcus suis to Host Cells and Its Inhibition by Carbohydrate Ligands."* Biology 2(3): 918-935.

[77] Johansson, E.M., Crusz, S.A., Kolomiets, E., Buts, L., Kadam, R.U., Cacciarini, M., Bartels, K.M., Diggle, S.P., Camara, M., Williams, P., Loris, R., Nativi, C., Rosenau, F., Jaeger, K.E., Darbre, T., and Reymond, J.L. (**2008**). *"Inhibition and dispersion of Pseudomonas aeruginosa biofilms by glycopeptide dendrimers targeting the fucose-specific lectin LecB."* Chem Biol 15(12): 1249-57.

[78] Kadam, R.U., Bergmann, M., Hurley, M., Garg, D., Cacciarini, M., Swiderska, M.A., Nativi, C., Sattler, M., Smyth, A.R., Williams, P., Camara, M., Stocker, A., Darbre, T., and Reymond, J.L. (**2011**). *"A glycopeptide dendrimer inhibitor of the galactose-specific lectin LecA and of Pseudomonas aeruginosa biofilms."* Angew Chem Int Ed Engl 50(45): 10631-5.

[79] Kolomiets, E., Johansson, E.M., Renaudet, O., Darbre, T., and Reymond, J.L. (**2007**). *"Neoglycopeptide dendrimer libraries as a source of lectin binding ligands."* Org Lett 9(8): 1465-8.

[80] Zhisheng Chen, C., L. Cooper, S., and C. Beck Tan, N. (**1999**). *"Incorporation of dimethyldodecylammonium chloride functionalities onto poly(propylene imine) dendrimers significantly enhances their antibacterial properties."* ChemComm(16): 1585-1586.

[81] Chen, C.Z., Beck-Tan, N.C., Dhurjati, P., van Dyk, T.K., LaRossa, R.A., and Cooper, S.L. (**2000**). *"Quaternary Ammonium Functionalized Poly(propylene imine) Dendrimers as Effective Antimicrobials: Structure−Activity Studies."* Biomacromolecules 1(3): 473-480.

[82] Rasines, B., Hernandez-Ros, J.M., de las Cuevas, N., Copa-Patino, J.L., Soliveri, J., Munoz-Fernandez, M.A., Gomez, R., and de la Mata, F.J. (**2009**). *"Water-stable ammonium-terminated carbosilane dendrimers as efficient antibacterial agents."* Dalton Trans(40): 8704-13.

[83] Ortega, P., Copa-Patino, J.L., Munoz-Fernandez, M.A., Soliveri, J., Gomez, R., and de la Mata, F.J. (**2008**). *"Amine and ammonium functionalization of chloromethylsilane-ended dendrimers. Antimicrobial activity studies."* Org Biomol Chem 6(18): 3264-9.

[84] Xue, X., Chen, X., Mao, X., Hou, Z., Zhou, Y., Bai, H., Meng, J., Da, F., Sang, G., Wang, Y., and Luo, X. (**2013**). *"Amino-terminated generation 2 poly(amidoamine) dendrimer as a potential broad-spectrum, nonresistance-inducing antibacterial agent."* Aaps j 15(1): 132-42.

[85] Lopez, A.I., Reins, R.Y., McDermott, A.M., Trautner, B.W., and Cai, C. (**2009**). *"Antibacterial activity and cytotoxicity of PEGylated poly(amidoamine) dendrimers."* Mol Biosyst 5(10): 1148-56.

[86] Wang, L., Erasquin, U.J., Zhao, M., Ren, L., Zhang, M.Y., Cheng, G.J., Wang, Y., and Cai, C. (**2011**). *"Stability, antimicrobial activity, and cytotoxicity of poly(amidoamine) dendrimers on titanium substrates."* ACS Appl Mater Interfaces 3(8): 2885-94.

[87] Xue, X.Y., Mao, X.G., Li, Z., Chen, Z., Zhou, Y., Hou, Z., Li, M.K., Meng, J.R., and Luo, X.X. (**2015**). *"A potent and selective antimicrobial poly(amidoamine) dendrimer conjugate with LED209 targeting QseC receptor to inhibit the virulence genes of gram negative bacteria."* Nanomedicine 11(2): 329-39.

[88] Curtis, M.M., Russell, R., Moreira, C.G., Adebesin, A.M., Wang, C., Williams, N.S., Taussig, R., Stewart, D., Zimmern, P., Lu, B., Prasad, R.N., Zhu, C., Rasko, D.A., Huntley, J.F., Falck, J.R., and Sperandio, V. (**2014**). *"QseC inhibitors as an antivirulence approach for Gram-negative pathogens."* MBio 5(6): e02165.

[89] Lowery, C.A., Abe, T., Park, J., Eubanks, L.M., Sawada, D., Kaufmann, G.F., and Janda, K.D. (**2009**). *"Revisiting AI-2 quorum sensing inhibitors: direct comparison of alkyl-DPD analogues and a natural product fimbrolide."* J Am Chem Soc 131(43): 15584-5.

[90] Garner, A.L., Park, J., Zakhari, J.S., Lowery, C.A., Struss, A.K., Sawada, D., Kaufmann, G.F., and Janda, K.D. (**2011**). *"A multivalent probe for AI-2 quorum-sensing receptors."* J Am Chem Soc 133(40): 15934-7.

[91] Kolb, H.C., Finn, M.G., and Sharpless, K.B. (**2001**). *"Click Chemistry: Diverse Chemical Function from a Few Good Reactions."* Angew Chem Int Ed Engl 40(11): 2004-2021.

[92] Hein, J.E. and Fokin, V.V. (**2010**). *"Copper-catalyzed azide-alkyne cycloaddition (CuAAC) and beyond: new reactivity of copper(i) acetylides."* Chem Soc Rev 39(4): 1302-1315.

[93] Sashiwa, H., Shigemasa, Y., and Roy, R. (**2001**). *"Chemical Modification of Chitosan. 10.1 Synthesis of Dendronized Chitosan−Sialic Acid Hybrid Using Convergent Grafting of Preassembled Dendrons Built on Gallic Acid and Tri(ethylene glycol) Backbone."* Macromolecules 34(12): 3905-3909.

[94] Meunier SJ., W.Q., Wang S-N., Roy R. (**1997**). *"Synthesis of hyperbranched glycodendrimers incorportaing alpha-thiosialosides based on gallic acid core. ."* Can J Chem 75(11): 1472-82.

[95] Sousa-Herves, A., Novoa-Carballal, R., Riguera, R., and Fernandez-Megia, E. (**2014**). *"GATG dendrimers and PEGylated block copolymers: from synthesis to bioapplications."* Aaps j 16(5): 948-61.

[96] Albertazzi, L., Fernandez-Villamarin, M., Riguera, R., and Fernandez-Megia, E. (**2012**). *"Peripheral functionalization of dendrimers regulates internalization and intracellular trafficking in living cells."* Bioconjug Chem 23(5): 1059-68.

[97] de la Fuente, M., Ravina, M., Sousa-Herves, A., Correa, J., Riguera, R., Fernandez-Megia, E., Sanchez, A., and Alonso, M.J. (**2012**). *"Exploring the efficiency of gallic acid-based dendrimers and their block copolymers with PEG as gene carriers."* Nanomedicine (Lond) 7(11): 1667-81.

2. Material and Methods

2.1 CHEMICALS

All reagents were of analytical grade and used as received except where otherwise stated. 2-Butyne-1,4-diol was purchased from Sigma-Aldrich and was recrystallized in ethyl acetate. Triphenylphosphine (PPh_3) was purchased from Aldrich and was recrystallized in EtOH. Phosphate-buffered saline (PBS) (Dulbecco A) was purchased from Oxoid. 4,5-Dihydroxy-2,3-pentandione (DPD) was purchased from Ommscientific®. Amberlite IR-120 cationic exchange resin (Sigma-Aldrich) was washed with DCM (50 mL), MeOH (50 mL) and H_2O (50mL) prior to use. Baclight™ Bacterial Viability kit (Life technologies L32856) was used for fluorescent live/dead staining for flow cytometry. All other chemicals were purchased from Sigma-Aldrich or Acros and were used without further purification. All solvents were HPLC grade, purchased from Fisher Scientific or Sigma-Aldrich and used without further purification. Water was of Milli-Q grade.

2.2. INSTRUMENTATION

Coulter Particle Size Analyser

Sizes of bacterial clusters were measured on Coulter LS230 particle size analyser (Beckman Coulter, High Wycombe, USA) using laser diffraction.

DLS

Dendrimer hydrodynamic diameter were measured by Dynamic Light Scattering (DLS) on a Nano-s Zetasizer (Malvern Instruments Ltd) at 25 °C in 10 mM NaH_2PO_2 with 10% HCl 0.1 M or in 0.15 M LiCl solutions. Samples were measured at 1 mg/mL concentration.

ESI-FIA-TOF Mass Spectrometry

Electrospray Ionization (ESI) Flow injection Analysis (FIA) Time-of-flight (TOF) mass spectrometry was carried out on Tandem HPLC (Agilent 1100)-MS (Bruker Microtof) by the RIAIDT service, University of Santiago de Compostela. Source ESI was equipped with gas flow counter current of 1 μL/min under temperature control.

Flow Cytometry

Flow Cytometry was performed on a BD LSRII Flow Cytometer.

Fluorimeter

Labelling of G3-N_3 dendrimer with MCCA fluorophore was confirmed with Varian Cary Eclipse fluorescence spectrophotometer.

Infrared spectroscopy

Fourier Transformed Infrared Spectroscopy (FT-IR) spectra were recorded on a Bruker IFS-66v using KBr pellets or neat samples (CsI window)

MALDI-TOF Mass Spectrometry (MS)

MALDI-TOF MS of the dendrimers at the azide stage were performed on a 4800 MALDI-TOF/TOF analyzer (Applied Biosystems) by RIAIDT service, University of Santiago de Compostela. Samples were dissolved in MeOH supplemented with NaCl as cationizing agent, and 2-(4-hydroxyphenylazo)benzoic acid (HABA) or 2,5-dihydroxybenzoic acid (DHB) as matrices. Mass spectrometry of the G3-N_3 dendrimer did not yield good quality MALDI spectra, which could have been due to the high molar mass of the dendrimer.

Microscopy

L3001 Epifluorescent Microscope was used for optical imaging. Zeiss LSM 880 confocal laser microscopy was used for fluorescent microscopy imaging.

NMR

Nuclear Magnetic Resonance (NMR) spectra were recorded on a Varian Mercury 300 MHz, Varian Innova 500 or Varian NMR Innova 750 MHz spectrometers. Chemical shifts are reported in ppm (δ units) downfield from solvent peak (D_2O, d6-DMSO, MeOD or $CDCl_3$).

Size Exlusion Chromatography (SEC)

All Size Exclusion Chromatography (SEC) was performed using an Agilent 1100 series separation module with an Agilent 1100 series UV-detector using a PSS SDV pre-column (5 μm, 8 x 50 mm), a PSS SDV Linear S column (5 μm, 8 x 300 mm) for dendrimers with terminal azides, and a PSS SDV Lux Linear

M column (5 μm, 8 x 300 mm) or Suprema Lux 100A and Suprema pre-column for aqueous soluble AAC-functionalised dendrimers. SEC for Gn-N_3 dendrimers were performed with THF as the eluent at 1 mL/min and filtered through 0.45 μm before injection. For AAC-functionalized dendrimers the SEC was performed in 150 mmol LiCl at 1 mL/min and filtered through 0.45 μm before injection

Tecan Reader

Luminescence and OD_{600} were measured in a Tecan Infinite Pro 200 Reader.

TLC

Thin-layer chromatography (TLC) was done on silica 60/F-254 aluminium-backed plates (E. Merck) in appropriate solvent mixture.

Ultrafiltrator

Ultrafiltration was performed on Amicon stirred cells with Amicon YM1, YM3, and YM5 membranes.

2.3 METHODS

2.3.1 Synthesis

General purification methods

When aqueous workups were implemented, organic layers were dried with anhydrous Na_2SO_4 followed by filtration in sintered funnel pore size 2. Automated column chromatography was performed with 70-230 mesh silica from Merck automated column chromatographic purification was performed on a MPLC Teledyne ISCO CombiFlash RF – 200 psi with a RediSepRf normal-phase 12 g silica columns, unless otherwise stated.

Protocol 1. General method for the synthesis of GATG dendrimers

The synthesis of the repeating unit of GATG dendrimers in large scale has been reported by our group [1] and was previously prepared in-house.

Gn-N_3. Dried Et_3N (3 equiv. per NH_2) was added under argon to a stirred solution of Gn-NH_2·HCl in MeCN (0.1 M per NH_2) and heated at 60 ºC during 1 h or until the contents of the reaction vessel were completely soluble. The solution was left to reach room temperature and then GATG repeating unit (R.U.) (1.25 equiv. per NH_2), HOBt (1.25 equiv. per NH_2) and EDC.HCl (1.25 equiv. per NH_2) were added sequentially. After 12 h of stirring, the solvent was concentrated and the mixture was dissolved in dichloromethane (DCM) and washed with H_2O (3x). The organic layer was dried ($MgSO_4$) and concentrated

to give a crude product that was purified by automated Medium Pressure Liquid Chromatography (MPLC) (eluent gradient from hexane to EtOAc/MeOH 30% in neutral oxide alumina column and basic oxide alumina solid cartridge, 10 min) to afford the pure product.

Gn-NH_2. PPh_3 (1.25 equiv. per N_3) was added to a solution of Gn-N_3 in MeOH/$CHCl_3$/H_2O 5:5:1 (0.1 M per N_3). The mixture was stirred at room temperature for 6h. After the addition of a 3 M aq. HCl solution (2 equiv. per NH_2) the solvent was evaporated. The crude product was dissolved in H_2O and filtrated through cotton. Then, it was washed with DCM (3 x) and lyophilized to give pure Gn-NH_2. The complete disappearance of the azide band in FT-IR at 2100 cm^{-1} as well as the disappearance of the CH_2N_3 signal in the ^1H NMR spectrum confirmed the completion of the reaction.

Protocol 2. General method for the conjugation of alkynated ligands to GATG–N_3 dendrimers through Thermal Azide-Alkyne Cycloaddition

Dendrimer and alkynated ligand (2 equiv. per N_3) were added to a small Schlenk-tube flask. tBuOH/H_2O (1:1) was added to a final concentration of 2M per N_3. The reaction tube was sealed and heated at 110°C. Reaction was monitored by IR until full conjugation was achieved (no N_3 signal was visible). Functionalized dendrimers were purified by ultrafiltration in H_2O in Amicon stirred cells with Amicon YM1, YM3 and YM5 membranes.

2.3.2 *In Vitro* Experiments

Bacterial strains and growth conditions

V. harveyi BB170 [2] and MM32 [3] were gifts from Bonnie Bassler (Department of Molecular Biology, Princeton University). Both strains were grown from frozen stock on LB agar plates containing 50 μg/mL kanamycin. Bacteria were incubated overnight at 30 °C.

Protocol 3. Boron depletion assay and preparation of AB medium

Boron-depleted Autoinducer Bioassay (AB) Medium previously described [3, 4] was used for the luminescence assay and was prepared following previously reported conditions.

Protocol 4. Luminescence/OD assay

A single colony of *V. harveyi* from LB agar plates was used to inoculate 2 mL LB medium containing 50 μg/mL kanamycin and incubated overnight at 30°C. Bacteria was diluted to Optical density 600 (OD_{600}) = 1.0 in boron-depleted AB medium and then inoculated in the same medium (5000:1). For MM32 boric acid was added to a final concentration of 400 μM, and DPD added to a final concentration of 22 μM. For BB170 boric acid was added to a final concentration of 22 μM. Since MM32 is not able to produce DPD, this way the limiting concentration for formation of S-THMF-borate induced luminescence is 22 μM for both bacterial strains. Dendrimer stock solutions were prepared in dH_2O with a concentration 10 times higher than final concentration. Selected dendrimers (20 μl of stock solutions) were incubated with 180 μL of bacteria

suspension (~10^4 CFU/mL) in a 96-well plate and mixed well. Light production and OD_{600} were recorded at 30 °C every 30 min for at least 10h in a 96-well plate. For MM32 a 96-well plate was incubated for 2 h at 30 °C prior to recording. Each compound was tested over at least 3 different concentrations; each concentration was run in triplicates. Experiment was repeated at least twice. For MM32, the magnitude of the value for the luminescence in the presence of dendrimers was divided by the magnitude of the value for luminescence for bacteria alone for 4 h, 8 h, 12 h and 16 h in order to present the relative luminescence. For BB170, the time (in 30 min intervals) to reach initial light production after decay phase (*Figure 4.7*) was presented as recovery time. Calculations for relative luminescence and recovery time were conducted for each individual sample.

Protocol 5. Clustering assay with particle size diffraction analyser

A single colony of *V. harveyi* from LB agar plates was used to inoculate 2 mL LB medium containing 50 μg/mL kanamycin and incubated overnight at 30°C. Bacteria were centrifuged at 9000 rpm for 5 min at 4°C, the supernatant was discarded and bacteria re-suspended in PBS. This washing step was repeated 2 times and bacteria were finally re-suspended at OD_{600} = 1.0 and passed through a 5 μm filter. Aliquots of the bacteria culture were mixed with known volumes of stock solutions of dendrimer in dH_2O. The values of the dendrimer concentrations reported correspond to the final concentration in the bacteria-suspension. The suspension was added to the flow cell filled with H_2O (<14 mL) at medium stirring (setting 5-6) to the required optical obstruction indicated by the built-in software (8-12%, between 500-1500 μL). Particle size

ranges were defined using PSS-Duke standards (Polymer Standard Service), Kromatek Ltd., Dunmow, UK). Particle size or cluster size distribution was determined as a function of the particle diffraction using the Coulter software (version 2.11) and plotted as a function of the percentage of distribution volume. Cluster size was measured in triplicates at each time point. Experiments were repeated three times.

Protocol 6. Microscopy

Aliquots (10 μL) of dendrimer-bacteria suspension used for measuring cluster size at the final time point (60 min) for each sample were mounted on a glass slip with a cover slip for optical and microscopy imaging. For confocal microscopy, 10 μL G3-NH_2-MCCA was added to 90 μL bacterial suspension in Phosphate buffer saline (PBS) (same as above) and incubated for 60 min. SYTO9 stain (1 μL of 0.033 mM solution in Dimethyl sulfoxide (DMSO)) was then added to the sample and incubated in the dark for 10 min at room temperature prior to imaging. For SYTO9; λ_{exc} = 488nm and λ_{em} = 522nm, for MCCA; λ_{exc} = 405nm and λ_{em} = 460nm.

Protocol 7. Colony Forming Unit (CFU) assay

A single colony of *V. harveyi* from Lyosgen Broth (LB)-agar plates was used to inoculate 2 mL LB medium containing 50 μg/mL kanamycin and incubated overnight at 30 °C. Bacteria were diluted to OD_{600} = 1.0 in boron-depleted AB medium and then inoculated in the same medium (5000:1). Boric acid was added to a final concentration of 22 μM. An aliquot (180 μL) of the inoculated AB medium was added to each well of a 96-well plate and mixed with 20μL of

the sample to be analysed. For each indicated time point, 20 μL sample was removed from each well and serial diluted in PBS. A sample (20 μL) of each dilution was plated in triplicates on LB-agar plates containing 50 μg/mL kanamycin. Plates were incubated over night at 30 °C and the number of colonies was counted the following day.

Protocol 8. Membrane Permeability using Flow Cytometry

A single colony of *V. harveyi* from LB agar plates was used to inoculate 2 mL LB medium containing 50 μg/mL kanamycin and incubated overnight at 30°C. Bacteria were centrifuged at 9000 rpm for 5 min, supernatant was discarded and bacteria were re-suspended in AB medium or PBS at OD_{600} = 1.0. For membrane permeability during aggregation assay in PBS; 90 μL of the bacteria culture was added to 10 μL of stock solutions of dendrimer in dH_2O or dH_2O alone (control) and incubated for 1 h at room temperature. A mixture (1 μL) of SYTO9 stain (0.033 mM in DMSO) and Propidium Iodide (20 mM in DMSO) (PI) 1:1.5 was added to each sample and incubated in the dark for 10 min at room temperature prior to experiment. For membrane permeability during luminescence experiment; bacteria were diluted 5000-fold in AB medium. 90 μL bacteria in AB medium was mixed with 10 μL of stock solutions of dendrimer in dH_2O or d H_2O alone (control). The bacteria-dendrimer mixture was incubated at 30 °C for 10 h thereafter centrifuged for 5 min at 9000 rpm and re-suspended in 500 μL of 0.85% NaCl. As before, 1 μL of a mixture of SYTO9 stain (0.033 mM in DMSO): PI (200 mM in DMSO) 1:1 was added to each sample and incubated in the dark for 10 min at room temperature prior to experiment. The negative control was incubated with 70% i-PrOH for 1 h

followed by 2 washes with media (centrifugation 10 000 rpm, 5 min, room temperature). Bacteria were counted in Flow Cytometer (BD LSRII Flow Cytometer), 100 000 events per sample were counted. The values of the dendrimer concentrations reported correspond to the final dendrimer concentration in the bacterial suspension. Each condition was done in triplicate and the experiment was repeated three times. Data were analysed using Kaluza® Flow Analysis Software (Beckman Coulter Inc.)

2.4 REFERENCES

[1] Amaral, S.P., Fernandez-Villamarin, M., Correa, J., Riguera, R., and Fernandez-Megia, E. (**2011**). *"Efficient multigram synthesis of the repeating unit of gallic acid-triethylene glycol dendrimers."* Org Lett 13(17): 4522-5.

[2] Bassler, B.L., Wright, M., Showalter, R.E., and Silverman, M.R. (**1993**). *"Intercellular signalling in Vibrio harveyi: sequence and function of genes regulating expression of luminescence."* Mol Microbiol 9(4): 773-86.

[3] Miller, S.T., Xavier, K.B., Campagna, S.R., Taga, M.E., Semmelhack, M.F., Bassler, B.L., and Hughson, F.M. (**2004**). *"Salmonella typhimurium recognizes a chemically distinct form of the bacterial quorum-sensing signal AI-2."* Mol Cell 15(5): 677-87.

[4] Greenberg, E.P., Hastings, J.W., and Ulitzur, S. (**1979**). *"Induction of luciferase synthesis in Beneckea harveyi by other marine bacteria."* Arc Microbiol 120(2): 87-91.

3. Synthesis and characterisation of functionalized GATG Dendrimers

3.1 INTRODUCTION

The active form of AI-2 recognized by *V. harveyi* is the furanosyl borate (S-THMF borate) formed when DPD complexes with borate in the marine environment (*Figures 1.3, 3.1*) [1-3]. Boric/boronic acids bind strongly to molecules containing diol moieties, through reversible ester formation. Thus, for control of AI-2 activity, a diol moiety could be used to bind the borate in the medium and thereby inhibit the formation of S-THMF borate (*Figure 3.2*) [4].

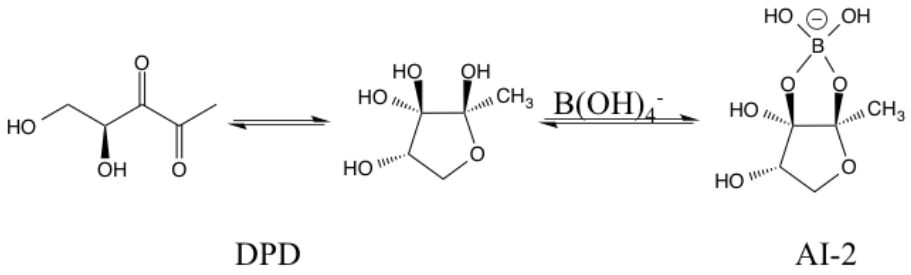

Figure 3.1 Structures of DPD and the S.THMF-borate (AI-2) formed in the presence of boric acid. Figure adapted from reference [5].

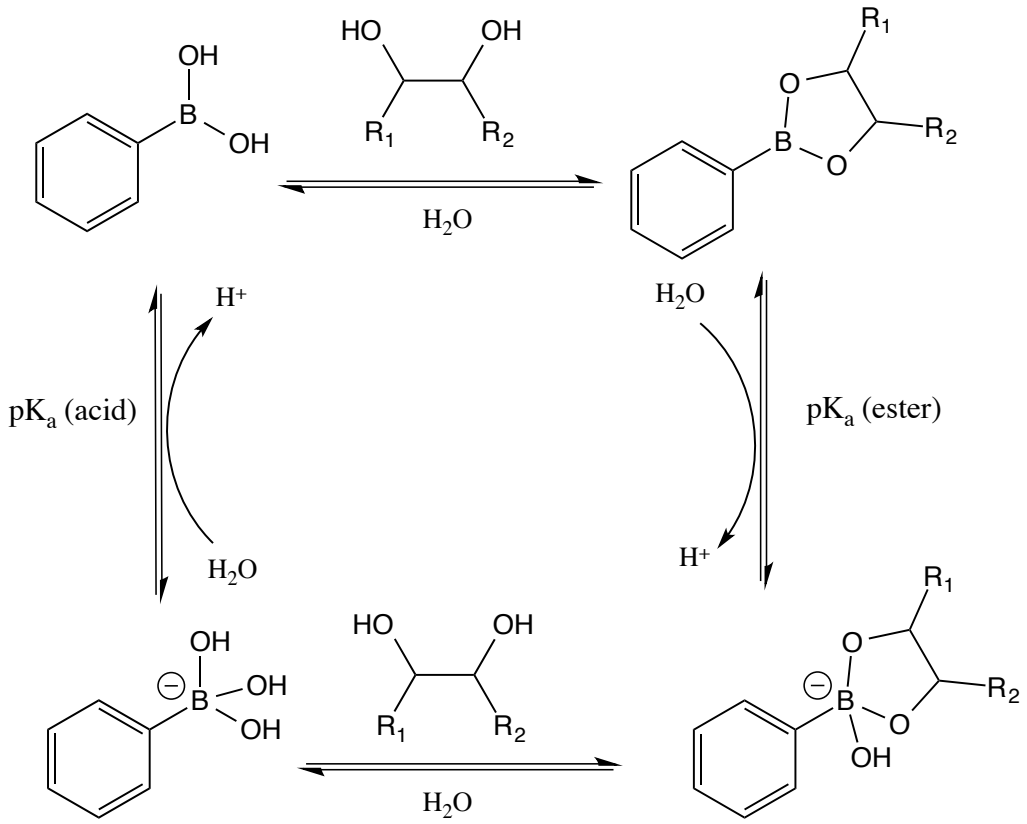

Figure 3.2 Equilibrium involved in diol exchange with phenylboronic acid and formation of the esters. Figure adapted from reference [6].

The affinity for boronates by different diol moieties were investigated by Xue and colleagues with the aim to design synthetic polymers decorated with diols for quenching of AI-2 by high affinity binding to the boric acid in the media [7]. They found the affinity to be in the following order: linear diols (polyvinyl alcohol) < cyclic diols (sugars) < aromatic diols (catechol). The synthetic polymers containing carbohydrate and catechol moieties were both able to quench QS signalling in *V. harveyi* MM32. The study presented here was aimed to prepare dendrimers functionalized with different diols, mimetic of the polymers previously reported by Xue and colleagues [7] for quorum quenching of AI-2 in *V.harveyi*, but with the potential for finer control of QS activity, as

the dendritic arcitecture enables more precise control over the relative number and position of the functional groups compared to polymers.

As outlined in Chapter 1, AAC offers a possibility for the efficient formation of triazole linkages from azides and alkynes. The synthesis of ligands with internal alkynes instead of terminal, results in two functional groups per azide, converting the triazole in the branching point of the dendrimer, and in doing so increases the multivalency of the dendrimer two-fold compared to ligands with terminal alkynes *(Figure 3.3)*.

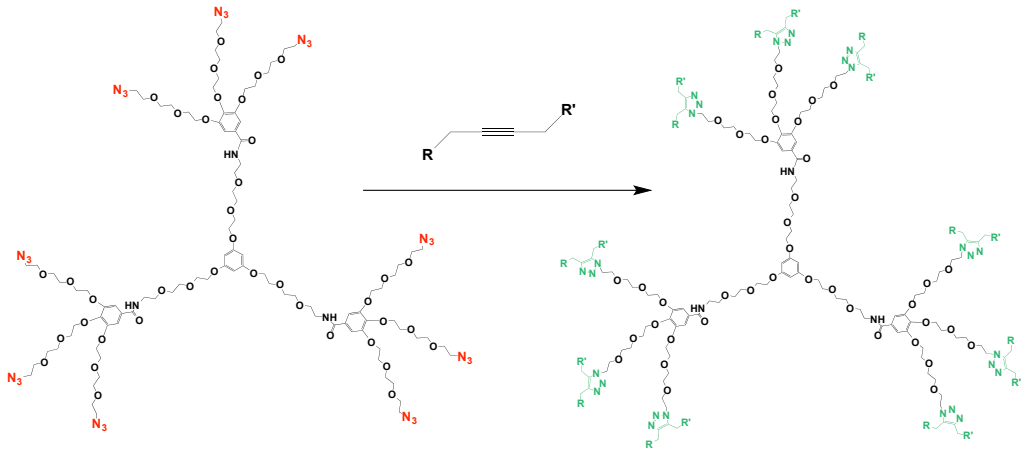

Figure 3.3 Functionalization of dendrimers with terminal azides through AAC with alkynated ligand.

Using metals such as Cu(I) as catalyst for the AAC (named CuAAC), can lead to difficulties in getting pure final products and even small traces of the metal can be toxic and influence bioactivities [8, 9]. To avoid this, the aim was to functionalise the dendrimers using catalyst-free thermal reactions. In contrast to CuAAC, thermal AAC allows for a cycloaddition with an internal alkyne.

AAC reactions using traditional heating methods can take several days depending on how activated the triple-bond of the reactant is and the conditions of the reaction [10]. In order to develop a faster and clean thermal AAC, our initial strategy was to use microwave-assisted AAC. The main advantage with using this approach is the decrease in reaction time. Although it is generally accepted now that most reported examples rely on thermal microwave effects (bulk thermal phenomena), there are also examples of non-thermal microwave effects associated to the orientation of dipolar molecules in the presence of electric field [11]. It was intended to exploit the dipolar nature of the AAC reaction in this context.

The first aim of this chapter was to synthesise alkynated ligands with diol moieties for the quenching of AI-2 and develop a method for their fast, efficient and reliable catalyst-free AAC conjugation to dendrimers of various generations.

Another strategy for the inhibition of AI-2 is to mimic the boronic acid binding to DPD and to quench the active form of AI-2 for *V. harveyi* (S-THMF-borate, *Figure 3.1*). Ni and colleagues evaluated a library with boronic acid derivatives for the inhibition of luminescence in *V. harveyi* MM32 and found five candidates with IC_{50} values in the single micro molar range [12]. They shared some common features; they were all phenylboronic acids with low pK_a and without ionisable functional groups (amine or carboxyl groups). The second aim of this chapter was to decorate dendrimers with phenylboronic acids that could quench the AI-2 by targeting the DPD molecule (*Chapter 1, Figure 1.4*).

In addition, cationic dendrimers of different generation were synthesised for the investigation of bacterial clustering through electrostatic interactions.

3.2 EXPERIMENTS

3.2.1 SYNTHESIS OF LIGANDS

Alkynated ligands with different diol moieties were synthesised (diol, tetraol, glucose and mannose) (*Figure 3.4*). All final ligands were characterized by MALDI-TOF Mass Spectrometry, ^{1}H and ^{13}C-NMR and Infrared Spectroscopy and have not been previously reported in the literature.

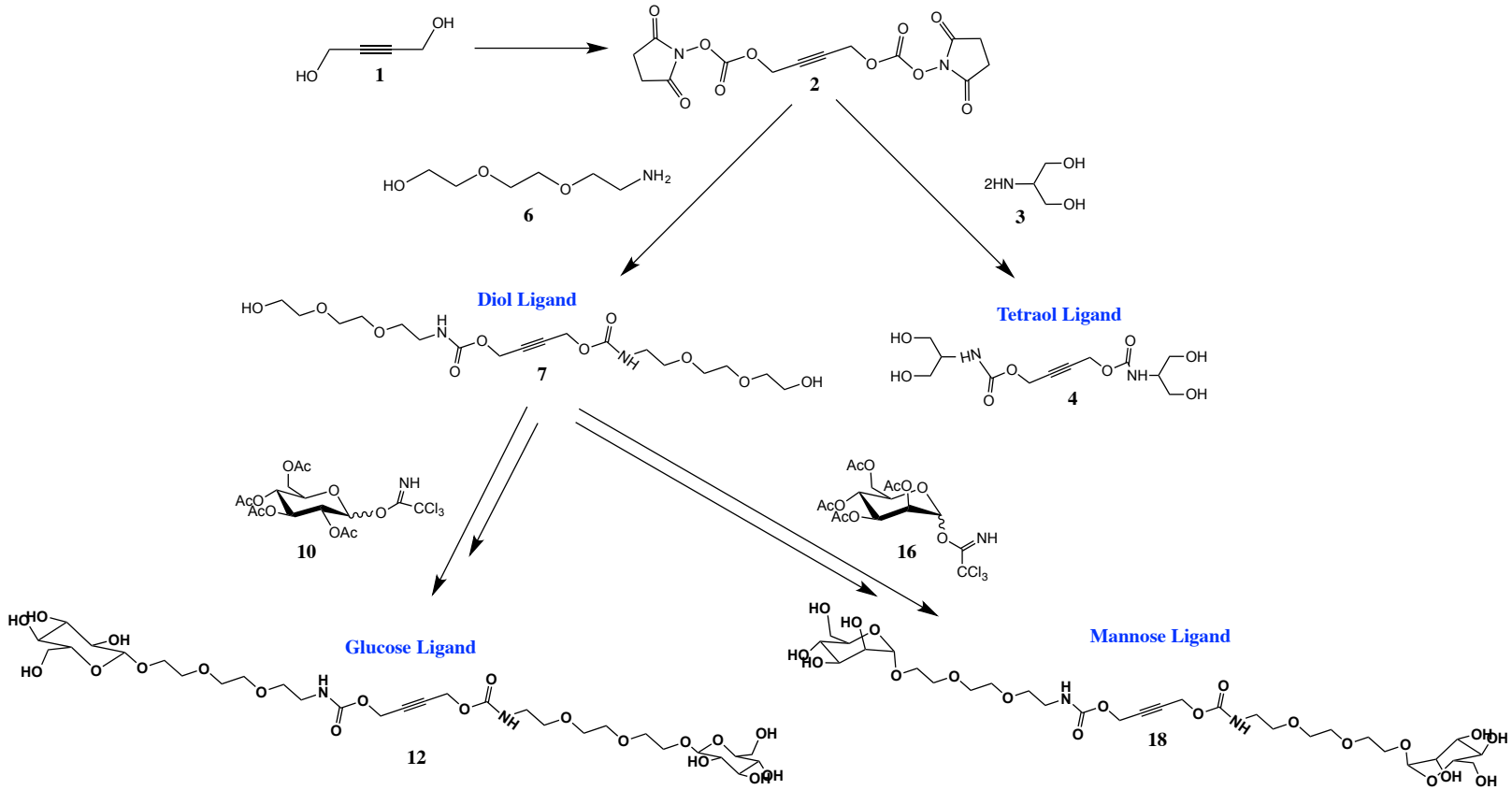

Figure 3.4 Synthesis of Tetraol (**4**), Diol, (**7**), Glucose (**12**) and Mannose (**18**) ligands.

3.2.1.1 Synthesis of Tetraol Ligand (4)

But-2-yne-1,4-diyl bis(2,5-dioxopyrrolidin-1-yl) bis(carbonate) (**2**)

2-Butyne-1,4-diol (**1**) (1.0 g, 0.012 mol) was dissolved in dry MeCN (36 mL). DSC (5.95 g, 0.023 mol) and dry pyridine (1,9 mL, 0.023 mol) were added and the reaction was left under argon at room temperature overnight. After evaporation, the product was partitioned between 1M HCl (60 mL) and EtOAc (90 mL). The organic phase was washed with 1M HCl (60 mL), H_2O (3 x 60 mL) and brine (60 mL). Then, it was dried and concentrated to afford **2** as a white solid (3.83 g, 90 %)

^{1}H-NMR (300 MHz, DMSO) δ_H 5.21 (s, 4H) 2.81 (s, 8H). ^{13}C-NMR (75 MHz, DMSO) δ_C 169.8, 150.9, 81.6, 58.4, 25.4 ESI-MS m/z 391.04 [M + Na^+] MS Calculated for $C_{14}H_{12}N_2NaO_{10}$ (M + Na^+): 391.0384, found 391.0387.

But-2-yne-1,4-diyl bis((1,3-dihydroxypropan-2-yl)carbamate) (**4**)

Active carbonate **2** (1.23 g, 3.34 mmol) was dissolved in dry MeCN (67 mL). Serinol (**3**) (1.83 g, 20.02 mmol) and dry Et_3N (2.8 mL, 20.0 mmol) were added and reaction was left stirring argon at room temperature overnight. After evaporation under reduced pressure, the crude product was purified by column chromatography (Combiflash silica, DCM/MeOH, 0-20% MeOH) to obtain **4** as a white solid (0.72 g, 68%).

^{1}H-NMR (300 MHz, CD_3OD), δ_H 4.70 (s, 4H), 3.68-3.55 (m, 10H). ^{13}C-NMR (75 MHz, CD_3OD) δ_C 157.8, 80.1, 62.2, 59.1, 53.2. ESI-MS m/z 343.11 [M + Na^+], MS Calculated for $C_{12}H_{20}N_2NaO_8$ [M + Na^+]: 343.1112, found 343.1106. IR (MeOH) ν_{max} 3331, 1704, 1544, 1269, 1038 cm^{-1}.

3.2.1.2 Synthesis of Diol Ligand (7)

2-(2-(2-azidoethoxy)ethoxy)ethan-1-ol (**5**) was synthesized previously in the group, following a one-step procedure from 2-(2-(2chloroethoxy)ethoxy)ethan-1-ol [13] (*Figure 3.8*).

2-(2-(2-aminoethoxy)ethoxy)ethan-1-ol (**6**)

Azide **5** was hydrogenated (hydrogen atmosphere) with H_2 over PdC in dry MeOH according to a previous published protocol [14] as follows: compound **5** (2.38 g, 13.59 mmol) was dissolved in MeOH (45 mL). Air was replaced with argon bubbled through the solution for 10 min. Pd/C (10%) (0.48g) was added to reaction. Argon was replaced with H_2. After 24h of stirring, NMR showed complete hydrogenation. H_2 was replaced with argon. The reaction contents were filtered over celite and MeOH was evaporated under reduced pressure to afford amino-alcohol **6** as a colourless oil (2.03 g, 100%).

But-2-yne-1,4-diyl bis((2-(2-(2-hydroxyethoxy)ethoxy)ethyl)carbamate) (**7**)

Aminoalcohol **6** (1.0 g, 6.83 mmol) was dissolved in dry DCM (5.7 mL). Dry Et_3N (0.95 mL, 6.83 mmol) was added and the mixture was left to stir under argon for 10 min. Then, active carbonate **2** (0.42 mg, 1.14 mol) was added and reaction was left stirring under argon at room temperature overnight. The solvent was evaporated under reduced pressure and crude product was purified by column chromatography (Combiflash silica, DCM/MeOH, 0-10% MeOH) to give **7** as a clear oil (0.45 g, 90%).

^{1}H-NMR (300 MHz, $CDCl_3$), δ_H 4.69 (s, 4H) 3.73-3.70 (m, 4H), 3.63-3.53 (m, 16H), 3.37-3.32 (m, 4H). ^{13}C-NMR (75MHz, $CDCl_3$) δ_C 155.7 , 81.1, 72.6, 70.7, 70.2, 69.9, 61.4, 52.5, 40.8. ESI-MS m/z MS Calculated for $C_{18}H_{32}N_2NaO_{10}$ [M + Na^+]: 459.1949, found 459.1950. IR (MeOH) ν_{max} 3331, 2875, 1703, 1536, 1252, 1098 cm^{-1}.

3.2.1.3 Synthesis of Glucose Ligand

The glucose-ligand with an internal alkyne was synthesised following a two-step procedure from glucose-trichloroacetimidate [15] (**10**) and diol **7**. D-glucose pentaacetate was mono-deprotected as described in the literature [16] to gain **9**, Subsequent elaboration of **9** (1.2 g, 3.4 mmol) as described in literature [15], afforded the glucose-trichloroacetimidate **10.**

2-(acetoxymethyl)-6-hydroxytetrahydro-2H-pyran-3,4,5-triyl triacetate (**9**)
Compound **8**, (5.0 g, 12.0 mmol) was dissolved in THF (60 mL) under argon. $BnNH_2$ (2.1 mL, 19.2 mmol) was added and reaction was left to stir at room temperature for 14h. The solvent was evaporated under reduced pressure and the product was partitioned between 1M HCl (60 mL) and DCM (90 mL). The organic phase was washed with 1M HCl (3 x 60 mL), H_2O (4 x 60 mL) and brine (60 mL). After the crude product was dried and concentrated the product was purified by column chromatography (Combiflash silica with hexane/EtOAc 10-50% EtOAc) to give **9** (3.5 g, 78%) as white solid.

^{1}H NMR (300 MHz, DMSO-d_6) δ: 6.17 (d, *J* = 3.7 Hz, 1H) 5.34 (t,1H), 5.08 (t, 1H), 5.01 (d, 1H), 4.17 (d, 2H), 4.07 – 3.93 (m, 1H), 2.01 (s, 3H), 2.00 (s, 3H), 1.99(s, 3H), 1.98(s, 3H).

2-(acetoxymethyl)-6-(2,2,2-trichloro-1-iminoethoxy)tetrahydro-2H-pyran-3,4,5-triyl triacetate (**10**)

Compound **9** (1.2 g, 3.4 mmol) was dissolved in DCM (14 mL) under argon. Trichloroacetonitrile (2.1 mL, 20.5 mmol) was added and then reaction was cooled to 0 °C with an ice bath and left for 15 min. DBU (0.26 mL, 1.7 mmol) was added drop wise and reaction was left to stir in water bath for 24 h. The solvent was evaporated under reduced pressure and the crude product was purified by column chromatography (Combiflash silica with hexane/EtOAc 10-30% EtOAc) to give D- trichloroacetimidate **10** (1.4 g, 83%) a yellow oil.

Subsequent elaboration of **9** (1.2 g, 3.4 mmol) as described in literature [15], afforded the glucose-trichloroacetimidate **10** (1.4 g, 83%).

^{1}H NMR (250 MHz, $CDCl_3$) δ_H 8.68 (s, 1H), 6.55 (d, *J* = 3.7 Hz, 1H), 5.62 – 5.47 (m, 1H), 5.23 – 5.03 (m, 2H), 4.30-4.09 (m 2H), 2.07 (s, 3H), 2.04 (s, 3H), 2.01 (s, 3H), 2.01 (s, 3H).

Protected glucose ligand (**11**)

2-(acetoxymethyl)-6-10,17-dioxo-26-3,4,5-triacetoxy-6-(acetoxymethyl)tetrahydro-2H-pyran-2-yl)oxy)-3,6,11,16,21,24-hexaoxa-9,18-diazahexacos-13-yn-1-yl)oxy)tetrahydro-2H-pyran-3,4,5-triyl triacetate

Molecular sieves (4Å) were dried in at 500 °C overnight and left to cool to room temperature under vacuum in the presence of anhydrous phosphorus pentoxide. Diol **7** (0.11 g, 0.26 mmol) and **8** were dissolved in dry DCM (10.4 mL). Dry 4Å molecular sieves were added and the reaction was left to stir for 10 min at room temperature under argon. Then, it was cooled to 0 °C with an ice bath and left stirring for 10 min. $BF_3{\cdot}Et_2O$ (0.013 mL, 0.10 mmol) was added dropwise and the reaction was left at 0 °C for 1 h. The ice bath was removed and after 4 h at room temperature, Et_3N (0.050 mL) was added. The solvent was evaporated under reduced pressure and the crude product was purified by column chromatography (Combiflash silica with hexane/EtOAc 50-60% EtOAc) to give **11** (0.21 g, 76%.) as yellow oil. The product was 100% in β-configuration (J = 7.9 Hz)

^{1}H-NMR (500 MHz, $CDCl_3$,), δ_H 5.21-5.17 (m, 2H, H3), 5.09-5.05 (m, 2H), 5.0-4.96 (m, 2H), 4.71 (s, 1H), 4.62-4.60 (d, J = 7.9 Hz, 2H), 4.27-4.23 (m, 2H), 4.14-4.12 (m, 2H), 3.96-3.93 (m, 2H), 3.76-3.69 (m, 2H), 3.60-3.54 (m, 16H) 3.39-3.35 (m, 4H). 2.08-2.00 (m, 24H). ^{13}C-NMR (75MHz, $CDCl_3$) δ_C 170.2, 170.1, 169.3, 169.3, 155.5, 100.7, 81.1, 72.7, 71.7, 71.2, 70.5, 70.2, 68.3, 61.9, 52.4, 40.8, 20.6, 20.6, 20.5. ESI-MS m/z 1119. [M + Na^+]: 1097.41 [M^+] MS Calculated for $C_{46}H_{69}N_2O_{28}$ (M^+): 1097.4031, found 1097.4066. IR (MeOH) ν_{max} 1750, 1368, 1038 cm^{-1}.

Glucose ligand **(12)**

10-oxo-1-3,4,5-trihydroxy-6-(hydroxymethyl)tetrahydro-2H-pyran-2-yl)oxy)-3,6,11-trioxa-9-azapentadec-13-yn-15-yl (2-(2-(2-3,4,5-trihydroxy-6-(hydroxymethyl)tetrahydro-2H-pyran-2-yl)oxy)ethoxy)ethoxy)ethyl)carbamate

Protected glucose ligand **11** (0.41 g, 3.7 mmol) was dissolved in dry MeOH (56 mL). Sodium methoxide in dry MeOH (1 M) was added until reaction reached pH 9. The reaction was left for one hour at room temperature. Amberlite IR-120 was added until reaction reached neutral pH, after which the mixture was filtered over sintered funnel pore size 2. The solvent was evaporated and compound was freeze-dried with liquid N_2 in milliq H_2O to obtain **12** (0.28 mg, 99%) as a white foam. The product was 100% in β-configuration (J = 7.9 Hz)

^{1}H-NMR (500 MHz, D_2O), δ_H 4.73 (s, 4H), 4.51-4.49 (d J = 7.9 Hz, 2H), 4.10-4.06 (m, 2H), 3.94- 3.91 (m, 2H), 3.77-3.72 (m, 14H), 3.64-3.62 (m, 4H), 3.49-3.45 (m, 4H), 3.41-3.29 (m, 8H). ^{13}C-NMR (75 MHz, D_2O) δ_C 157.6, 102.2, 81.4, 75.9, 75.7, 66.7, 69.9, 69.6, 69.4, 69.2, 68.7, 60.8, 52.9, 40.1. ESI-MS m/z 783.30 [M + Na^+] MS Calculated for $C_{30}H_{52}N_2NaO_{20}$ [M + Na^+]: 783.3006, found 783.2988. IR (MeOH) ν_{max} 3369, 2921, 1708, 1257, 1038 cm^{-1}.

3.2.1.4 Synthesis of Mannose Ligand (18)

The mannose ligand was synthesised according to the same procedure as the glucose ligand, starting from mannose -trichloroacetimidate **16** and diol ligand **7**. Mannose trichloroacetimidate **16** was synthesized from D-mannose **13** in a three-step reaction as previously reported, described in brief below [15].

6-(acetoxymethyl)tetrahydro-2H-pyran-2,3,4,5-tetrayl tetraacetate (**14**)
D-mannose (5.0 g, 27.7 mmol) was dissolved in dry pyridine (100 mL) under argon. 26 mL Ac_2O (26 mL, 0.27 mol) and dimethylamine pyridine (0.34 g,

0.027 mmol) were added and reaction was left to stir for 16h at room temperature. After evaporation, the product was partitioned between 1M HCl (60 mL) and DCM (90 mL). The organic phase was washed with 1M HCl (5 x 60 mL), H_2O (5 x 60 mL) and brine (60 mL). Then, it was dried and concentrated to afford D-mannose pentaacetate **14** as a white solid (10.8 g, 100%)

^{1}H NMR (250 MHz, $CDCl_3$) δ_H 6.12 (d, J = 1.9 Hz, 1H), 5.39–5.34 (m, 2H), 5.29-5.26 (m, 1H), 4.37-4.05 (m, 3H), 2.19 (s, 3H), 2.18 (s, 3H), 2.11 (s, 3H), 2.07 (s, 3H), 2.02 (s, 3H).

2-(acetoxymethyl)-6-hydroxytetrahydro-2H-pyran-3,4,5-triyl triacetate (**15**)
Compound **14**, (5.5 g, 14.1 mmol) was dissolved in THF (64 mL) under argon. $BnNH_2$ (2.3 mL, 21.1 mmol) was added and reaction was left to stir at room temperature for 14h. The solvent was evaporated under reduced pressure and the product was partitioned between 1M HCl (60 mL) and DCM (90 mL). The organic phase was washed with 1M HCl (3 x 60 mL), H_2O (4 x 60 mL) and brine (60 mL). After the crude product was dried and concentrated the product was purified by column chromatography (Combiflash silica with hexane/EtOAc 10-50% EtOAc) to give **15** (4.2 g, 85%) as white solid.

^{1}H NMR (250 MHz, $CDCl_3$) δ_H 5.41 (d, J = 10.02, 3.21 Hz, 1H), 5.33-5.21(m, 3H), 4.29-4.09 (m, 2H), 2.15 (s, 3H), 2.10 (s, 3H), 2.04 (s, 3H), 1.99 (s,2H).

2-(acetoxymethyl)-6-(2,2,2-trichloro-1 iminoethoxy) tetrahydro-2H-pyran-3,4,5-triyl triacetate (**16**)

Compound **15** (2.6 g, 7.4 mmol) was dissolved in DCM (30 mL) under argon. Trichloroacetonitrile (4.5 mL, 44.4 mmol) was added and then reaction was cooled to 0 °C with an ice bath and left for 15 min. DBU (0.55 mL, 3.7 mmol) was added drop wise and reaction was left to stir in water bath for 24 h. The solvent was evaporated under reduced pressure and the crude product was purified by column chromatography (Combiflash silica with hexane/EtOAc 10-30% EtOAc) to give D- trichloroacetimidate **16** (3.15 g, 86%).

^{1}H NMR (250 MHz, $CDCl_3$) δ_H: 8.77 (s, 1H), 6.28 (d, J = 1.79 Hz, 1H), 5.48-5.37 (m, 3H), 4.32-4.16 (m, 2H), 2.20 (s, 3H), 2.09 (s, 3H), 2.07 (s, 3H), 2.01 (s, 3H).

Protected Mannose ligand (**17**)

2-(acetoxymethyl)-6-((10,17-dioxo-26-3,4,5-triacetoxy-6-(acetoxymethyl)tetrahydro-2H-pyran-2-yl)oxy)-3,6,11,16,21,24-hexaoxa-9,18-diazahexacos-13-yn-1-yl)oxy)tetrahydro-2H-pyran-3,4,5-triyl triacetate

Molecular sieves (4Å) were dried at 500 °C overnight and left to cool to room temperature under vacuum in the presence of anhydrous phosphorus pentoxide. Diol **7** (0.33 g, 0.76 mmol) and **16** were dissolved in dry DCM (30 mL) under argon. Dry 4Å molecular sieves were added and the reaction was left to stir for 10 min at room temperature. Then, it was cooled to 0 °C with an ice bath and left for another 10 min. $BF_3{\cdot}Et_2O$ (0.038 mL, 0.31 mmol) was added drop wise and reaction was left at 0°C for 1h. The ice bath was removed and after 4h at

room temperature Et_3N (0.150 mL) was added. The solvent was evaporated under reduced pressure and the crude product was purified by column chromatography (Combiflash silica hexane/EtOAc, 50-60% EtOAc) to give **17** as off-white solid (0.40 g, 48%). The product was 100% in α-configuration (*J* = 1.7Hz).

^{1}H-NMR (750 MHz, $CDCl_3$), δ_H 5.36-5.24, (m, 6H), 4.87-4.86 (d, *J* = 1.7 Hz, 2H), 4.69 (s, 4H), 4.30-4.24 (m, 2H), 4.10-4.03 (m, 4H), 3.81-3.52 (m, 22 H), 3.39-3.36 (m, 4H), 2.14 – 1.97 (m, 24H). ^{13}C-NMR (750 MHz, $CDCl_3$) δ_C 170.7, 170.0, 169.9, 169.7, 155.5, 97.7, 81.1, 70.6, 70.3, 70.0, 69.9, 69.5, 69.0, 68.4, 67.4, 66.1, 62.4, 52.5, 40.9, 20.9, 20.7, 20.7. ESI-MS m/z 1097.40 (MH^+), 1119.38 [M + Na^+] MS Calculated for $C_{46}H_{69}N_2O_{28}$ [M^+]: 1097.4031, found 1097.4035. IR (MeOH) ν_{max} 1739, 1368, 1217,1043cm^{-1}.

Mannose ligand (**18**)

(6-((10,17-dioxo-26-3,4,5-trihydroxy-6 (hydroxymethyl)tetrahydro-2H-pyran-2-yl)oxy)-3,6,11,16,21,24-hexaoxa-9,18-diazahexacos-13-yn-1-yl)oxy)-4,5-dihydroxy-2-(hydroxymethyl)tetrahydro-2H-pyran-3-yl acetate)

Protected mannose **17** (0.43 g, 0.4 mmol) was dissolved in dry MeOH (60 mL). Sodium methoxide in dry MeOH (1 M) was added until reaction reached pH 9. Reaction was left for one hour at room temperature. Amberlite IR-120 was added until the reaction reached neutral pH, after which the mixture was filtered over sintered funnel pore size 2. The solvent was evaporated and compound was freeze-dried to obtain **18** as white foam (0.3 g, 97 %). The product was 100% in α-configuration (*J* = 1.7Hz).

^{1}H-NMR (750 MHz, D_2O), δ_H 4.90 (d, *J* = 1.7Hz, 2H), 4.73 (s, 4H), 3.96-3.97 (m, 2H), 3.91-3.89 (m, 4H), 3.84-3.83 (m, 2H), 3.78-3.66 (m, 20H), 3.64-3.63 (m, 4H), 3.36-3.35 (m, 4H). ^{13}C-NMR (125 MHz, D_2O) δ_C 157.5, 99.9, 81.3, 72.7, 70.5, 70.0, 69.6, 69.5, 69.4, 69.2, 66.72, 66.3, 60.9, 52.8, 40.1. ESI-MS m/z 783.30 [M + Na^+], MS Calculated for $C_{30}H_{52}N_2NaO_{20}$ [M + Na^+]: 783.3006, found 783.3009. IR (MeOH) ν_{max} 3342, 2928, 1706,1255,1057 cm^{-1}.

3.2.2 SYNTHESIS OF GATG DENDRIMERS

The synthesis and characterisation of GATG dendrimers G1-G3 was developed by my colleague Sandra P. Amaral. Her thesis is in preparation and will be defended at the University of Santiago de Compostela (Amaral, S.P., *et.al Manuscript in preparation).*

3.2.2.1 Synthesis of Core (32)

(1,3,5-tris(2-(2-(azidomethoxy)ethoxy)ethoxy)benzene)

To a solution of 1-azido-2-[2-(2-chloroethoxy)ethoxy]ethane (**31**) [13] (2.40 g, 8.42 mmol) in DMF (4.8 mL), phloroglucinol (0.34 g, 2.41 mmol), dry K_2CO_3 (3.30 g, 24.05 mmol) and 18C6 (64.00 mg, 0.24 mmol) were sequentially added. The resulting mixture was heated at 100 ºC for 32 h under argon. After cooling down to room temperature, the solvent was evaporated and the resulting crude product was passed through a pad of neutral aluminium oxide (eluent gradient from hexane to acetone) to remove the solid residues. The filtrate was concentrated and the resulting residue was purified by MPLC (3.00 g silica column, eluent gradient from hexane to acetone) to yield the product **32** (1.10 g, 76%) as pale yellow oil.

^{1}H NMR (250 MHz, $CDCl_3$) δ_H: 6.08 (s, 3H), 4.06-4.03 (m, 6H), 3.82-3.79 (m, 6H), 3.72-3.62 (m, 18H), 3.36 (t, *J*=5.3 Hz, 6H). ^{13}C NMR (64 MHz, $CDCl_3$) δ_C: 160.1, 93.9, 70.4, 70.3, 69.7, 69.3, 67.0, 50.3. ESI-MS: *m/z* Calculated for $C_{24}H_{40}N_9O_9^+$: 598.3. Found $[M+H]^+$: 598.3. Elem. Anal. Calculated for $C_{24}H_{39}N_9O_9$: C, 48.23; H, 6.58; N, 21.09. Found: C, 47.96; H, 6.74; N, 21.31. IR (KBr) ν_{max}: 2924, 2872, 2107, 1599, 1125 cm^{-1}

3.2.2.2 Synthesis of GATG Repeating unit

The efficient synthesis of the repeating unit for GATG dendrimer (**21**) has been reported in medium-to-large scale by our group [13] and was prepared in-house.

3.2.2.3. Synthesis of GATG Dendrimers G1-G3

G0-NH_2 (**25**)

Ph_3P (1.25 equiv. per N_3) was added to a solution of core **35** in MeOH/$CHCl_3$/H_2O 5:5:1 (0.1 M per N_3). The mixture was stirred at room temperature for 6 h. After the addition of a 3 M HCl solution (2 equiv. per NH_2) the solvent was evaporated and the crude dissolved in water (30.0 mL). The crude product **25** was dissolved in H_2O and filtrated through cotton to the decantation funnel to eliminate part of the white precipitates. The mixture was washed with DCM (3 x 15 mL) and lyophilized to give white foam. The complete disappearance of the azide band in FT-IR at 2100 cm^{-1} as well as the disappearance of the CH_2N_3 signal in the ^{1}H NMR spectrum shows that the reaction was completed.

G1-N_3 (**27**)

Dried Et_3N (3 equiv. per NH_2) was added under Argon to a stirred solution of G0-NH_2·HCl (**25**) in MeCN (0.1 M per NH_2) and heated at 60 ºC during 1 h or until everything was clearly soluble. The solution was left to reach room temperature and then 3,4,5-tri-{2-[2-(2azidoethoxy)ethoxy]ethyl}benzoic acid (**26**) (R.U., 1.25 equiv. per NH_2), HOBt (1.25 equiv. per NH_2) and EDC·HCl (1.25 equiv. per NH_2) were sequentially added. After 12 h, the solvent was concentrated and the reaction mixture was dissolved in DCM and washed with H_2O (3x). The organic layer was dried ($MgSO_4$) and concentrated to give a crude product that was purified by automated MPLC (eluent gradient from hexane to EtOAc/MeOH 30% in neutral alumina refilled column and basic alumina filled solid cartridge, 10 min) to afford **27** a colourless dense oil (165.4 mg, 95%).

^{1}H NMR (500 MHz, $CDCl_3$) δ_H: 7.06 (s, 6H), 6.70–6.75 (m, 3H), 6.05 (s, 3H), 4.19 (m, 18H), 4.03 (t, 6H), 3.86-3.65 (m, 108H), 3.37 (t, 18H). ^{13}C NMR (75 MHz, $CDCl_3$) δ_C: 166.9, 160.4, 152.4, 129.7, 107.0, 94.3, 72.3, 70.7, 70.6, 70.5, 70.2, 70.0, 69.7, 69.6, 69, 67.3, 50.6, 39.9. MALDI-TOF MS (HABA, reflected mode): *m/z* calculated for $C_{99}H_{156}N_{30}O_{39}Na$: 2412.1. Found $[M + Na]^+$: 2412.3. IR (KBr) ν_{max}: 3295, 2926, 2872, 2105, 1653, 1121 cm^{-1}.

G1-NH_2 (**28**)

Ph_3P (1.25 equiv. per N_3) was added to a solution of G1-N_3 (**27**) in MeOH/$CHCl_3$/H_2O 5:5:1 (0.1 M per N_3). The mixture was stirred at room temperature for 6 h. After the addition of a 3 M HCl solution (2 equiv. per

NH_2) the solvent was evaporated and the crude product dissolved in H_2O (30.0 mL). After filtration through cotton, the solution was washed with DCM (3 x 15 mL) and lyophilized to give **28** as a white foam. The complete disappearance of the azide band in FT-IR at 2100 cm^{-1} as well as the disappearance of the CH_2N_3 signal in the ^1H NMR spectrum confirmed the completeness of the reaction.

^1H NMR (500 MHz, CD_3OD) δ_H: 7.3 (s, 6H), 6.16 (s, 3H), 4.32-4.26 (m, 18H), 4.10 - 4.09 (m, 6H), 3.95-3.72 (m, 96H), 3.64-3.62 (m, 6H), 3.21-3.17 (m, 18H). IR (KBr) ν_{max}: 2929, 1584, 1119 cm^{-1}.

G2-N_3 (**29**)

Dried Et_3N (3 equiv. per NH_2) was added under Argon to a stirred solution of G1-NH_2 (**28**) in MeCN (0.1M per NH_2) and heated at 60 ºC during 1h or until everything was clearly soluble. The solution was left to reach r.t. and then 3,4,5-tri-{2-[2-(2-azidoethoxy)ethoxy]ethyl}benzoic acid (**26**) (R.U., 1.25 equiv. per NH_2), HOBt (1.25 equiv. per NH_2) and EDC·HCl (1.25 equiv. per NH_2) were sequentially added. After 12 h, the solvent was concentrated and the reaction mixture was dissolved in DCM and washed with H_2O (3x 15mL). The organic layer was dried ($MgSO_4$) and concentrated to give a crude product that was purified by automated MPLC (eluent gradient from hexane to EtOAc/MeOH 30% in filled neutral oxide alumina column) to afford **29**, as a yellow dense oil (85%).

^{1}H NMR (300 MHz, $CDCl_3$) δ_H: 7.08-6.98 (m, 24H), 6.98-6.96 (m, 12H), 6.05 (s, 3H) 4.17–4.16 (m, 72H), 4.01-4.00 (m, 6H), 3.82-3.65 (m, 344H), 3.41–3.36 (m, 54H). ^{13}C NMR (75 MHz, $CDCl_3$) δ_C: 166.9, 160.3, 152.2, 141.1, 129.5, 106.8, 94.1, 72.2, 70.6, 70.5, 70.4, 70.1, 69.8, 69.6, 68.8, 50.4, 39.8. MALDI-TOF MS (HABA, reflected mode): *m/z* calculated for $C_{324}H_{511}N_{89}O_{129}Na$: 7792.0. Found $[M + Na]^+$: 7791.9. IR (KBr) ν_{max}: 3288, 2926, 2872, 2105, 1652, 1120 cm^{-1}.

G2-NH_2

Ph_3P (1.25 equiv. per N_3) was added to a solution of G2-N_3 (**29**) in MeOH/$CHCl_3$/H_2O 5:5:1 (0.1 M per N_3). The mixture was stirred at room temperature for 6 h. After the addition of a 3 M HCl solution (2 equiv. per NH_2) the solvent was evaporated and the crude product dissolved in H_2O (30.0 mL). After filtration through cotton, the solution was washed with DCM (3 x 15 mL) and lyophilized to give G2-NH_2 as a white foam. The reaction was shown to be complete by azide band disappearance as described above.

^{1}H NMR (500 MHz, CD_3OD) δ_H: 7.31-7.26 (m, 24H), 6.17 (s, 3H), 4.29 -4.20 (m, 72H), 4.11 - 4.09 (m, 6H), 3.93 – 3.72 (m, 312H), 3.62 – 3.60 (m, 24H), 3.19 – 3.16 (m, 54H). IR (KBr) ν_{max}: 2929, 1638, 1118 cm^{-1}.

G3-N_3

Dried Et_3N (3 equiv. per NH_2) was added under Argon to a stirred solution of G2-NH_2 in MeCN (0.1M per NH_2) and heated at 60 ºC during 1h or until everything was clearly soluble. The solution was left to reach r.t. and then

3,4,5-tri-{2-[2-(2-azidoethoxy)ethoxy]ethyl}benzoic acid (**26**) (R.U., 1.25 equiv. per NH_2), HOBt (1.25 equiv. per NH_2) and EDC·HCl (1.25 equiv. per NH_2) were sequentially added and reaction was stirred for 24h at room temperature. Then, acetone was added to the reaction and this mixture ultra filtrated with Acetone/water 3:2 (3 washes, regenerated cellulose membrane M_w cut-off 3000 Da). The obtained crude product was concentrated to afford a yellow dense oil (84%).

^{1}H NMR (300 MHz, $CDCl_3$,) δ_H: 7.27 (s, 78H), 7.11-7.10 (m, 39H), 6.03 (s, 3H) 4.27-4.16 (m, 234H), 3.90-3.65 (m, 453H), 3.40-3.37 (m, 162H). ^{13}C NMR (75 MHz, $CDCl_3$) δ_C: 166.9, 160.3, 152.3, 141.2, 129.6, 106.9, 94.2, 72.3, 70.7, 70.6, 70.4, 70.1, 69.9, 69.7, 68.9, 50.6, 39.9. IR (KBr) ν_{max}: 3300, 2926, 2872, 2105, 1652, 1119 cm^{-1}.

G3-NH_2

Ph_3P (1.25 equiv. per N_3) was added to a solution of G2-N_3 (**29**) in MeOH/$CHCl_3$/H_2O 5:5:1 (0.1 M per N_3). The mixture was stirred at room temperature for 6 h. After the addition of a 3 M HCl solution (2 equiv. per NH_2) the solvent was evaporated and the crude product dissolved in H_2O (30.0 mL). After filtration through cotton, the solution was washed with DCM (3 x 15 mL) and lyophilized to give G3-NH_2 as a white foam (96%). The reaction was shown to be complete by azide band disappearance as described above.

^{1}H NMR (500 MHz, CD_3OD) δ_H: 7.32 -7.27 (m, 78H), 6.18 (s, 3H), 4.29 -4.19 (m, 234H), 4.11 (bs, 6H), 3.92- 3.60 (m, 1038H), 3.20- 3.16 (m, 162H IR (KBr) ν_{max}: 2878, 1638, 1117 cm^{-1}

3.2.3 AAC FUNCTIONALIZATION OF GATG DENDRIMERS

GATG dendrimers of generations G1 and G3 were functionalised with the above ligands (diol, tetraol, glucose and mannose) through thermal AAC reaction or microwave-assisted AAC as described in Chapter 2. The reaction was followed by infrared and the disappearance of the azide IR absorption at 2100 cm^{-1}. After complete functionalization products were purified by ultrafiltration in H_2O. Final compounds were characterised by ^{1}H and ^{13}C-NMR, infrared and DLS.

G1-Tetraol

G1-Tetraol was obtained through microwave-assisted AAC. A solution of tetraol ligand (**4**) (0.17 g, 0.52 mmol, 1.5 equiv. per N_3) and G1-N_3 (**23**) (0.092 g, 0.04 mmol) in tBuOH/H_2O (1:1) (0.17 mL) was irradiated in a microwave tube for 4 h at 100 °C (fixed-power 100W, airflow 14 psi). After evaporation, the crude product was purified by ultrafiltration with YM1 membranes (3x30 mL H_2O) to give G1-Tetraol as an off white solid (0.12 g, 61%). ^{1}H-NMR (500 MHz, D_2O) δ_H 7.10 (s, 6H), 5.95 (s, 3H), 5.29-5.12 (m, 36H), 4.60 (s, 18H), 4.10 (m, 18H), 3.89 (s, 24H), 3.75-3.54 (m, 175H). ^{13}C-NMR (125 MHz, D_2O) δ_C 168.9, 159.9, 157.4, 156.9, 151.7, 141,9, 139.6, 132.5, 129.2, 106.2, 102.5, 94.1, 72.0, 70.0, 69.9, 69.8, 69.7, 69.5, 69.5, 69.4, 60.0, 69.0, 68.8, 69.6, 68.3, 67.1, 60.7, 60.7, 57.0, 54.4, 54.4, 53.8, 48.6, 39.8. IR (MeOH) ν_{max} 3324, 2881, 1704, 1539, 1242, 1068 cm^{-1}.

G1-Diol

G1-Diol was obtained through microwave-assisted AAC. A solution of diol ligand (**7**) (0.15 g, 0.45 mmol, 1.2 equiv. per N_3) and G1-N_3 (**23**) (0.076 g, 0.032 mmol) in tBuOH/H_2O (1:1) (0.14 mL) was irradiated in a microwave tube for 2.5 h at 110 °C (fixed-power 100W, airflow 14 psi). After evaporation, the crude product was purified by ultrafiltration with YM1 membranes (3x50 mL H_2O) to give G1-Diol as a yellow oil (0.17 g, 84%).

^{1}H-NMR (500 MHz, D_2O) δ_H 7.14 (s, 6H), 5.99 (s, 3H), 5.29-5.16 (m, 36H), 4.62 (s, 18H), 4.12-4.09 (m, 18H), 3.94-3.90 (m, 24H), 3.75-3.54 (m, 264H), 3.26 (m, 36H) ^{13}C-NMR (125 MHz, D_2O) δ_C 168.6, 160.0, 157.5, 156.9, 151.9, 141.9, 139.7, 132.7, 129.2, 106.2, 94.2, 72.10, 71.7, 69.9, 69.8, 69.6, 69.4, 69.2, 69.1, 69.0, 68.9, 68.4, 67.2, 63.8, 60.3, 56.9, 53.8, 48.6, 40.1, 39.8. IR (MeOH) ν_{max} 3376, 2876, 1713, 1544, 1253, 1117 cm^{-1}.

G3-Diol

G3-Diol was obtained through microwave-assisted AAC. A solution of diol ligand (**7**) (0.16 g, 0.35 mmol, 1.2 equiv. per N_3) and G3-N_3 (0.088 g, 0.0037 mmol) in tBuOH/H_2O (1:1) (0.15 mL) was irradiated in a microwave tube for 2 h 15 min at 110 °C (fixed-power 100W, airflow 20 psi). After evaporation, the crude product was purified by ultrafiltration with YM1 membranes (3x50 mL H_2O) to give G3-Diol as a yellow oil (0.17 g, 76%).

^{1}H-NMR(300 MHz, D_2O) δ_H 7.16 (s, 78H), 6.09 (s, 3H), 5.28-5.17 (m, 324H), 4.62 (s, 162H), 4.11 (bs, 468H), 3.89-3.58 (m, 2268H), 3.25 (bs, 324H) ^{13}C-NMR (125 MHz, D_2O) δ_C 168.4, 160.0, 157.4, 156.9, 151.9, 141.9, 139.8, 132.7, 132.7, 106.2, 94.2, 72.2, 71.8, 69.9, 69.6, 69.5, 69.2, 69.1, 68.9, 68.4, 67.2, 60.3, 57.0, 53.8, 48.6, 40.2, 39.8. IR (MeOH) ν_{max} 3376, 2876, 1713, 1544, 1253, 1117 cm^{-1}.

G1-Glucose

G1-Glucose was obtained through microwave-assisted AAC. A solution of glucose ligand (**12**) (0.16 g, 0.35 mmol, 1.2 equiv. per N_3) and G1-N_3 (**23**) (0.290 g, 0.038 mmol) in tBuOH/H_2O (1:1) (0.16 mL) was irradiated in a microwave tube for 2 h 15 min at 110 °C (fixed-power 100W, airflow 20 psi). After evaporation, the crude product was purified by ultrafiltration with YM1 membranes (3x30 mL H_2O) to give G1-Glucose an off white solid (0.22 g, 67%).

^{1}H-NMR(500 MHz, D_2O) δ_H 7.14 (s, 6H), 5.98 (s, 3H), 5.29-5.17 (m, 36H), 4.63 (2, 36H), 4.46-4.44 (d, 18H) 3.91-3.89 (m, 18H) 3.78- 3.37 (m, 376H) 3.28-3.25 (m, 36H) ^{13}C-NMR (125 MHz, D_2O) δ_C 168.8, 160.0, 157.5, 156.97, 151.9, 141.9, 139.7, 132.7, 129.2, 106.2, 102.2, 94.2, 75.9, 75.7, 73.1, 72.1, 71.7, 70.0, 69.8, 69.7, 69.6, 69.6, 69.4, 69.3, 69.2, 69.1, 68.9, 68.6, 68.4, 67.2, 60.8, 60.3, 57.0, 53.8, 48.7, 40.1, 39.8. IR (MeOH) ν_{max} 3352, 2877, 1707, 1252, 1078 cm^{-1}.

G3-Glucose

G3-Glucose was obtained through thermal AAC. Glucose ligand (**12**) (0.026, 0.034 mmol, 1.2 equiv. per N_3) and G3-N_3 (0.005 g, 20 μmol) were dissolved in tBuOH/H_2O (5:1) (17μL) in a Schlenk flask and heated for 14 h at 120 °C. The reaction mixture was purified by ultrafiltration with YM5 membranes (5x20 mL H_2O) to give G3-Glucose an off white solid (0.013 g, 74%). ^{1}H-NMR (500 MHz, D_2O) δ_H 7.09-6.88 (m, 78H), 5.22-5.12 (m, 324H), 4.57 (s, 162H), 4.39 (s, 162H), 4.06-3.96 (m, 468H), 3.85-3.30 (m, 3402H), 3.25-3.20 (m, 324H). IR (MeOH) v_{max} 3352, 2925, 1707, 1252, 1078 cm^{-1}.

G1-Mannose

G1-Mannose was obtained through thermal AAC. Mannose ligand (**18**) (0.11, 0.15 mmol, 1.4 equiv. per N_3) and G1-N_3 (**23**) (0.027 g, 0.011 mmol) were dissolved in tBuOH/H_2O (1:1) (0.07 mL) in a Schlenk flask and heated for 64 h at 120 °C. The reaction mixture was purified by ultrafiltration with YM1 membranes (3x30 mL H_2O) to give G1-Mannose as an off white solid (0.062 g, 60%).

^{1}H-NMR (300 MHz, D_2O) δ_H 7.15 (s, 6H), 6.00 (s, 3H), 5.30-5.18 (m, 36H), 4.87 (s, 18H) 4.64 (s, 36H), 4.14 - 4.19 (m, 18H), 3.96-3.54 (m, 376H), 3.28-327 (m, 36H) ^{13}C-NMR (D_2O, 125 MHz) δ_C 168.7, 159.92 157.4, 156.9, 151.8, 141.9, 139.6, 132.7, 129.2, 106.1, 99.8, 94.1, 72.7, 70.4, 69.9, 69.5, 69.1, 69.1, 69.1, 69.9, 68.9, 68.3, 67.1, 66.5, 66.2, 60.8, 56.9, 53.8, 48.6, 40.0, 39.7. IR (MeOH) v_{max} 3352, 2923, 1716, 1252, 1101 cm-^{1}.

G3-Mannose

G3-Mannose was obtained through thermal AAC. Mannose ligand (**18**) (0.026, 0.034 mmol, 1.2 equiv. per N_3) and G3-N_3 (0.005 g, 20 μmol) were dissolved in tBuOH/H_2O (5:1) (17μL) in a Schlenk flask and heated for 14 h at 120 °C . The reaction mixture was purified by ultrafiltration with YM5 membranes (5x20 mL H_2O) to give G3-Mannose an off-white solid (0.017 g, 93%). ^{1}H-NMR (500M Hz, D_2O) δ_H 7.17-6.93 (m, 78H), 5.30-5.20 (m, 324H), 4.88 (bs, 162H), 4.65 (bs, 162H), 4.15-4.12 (m, 468H), 3.97-3.56 (m, 3402H), 3.28 (s, 324H). IR (MeOH) ν_{max} 3352, 2923, 1716, 1252, 1101 cm-^{1}.

3.2.4 BORONIC ACID FUNCTIONALISATION OF GATG DENDRIMERS

GATG dendrimers G1 and G3 were functionalized with phenylboronic acid through an adapted protocol developed by our group for boronic acid-dendrimers with polyethylene glycol chains. (Amaral S.P. et al. Manuscript in preparation).

G1-B(OH)$_2$

PPh_3 (185 mg, 0.7 mmol, 1.1 equiv. per N_3) was added to a solution of G1-N_3 (170 mg, 0.07 mmol) in MeOH/H_2O (95:5, 6.5mL). After 16h of stirring at room temperature, 2-formylphenylboronic acid (144 mg, 0.9 mmol, 1.5 equiv. per N_3) was added and the reaction was left overnight. Then, $NaBH_4$ (36 mg, 0.9 mmol, 1.5 equiv. per N_3) was added and the reaction allowed for stir 8 h.

Purification of the reaction mixture by ultrafiltration, (YM1, first acetone/H_2O 1:1, 3 x 15mL followed by H_2O) afforded G1-$B(OH)_2$ as a white solid (9 mg, 5% yield)- The low yield was attributed to difficulties with separation.

^{1}H NMR (500 MHz, CD_3OD) δ_H: 7.42-7.38 (t, 6H), 7.22-6.95 (m, 36H), 5.98 (s, 3H), 4.03-3.68 (m, 114H), 3.57 – 3.55 (m, 6H), 3.06 (s, 18H). IR (MeOH) ν_{max} 3491, 2874, 1582, 1115, 754 cm^{-1}.

G3-$B(OH)_2$

PPh_3 (60 mg, 0.7 mmol, 1.1 equiv. per N_3) was added to a solution of G1-N_3 (60 mg, 0.0025 mmol) in MeOH/H_2O (95:5, 2.1 mL). After 17h of stirring at room temperature, 2-formylphenylboronic acid (46 mg, 0.3 mmol, 1.5 equiv. per N_3) was added and the reaction was left overnight. Then, $NaBH_4$ (11.5 mg, 0.3 mmol, 1.5 equiv. per N_3) was added and the reaction allowed for stir 8 h. Purification of the reaction mixture by dialysis, mw cut-off, 1000 Da MeOH/H_2O (3:2) (3 x 1000mL) followed by dialysis in H_2O (3 x 1000mL) afforded G3-$B(OH)_2$ as a white solid (80 mg, 98% yield).

^{1}H-NMR(500 MHz, D_2O) δ_H 7.34-7.31 (m, 78H), 7.12-6.88 (m, 324H), 5.98 (s, 3H), 3.94-3.45 (m, 1200 H) 2.96 (s, 162H) ^{13}C-NMR (125 MHz, D_2O) δ_C 168.23. 160.44, 151.57, 140.98, 128-96, 127.32, 126.91, 122.37, 105.99, 94.61, 71.93, 69.86, 69.43, 68.94, 68.13, 66.76, 52.36, 45.63, 39.54 IR (MeOH) ν_{max} 3491, 2874, 1582, 1115, 752 cm^{-1}.

3.3 RESULTS AND DISCUSSION

3.3.1 SYNTHESIS OF LIGANDS

3.3.1.1. Synthesis of Tetraol Ligand

An alkynated ligand with two hydroxyl groups in each end (tetraol) was synthesised based on the hypothesis that it would have an increased affinity for boric acid compared to linear diols such as polyvinyl alcohol (PVA), previously evaluated by Xue and colleagues due to the *cis*-conformation of the diol pair [7].

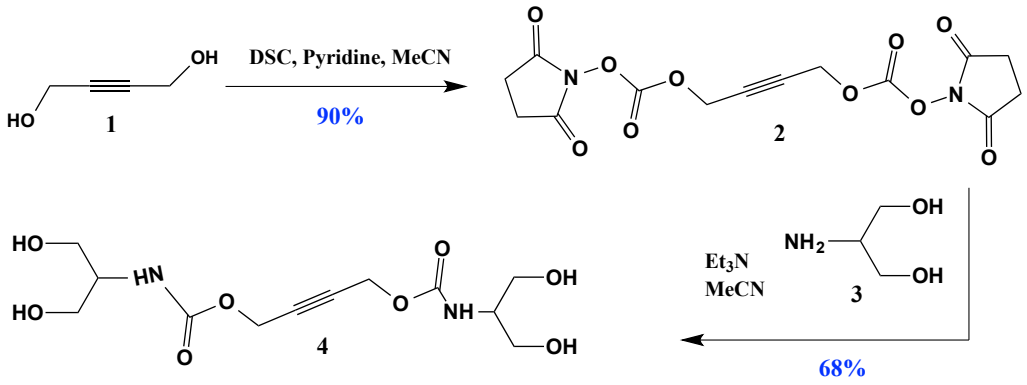

Figure 3.5 Syntheses of Tetraol ligand with an internal alkyne (**4**).

The tetraol-alkyne-ligand was synthesized following a two-step reaction from 2-butyne-1,4-diol (*Figure 3.5*). The first step was by a modified protocol previously reported [17], where 2-butyne-1,4-diol is activated with a good leaving group, N-hydroxysuccinimide (NHS). In this reaction, the alcohol groups in 2-butyne-1,4-diol reacted via nucleophilic attack on the carbonyl of the N, N'-disuccinimidyl carbonate (DSC) after formation of the active carbonate **2** (*Figure 3.5, 3.6*). Pyridine, the excess of DSC and NHS were removed by aqueous workup. The product, but-2-yne-1,4-diyl bis(2,5-

dioxopyrrolidin-1-yl) dicarbonate (**2**) was obtained in good yield (90%). Characterization was done by ^{1}H and ^{13}C-NMR, comparing with similar products previously reported [17] and confirmed with mass spectrometry (*Appendix, Figures A1-A2*).

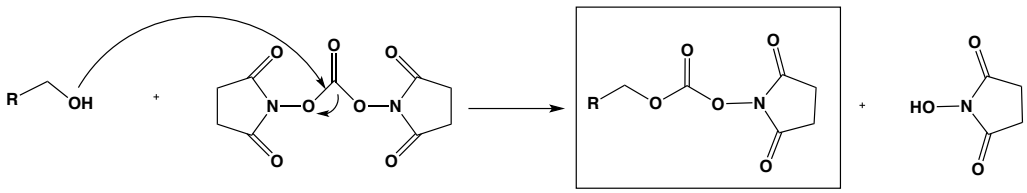

Figure 3.6 Mechanism of the formation of active carbonate

In the second step, the activate carbonate (**2**) reacts with the amine group of the serinol (**3**) to form a carbamate with an internal alkyne (**4**) (*Figure 3.7*). The reaction was followed by TLC to confirm reaction was complete and that no mono-substituted active carbonate or hydrolysed alcohol remained.

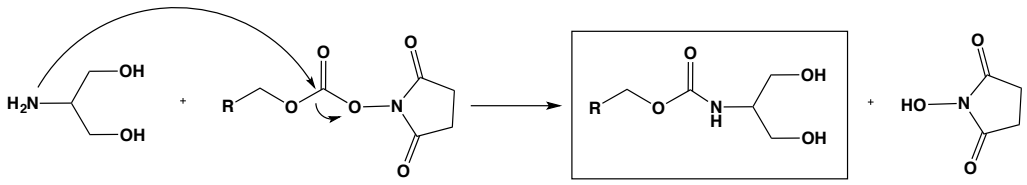

Figure 3.7 Mechanism of amine substitution of the active carbonate.

The purification of the product was complicated due to the fact that the final compound contained four alcohol functional groups that can interact with the

silica during column chromatography and thereby retain the product in the column during purification. The leaving group, NHS has a similar retention factor (RF) to that of the desired product and the most challenging part of the purification was the separation of product from the NHS. The use of 1% acetic acid to elute the product more quickly was unsuccessful; removal of the acetic acid was quite challenging, with traces still present even after multiple freeze-drying cycles.

Final conditions for purification involved Combiflash silica column chromatography with DCM in gradient 0-20 % with MeOH, to obtain the final product in good yield (68%). The ligand appeared to be stable in tBuOH/H_2O under thermal microwave-assisted conditions (200 W, 100 °C, 1 h). This was the first time this product has been described and the product was therefore characterised with ^{1}H-NMR (*Figure 3.8*), ^{13}C-NMR, Mass Spectrometry and Infrared Spectroscopy (*Appendix, Figures A3-A5*). ^{1} H-NMR confirms the removal of the leaving group (NHS) at 2.8 ppm and the appearance of the serinol-specific multiple at 3.68 -3.55 ppm (*Figure 3.8*). The tetraol ligand was used to functionalise GATG dendrimer of G1-N_3

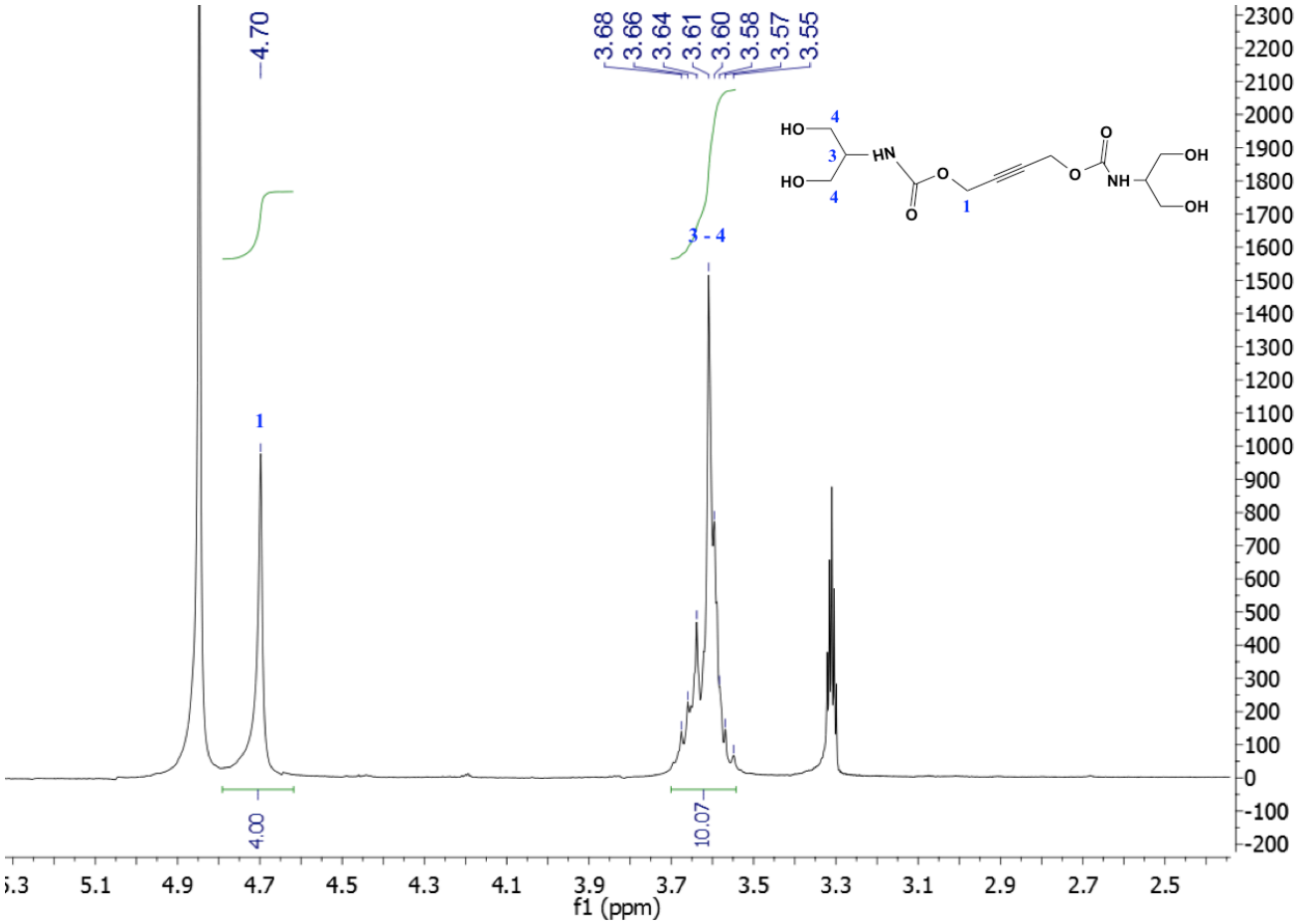

Figure 3.8 ^{1}H-NMR of tetraol ligand in CD_3OD

3.3.1.2. Synthesis of Diol ligand (7)

An alkynated diol with terminal hydroxyl groups was synthesised with the consideration that the affinity for boric acid might be lower than that of the carbohydrates[7]. The diol-functionalised dendrimer could be used as a negative control for the quorum quenching and bacteria clustering and to be compared with the tetraol and carbohydrate ligands.

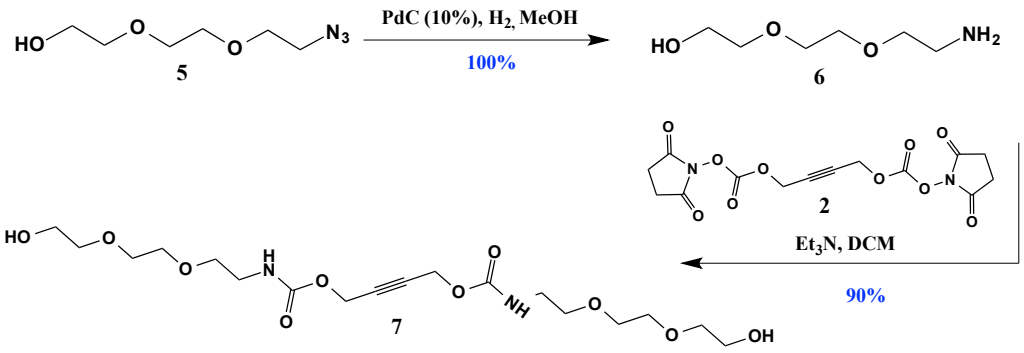

Figure 3.9 Syntheses of diol-alkyne ligand (7) synthesised in a three-step sequence.

A diol-ligand (**7**) was successfully synthesised using a similar protocol as for tetraol ligand, changing the serinol for 2-(2-(2-aminoethoxy)ethoxy)ethan-1-ol (**6**). Compound (**6**) was easily prepared through a reported protocol [14], by reduction of the azide group as of -2(2-(2-azidoethoxy)ethoxy)ethan-1-ol (**5**) previously prepared in our group [13], with H_2 and Pd-C (*Figure 3.9*). Aminoalcohol **6** was characterised by ^{1}H and ^{13}C-NMR and compared with literature [14]. In the following step, compound **6** reacted with the activated carbonate **2** to form a dicarbamate following the above protocol used for the tetraol *(Figures 3.5)*. The reaction was followed by TLC to confirm that the reaction was complete and the absence of mono-substituted products.

Similar to the tetraol ligand, the purification was complicated due to the fact that the final compound contained two alcohols that can interact with the silica of the column chromatography. However, using similar purification conditions (DCM with 0-10% MeOH) as for the tetraol, the final compound could be obtained in very good yield (90%). The diol ligand was stable under microwave conditions (100 W, 100 °C, 2 h) and accordingly, it was used both as a ligand for functionalization of the dendrimer and for the Schmidt's glycosylation to gain mannose and glucose ligands. This was the first time this product has been described and so it was characterised by ^{1}H-NMR (*Figure 3.10*), ^{13}C-NMR, Mass Spectrometry and Infrared (*Appendix Figures A6-A8*). ^{1}H-NMR confirms the removal of the leaving group (NHS) at 2.8ppm and the appearance of carbamate bound chain at 3.71-3.23 ppm (*Figure 3.10*). This long diol ligand was used to functionalise GATG dendrimer of G1-N_3 and G3-N_3.

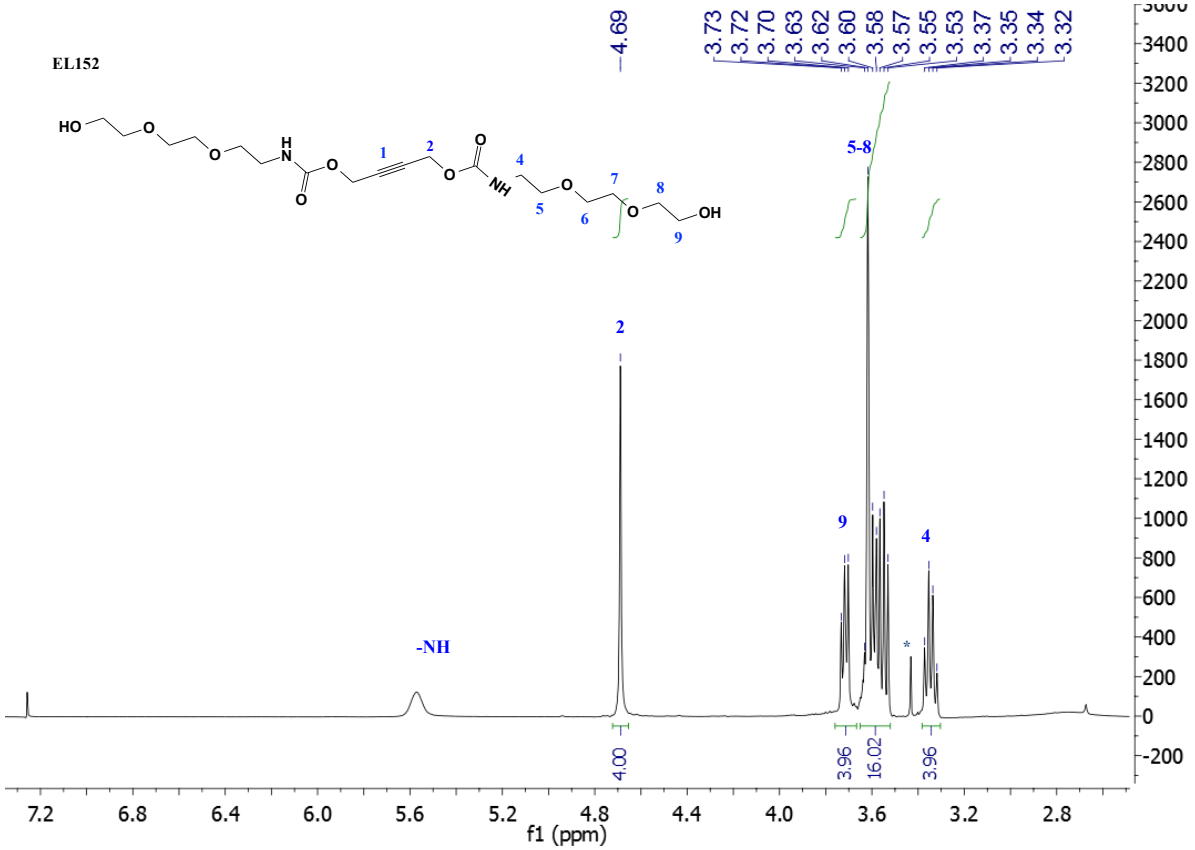

Figure 3.10 ^{1}H-NMR of diol ligand in $CDCl_3$ (*accounts for residual CH_3OH).

3.3.1.3. Synthesis of Glucose and Mannose Ligands

Glucose ligand was synthesised to mimic the diol moiety of the linear polymers synthesised by Xue and colleagues [7], capable of inhibiting quorum sensing molecule AI-2 in *V. harveyi* MM32. They reported that the affinity for boric acid and phenylboronic acid was shown to be higher for cyclic diols such as carbohydrates compared to linear diols. Although the affinity was lower for carbohydrates compared to the catechol moiety, carbohydrates have been shown to be active bacterial sequestering agents though carbohydrate- lectin-binding [18, 19] Springsteen and Wang reported higher affinity of D-mannose than D-glucose for phenylboronic acid, which was the rational for synthesising both mannose- and glucose -ligands [4]. In addition, D-α-mannose is known to bind to *E. coli,* a human relevant pathogen that also releases AI-2 [20].

Even through the stereochemistry of the carbohydrate is not likely to effect the quorum sensing quenching of AI-2, it might be of importance for bacteria clustering. Accordingly, an α-mannose ligand was synthesised (*Figure 3.12*) for the possibility of evaluating binding affinity to *E. coli* and induction of clustering with α-mannose-specific lectins. For the purpose of comparison in bacteria clustering between linear glucose polymer previously synthesised in our group and globular dendrimers, it was decided to synthesise glucose ligand in the β-form (*Figure 3.11*) [7].

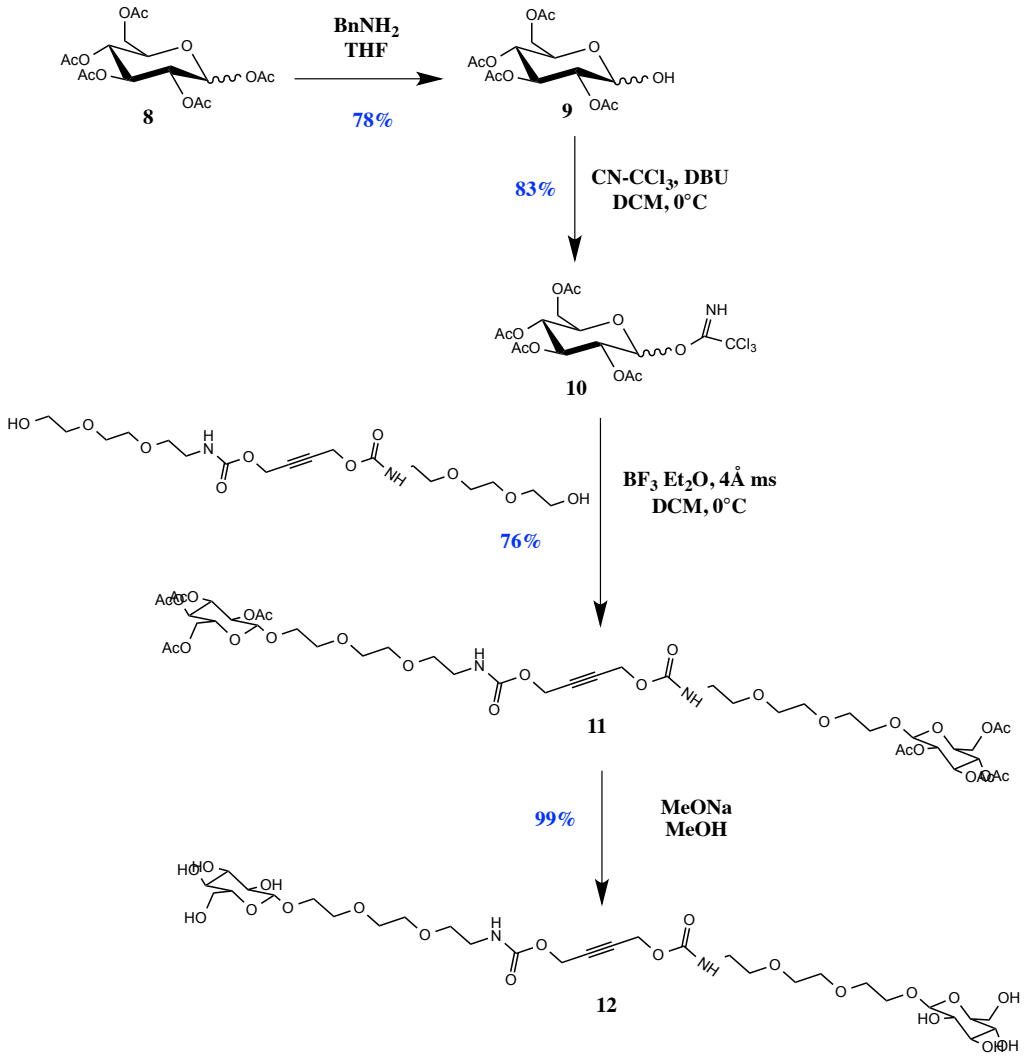

Figure 3.11 Synthesis of glucose ligand with an internal alkyne.

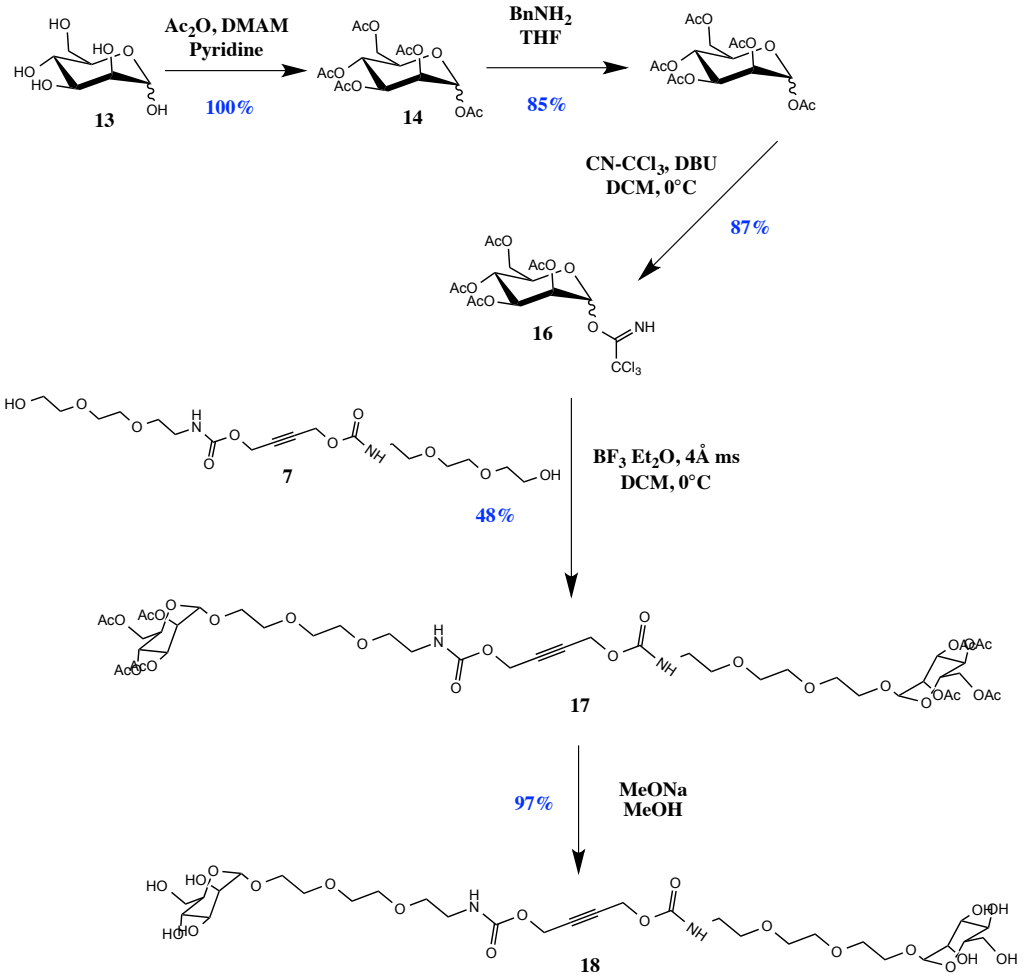

Figure 3.12 Synthesis of mannose ligand with an internal alkyne.

The Schmidt glycosylation is a Lewis acid-activated reaction between a thricloroacetimidate and an alcohol, where the formation of α/β selectivity can be controlled (*Figures 3.13-3.14*). The protecting acetyl group at the C2 position of the sugar participates in the glycosylation of the hydroxyl group through neighbouring group participation [21].

Tetraacetate glucose-trichloroacetimidate was synthesized from D-glucose pentaacetate in a two-step reaction and tetraacetate mannose-trichloroacetimidate was synthesized from D-mannose in a three-step process

following previously reported procedures [15, 16]. Both sugars were protected with acetyl groups, followed by selective monodeprotection at the anomeric position.

The $BF_3 \cdot OEt_2$, used in catalytic concentrations, activates the anomeric leaving group trichloroacetimidate, which is present in both α and β anomeric positions, resulting in the formation of an oxacarbenium ion (*Figure 3.13*). Due to the present acetyl group in the C2 position, the more stable five-member acetoxonium-ion will be formed. The acetoxonium-ion can, in the case of glucose only be formed in an axial conformation [21]. The alcohol attack on the anomeric position can therefore only occur in the equatorial position, hence the selective formation of β-linked glycosylation where the anomeric carbon is in equatorial position.

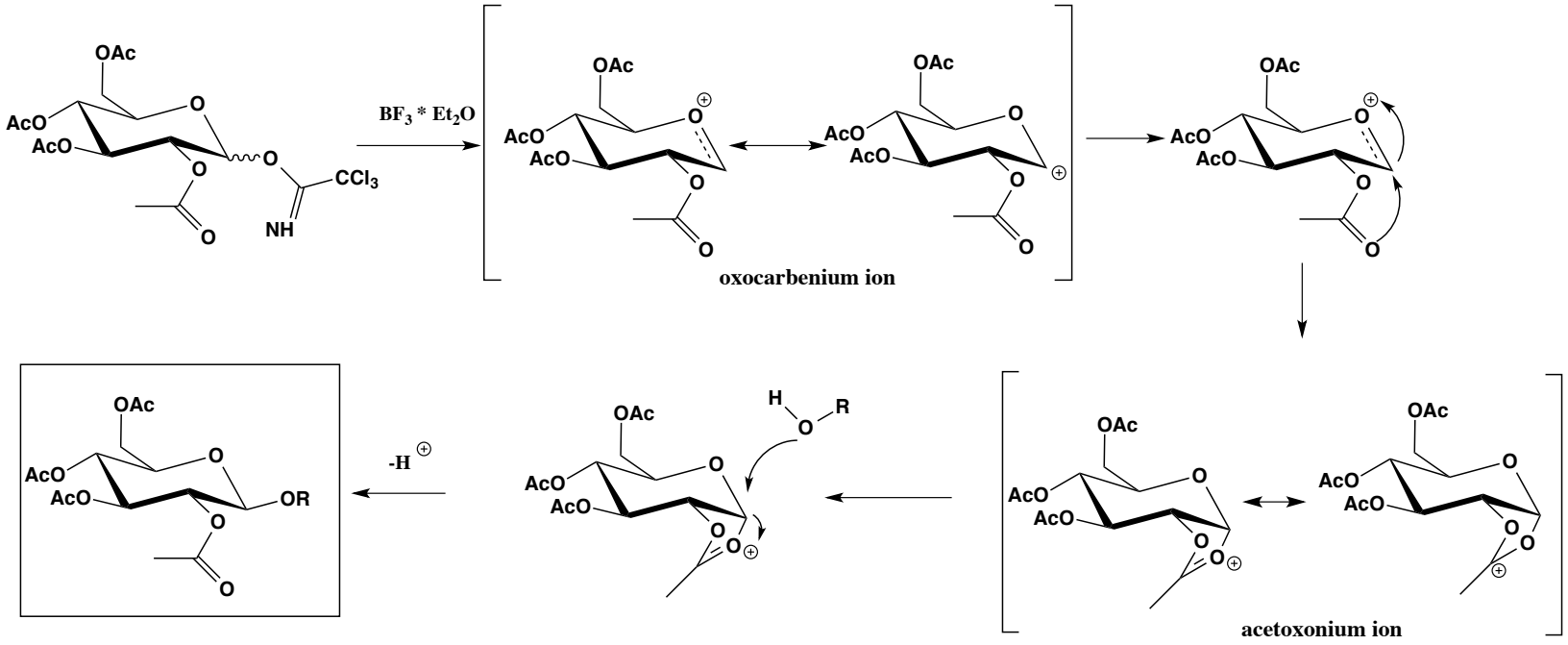

Figure 3.13 Mechanism for the glycosylation of alcohols with $BF_3 \cdot Et_2O$ as catalyst. Selective formation of β -glucose derivatives.

In the case of mannose, the same principle applies, but due to the conformation of the C2 neighbouring group (equatorial), the Schmidt's glycosylation will lead to selective formation of α-linked products with anomeric carbon substituent group in the axial position (*Figure 3.14*).

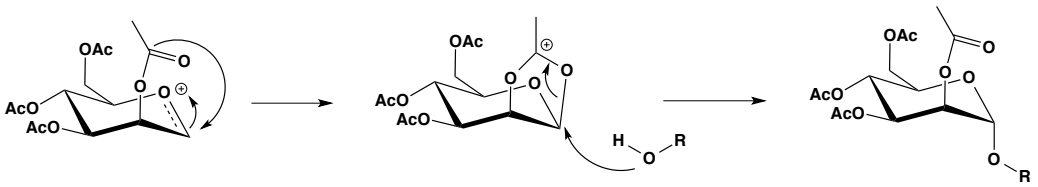

Figure 3.14 Mechanism for selective formation of α-mannose derivatives.

Several protocols for the synthesis of the sugar ligands with internal alkyne were evaluated, the initial strategy was conjugate directly the protected sugar-trichloroacetimidate to the 2-butyne-1,4-diol to get compound (**19**) (*Figure 3.15*).

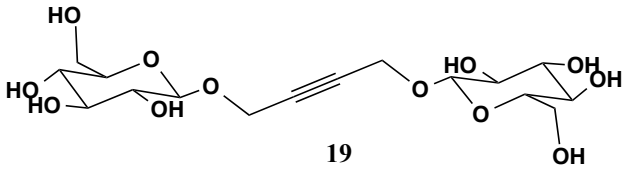

Figure 3.15 Structure of short arm sugar ligand with an internal alkyne

The synthesis was successful and after purification, the acyl-protected glucose and mannose ligands were obtained in yields above 80%. Products were confirmed by ^{1}H-NMR (*Appendix Figure A9*) and compared to previous published mannose derivatives [22].

However, after deprotection and gaining of the final sugar products (**19**), the ligands were not stable under the conditions needed for the AAC conjugation of the ligand to dendrimer (120 °C for 2 h) as both the mannose and glucose ligand (**31**) decomposed under these conditions, as observed by TLC and ^{1}H-NMR. It was hypothesised that the reason for the unstable molecule under thermal conditions was the close proximity of the alkyne to the carbohydrate. Therefore, it was decided to synthesise a sugar ligand starting from the diol mimetic of the tetraol ligand **4,** which was stable under the AAC conditions and which been successfully conjugated to G1 dendrimer. The Schmidt glycosylation with $BF_3{\cdot}OEt_2$ as Lewis acid was again used, but rather than using 2-butyne-1,4-diol, starting from a new diol with structure similar to the tetraol ligand (*Figure 3.16*). The hypothesis was that the increased distance between alkyne and anomeric position of the sugar in combination with the carbamate group could improve the stability.

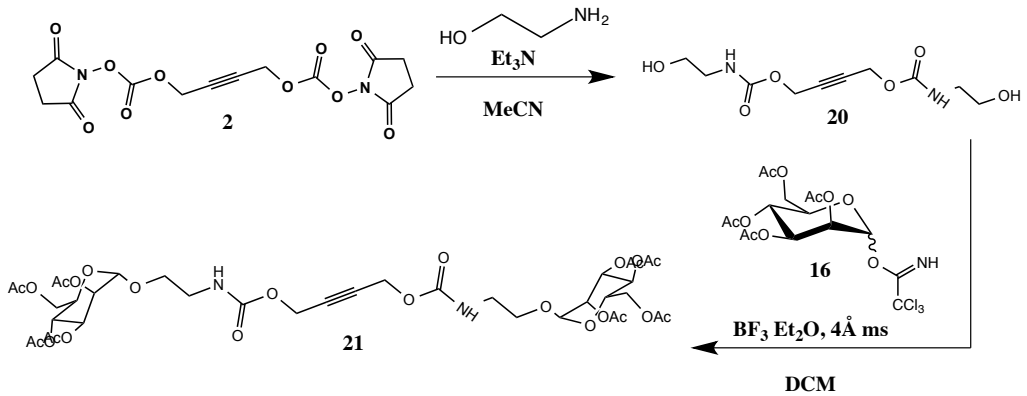

Figure 3.16 Synthetic strategy for compound (**21**).

A new ligand with internal alkyne and terminal hydroxyl groups (**20**) was successfully synthesised using the same protocol as for tetraol ligand, replacing

the serinol with ethanolamine (*Figure 3.16, Appendix Figure A10*). However, the Schmidt glycosylation did not generate the desired product (**21**). Several Lewis acids and optimisation steps were evaluated without success (*Appendix Table A1*), in all cases either no product was obtained at all, or a very unstable product was obtained. It seemed to proceed from N-glycosylation probably through a five-membered ring intermediate, once the desired product was obtained. To avoid this, a further increased distance between the carbamate linkage and the sugar moiety was explored.

In order to increase the chain length, diol ligand (**7**) was synthesised, as described above in section 3.3.1.2 (*Figure 3.5*). By doing so, 4 carbons and 2 oxygen atoms were added to the chain length compared to ethanolamine used in compound **21**. Again, $BF_3{\cdot}OEt_2$ was used as the Lewis acid, and after optimizing the protocol (*Appendix Table A2*), the Schmidt's glycosylation of the diol ligand **7** was successful with both mannose and glucose trichloroacetimidates. The purification was found to be more challenging than for the shorter glucose compound **21**, possibly due to the long flexible nature of the chain that could alter the interactions with the silica column (by combination of hydrogen bonding and hydrophobic associations). Final chromatography conditions were hexane/EtOAc (45:55). The protected glucose ligand **11** was obtained in good yield (76%) and the protected mannose ligand **17** in lower yield (48%). This was the first time these products have been described and they were therefore characterised by ^{1}H-NMR (*Figures 3.17 - 3.18*), and ^{13}C-NMR, Mass Spectrometry and Infrared for protected glucose ligand (*Appendix Figures A11, A13, A15)* and protected mannose ligand (*Appendix Figures A17, A19, A21).*

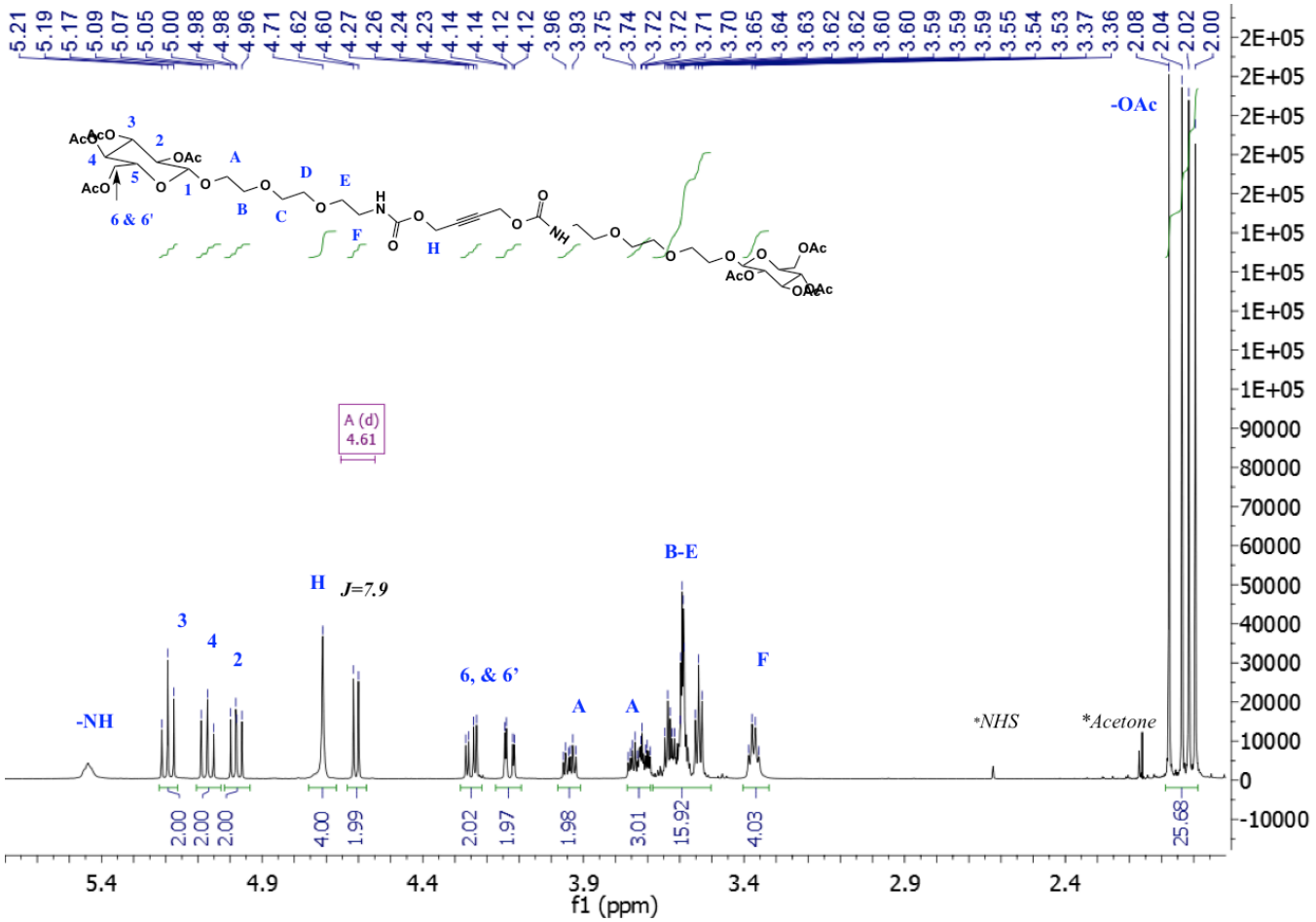

Figure 3.17 ^{1}H-NMR of protected glucose ligand **11** ($CDCl_3$). The J-coupling constant (7.9 Hz) confirms the β-conformation of glucose.

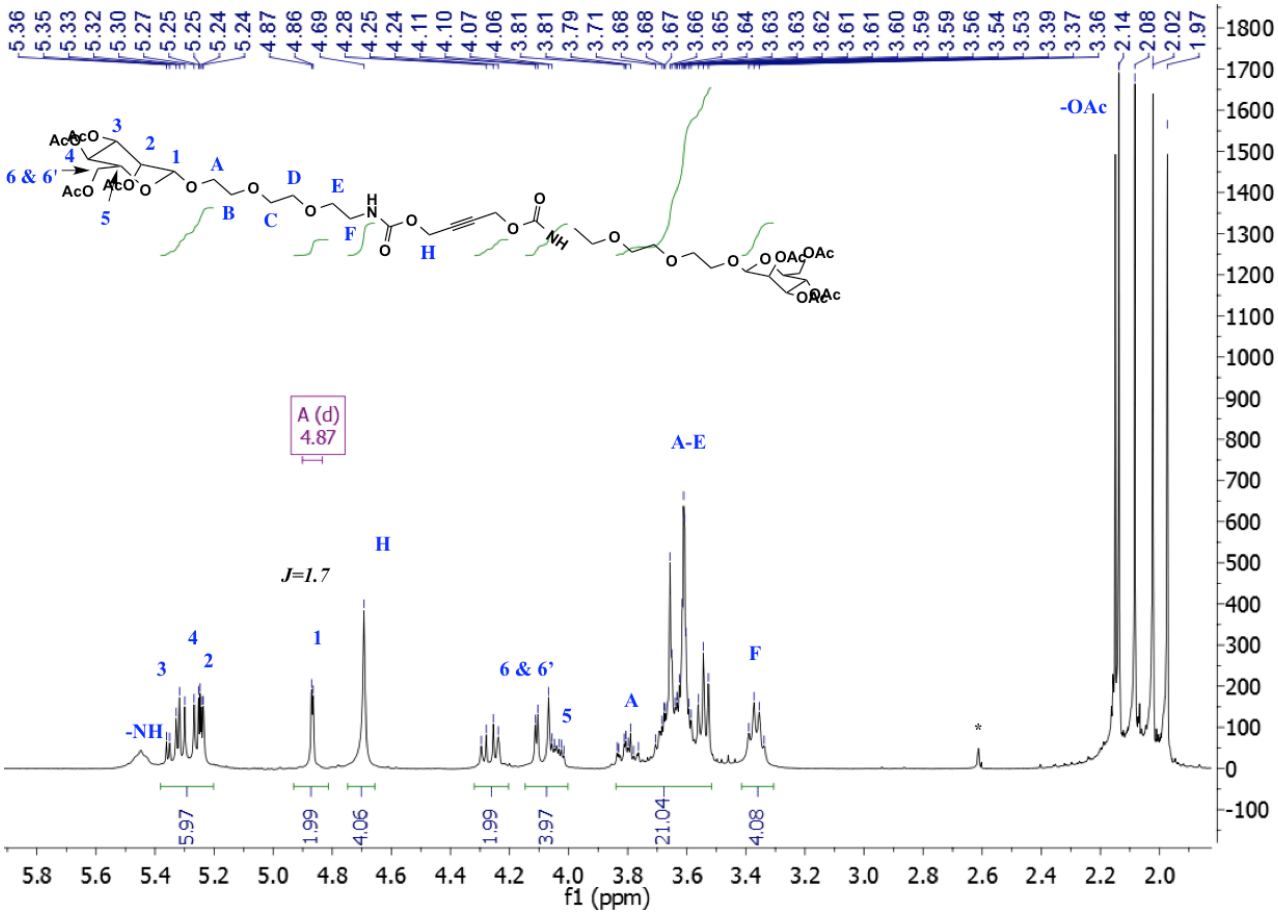

Figure 3.18 ^{1}H-NMR of protected mannose ligand (**17**) ($CDCl_3$). Trace of NHS is seen at 2.6ppm. The *J*-coupling constant (1.7 Hz) confirms the α-conformation of mannose.

The selective formation of α-mannose and β-glucose conjugates was confirmed by measuring the *J*-coupling constants of the anomeric peak (the distance in frequency units of Hz between the peaks of the anomeric doublet) [23]. The *J*-coupling is an interaction between proton nuclei connected by bonds and depends on both the number of bonds and their configuration. The angle between the hydrogens at C1 and C2 changes if the sugar is in α or β configuration, and therefore also the *J*-coupling changes. β-D-Glucose has an equatorial substituent group at the C2 position, which means that the H in C2 position is axial (*Figure 3.19*). When the H_1-H_2 relationships are axial-axial the *J*-coupling has a value between 7-9 Hz and the glucose is in β-configuration [23, 24]. For an axial-equatorial coupling associated with α-glucose the values are between 2-4 Hz. The *J*-coupling constant measured for the glucose ligand (7.9 Hz) confirmed the β-configuration.

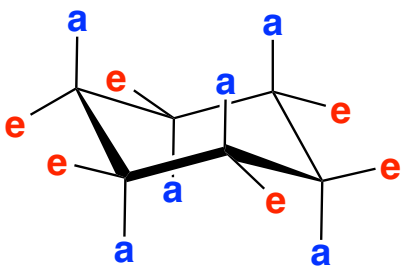

Figure 3.19 Axial (a) and equatorial (e) positions in the chair conformation of cyclohexane.

The α-D-mannose ligand has the substituent group in the C2 position in axial configuration, so the H at C2 is equatorial. The anomeric proton is equatorial (the anomeric substituent group is in axial position). The α-configuration in mannose, associated with equatorial-equatorial H_1–H_2 relationship has a reported *J*-coupling constant around 1.6 Hz, with values around 0.8 Hz for

axial-equatorial coupling (β-configuration) [24]. The experimental *J*-coupling constant of mannose ligand **17** (1.7 Hz) confirmed the α-configuration.

The mannose and glucose ligands were deprotected through Zemplén deacetylation, by treatment with catalytic amounts of sodium methoxide in methanol (*Figure 3.20*) [25]. Sodium methoxide catalyzeses the deacetylation with concomitant formation of new alcoxide groups, as a source for new methoxide anions. Once deprotection was complete, after approximatly 1.5 h, the reaction was neutralised with Amberlite IR-120 (H^+) ion exchange resin for protonation of methoxide anions and removal of sodium cations, prior to filtration and lyophilisation. The complete deprotection was followed with TLC and confirmed by ^{1}H-NMR and the disappearance of the characteristic acetyl signals at 2.14-1.97ppm (*Figure 3.21*). The deacetylation was successful and the deprotected mannose (**19**) and glucose (**12**) ligands were obtained in quantitative yields.

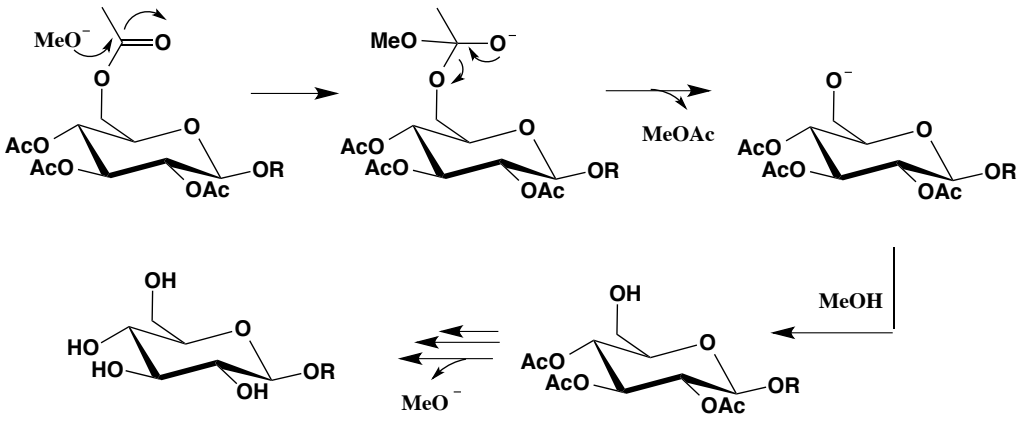

Figure 3.20 Mechanism of Zemplén deacetylation for glucose protected with acetyl groups [25]

The final glycosylated ligands were characterised with ^{1}H-NMR (*Figure 3.21, 3.22*) and ^{13}C-NMR, Mass Spectrometry and Infrared for glucose (*Appendix Figures A12, A14, A16)* and mannose (*Appendix Figures A18, A20, A22).* The ligands were stable under AAC and thermal conditions (120 °C, 2 h), confirmed by TLC and ^{1}H-NMR and the resulting products were used to functionalise the GATG dendrimer of G1-N_3 and G3-N_3

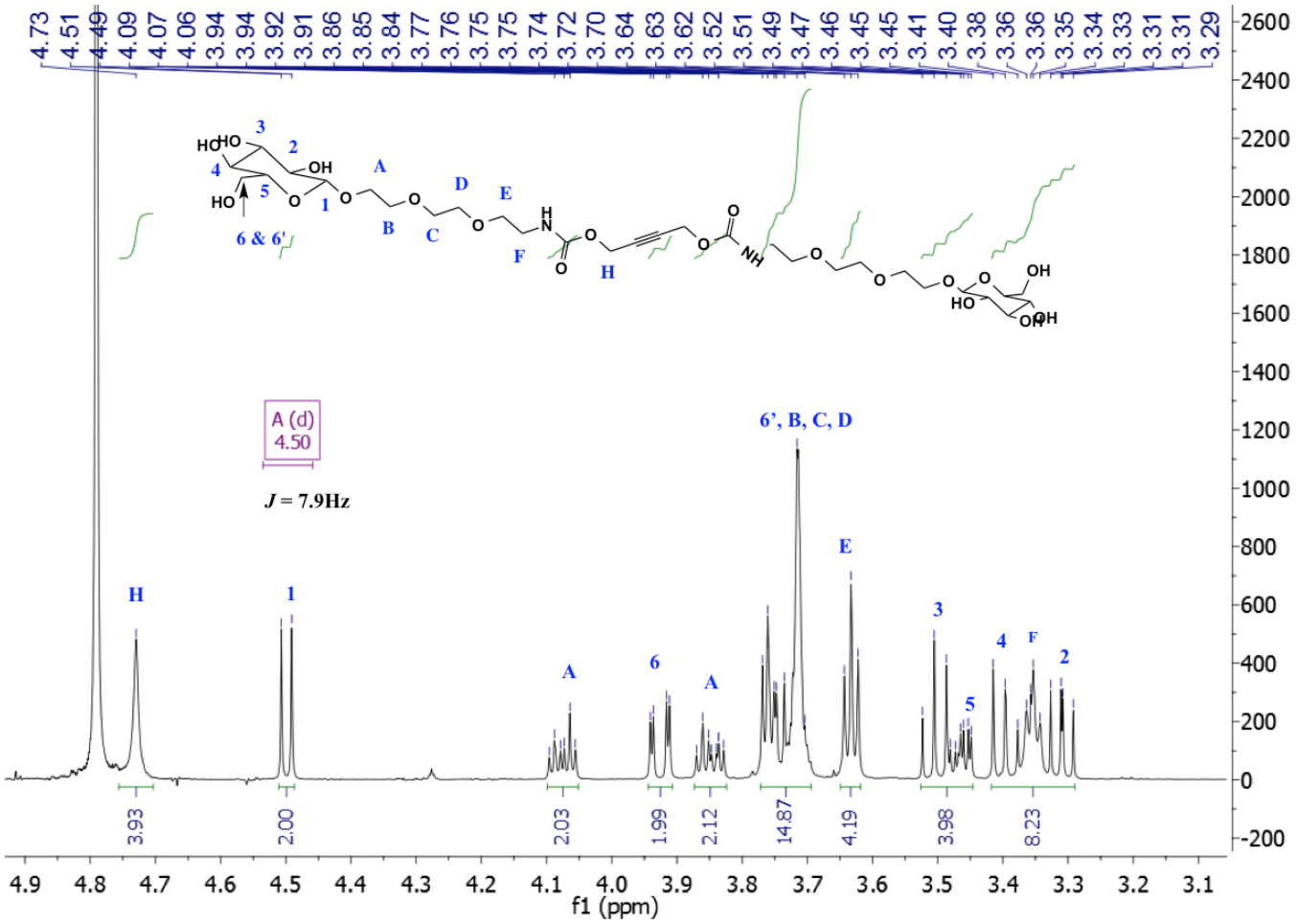

Figure 3.21 ^{1}H-NMR of glucose ligand (**12**) in D_2O. The *J*-coupling constant of 7.9 Hz shows the glucose is in β-configuration.

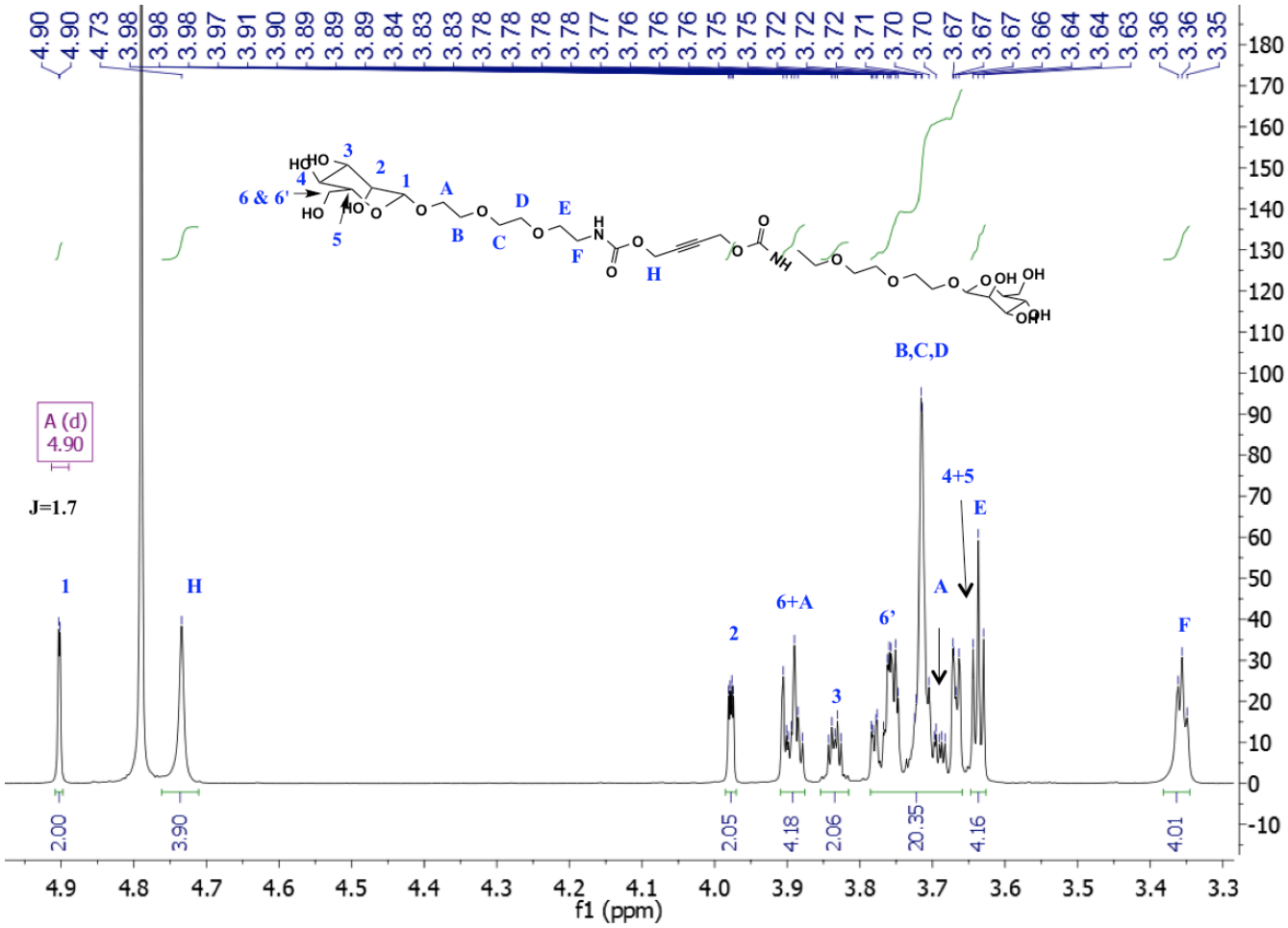

Figure 3.22 ^{1}H-NMR of mannose ligand (**19**) in D_2O. The *J*-coupling constant of 1.7 Hz shows the mannose is in α configuration.

3.3.2. SYNTHESIS OF DENDRIMERS

It was the main objective to grow each generation of dendrimers through microwave-assisted AAC, instead of using traditional heating methods such as oil baths or heating jackets. A wide range of microwave-assisted chemical reactions have been described including the thermal 1,3-dipolar cycloaddition and the Cu(I)-catalysed variant, for instance for the functionalization of dendrimers with peptides [26, 27].

3.3.2.1 Microwave assisted synthesis of dendrimers through Azide-alkyne cycloaddition.

Dendrimers prepared through catalyst-free click chemistry have been recently described by the group of Morin [10]. They presented an interesting approach for the efficient divergent synthesis of dendrimers through azide-alkyne cycloaddition (AAC) under thermal conditions, while avoiding the use of toxic metals and chemicals that can interfere when dendrimers are applied to biological systems. To further exploit this concept, it was aimed to synthesize a new family of dendrimers containing internal alkynated ethers instead of the more sensitive esters [10], which can be hydrolysed in water. Thus as depicted in Figure 3.22, building dendritic structures from a core with terminal azides and repeating units bearing internal alkynes, through thermal AAC.

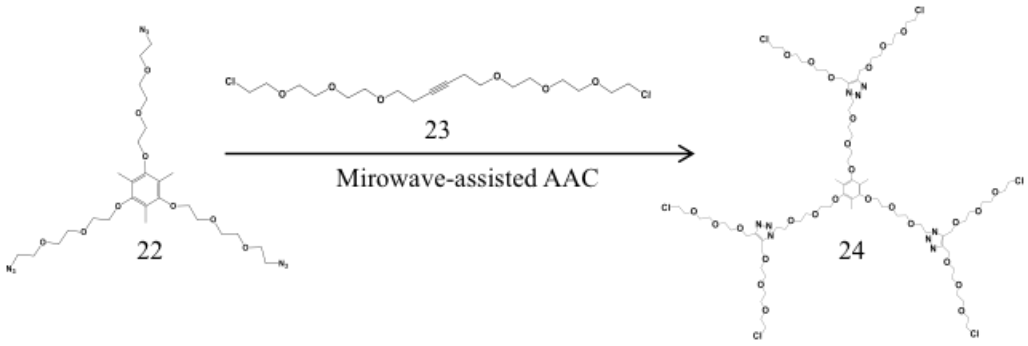

Figure 3.23 Strategy for microwave-assisted synthesis of dendrimers through AAC.

New core

The core (**32**) used in our group for the synthesis of GATG dendrimers (*Figures 3.24-3.25*) is synthesised in a four-step process with yields usually around 60%, albeit with some difficulties to purify after the last step (Amaral *et. al. Manuscript in preparation*). Therefore, the aim was to develop a more efficient synthesis of a related core molecule (**22**) to be used in the development of the new AAC dendritic family (**24**) (*Figure 3.23*). The core molecule was synthesised in a one-step reaction, (*Appendix A23)* and obtained in 66% yield after column chromatography.

Repeating unit for microwave-assisted AAC dendrimers

The synthesis of an ethylene-oxide based repeating unit with an internal alkyne and terminal chlorides (**23**), was synthesised using two different conditions; 1) 50% aqueous NaOH with the phase transfer agent nBu_4NHSO_4, and 2) NaH in THF. Under either conditions, repeating unit **23** was difficult to get in a clean reaction, leading to many different spots by TLC, yields below 20%, and

starting material left even after 48 h of reaction time at 60 °C (*Appendix, Table A3).*

Microwave-assisted AAC dendrimers

Unfortunately, the use of **23** for the preparation of dendrimers starting from previous core **22** was also unsuccessful, with reactions suffering from low reproducibility and yields (*Described in Appendix A25*).

Because the main focus of this project was to study the interaction of functionalized dendrimers with bacteria, it was decided not to further pursue the strategy of synthesising new dendrimers through thermal AAC. Instead it was decided to rely on GATG dendrimers (Amaral P.S. *et. al. Manuscript in preparation*) and to conjugate the alkynated ligands to the GATG azide terminal groups through catalyst-free AAC.

3.3.2.2 Synthesis of GATG dendrimers

This synthetic route and characterisation of GATG dendrimers was developed by Sandra P. Amaral (Amaral P.S. et.al. *Manuscript in preparation*). Thesis to be submitted at University of Santiago de Compostela Spain.

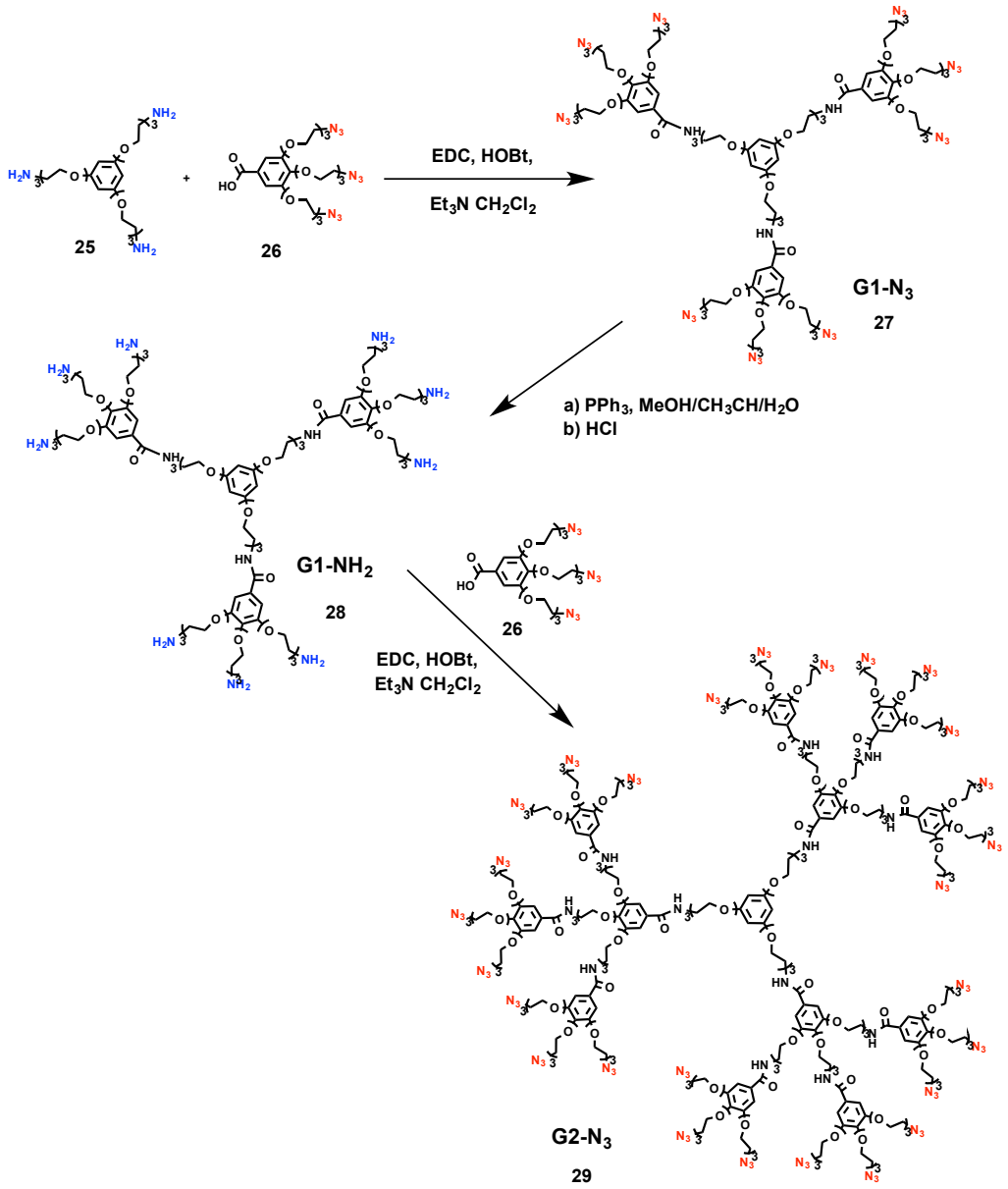

Figure 3.24 Synthesis of GATG dendrimer G_1-N_3 (**27**), G_1-NH_2 (**28**) and G_2-N_3 (**29**). Figure from (Amaral, S.P., *et.al.* Manuscript in preparation)

GATG Core

The GATG core was synthesised from compound **30** previously described [13] to form compound **32** (*Figure 3.25*). The first step involved a nucleophilic attack of the hydroxyl group of **5** to $SOCl_2$ to get obtain chloroalkane **30** as

previously reported [13]. For conjugation of this product to phloroglucinol the electrophilicity of **30** was increased by substitution of the chloroalkane with iodine in acetone to from **31**. In the last step of the reaction, after deprotection of the phenol groups with carbonate, the nucleophilicity of the resulting phenyloxides was increased by the use of 18-crown-6 for trapping the potassium ion. After purification by column chromatography the core **32** carrying 3 terminal azides was obtained in a yield around 60%.

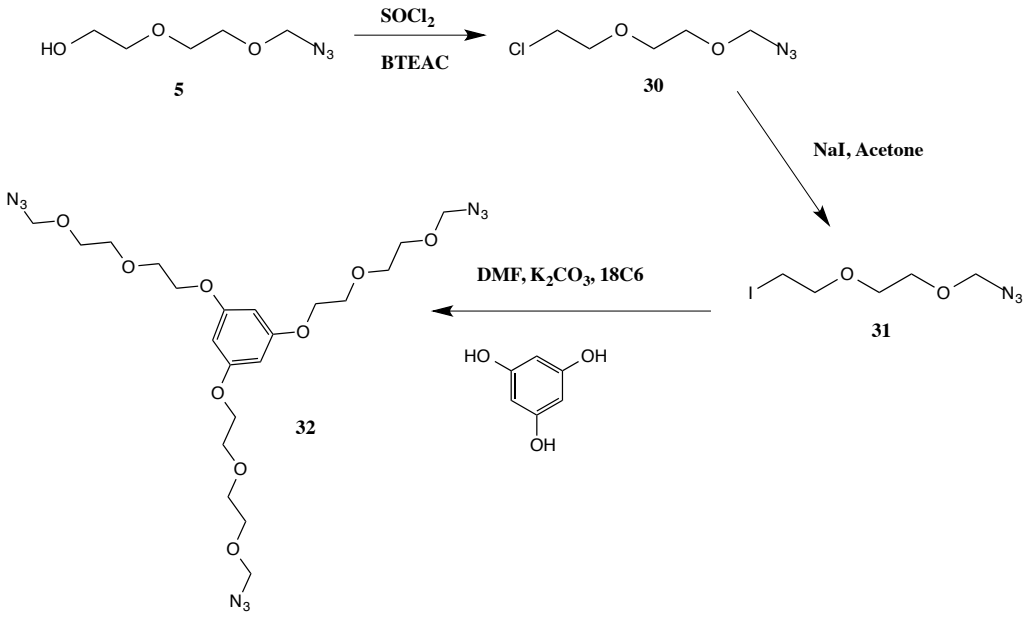

Figure 3.25 Synthesis of core **32** (Amaral. S. P. Manuscript in preparation).

GATG Repeating unit

The efficient synthesis of the repeating unit for GATG dendrimer (**26**) in large scale has been previously reported [13].

GATG divergent synthesis

The terminal azides of the core **32** were reduced under Staudinger conditions (*Figure 3.26)* with PPh_3 in a solvent mixture of methanol, chloroform and water, followed by protonation with HCl to obtain G0-NH_2·HCl (**25**).

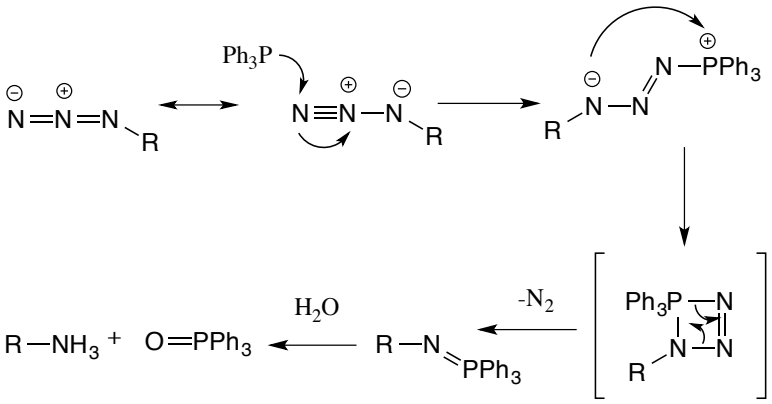

Figure 3.26 Mechanism of Staudinger reduction of azide to amine in the presence of PPh_3.

The reaction was followed by infrared and ^{1}H-NMR, observing the disappearance of the azide peak at 2100 cm^{-1} by infrared (*Figure 3.27*) and a triplet/multiplet around 3.40ppm by ^{1}H-NMR, characteristic of the methylene protons alpha to the azide group (*Figure 3.28*). The repeating unit **26** was coupled to G0-NH_2·HCl (**25**) through formation of an amide bond between the carboxylic acid of the repeating unit and the amine at the core (*Figure 3.30).* EDC and HOBt were used as coupling agents, producing the first generation GATG dendrimer G1-N_3 (**27**) and the corresponding urea. The reaction was followed by the appearance of the already mentioned triple/multiplet around 3.40ppm ($CDCl_3$) and the disappearance of the amine peak (MeOD) around 3.21-3.17 ppm for the methylene proton in a position alpha to the amino groups (*Figure 3.28*). The resultant product was purified by column chromatography.

Following similar reaction conditions second- and third-generation dendrimers G2-N_3 and G3-N_3 were obtained. The final products were characterized by ^{1}H-NMR, ^{13}C-NMR and MALDI-TOF Mass Spectrometry. Size-Exclusion Chromatography (SEC) (*Figure 3.29*) confirmed the identity of these GATG dendrimers. The size of the dendrimers was measured in their amine form by Dynamic Light Scattering (DLS) (*Table 3.1*). GATG dendrimers of generation G1, G2 and G3 with terminal azides were successfully synthesised and were then functionalised with ligands carrying internal alkynes through AAC. In addition, dendrimers were functionalised with boronic acids (See 3.3.5) These dendrimers, along with the amino-functionalized dendrimers were tested for antibacterial properties (see Chapter 4-6).

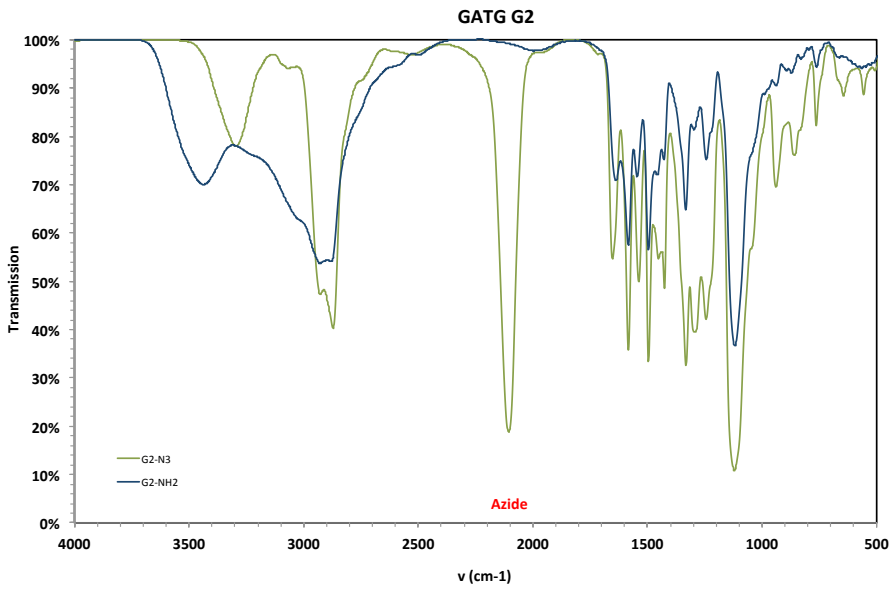

Figure 3.27 Infrared spectra of GATG dendrimer G2-N_3 (green) and G2-NH_2 (blue) confirm the complete reduction of the azide groups.

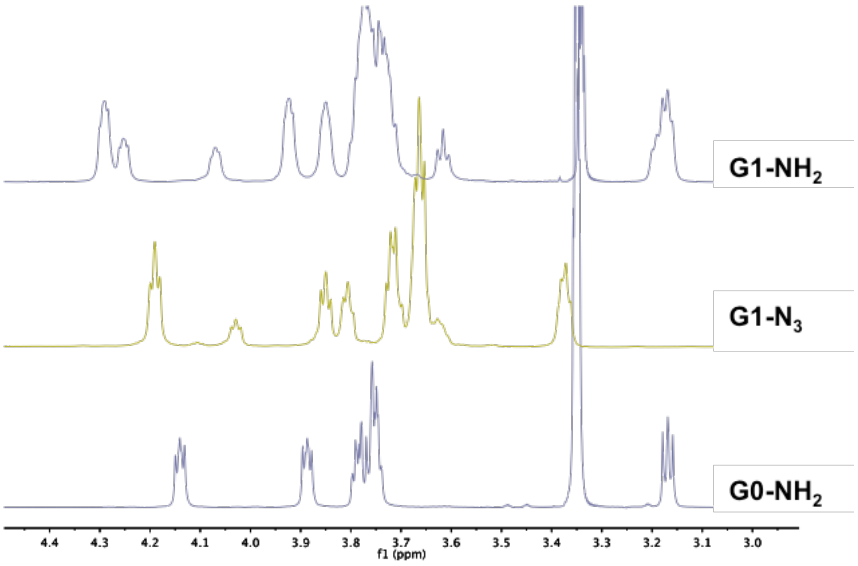

Figure 3.28 ^{1}H-NMR spectra of G0-NH_2, G1-N_3 and G1-NH_2. The reduction of azides was followed by the disappearance of the methylene proton in a position alpha the azide group (3.37 ppm) and the appearance of methylene proton alpha to the amino groups (3.18 ppm). ^{1}H-NMR was performed in CD_3OD.

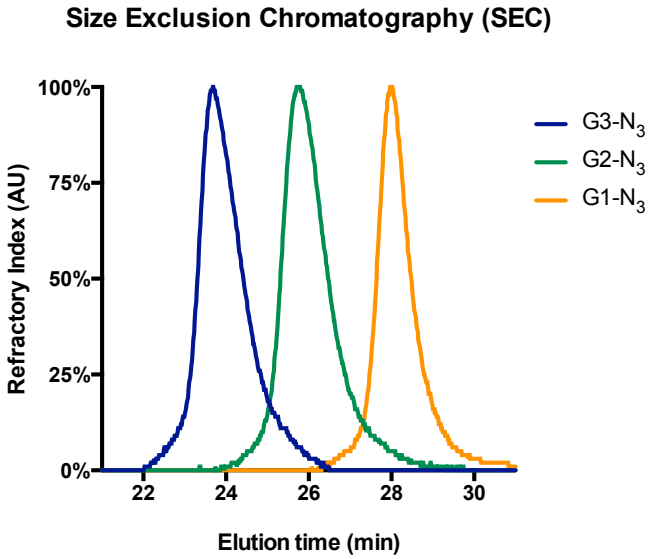

Figure 3.29 Size Exclusion Chromatography for GATG dendrimer G1-N_3 (orange), G2-N_3 (green) and G3-N_3 (blue). THF was used as an eluent at 1 mL/min and samples were filtered through 0.45 µm before injection.

Cationic Dendrimers			
	Amines	Theoretical Mw	Size (nm)
G1-NH_2	9	2 389	n/a
G1-NH_2	27	7 765	3.62 ± 0.42
G3-NH_2	81	23 891	5.68 ± 0.39

Table 3.1 Number of surface amines, calculated molecular weight and size (as determined by DLS at 25 °C with hydrochloride amino dendrimers (1.5 mg/mL) in a 10 mM NaH_2PO_4 10% HCl 0.1M solution

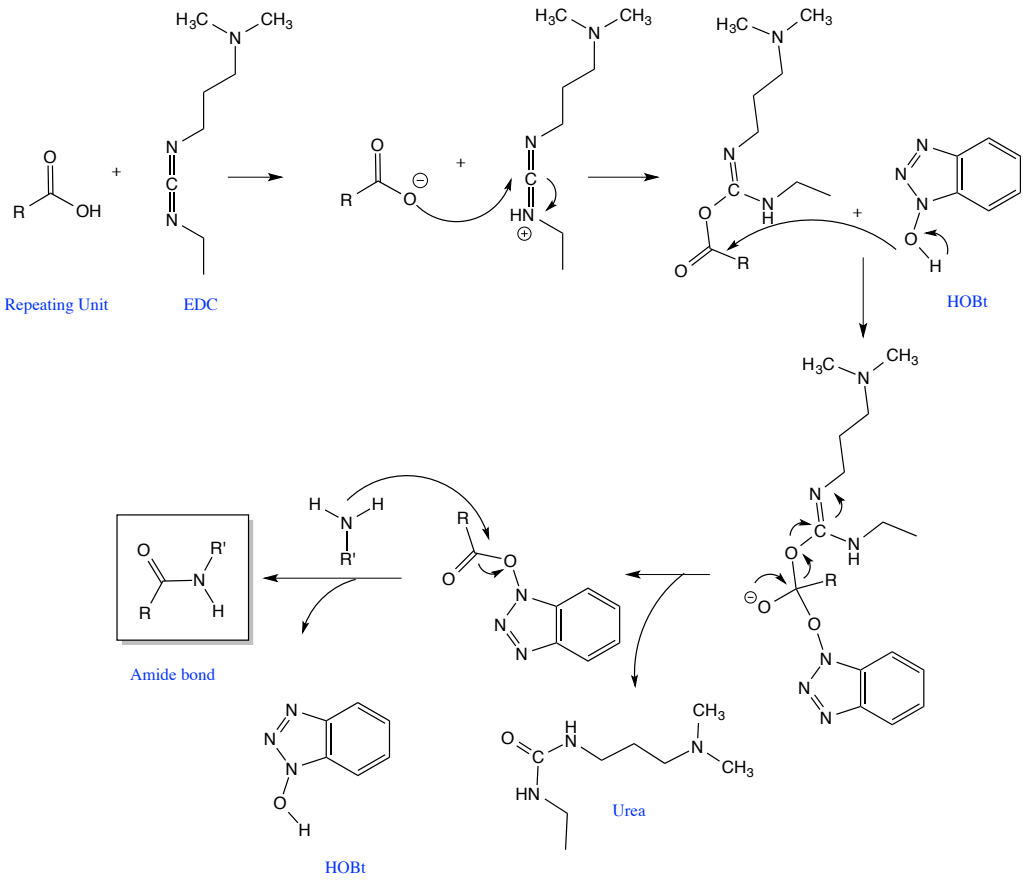

Figure 3.30 Mechanism of formation of an amide bond between the carboxylic acid of the repeating unit and the amine of the core, using EDC and HOBt as coupling agents. Figure modified from [28].

3.3.3 AAC FUNCTIONALIZATION OF GATG DENDRIMERS

Dendrimers grow in multivalency and size with each generation enabling precise control over both. The aim of this PhD was to understand how size and number of functional groups affects the interactions with bacteria. In order to evaluate any significant differences between the dendrimers in these two properties, dendrimers of generation G1 (9 azides) and G3 (81 azides) were chosen. The larger dendrimer was expected to have 9 times as many functional groups in the periphery and a significant difference in size.

3.3.3.1. Microwave-assisted functionalization of GATG dendrimer through Azide-Alkyne Cycloaddition

The initial strategy was to functionalise the dendrimers through microwave-assisted AAC. It was expected to be able to reach high temperature and a homogenous heat transfer in the sample, thereby facilitating the AAC reaction and shortening the reaction time. A wide range of reaction have been performed using microwave-assisted synthesis, including reactions of compounds with internal alkynes and azidomethyl phosphonates [26]. Esters derived from acetylenedicarboxylic acid have successfully been used for the microwave-assisted AAC divergent synthesis of new families of dendrimers (Correa J.F., Amaral S.P., *et. al. Manuscript in preparation*). Based on this synthesis route, a fixed power setting with air-cooling was used. The fixed-power setting was aimed to ensure that the microwave would irradiate the sample with appropriate power to keep the temperature at the target level. Control of the target temperature for the microwave was based on Infrared

measurement of the outside wall of the vial. The air-cooling reduced the temperature so that more radiation was needed to keep the sample at target temperature, thus increasing the effect from microwave radiation.

Using (**5**) as model system together with the tetraol ligand (**4**), optimizations of solvents, microwave power, target temperature, air cooling and equivalence of ligand were performed to find conditions suitable for the microwave-assisted AAC functionalization of the GATG dendrimers (*Figure 3.32*). The goal was to get full functionalization (100% conversion) of dendrimers without any decomposition of the material (*Table 3.2*). A t-BuOH/water mixture was preferred to water mixtures with THF and DMSO, which seemed to give small amounts of decomposition. Using higher fixed power settings (200 W) has been shown to make the temperature control more challenging, while a lower power (80 W) might fail to reach a temperature of 100 °C and therefore increase the reaction time. Therefore, the microwave settings were fixed at 100 W, with a target temperature of 100 °C and air-cooling of 14 psi. After 4 h, with 1:1 molar ratio of the reactants in t-BuOH-H_2O, the conversion was 100 % using the model system (as measured by integration of the azide triplet at 3.38-3.34 ppm relative to the triazole peaks at 5.29-5.12 ppm in ^{1}H-NMR)

The G1-N_3 was functionalised with tetraol ligand (**4**), using the conditions from the model system, increasing the number equivalents of the ligand to 1.5 to ensure a faster and complete functionalization. The reaction was followed by infrared (disappearance of the azide peak at ca 2100 cm^{-1}) and was run for 4.5 h, to 100% conversion. The peaks at 5.29-5.26ppm and 5.17-5.12ppm (*Figure 3.31, 3.36*) were representative of the protons of the carbon alpha to the triazole. When the reaction was run at higher power setting (150 W), the tetraol

ligand was completely decomposed. A small degree of decomposition was observed also in the ^{1}H-NMR spectra for the reaction with 100 W microwave power (*Figure 3.31*).

It was rationalized that as a result of the high temperature conditions, intramolecular cleavage of the carbamate bond was taking place with participation of the serinol hydroxyl groups through a five-membered ring. As a result, a product identical to that obtained by AAC with 2-butyne-1,4-diol (**1**) was isolated. Thus, the protons of the alpha carbon were shifted upfield, to 4.67 ppm as visible in the ^{1}H-NMR spectra (*Figure 3.31*). Integration of the protons of the alpha-carbon to the triazole with the tetraol ligand compared to the alpha carbon protons to the 2-butyne-1,4-diol (decomposed ligand) made it possible to calculate the degree of decomposition, which for G1-tetraol was 5%.

Reaction	Power	Temp (maxtemp)	Cooling (psi)	Ligand Eq.	Time(h)	Conversion	Notes
Model + Tetraol	**200W**	**100**	20	1	1	63 %	NMR Ok.
Model + Tetraol	**100W**	**100**	14	1	4	100%	Decreased cooling to 14.
Model + Tetraol	**80W**	**90**	14	1	4.5	80 %	NMR Ok.
G1+Tetraol	**150W**	**100** (126)	20	1.2	2.5	100%	100% decomposition
G1+Tetraol	**100W**	**100** (115)	14	1.5	4	100%	5 % Decomposition after purification
G1+Tetraol	**80W**	**80** (94)	14	2	2	70%	More decomposition with more eq. of ligand

Table 3.2 Optimization of microwave-assisted AAC using model system and G1-N_3. The microwave settings were fixed power. The best conditions were found to be 100W, with target temperature 100°C, cooling 14 psi in t-BuOH/H_2O (1:1). Conversion was measured by integration of the CH_2 alpha to azide signal in ^{1}H-NMR (3.38-3.34ppm) to the CH_2 alpha to triazole signal (5.29-5.12 ppm).

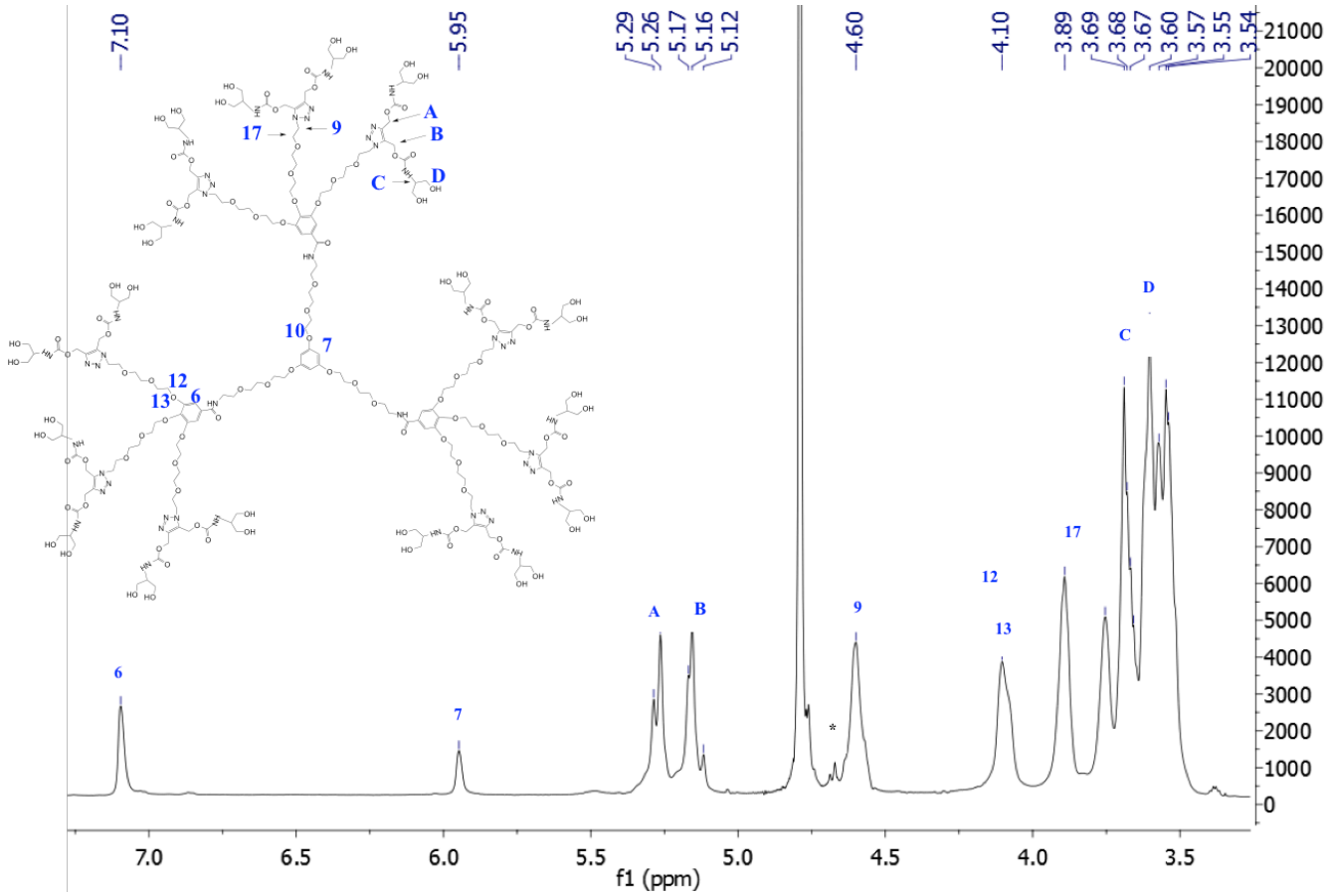

Figure 3.31 ^{1}H-NMR of G1-Tetraol in D_2O. The degree of decomposition (*) was measured by integration compared to alpha to the triazol (peak A and B) at 5.29-5.12 ppm.

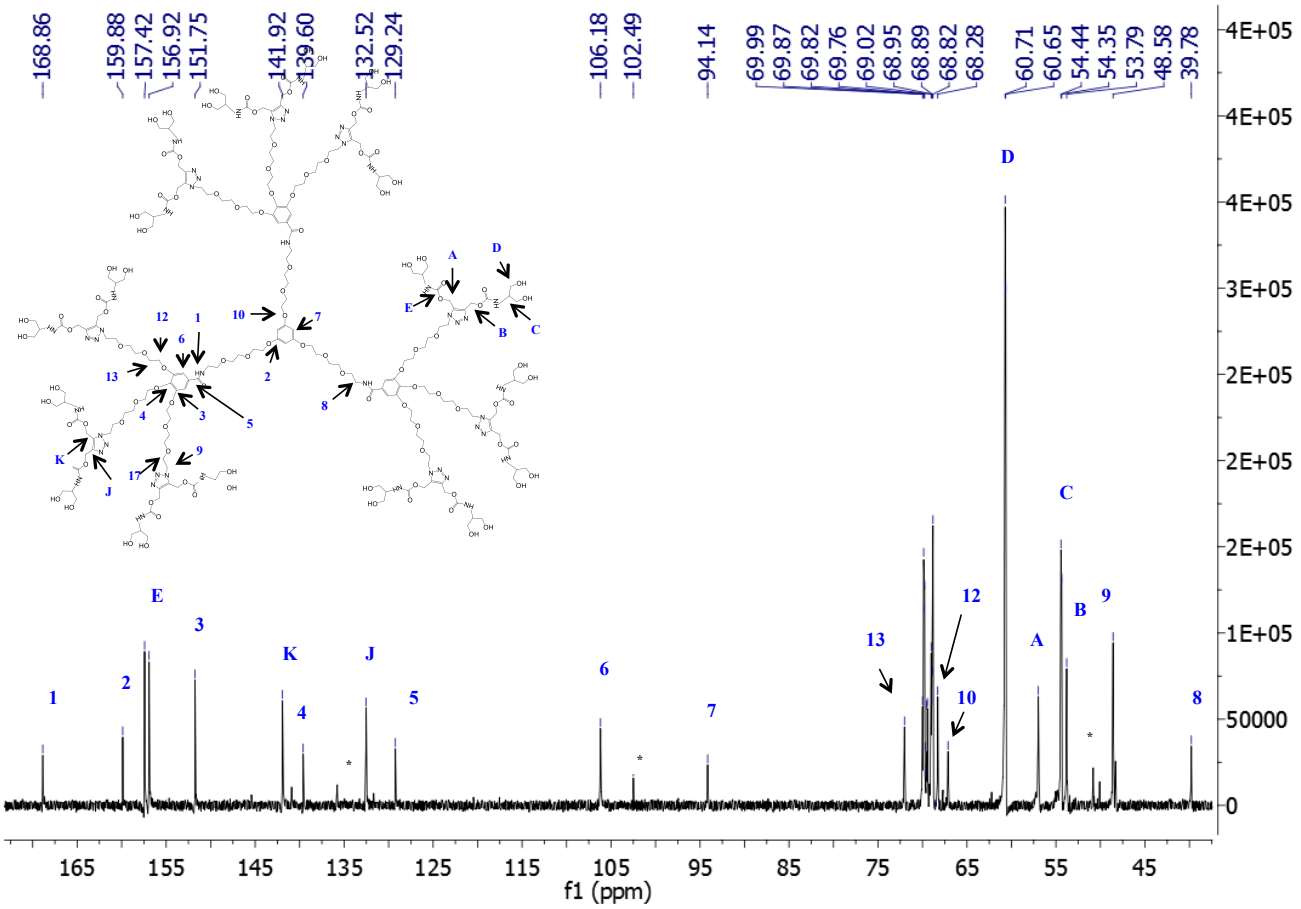

Figure 3.32 ^{13}C-NMR of G1-Tetraol in D_2O.

G1-diol and G1-glucose were synthesised using similar conditions used to the synthesised G1-tetraol. The target temperature was increased to 110 °C and the cooling 20 psi and equivalence of ligand reduced to 1.2. Reactions were followed by infrared (*Figures 3.33, 3.34*) and full conversion was reached after 2 h 15 min.

However, using the same conditions for functionalization of the higher generations (G3) was more challenging. The G3 was conjugated with the diol ligand (**7**) using the same conditions, although with some degree of decomposition. Decomposition was also observed when AAC conditions from G1 were applied to G3 with tetraol- (**4**) and glucose-ligands (**12**). Using lower temperature and power (80 °C/80 W) increased the reaction time but did not avoid the decomposition.

As observed, the reaction mean temperature was increased during the time course of all the microwave-assisted AAC experiments, and maximal temperature reached 14 – 26 °C above target temperature for G1-tetraol (*Table 3.2*). As a consequence, although all the ligands alone were stable under the microwave-assisted conditions, when used in the reaction with the dendrimer, ligand decomposition was observed for the pairs G1-tetraol and G3- diol. More decomposition was obtained with higher dendrimer generations when the same conditions were applied. It was rationalized that the high temperatures required for the reaction to proceed resulted in decomposition of the dendrimers under the conditions developed for the model system, while the use of lower temperatures and power prevented the reaction from occurring in times short enough to make the reaction efficient. The successful microwave-assisted

synthesis of dendrimers by AAC developed by our group (Correa, J.F., Amaral S.P., *et al. Manuscript in preparation*) was indeed done under much milder reaction conditions because of the activated nature of internal alkynes derived from acetylenedicarboxylic acid. The prolonged time in combination with poor temperature control could explain why the microwave-assisted AAC was unsuccessful for higher generations. In addition, the temperature fluctuation and maximal temperatures during the reactions under microwave irradiation were not reproducible between repeated experiments with the same ligand either for G1 or G3.

Although G1-tetraol, G1-diol, G3-diol G1-glucose were obtained through microwave-assisted AAC with only small decomposition in some cases (G1-tetraol, G3-diol), the G3 derivatives of tetraol, glucose and mannose could not be functionalised under these conditions. A thermal AAC reaction, using a heat bath to increase the temperature, although prolonging the reaction time, enabled better control over the temperature and was considered a better alternative than microwave-assisted AAC for the conjugation of these ligands to GATG dendrimers. To obtain good, reliable conjugation of GATG dendrimers with the above alkynated ligands, in the absence of any catalyst it was decided to test whether thermal AAC conditions could represent any advantage compared to microwaves. Clearly, longer reaction times were expected, but in the absence of decomposition, they would represent better conditions for the functionalization of dendrimers if reaction times below 10 h under aqueous conditions could be developed by tuning the temperature and the dendrimer-ligand ratio.

3.3.3.2. Thermal Azide-alkyne cycloaddition for functionalization of GATG dendrimers

The synthesis of model compounds and the optimization for the thermal reactions (Table 3.3 and Figure 3.33) was done by Dr. Juan Francisco Correa at University of Santiago de Compostela Spain.

To see how conditions from microwave-assisted AAC would translate into thermal AAC, the same temperature, solvent and number of equivalents of ligand were used as initial conditions for the synthesis of G1-mannose. The thermal reaction was performed using a small Schlenk- flask in a silicon oil bath; conversion was followed by infrared spectroscopy. The small volume of the sample (0.05 mL) and the temperature being above boiling point (*t*-BuOH boiling point 82 -83 °C) lead to difficulties for adequate stirring of reaction. An extra 0.05 mL of solvent and 0.2 equiv. per N_3 of mannose ligand were added to the reaction, and after 64 h the reaction was complete. The reaction was clearly much slower compared to the microwave conditions of 2-4 h.

A series of reactions with a model system (*Figure 3.33*) was performed to understand the importance of solvent and temperature on the kinetics of the reaction with the aim to find the conditions for the most efficient conversion and a faster reaction time (*Table 3.3*). The model ligand (**5**) contained the same basic structure as the final target compound, with carbamate functionalities adjacent to the alkyne and was prepared in-house following same conditions as for tetraol and diol synthesis, by activation of (**1**) with DSC and amine substitution with propylamine (*Figure 3.33*). The number of equivalents of ligand was kept at 1 per N_3 in the model system.

Reaction	Solvent	Temp (ºC)	Solvent Conc. (M/N_3)	Reaction time (h)	Conversion (by IR)
1	tBuOH/H_2O 1:1	100	1	9	90 %
2	tBuOH/H_2O 4,75:1	100	1	9	85 %
3	tBuOH/H_2O 3,3:1	100	1	9	85 %
4	tBuOH	100	1	9	95 %
5	tBuOAc	100	1	9	95 %
6	AcoPr	110	1	9	90 %
7	tBuOAc	100	2	9	90 %
8	tBuOAc	110	1	6	100 %
9	tBuOAc	120	1	4	100 %

Table 3.3 Optimization of thermal AAC using model system. Conversion was measured by integration of the CH_2 alpha to the azide signal by ^{1}H-NMR to CH_2 alpha to the triazole signal.

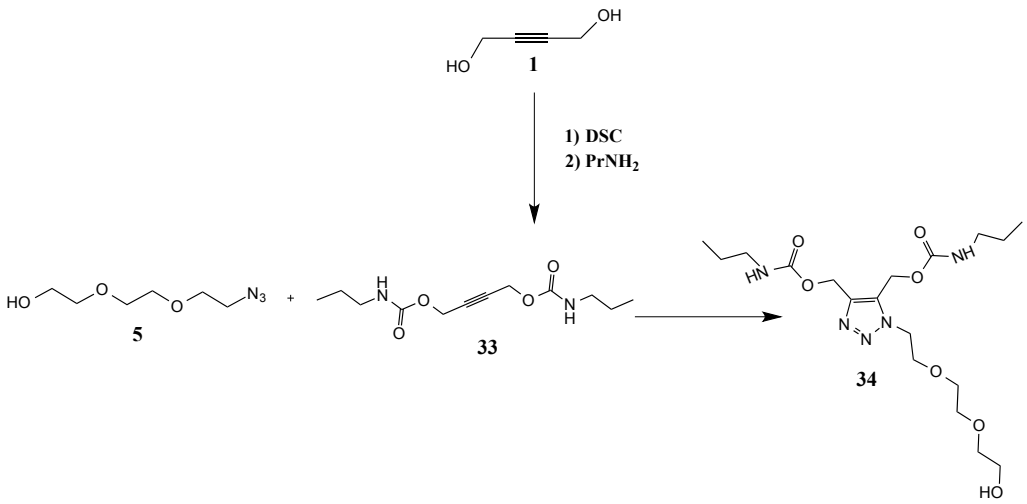

Figure 3.33 Models reaction for the optimization of conditions for thermal AAC.

The conversion was measured by integration of the CH_2 alpha to the azide signal by ^{1}H-NMR to the CH_2 alpha to the triazole signal. Measuring conversion with NMR or IR is not very accurate and generally has a deviation of 5-10%. The calculated values serve as an indication of what factors are important to increase the conversions. The conversion decreased slightly with increased amount of water in the solvent mixture (*Table 3.3)* while using the tBuOH alone gave the shortest reaction time (Reaction 4, 14 h). The use of

tBuOAc with a higher boiling point than tBuOH (97.8 °C compared to 82-83 °C), afforded the same reaction time (Reaction 5) pointing to a low solvent effect in the kinetics. The solvent concentration was not important for the kinetics of the reaction, when increased from 1 M azide concentration to 2 M, the conversions did not increase. The most important factor for the increase in conversion, except for the equivalents of the ligand, was the temperature. By increasing from 100 to 120 °C, the reaction time to completeness decreased from over 9 h to 4 h for the model system. It was known from previous experiments that functionalization of dendrimers was slower than for the model system, so the equivalents of ligand were increased from 1 to 2, which resulted in faster reaction according to a first order kinetics.

Following these conditions, G3-Glucose and G3-mannose were synthesised using a thermal AAC reaction. By increasing the temperature to 120 °C, and the number equivalents of ligands (from 1.2 to 2 equiv. per N_3) the reaction time for the functionalization of the dendrimer was decreased from >60 h to 14 h. However, the reaction was not followed during the complete time period of the reaction, and based on the thermal AAC using the model system, it is believed it is possible that the reaction time could be further reduced. The reaction conditions were reproducible and no decomposition was observed.

All AAC reactions (thermal and microwave-assisted) were followed by infrared spectroscopy via the disappearance of the azide-peak at 2100cm^{-1}) as presented in (*Figures 3.34-3.35 and Appendix Figures A29-A32*).

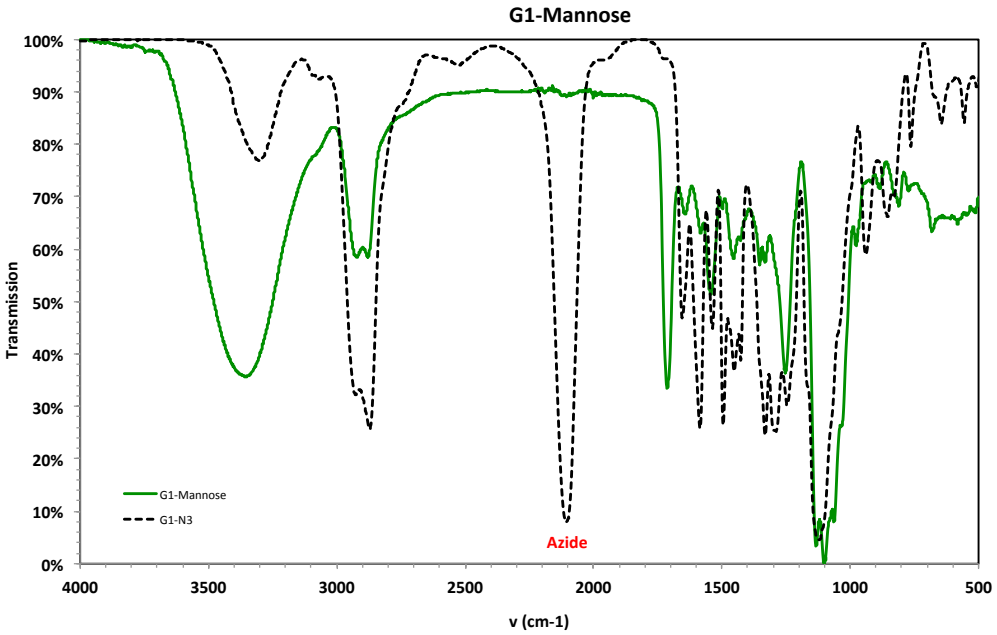

Figure 3.34 Infrared spectra of G1-Mannose (MeOH) prepared under thermal AAC conditions. The complete functionalization was confirmed by the disappearance of the azide peak of G1-N_3 (2106 cm^{-1}).

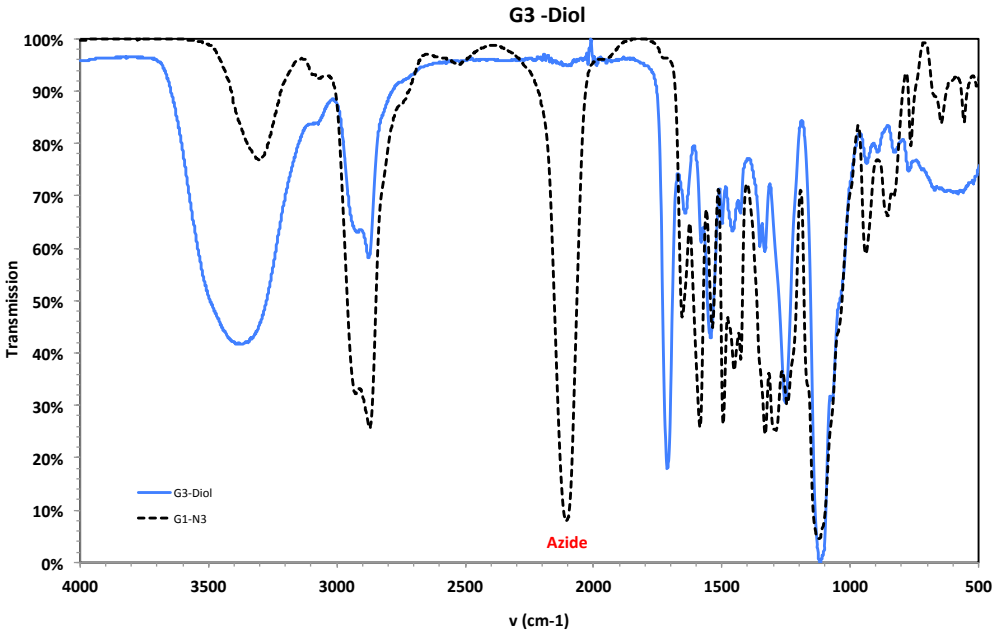

Figure 3.35 Infrared spectra of G3-Diol (MeOH) prepared with microwave-assisted AAC. The complete functionalization was confirmed by the disappearance of the azide peak of G-N_3 (2106 cm^{-1}).

Dendrimers were characterised with NMR, SEC, DLS. (*Figures 3.36,3.37 and Appendix Figures A25-A34*). The disappearance of the CH_2 alpha to the azide signal (3.37 ppm) and the appearance of the CH_2 alpha to the triazole signal (5.29-5.16ppm), as seen by ^{1}H-NMR confirmed successful AAC reactions (*Figure 3.36*).

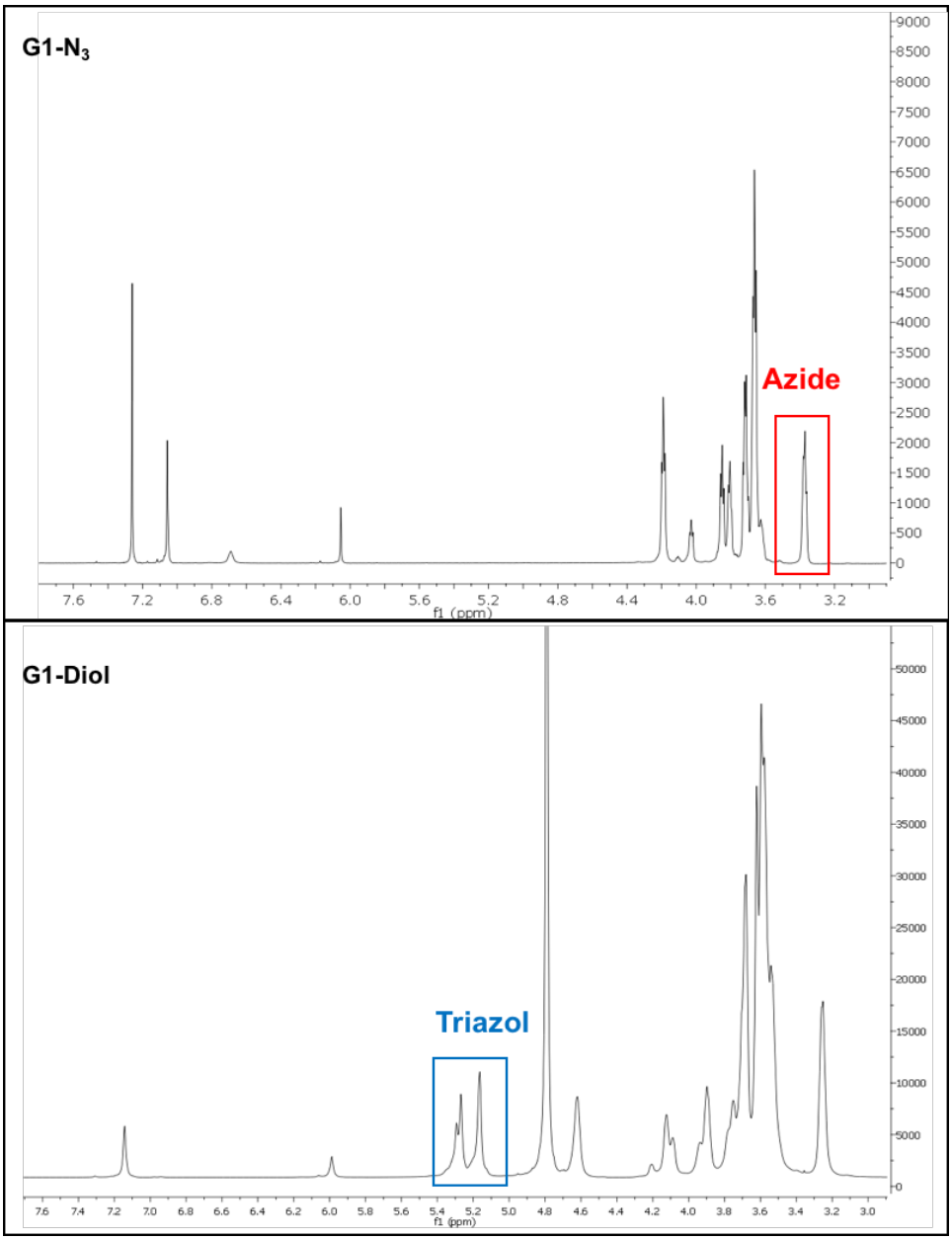

Figure 3.36 ^{1}H-NMR spectra of G1-N_3 and G1-Diol. AAC confirmed by the disappearance of the CH_2 alpha to the azide signal (3.37 ppm, azide) and the appearance of the CH_2 alpha to the triazole signal (5.29-5.16ppm, triazol), ^{1}H-NMR for the G1-N_3 was performed in $CDCl_3$ and G1-Diol in D_2O

Remarkably, functionalised dendrimers were monodisperse as observed by SEC *(Figure 3.37 and Appendix Figure A34*).

The size range was 3 nm for generation G1 and around 8-10 nm for G3, as determined by DLS (*Figure 3.38, Table 3.3*). A summary of the characteristics of the AAC-functionalised dendrimers is presented in *Table 3.4*

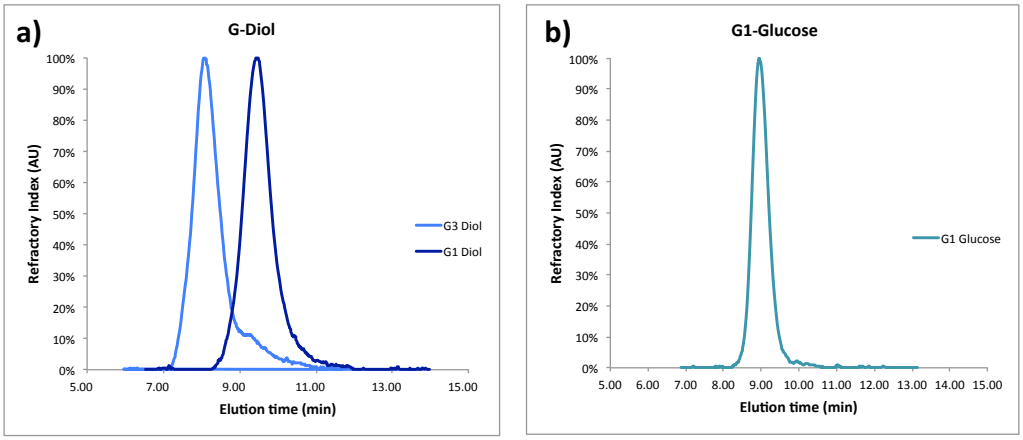

Figure 3.37 Size Exclusion Chromatography for GATG dendrimer a) G1-Diol (dark blue) and G3-Diol (light blue) and b) G1-Glucose. 150 mmol LiCl was used as an eluent at 1 mL/min and samples were filtered through 0.45 μm before injection.

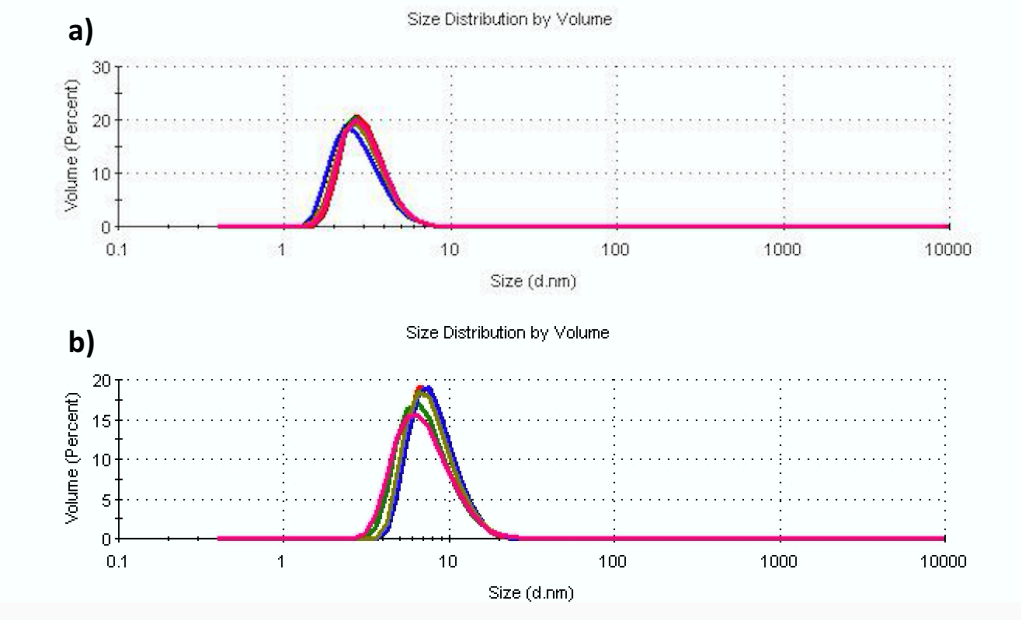

Figure 3.38 Dynamic Light Scattering (DLS) as size distribution by volume for G1-Diol (a) and G3-Diol (b). Samples at 1 mg/mL in 150 mmol LiCl. Shown are five measurements of each sample.

Dendrimer	G1			G3		
	Theoretical MW	Functional groups	Size	**Theoretical MW**	Functional groups	Size
Gn-Diol	6332.59	18	3.1 nm	59 382.36	162	8.1 nm
Gn-Tetraol	5279.39	18	3.6 nm	-	-	-
Gn-Glucose	9251.12	18	3.7 nm	85 649.13	162	10.0 nm
Gn-Mannose	9251.12	18	3.5 nm	85 649.13	162	9.1 nm

Table 3.4 Summary of characterisation of G1 and G3 dendrimers functionalised through AAC. Molecular weight (MW), Number of functional groups (-OH, -$(OH)_2$, -Glucose, -Mannose), Size as measured by DLS in 150mmol LiCl.

The functionalised G1 dendrimers were obtained in lower yields than G3 (60-84%) after ultrafiltration in H_2O. TLC and NMR of the crude product confirmed only the presence of excess ligand and functionalised dendrimer

after AAC. The filtrate from purification contained only ligand and ligand linked to dendrimers, as confirmed by NMR and TLC, suggesting that the loss of mass is due to the purification associated with their low molecular weight (MW cut-off used 1000 Da). However, the G3 –mannose dendrimer was obtained in very good yields (93%), and the G3-diol and G3-glucose in 76% yields. The greater yields were likely due to the better retention of the higher molecular weight dendrimers during ultrafiltration. Using an acetone/water mixture might further increase the yields as the pores of the cellulose filter close under this solvent system, which could improve the retention of G1.

Due to the preliminary microbiological experiments with G1-tetraol (Chapter 4) and time constraints, the synthesis of G3-tetraol was not addressed within this thesis.

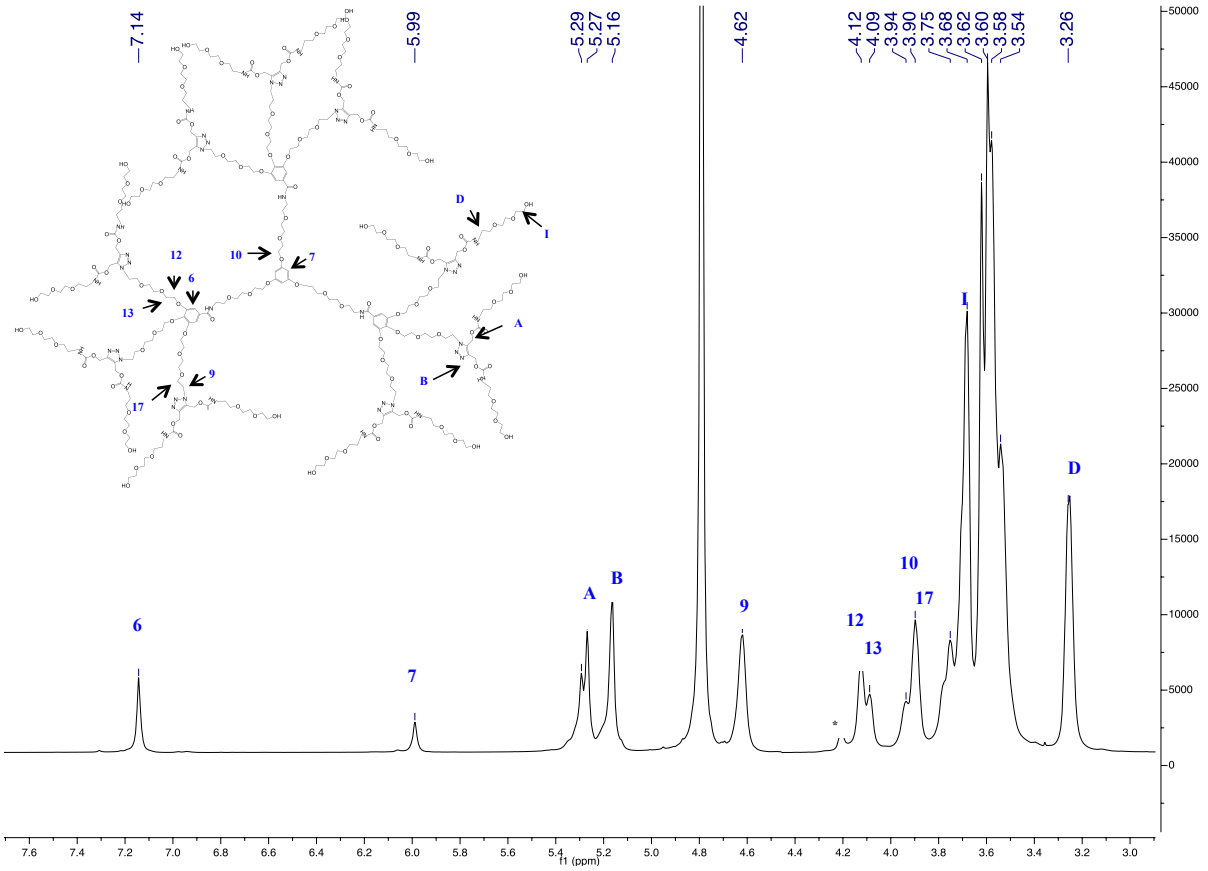

Figure 3.39 ^{1}H-NMR of G1-Diol in D_2O

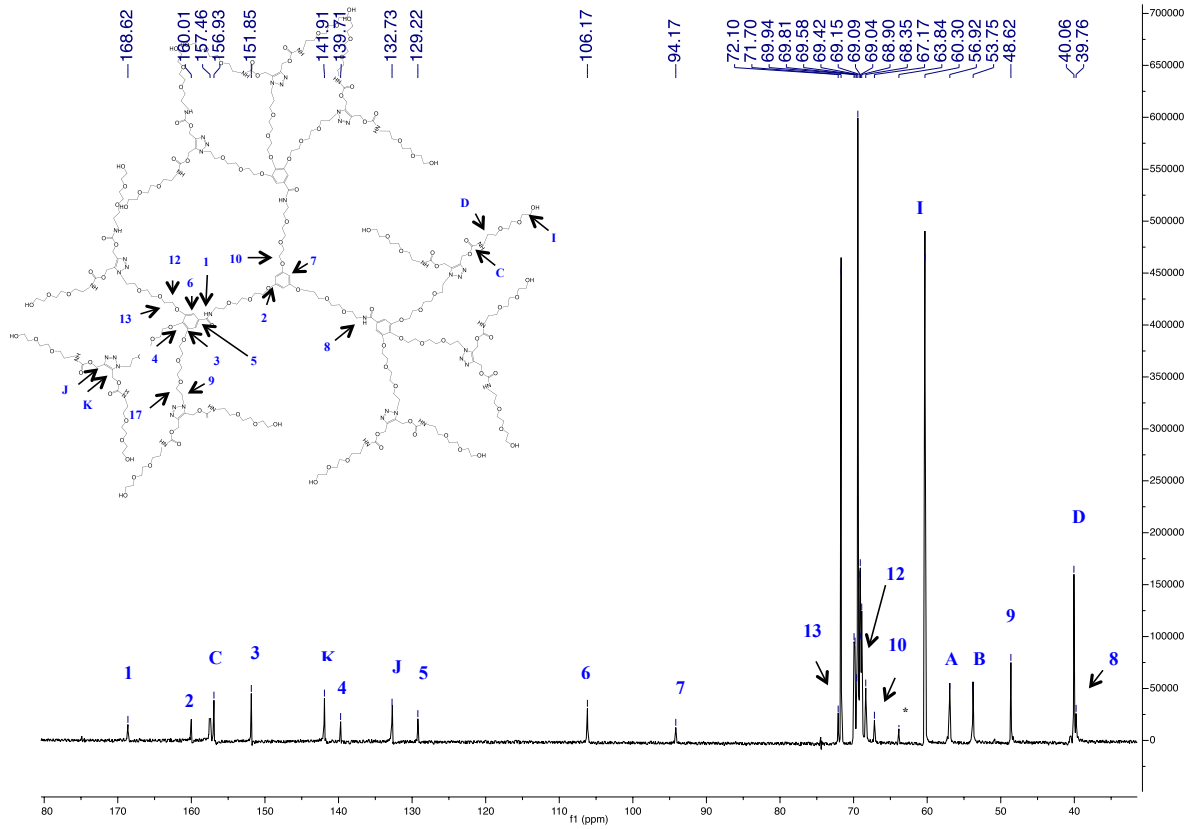

Figure 3.40 ^{1}H-NMR of G1-Diol in D_2O

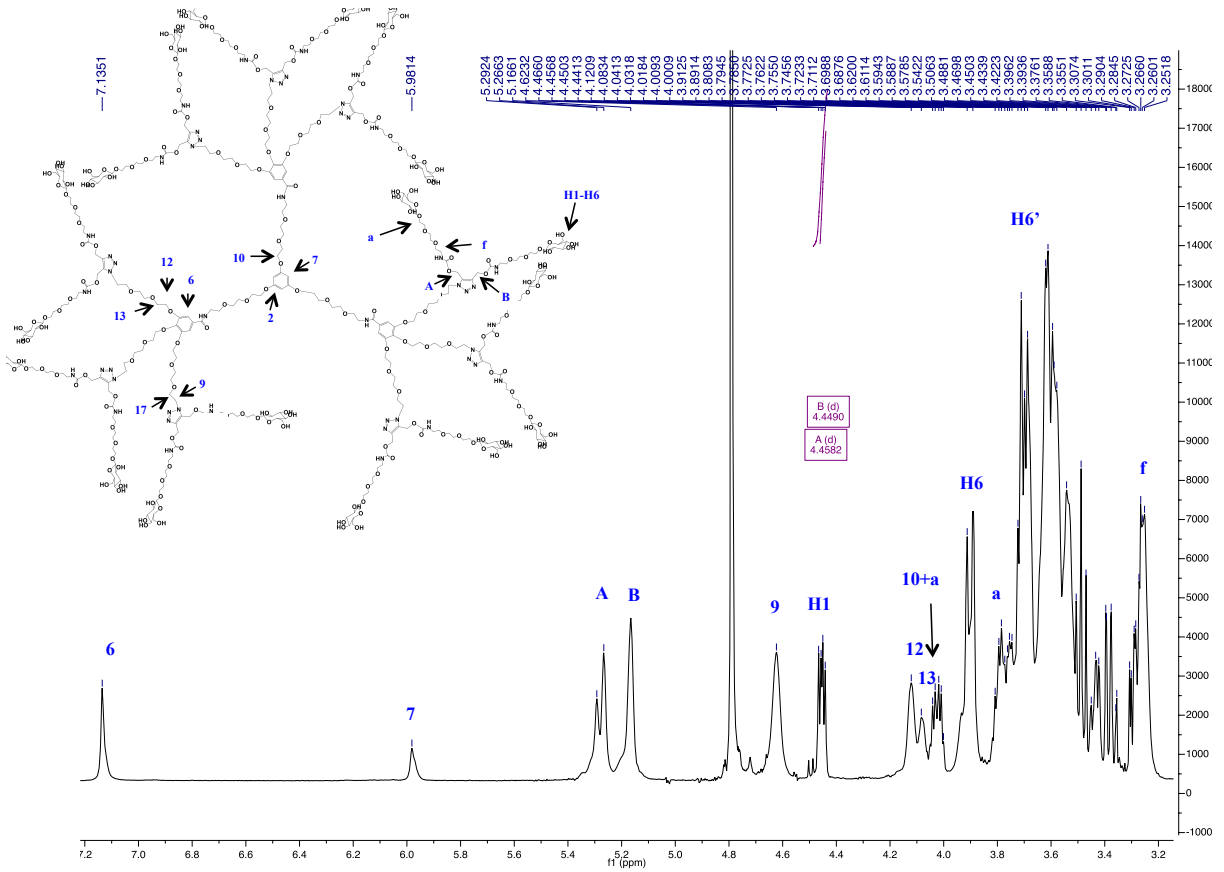

Figure 3.41 ^{1}H-NMR of G1-Glucose in D_2O. The anomeric position at 4.46-4.44 ppm is composed of two doublets with the *J*-coupling constant of 7.8 Hz each.

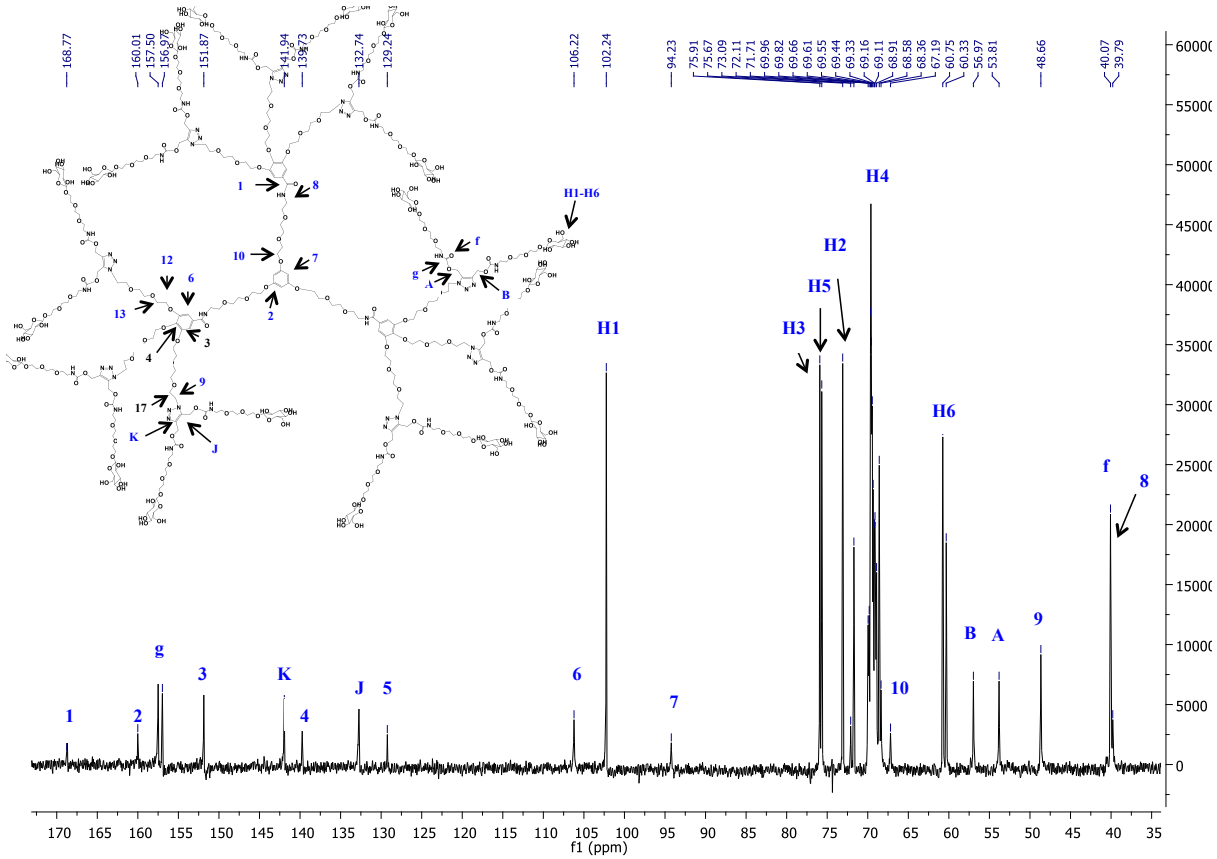

Figure 3.42 ^{1}H-NMR of G1-Glucose in D_2O

3.3.4. GATG Gn-B(OH)$_2$ dendrimers

Dendrimers with terminal phenylboronic acids were synthesised, following modified protocols of those previously established for PEG-GATG block copolymers in the group (Amaral et.al., *unpublished results*), aiming to substitute the borate binding to S-THMF and quenching of AI-2. In addition, these dendrimers might have affinity for the quinolone PQS, a QS molecule of the important human pathogen, *P. aeruginosa (Figure 3.43*).

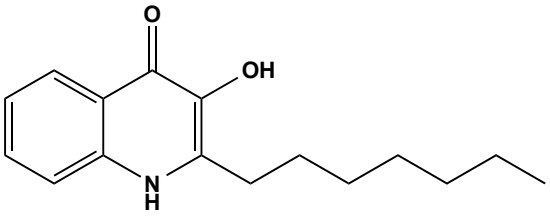

Figure 3.43 Structure of QS molecule PQS

A preliminary experiment showed solubility of PQS in the presence of phenyl-boronic acid in $CHCl_3$, while PQS was completely insoluble in $CHCl_3$ alone (data not shown) suggesting binding affinity of PQS to phenylboronic acid. However, due to the time constraint, these experiments were not further elaborated.

GATG dendrimers of generation G1 and G3 were functionalised with phenylboronic acid through a two-step-one-pot protocol (Amaral et.al., *unpublished results*). To this end, azides were reduced to primary amines in the presence of PPh_3, through Staudinger reactions. After complete reduction, as confirmed by infrared spectroscopy, 2-formylphenyl boronic acid was added to afford an imine (*Figure 3.44*). The nucleophilic amine attacks the carbonyl of

the aldehyde followed by proton transfer from the amine to the OH and removal of water forms the imine.

In the final step, $NaBH_4$ is added to the reaction to reduce the imine to an amine (*Figure 3.45)*. The hydride ion reacts with the electrophilic carbon atom, followed by protonation of the anion to generate the final amine.

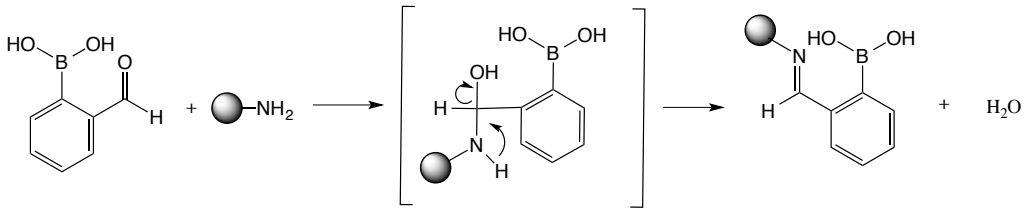

Figure 3.44 Mechanism of reaction between the aldehyde of 2-formylphenylboronic acid and the amine of the dendrimer to the formation of an imine.

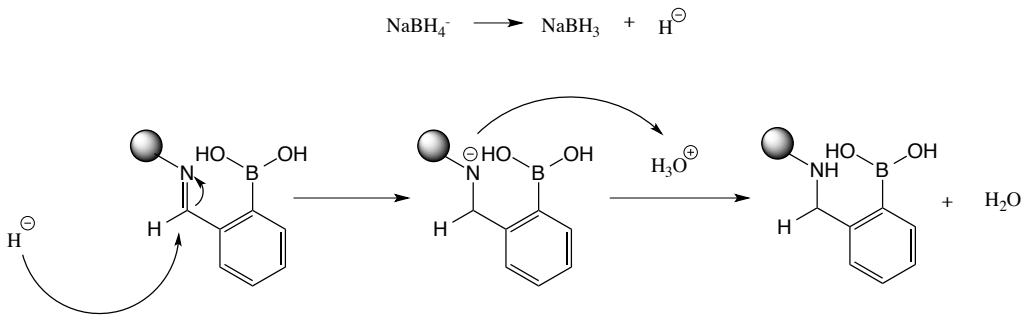

Figure 3.45 Mechanism of imine reduction to amine by $NaBH_4$

The G3-$B(OH)_2$ dendrimer was purified by dialysis and was obtained in excellent yields. (98%) However, the G1 analogue was more difficult to purify due to its small size, with dialysis with the MW cut-off 1Da affording only 5% yield.

In both examples, the complete reduction of azides was confirmed by infrared spectroscopy (*Figure 3.47)* and the functionalization with phenylboronic acid by integration in ^{1}H-NMR (*Figure 3.46 and Appendix Figure A35*) of the benzylic protons (alpha to phenylboronic acid) at 2.96ppm (A) and those of the phenylboronic ring at 7.12-6.88 ppm (B-E). ^{13}C-NMR for G3-$B(OH)_2$ is presented in *Appendix, Figure A36*. Due to the limited amounts available of G1-$B(OH)_2$, the ^{13}C-NMR of this sample was not recorded. Summary of characterisation is presented in *Table 3.5* and in section 3.2.4. Dendrimers G1 and G3 with boronic acid were completely water-soluble. No aggregation was observed by DLS (*Figure 3.48*). Due to strong binding to polyols, SEC was not performed to measure molar mass dispersity as boronic-dendrimers have been noted to be retained strongly on SEC columns.

Boronic acid Dendrimers			
	$B(OH)_2$	Theoretical MW	Size
G1-$B(OH)_2$	9	3 390.01	2.7 nm
G3-$B(OH)_2$	81	32 735.04	6.0 nm

Table 3.5 Summary of characterisation of G1-$B(OH)_2$ dendrimers. Molecular weight (Mw), Number of functional groups, Size as measured by DLS in 150 mmol LiCl at 1 mg/mL.

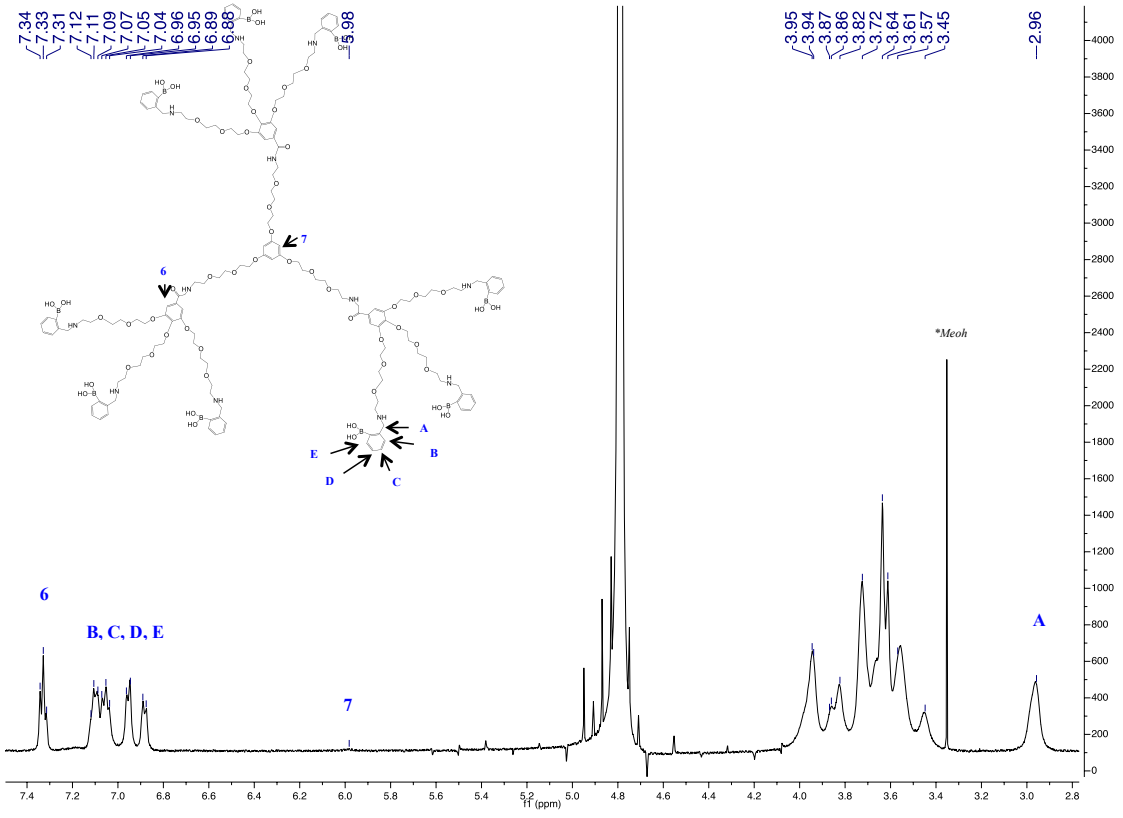

Figure 3.46 ^{1}H-NMR of G3-B(OH)$_2$ in D_2O. The complete conjugation of phenylboronic acid was confirmed by integration the benzylic protons (alpha to phenylboronic acid) (A) and those of the phenylboronic ring (B-E).

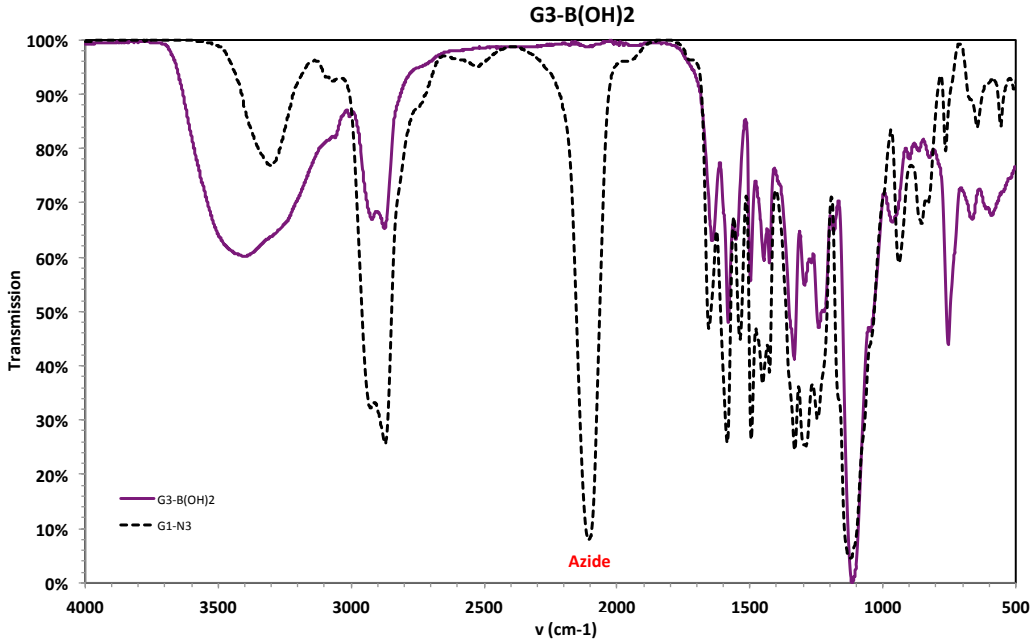

Figure 3.47 Infrared spectra of G3-B(OH)$_2$ (MeOH). The complete reduction of the azide was confirmed by the disappearance of the azide peak of G-N$_3$ (2106 cm^{-1}).

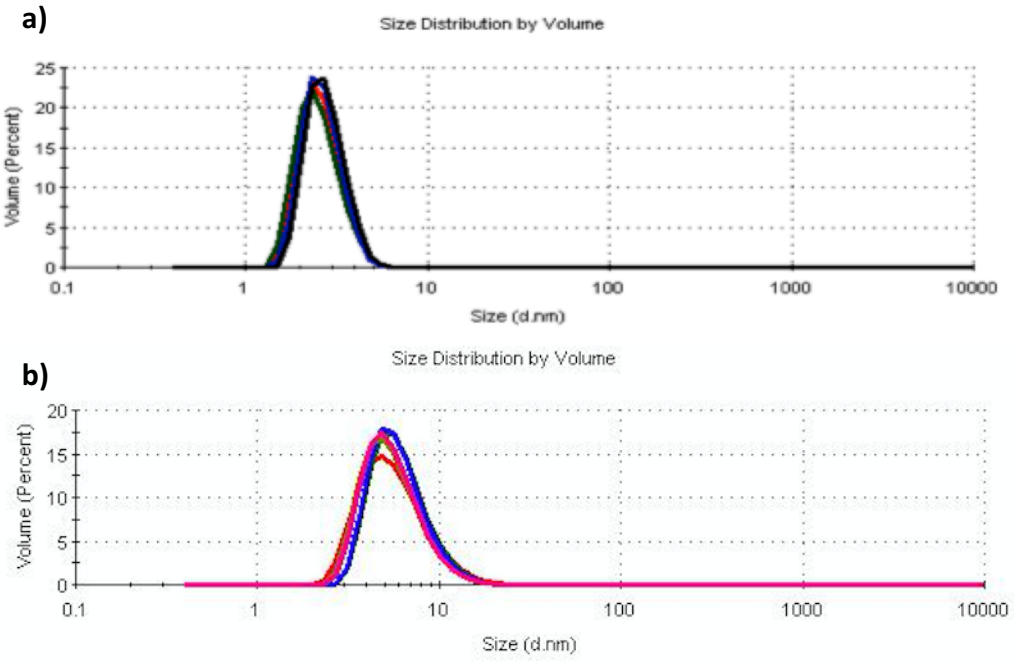

Figure 3.48 Dynamic Light Scattering (DLS) as size distribution by volume for G1-B(OH)$_2$ (a) and G3-B(OH)$_2$ (b). Samples at 1 mg/mL in 150 mmol LiCl. Shown are five measurements of sample.

3.4 CONCLUSIONS

In this chapter the synthesis and characterisation of novel alkynated ligands with diol, tetraol, glucose and mannose functionalities are described. A fast and efficient catalyst-free functionalization of dendrimer was developed using thermal AAC. The ligands were successfully conjugated to GATG dendrimers of G1 and G3, resulting in dendrimers with 18 and 162 functional groups in the periphery. The dendrimers were monodisperse, as confirmed by SEC and with a size range of 3-10 nm as determined by DLS.

GATG dendrimers of generation G1 and G3 were synthesised containing 9 and 81 phenylboronic acid functionalities in the periphery to be used for the quenching of S-THMF to inhibit the formation of STHMF-borate.

In addition, cationic dendrimers of generation G1, G2 and G3 with 9, 27 and 81 terminal primary amines were synthesised for clustering of anionic bacteria through electrostatic interactions.

3.5 REFERENCES

[1] Chen, C.Z. and Cooper, S.L. (2002a). *"Interactions between dendrimer biocides and bacterial membranes."* Biomaterials 23(16): 3359-68.

[2] Schauder, S., Shokat, K., Surette, M.G., and Bassler, B.L. (2001). *"The LuxS family of bacterial autoinducers: biosynthesis of a novel quorum-sensing signal molecule."* Mol Microbiol 41(2): 463-76.

[3] Chen, X., Schauder, S., Potier, N., Van Dorsselaer, A., Pelczer, I., Bassler, B.L., and Hughson, F.M. (2002b). *"Structural identification of a bacterial quorum-sensing signal containing boron."* Nature 415(6871): 545-9.

[4] Springsteen, G. and Wang, B. (2002). *"A detailed examination of boronic acid–diol complexation."* Tetrahedron 58(26): 5291-5300.

[5] Globisch, D., Lowery, C.A., McCague, K.C., and Janda, K.D. (2012). *"Uncharacterized 4,5-dihydroxy-2,3-pentanedione (DPD) molecules revealed through NMR spectroscopy: implications for a greater signaling diversity in bacterial species."* Angew Chem Int Ed Engl 51(17): 4204-8.

[6] Pappin, B., Kiefel, M.J., and Houston, T.A. (2012). Boron-Carbohydrate Interactions - Comprehensive studies on Glycobiology and Glycotechnology, INTECH Open Access Publisher.

[7] Xue, X., Pasparakis, G., Halliday, N., Winzer, K., Howdle, S.M., Cramphorn, C.J., Cameron, N.R., Gardner, P.M., Davis, B.G., Fernandez-Trillo, F., and Alexander, C. (2011). *"Synthetic polymers for simultaneous bacterial sequestration and quorum sense interference."* Angew Chem Int Ed Engl 50(42): 9852-6.

[8] Gaetke, L.M. and Chow, C.K. (2003). *"Copper toxicity, oxidative stress, and antioxidant nutrients."* Toxicology 189(1-2): 147-63.

[9] Kaplan, J.H. and Maryon, E.B. (2016). *"How Mammalian Cells Acquire Copper: An Essential but Potentially Toxic Metal."* Biophys J 110(1): 7-13.

[10] Arseneault, M., Levesque, I., and Morin, J.-F. (2012). *"Efficient and Rapid divergent synthesis of ethylene oxide containing dendrimers through catalyst-free click chemistry."* Macromolecules 45(9): 3687-3694.

[11] Kappe, C.O., Pieber, B., and Dallinger, D. (2013). *"Microwave effects in organic synthesis: myth or reality?"* Angew Chem Int Ed Engl 52(4): 1088-94.

[12] Ni, N., Chou, H.T., Wang, J., Li, M., Lu, C.D., Tai, P.C., and Wang, B. (2008). *"Identification of boronic acids as antagonists of bacterial quorum sensing in Vibrio harveyi."* Biochem Biophys Res Commun 369(2): 590-4.

[13] Amaral, S.P., Fernandez-Villamarin, M., Correa, J., Riguera, R., and Fernandez-Megia, E. (2011). *"Efficient multigram synthesis of the repeating unit of gallic acid-triethylene glycol dendrimers."* Org Lett 13(17): 4522-5.

[14] Airoldi, C., Zona, C., Sironi, E., Colombo, L., Messa, M., Aurilia, D., Gregori, M., Masserini, M., Salmona, M., Nicotra, F., and La Ferla, B. (2010). *"Curcumin derivatives as new ligands of Abeta peptides."* J Biotechnol 156(4): 317-24.

[15] Montanez, M.I., Hed, Y., Utsel, S., Ropponen, J., Malmstrom, E., Wagberg, L., Hult, A., and Malkoch, M. (2011). *"Bifunctional dendronized cellulose surfaces as biosensors."* Biomacromolecules 12(6): 2114-25.

[16] Cai, T.B., Lu, D., Tang, X., Zhang, Y., Landerholm, M., and Wang, P.G. (2005). *"New glycosidase activated nitric oxide donors: glycose and 3-morphorlinosydnonimine conjugates."* J Org Chem 70(9): 3518-24.

[17] Fujimoto, K., Oimoto, N., Katsuno, K., and Inouye, M. (2004). *"Effective stabilisation of [small alpha]-helical structures in short peptides with acetylenic cross-linking agents."* ChemComm(11): 1280-1281.

[18] Pasparakis, G. and Alexander, C. (2008). *"Sweet talking double hydrophilic block copolymer vesicles."* Angew Chem Int Ed Engl 47(26): 4847-50.

[19] Pasparakis, G., Cockayne, A., and Alexander, C. (2007). *"Control of bacterial aggregation by thermoresponsive glycopolymers."* J Am Chem Soc 129(36): 11014-5.

[20] Pieters, R.J. (2007). *"Intervention with bacterial adhesion by multivalent carbohydrates."* Med Res Rev 27(6): 796-816.

[21] Boltje, T.J., Buskas, T., and Boons, G.J. (2009). *"Opportunities and challenges in synthetic oligosaccharide and glycoconjugate research."* Nat Chem 1(8): 611-22.

[22] Bergeron-Brlek, M., Shiao, T.C., Trono, M.C., and Roy, R. (2011). *"Synthesis of a small library of bivalent alpha-D-mannopyranosides for lectin cross-linking."* Carbohydr Res 346(12): 1479-89.

[23] Jacobsen, N.E. (2007). NMR Spectroscopy Explained: Simplified Theory, Applications and Examples for Organic Chemistry and Structural Biology, Wiley.

[24] Bubb, W.A. (2003). *"NMR spectroscopy in the study of carbohydrates: Characterizing the structural complexity."* Concept Magnetic Res Part A 19A(1): 1-19.

[25] Wang, Z., *Zemplén Deacetylation.* , in *Comprehensive Organic Name Reactions and Reagents*, W. Z, Editor. 2010, John Wiley&Sons Inc. : Hoboken NJ.

[26] Lidström, P., Tierney, J., Wathey, B., and Westman, J. (2001). *"Microwave assisted organic synthesis - a review."* Tetrahedron 57: 9225-9283.

[27] Rijkers, D.T., van Esse, G.W., Merkx, R., Brouwer, A.J., Jacobs, H.J., Pieters, R.J., and Liskamp, R.M. (2005). *"Efficient microwave-assisted synthesis of multivalent dendrimeric peptides using cycloaddition reaction (click) chemistry."* ChemComm (Camb)(36): 4581-3.

[28] Chan, L.C. and Cox, B.G. (2007). *"Kinetics of amide formation through carbodiimide/N-hydroxybenzotriazole (HOBt) couplings."* J Org Chem 72(23): 8863-9.

4. Biological application studies of Hydroxyl-functionalized Dendrimers

4.1 INTRODUCTION

As outlined in Chapter 1, *V. harveyi* recognizes the furanosyl borate (S-THMF borate) formed when the carbohydrate precursor DPD complexes with borate in the marine environment [1]. The unique feature of AI-2 is its chemical structure, arising from the ability of boronic acids to bind covalently with 1,2 or 1,3 diols to form cyclic esters [2]. The rigid *cis*-conformation of saccharides forms stronger cyclic esters compared to linear diols, such as those in ethylene glycol or PVA and therefore DPD has a higher affinity for boric acid (Chapter 3, *Figure 3.2*) [2, 3].

Many bacteria have developed means to attach to host cells for effective colonization and initiate the infection pathway by expressing one or more than adherence factors (adhesins) [4]. Bacteria can have adhesins located on hair-like threads extending from the bacterial surface, referred to as fimbriae, or as a surface-anchored protein named afimbrial adhesin (*Figure 4.1*) [4]. Lectins that can bind complementary carbohydrates on host cell surface are the most common way for bacteria to attach to hosts. [5].

Free carbohydrate structures that bind to specific lectins can interfere with pathogen adhesion. The production of sugars has been evolved as an important

anti-infective strategy for infants, as the breast milk contains large amount of oligosaccharides acting as anti-adhesives [6].

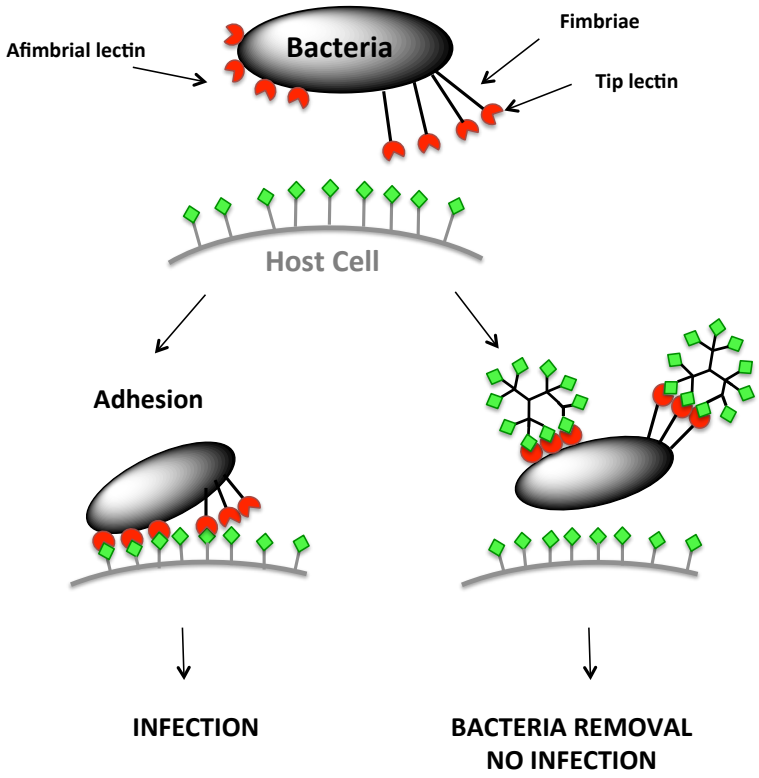

Figure 4.1 Bacterial adhesion and interference of multivalent carbohydrates. Afimbrial lectin and fimbriae projections containing lectins that recognize carbohydrates from the host cell surface. Multivalent carbohydrates can bind to bacteria and interfere with lectin-carbohydrate interactions crucial for adhesion. Non-adhering bacteria are removed by host clearing systems such as airflow, mucus or urine flow [4, 7].

Individual lectin-carbohydrate interactions are relatively weak. While most bacteria initially attach to surfaces via transient charge-charge and/or weak non-covalent hydrophobic interactions, medium-to long term bacterial adhesion relies on multivalent interactions where multiple binding sites lead to tight association [7]. These interactions take place on three levels, differing in the distance between the binding sites (*Figure 4.2*). Bacteria can bind with

multiple lectins to multiple sites on the host cell separated by large distances (1). A second level of multivalency involves binding with multiple sites with one cluster of associated carbohydrates (2). The third level takes place when a single lectin contains multiple binding sites (3).

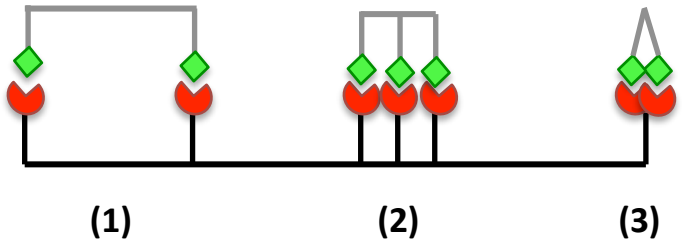

Figure 4.2 Three levels of multivalency in bacterial adhesion. (1) Large distance multivalent binding. (2) Binding within one cluster of lectin and (3) multiple binding sites within one lectin [7].

The aim of this study was to synthesise GATG dendrimers with diol moieties with affinity for boric acid present in the medium, interfere with the formation of the active S-THMF borate needed for QS induced phenotype in *V. harveyi*. Functionalized dendrimers of generation G1 and G3, as described in chapter 3, were used to obtain a significant difference in terms of size and number of functional groups and to study their effect on *V. harveyi* binding. Diol-functionalized dendrimers were incubated with bacteria in boron-depleted AB medium [1] as described previously (**protocol 3**) [8]. By depleting the medium of boron and adding a known concentration of boric acid, a controlled environment between DPD and boric acid was achieved that enabled the study of small variations in boric acid binding to diol-dendrimers. Based on the previous findings it was expected for the carbohydrate to have higher affinity for boric acid compared to the tetraol and diol [2, 3]. The tetraol containing two

diol functionalities on each arm would have higher affinity for boric acid compared to the diol with only a hydroxyl group on each arm. It was expected to see QS quenching with functionalized dendrimer to be increasing: carbohydrate > tetraol > diol. Described in this chapter is preliminary evaluation of the dual effect of quorum quenching and bacteria clustering with glucose- and mannose- functionalized dendrimers and a comparison with the diol- and tetraol dendrimers, expected to be capable of only interference with QS (*Figure 4.3*).

Structures of diol-dendrimers investigated in this chapter:

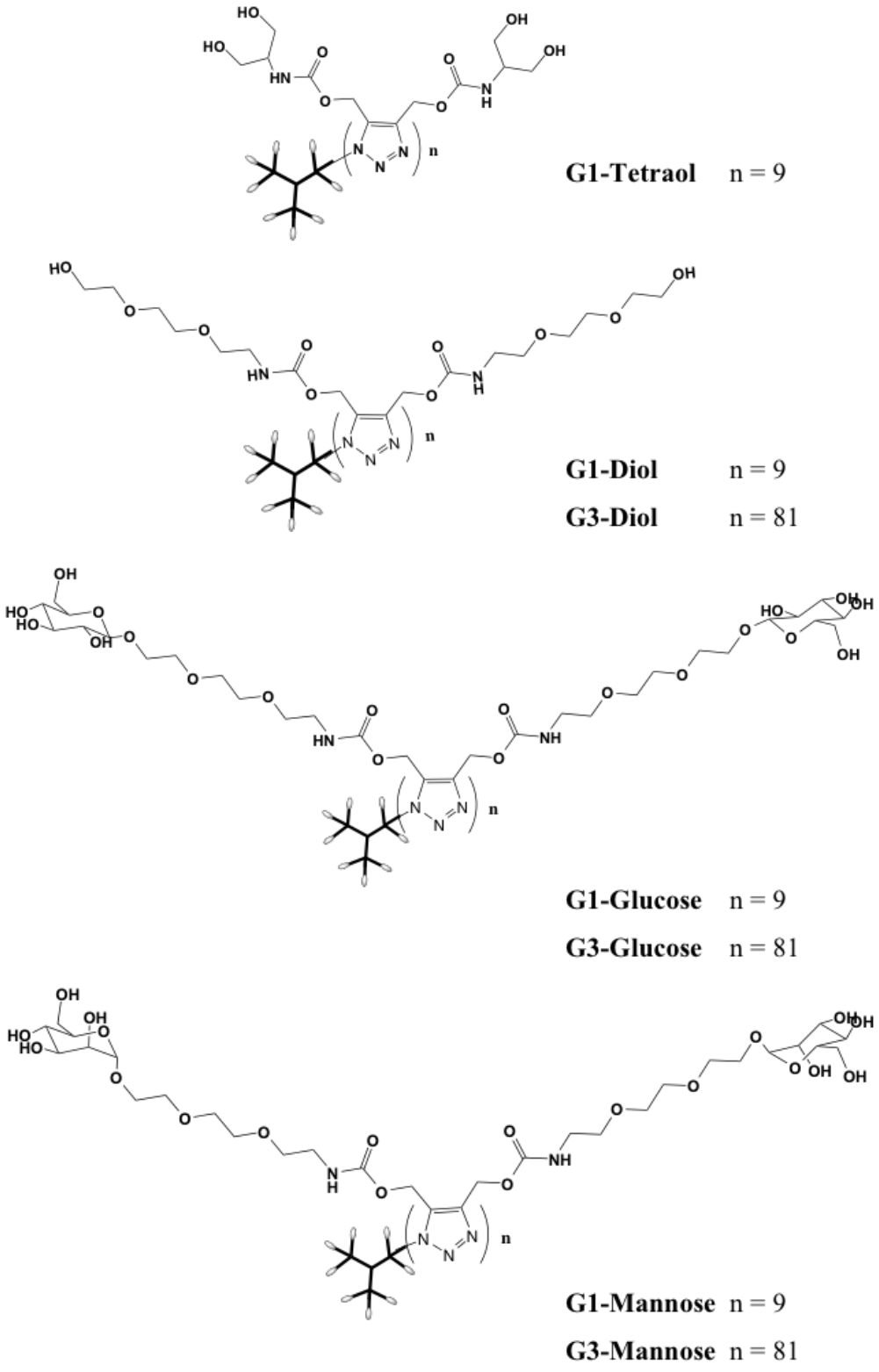

Figure 4.3 Structures of hydroxyl and glyco-functionalised dendrimers investigated in this chapter.

4.2. EXPERIMENTS

The protocols for the assays are all described in Chapter 2. In brief; for the **luminescence assay (protocol 4**), overnight cultured bacteria were adjusted to OD = 1.0 and diluted 5000-fold in boron-depleted AB medium. Boric acid was added to the medium with final concentrations of 400 μM for experiments with MM32 and 22 μM for BB170. In the assay with MM32, DPD was added to the medium to a final concentration of 22 μM. Since MM32 is not able to produce DPD, in this way the limiting concentration for the formation of S-THMF-borate induced luminescence is 22 μM for both bacterial strains. Dendrimer stock solutions were prepared in dH_2O with a concentration 10 times higher than the final concentration. Selected dendrimers (20 μL of stock solutions) was incubated with 180μl of bacteria suspension (~10^4 CFU/mL) in a 96-well plate at 30 °C. The final volume in each well was 200 μL. Optical density at 600 nm and luminescence were measured every 30 min for at least 10 h. Graphs show the mean values of data obtained with error bars, based on the Standard Deviations (SD) from the mean. For MM32, the magnitude of the value for the luminescence in the presence of dendrimers was divided by the magnitude of the value for luminescence for bacteria alone for 4 h, 8 h, 12 h and 16 h in order to present the relative luminescence. For BB170, the time (in 30 min interval) to reach initial light production after decay phase (*Figure 4.7*) was presented as recovery time. Calculations for relative luminescence and recovery time were conducted for each individual sample. Graphs show represent minimum, maximum and mean values.

For the **clustering assay** (**protocol 5**) overnight cultured bacterial suspensions were diluted to OD = 1.0 in PBS, passed through a 5 μm filter and incubated with or without dendrimers (final dendrimer concentrations 0.25 mg/mL and 0.5 mg/mL). At different time points 300-1000 μl of the mixture was added to the water-filled counter cell and cluster size was measured. Graphs show mean values from triplicate experiments.

For the **CFU assay (protocol 7)**, bacteria were incubated with dendrimers as for the luminescence assay. At each time point, an aliquot was collected, diluted in PBS and plated on LB-agar plates. Plates were incubated overnight at 30 °C and colonies were counted the following day. Graphical data represent mean values and error bars, SD.

All samples were evaluated in triplicate and experiments were repeated at least twice.

4.3 RESULTS

4.3.1 Luminescence of *V. harveyi* in the presence of Gn-OH

The diol concentrations of dendrimers (0.5 – 3 mM, *Table 4.1*) used were similar to that as that of diol-containing quorum quenching polymers (linear, carbohydrate and catechol) published by Xue and colleagues (0.1 mM – 5 mM) [3]. *V. harveyi* MM32 was incubated with diol-containing dendrimers with dendrimer concentrations ranging 0.5 mg- 1.5 mg/mL (*Figure 4.4*) except G1-glucose which was incubated with dendrimer concentrations of 0.38-4.5 mg/mL (*Figures 4.4-4.5*).

Dendrimer/ Polymer n = Diols	Dendrimer Conc (mg/mL)	Diol Concentration in bioluminescence experiment (mM)
G1-Diol n=9	0.5 – 1.5	0.7 – 2.1
G3- Diol n=81	0.5 – 1.5	0.7 – 2.0
G1-Tetraol n=18	0.5 – 1.5	1.7 – 5.1
G1-Glucose n=18	0.38 – 4.0	0.7 – 8.8
G3-Glucose n=162	0.5 – 1.5*	0.9 – 2.8*
G1-Mannose n=18	0.5 – 1.5	1.0 – 2.9
G3-Mannose n= 162	0.5 – 1.5*	0.9 – 2.8*

Table 4.1 Dendrimer and diol concentration for luminescence experiments with MM32 comparing [3]. * BB170 instead of MM32 strain. The carbohydrates contain multiple hydroxyl groups, but the only significant binding is only through the C4/C6 diol, diol concentration is therefore determined as one diol/carbohydrate [9].

The glucose functionality of the linear polymers was used at higher concentration (1.2 mM- 4.7 mM) than PVA (0.1 mM – 3.4 mM); therefore a higher diol concentration of G1-Glucose (up to 8.7 mM) (*Figure 4.5*) was tested in luminescence experiments with MM32. The carbohydrates contain multiple hydroxyl groups, but the only significant binding site is the C4/C6 diol, and therefore diol concentration was determined as one diol/carbohydrate [9]. Due to the very limited amount of G3-glucose and G3-mannose available, concentrations greater than 2.8 mM diol could not be evaluated in these experiments. Dendrimers functionalised with carbohydrates decreased luminescence produced by *V. harveyi* MM32 at early stages (4 h time point) of the experiment (*Figures 4.6-4.7*). However, after 8h the effect was reversed. After 12 h, bacteria incubated with any of the diol-dendrimers initiated more light production compared to the bacteria alone. There was an increase in OD_{600} when bacteria were incubated with G1-tetraol with G1-glucose at higher concentrations.

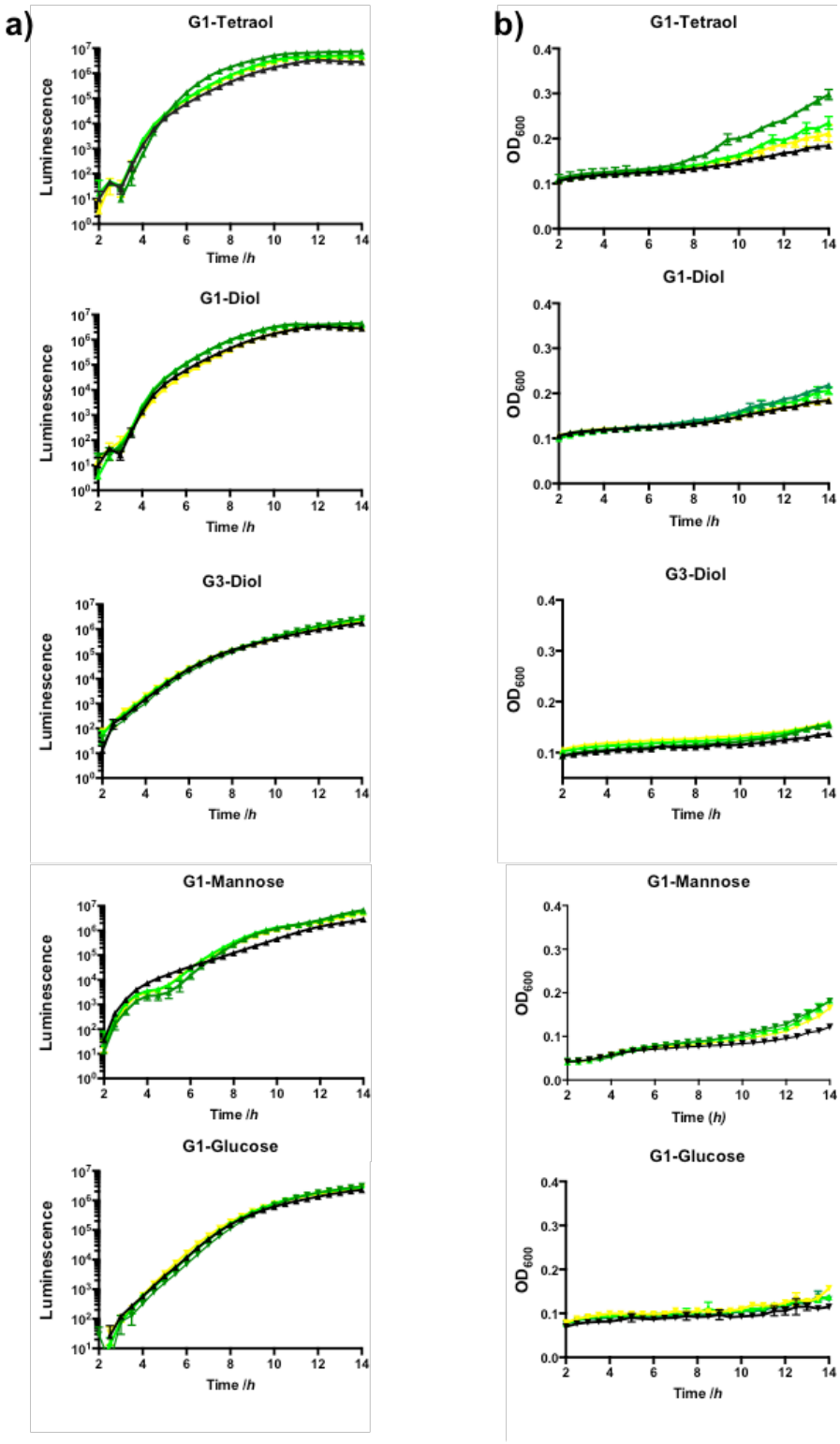

Figure 4.4 Luminescence (Relative Luminescence Units, RLU) of *V. harveyi* MM32 in the absence (black) and presence of dendrimers. Luminescence (a) and optical density (b) at 600 nm (OD_{600}) are presented. Final dendrimer concentrations 0.5 mg/mL (yellow), 1 mg/mL (light green) and 1.5 mg/mL (dark green). Except for G1-Glucose, which were 0.38 mg/mL (yellow), 0.75 mg/mL (light green) and 1.25 mg/mL (dark green).

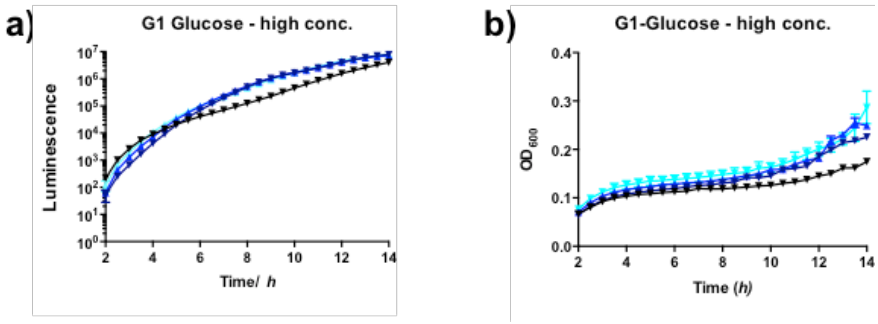

Figure 4.5 Luminescence (Relative Luminescence Units) of *V. harveyi* MM32 in the absence (black) and presence of high concentration G1-Glucose. Luminescence (a) and optical density (b) at 600 nm (OD_{600}) are presented. Final dendrimer concentrations 2 mg/mL (light blue), 3 mg/mL (royal blue) and 4.5 mg/mL (dark blue)

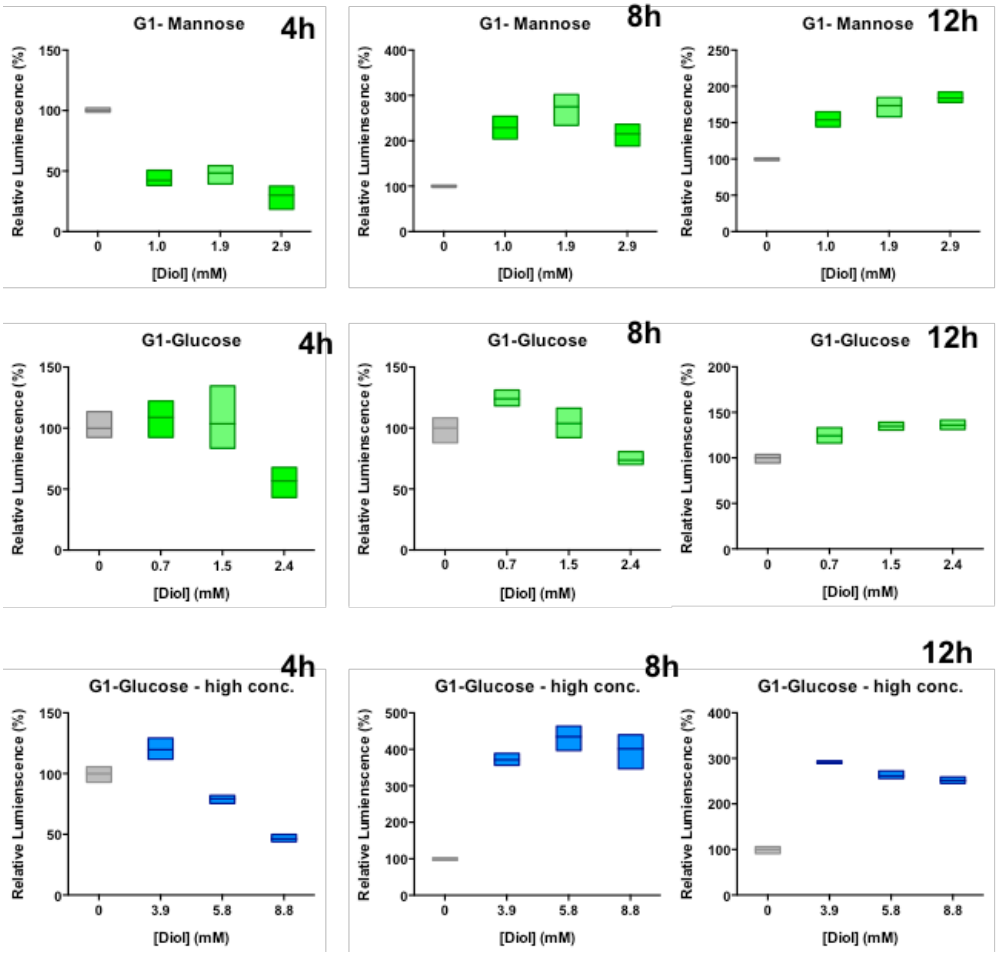

Figure 4.6 Effect of diol concentration on luminescence of MM32 in the presence of G1 carbohydrate dendrimers.

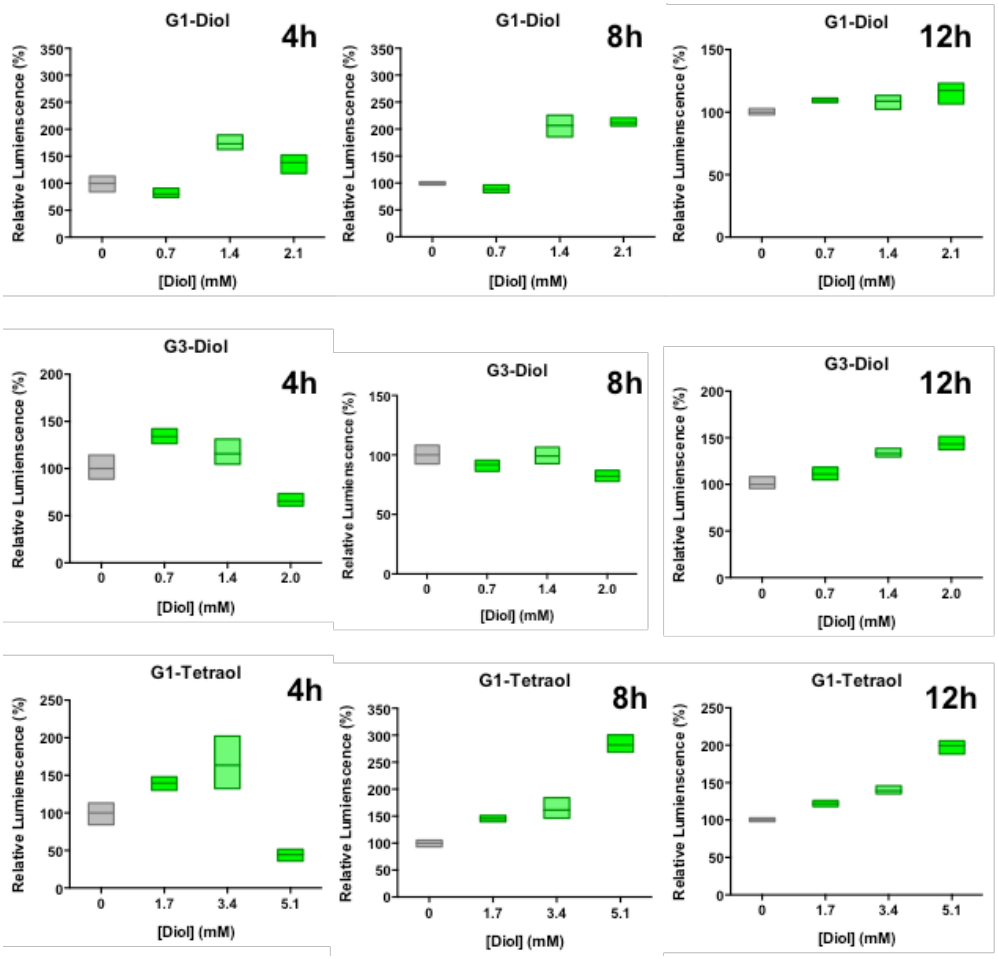

Figure 4.7 Effect of diol concentration on Luminescence (Relative Luminescence Units) of MM32 in the presence of G1-diol, G3-dol and G1-tetraol.

To see if the same effect on luminescence and optical density occurred when bacteria produced their own DPD, luminescence and optical density in the presence of dendrimers were measured using the *V. harveyi* BB170 strain. Quenching of quorum sensing molecules in *V. harveyi* BB170 can be observed as a shift to the right or a delay in the enhancement phase in the measured luminescence curve (*Figure 4.8*). The initial light production decreased down to minimum luminescence at the beginning of the experiment: this is the decay phase. The decrease in bioluminescence is due to the dilution of bacteria from

medium with high concentration of AI-2 (overnight growth) to medium with low concentration of AI-2 molecules. When bacteria density increases, then light production increased accordingly. The recovery time represents the time it took for the luminescence to reach the initial light production following the decay phase. An increase in luminescence and therefore faster recovery from the decay phase was expected to give a shorter recovery time, while with decreased luminescence it would take more time to reach the initial luminescence level and the recovery time would be longer.

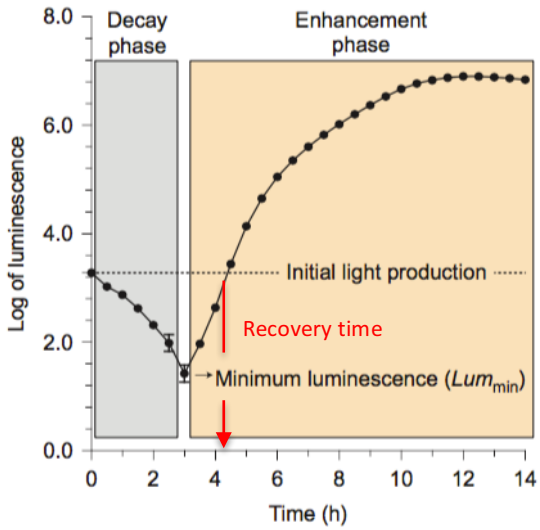

Figure 4.8 The luminescence (Relative Luminescence Units) of *V. harveyi* BB170. During the decay phase luminescence is reduced due to decreased bacteria density. After minimum luminescence follows an enhancement phase and increase in luminescence due to increased cell density. Image modified from [10]

V. harveyi BB170 was incubated with diol-containing dendrimer G1 (*Figure 4.9*) and G3 (*Figure 4.10*) with dendrimer concentrations of 0.5 mg- 1.5 mg/mL. A slight increase in recovery time (decreased luminescence) was observed at the highest concentration of G1-tetraol and G3-mannose while G3-diol, and G1- and G3-glucose all gave decreased recovery times (increased

luminescence) (*Figure 4.11*). There was an increase in OD_{600} for BB170 when incubated with the diol-dendrimers, which in some cases seemed to be concentration-dependent (G3-glucose, G3-diol). The increase in recovery time could be related to the increase in growth. The concentration-dependent increase in luminescence, observed with MM32 at later time points with the diol dendrimers was not found in the case of BB170.

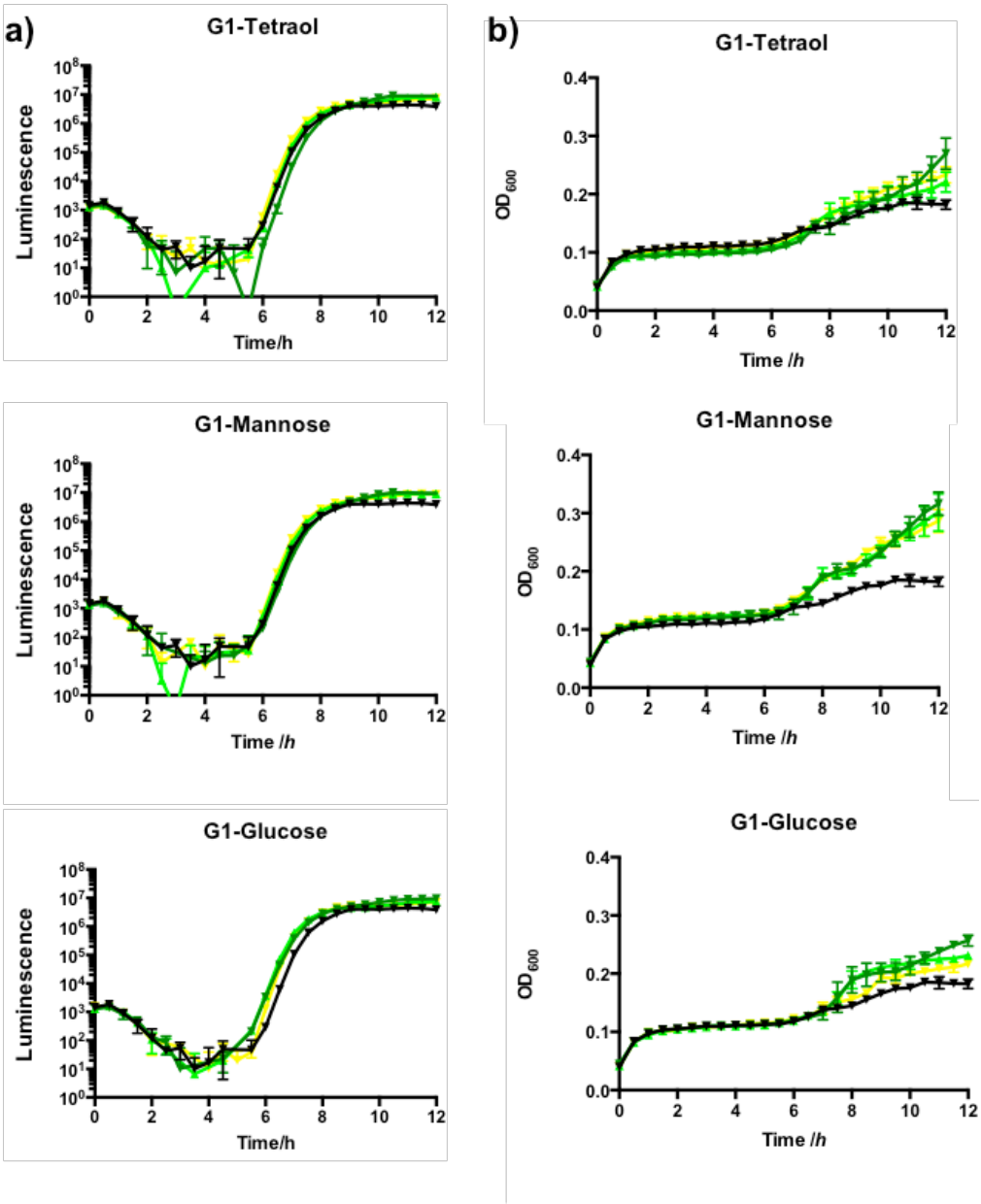

Figure 4.9 Luminescence (Relative Luminescence Units) of *V. harveyi* BB170 in the absence (black) and presence of G1 -dendrimers. Luminescence (a) and optical density (b) at 600 nm (OD_{600}) are presented. Final dendrimer concentrations: 0.5 mg/mL (yellow), 1 mg/mL (light green) and 1.5 mg/mL (dark green).

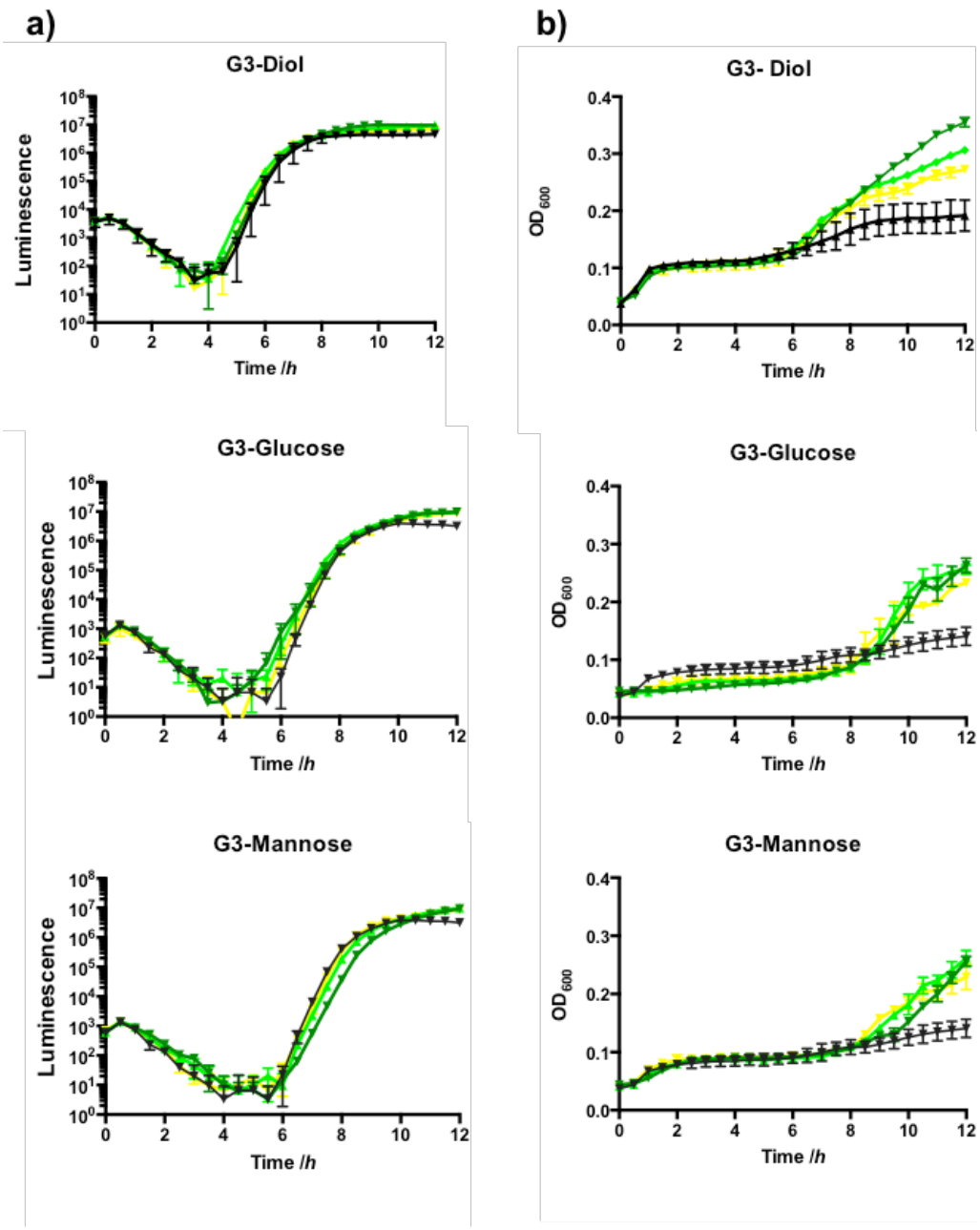

Figure 4.10 Luminescence (Relative Luminescence Units) of *V. harveyi* BB170 in the absence (black) and presence of G3 -dendrimers. Luminescence (a) and optical density (b) at 600 nm (OD_{600}) are presented. Final dendrimer concentrations: 0.5 mg/mL (yellow), 1 mg/mL (light green) and 1.5 mg/mL (dark green).

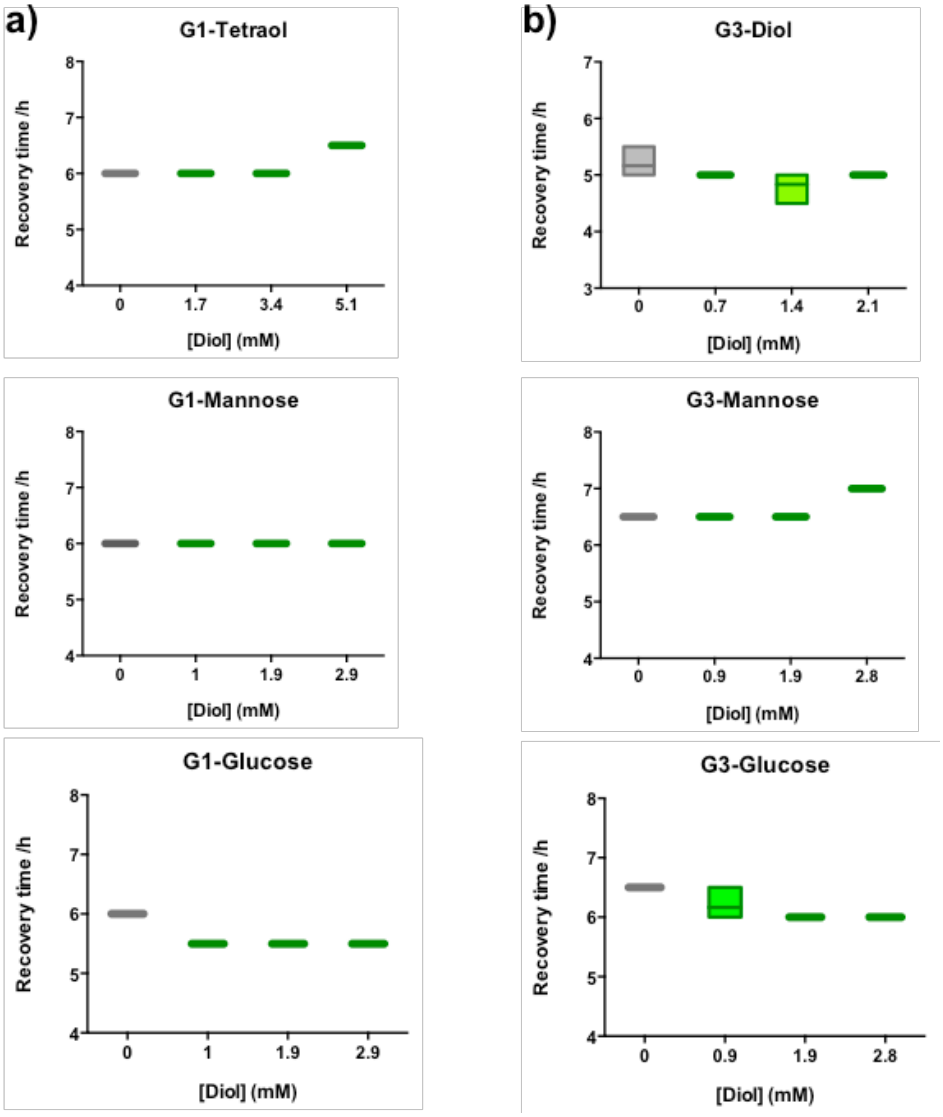

Figure 4.11 Effect of diol concentration on luminescence recovery time BB170 in the absence (grey) and presence of a) G1-dendrimers and b) G3-dendrimers.

There was an increase in OD_{600} when bacteria were incubated with diol-dendrimers, similar to assays with MM32. The trend was most pronounced in the case where BB170 was incubated with dendrimers of generation G3 (*Figure 4.8)*, but was visible also for G1 dendrimers (*Figure 4.7)* and for G1-tetraol and G1-diol when incubated with MM32 (*Figure 4.4*).

OD_{600} is a standard method to estimate the number of bacteria in a suspension, and measuring OD_{600} is often used to represent bacterial populations. The method is based on measuring the scattered light, by particles (in this case, bacteria) in suspension. The amount of scattered light is an indication of the biomass present. Light scattering is dependent on the size and shape of the particles (cells in this case). If bacteria aggregate into clusters, the size and shape changes, and as larger particles scatter more light, the optical density can increase, giving rise to an apparent increase of bacterial populations. Optical density has thus been used previously as a method to determine the degree of clustering of bacteria [3]. However, it is important to note that light scattering varies non-linearly with particle size, with an intensity dependence which scales with the sixth power of diameter.

4.3.2 Clustering of *V. harveyi* with Gn-OH

To determine if bacterial clustering was responsible for the increase in OD_{600}, dendrimers were incubated with *V. harveyi* and cluster size was measured with clustering assay according to previously reported protocols [11]. Dendrimers were incubated with *V. harveyi* BB170 and MM32 in PBS for 5-60 min, after which aliquots were placed in the water-filled counter cell and the cluster size was measured. Untreated bacteria have a size around 1 μm visualized with the grey area in *Figure 4.9.* Bacterial clustering can be seen as shift from the size of single bacteria to a population of larger sizes.

The diol and tetraol dendrimers were not expected to have a large effect on aggregation. However, it was surprising that the G3-glucose did not cause clustering of *V. harveyi*. Glycopolymers have been shown to be highly active at sequestering bacteria, clustering for example *E. coli* [7, 12-14]. *V. harveyi* have been shown to bind to both glucose and mannose and lectins responsible for binding these sugars are important for the formation of *Vibrio* biofilms, where adding mannose and glucose to growth media can interfere with the formation of biofilm [15, 16] Clustering of *V. harveyi* with glucose-polymers was also presented by Xue and colleagues [3]. With G1, due to their small size and limited number of functional groups, it was not anticipated to observe extensive aggregation even for the glyco-dendrimer expected to have affinity for the lectin of *V. harveyi* (Chapter 5).

No increase in aggregation size was observed for any of the diol-dendrimers after 5 min (*Figure 4.12*) (light blue line), 30 min (royal blue line) or 60 min

(dark blue line). No clustering was seen with *V. harveyi* BB170 (*Figure 4.12*) or MM32 *(Appendix Figure A36)*. Some larger aggregates were seen with sizes above 10 μm that were considered to be background clustering, as they were present in cases with bacteria alone and there was no shift in the smaller and middle-sized clusters formed. Due to material amount restrictions, the effects of G3-Glucose and G3-Mannose in the presence of BB170 were only measured after 60 min of incubation time.

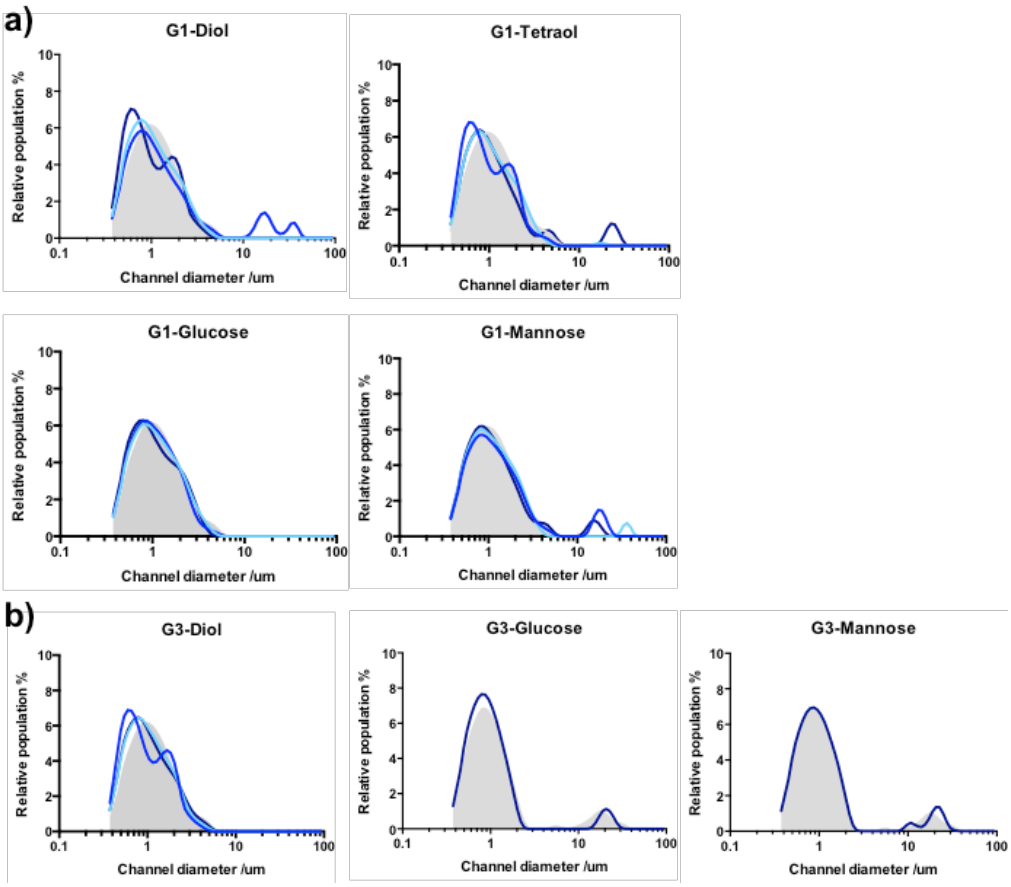

Figure 4.12 Size distribution of *V. harveyi* BB170 suspension (OD_{600} = 1.0) in the absence (grey) and presence of dendrimers after 5min (light blue), 30 min (royal blue) and 60 min (dark blue) Diol-functionalized dendrimer of generation G1 (a) and G3 (b). Final dendrimer concentration 0.5 mg/mL.

No aggregation of *V. harveyi* MM32 was observed by optical microscopy for diol dendrimers (*Figure 4.13)*. Due to time limits, no microscopy analysis was

possible for diol dendrimers incubated with BB170. However, there was no significant difference in the clustering between MM32 and BB170 as seen with amine-dendrimers in Chapter 5, (the MM32 shows slightly larger aggregation with cationic dendrimers) and no clustering was apparent in clustering measurements for either *V. harveyi* mutants. A possible explanation for the lack of clustering is that the carbohydrate concentration was too high (0.5 mg/mL, *Figure 4.12*) in the assay for clustering to occur. If dendrimers were coating the bacteria surface with carbohydrate moieties and not interacting with multiple cells, no significant clustering effect would be noticed.

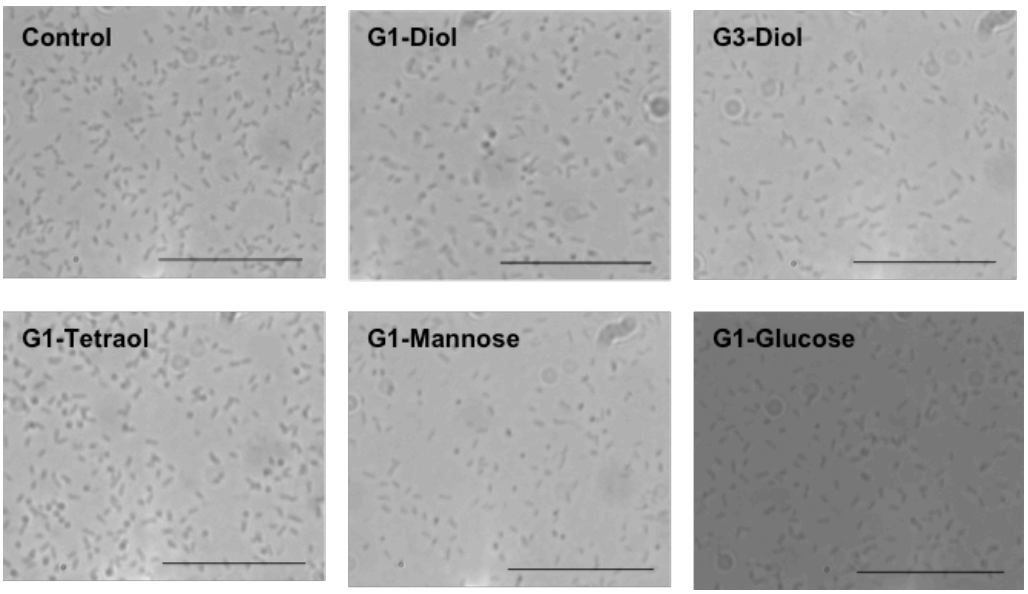

Figure 4.13 *V. harveyi* MM32 in the absence (Control) and presence of G1-Diol, G3-Diol, G1-Tetraol, G1-Mannose and G1-Glucose (100X magnification). The black bar represents 30 μm. Dendrimer concentration 0.5 mg/mL.

Dendrimer	Dendrimer Conc (mg/mL)	Dendrimer Conc (Molar)	Number of dendrimers/mL	Carbohydrate conc. (Molar)
G1-Long Diol	0.5	0.08 mM	$5 * 10^{16}$	-
G3-Long Diol	0.5	0.008 mM	$5 * 10^{15}$	-
G1-Tetraol	0.5	0.09 mM	$6 * 10^{16}$	-
G1-Glucose	0.5	0.05 mM	$3*10^{16}$	1 mM
G3-Glucose	0.5	0.006 mM	$3*10^{15}$	0.9 mM
G1-Mannose	0.5	0.05 mM	$3*10^{16}$	1 mM
G3-Mannose	0.5	0.006 mM	$3*10^{15}$	0.9 mM

Table 4.2 Concentration of dendrimer, and their number of carbohydrates and the calculated number of dendrimers per mL sample for the clustering assay. Dendrimer concentration 0.5 mg/mL. The concentration was kept the same between dendrimers of different generation and molecular weight, and thus the number of dendrimers per mL varies.

The increase in optical density measured when bacteria were incubated with diol-dendrimers could not be explained by an increase in aggregation. Another way to determine if bacteria are growing is by counting colony-forming units (CFU).

4.3.3 Colony Forming Unit counts in the presence of Gn-OH

V. harveyi MM32 was incubated the absence or presence of diol-dendrimers under same conditions as luminescence experiment (**protocol 5**). At each time point, aliquots were collected, diluted and plated on LB-agar plates in triplicates and incubated overnight. The number of CFU for each condition was counted. Due to time limits, cell plate counting assays were not possible for G3-mannose and G3-glucose.

There was an increase in cell counts after 8h for all diol-dendrimers (colour) incubated with MM32 compared to bacteria alone (black) (*Figure 4.14*). After 24 h, there was no difference in numbers of colonies when bacteria were incubated with diol-dendrimers, compared to bacteria in the absence of dendrimer (control). When *V. harveyi* BB170 was incubated with dendrimer in the more nutrient-rich LB medium, there was no difference in cell counts at any of the time points. (*Appendix Figure A37*). It should be noted that the cross-experiments with MM32 grown in LB medium and BB170 in AB-medium were not performed, and the comparisons between the two conditions were done across two different bacterial mutants. However, it seems that in the case of the less nutrient-rich AB medium, *V. harveyi* were growing more rapidly in the presence of diol-dendrimers.

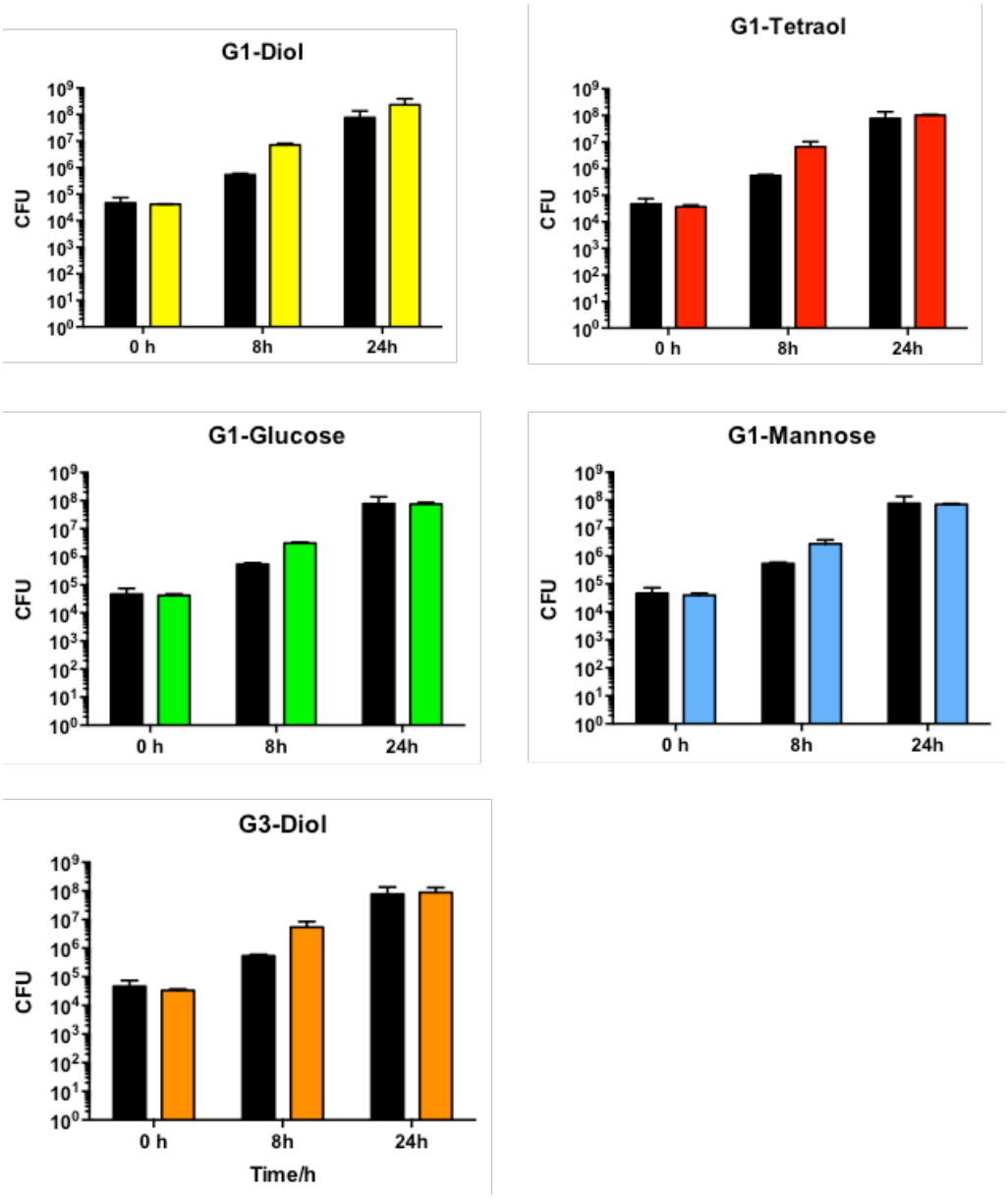

Figure 4.14 Colony Forming Unit (CFU) count for *V. harveyi* MM32 in AB medium, in the absence (black) and presence (colour) of diol-dendrimers at time point 0, 8 and 24 h. Dendrimer concentration 0.5 mg/mL.

4.4 DISCUSSION

Luminescence produced by *V. harveyi* MM32 was decreased in the presence of carbohydrate-dendrimers, at the early time point (4 h) compared to control (*Figure 4.6*). This decrease of luminescence was dose-dependent. G1-mannose produced less than half of luminescence compared to bacteria in the absence of any dendrimer (control). Dendrimers with high number of hydroxyl groups, G3 and G1-tetraol had a similar effect on MM32 luminescence with the higher concentrations most effective in quorum quenching (*Figure 4.7*). G1-tetraol (5.1mM) and G3-diol (2.0 mM) had inhibitory effects on bacterial luminescence at the highest diol concentration (5.1 mM and 2.0 mM respectively) although he opposite effect was again observed for the later time points. However, at later time point (8 h) the opposite effect was observed, luminescence produced by MM32 increased in the presence of the same dendrimer (*Figure 4.6*).

The concentrations of functional groups for the luminescence experiments were in the range used in previous assays it was therefore surprising that the dendrimers with similar ligands as the polymers did not have a greater inhibitory effect on the luminescence. (*Table 4.1*) [3]. It is possible that inhibition of luminescence could have been achieved at higher dendrimer concentrations, especially in the case of the larger G3 dendrimer functionalised with carbohydrates. Polymeric carbohydrates have displayed higher affinity for boric acids compared to linear diols, such as ethylene glycol or PVA [2, 3]. Due to time constraints, only G1-glucose was tested in higher concentrations than 5mM of diol.

It is thus possible that the diol-dendrimer had a dual effect on the MM32 bacterial strain, i.e. during an initial stage the dendrimer was quenching quorum sensing as seen by the decrease in luminescence, while at the later stages the dendrimers seemed to be promoting bacterial growth so any effect on QS was obscured due to increased numbers of bacteria.

At early time point, no significant increase in growth by OD was observed. However, it should be noted that using OD to determine bacterial growth at low cell densities, close to the detection limit of 0.01–0.02, is not a very accurate method for identifying differences in growth. The increase in OD_{600} observed when bacteria at later time points (8-12 h) could explain the increase in luminescence. Thus it could be considered that when bacterial density increased there were more bacteria that could respond to DPD in the assay. In addition, it is not clear from these experiments if the dendrimers formed bacterial clusters at the concentrations used in the luminescence assays, and thereby enhanced the luminescence output.

A possible explanation for the increase in growth could be that the bacteria were degrading the dendrimer or part of the dendrimer structure and using it as a carbon source in the nutrient-poor AB medium. The GATG dendrimers are based on gallic-acid and triethylene glycol chains, linked though amide, peptide like bonds. *V. harveyi* produces extracellular cysteine proteases, enzymes able to catalyse the hydrolysis of peptide bonds [17]. Several microorganisms, mainly gram-negative aerobic bacteria such as *Pseudomonas* are able to use poly-ethylene-glycol (PEG) as their sole carbon source [18-20]. Different PEG –degrading enzymes have been found to be associated with the

periplasmatic space of the Gram-negative bacteria, and the cleavage of the macromolecule proceeds through the attack of the terminal end of the poly-ether chain [18]. *Vibrio* species can use polyvinyl alcohol, a biodegradable polymer, as a source of carbon. In addition, Francis and colleagues were able to show certain bacterial species in addition were able to degrade the low-density-polyethylene, a non-biodegradable polymer, when blended with 5-30% PVA [21]. Gallic acid can be degraded by some species of *Pseudomonas* [22], however gallic acid derivates have been shown to have antibacterial effects in *V. harveyi* and other pathogenic *Vibrio* species [23]. Although it is not known whether *V. harveyi* can degrade polyethylene glycol chains, the bacteria has been reported to degrade PVA and synthesise enzymes able to catalyse the hydrolysis of peptide bonds. It is also possible that an impurity in the dendrimer sample was increasing growth, or that the hydroxyl groups of the dendrimer were chelating important co-factors such as iron, and thereby increasing growth.

The initial quorum quenching seen with MM32, was not as evident with BB170. Dendrimers with hydroxyl groups had a very small effect on the luminescence of *V. harveyi* mutant BB170. In the presence of the highest concentrations of G1-tetraol and G3-mannose luminescence was slightly decreased as observed by recovery time while luminescence increased in the presence of G3-diol, and G1- and G3-glucose compared to *V. harveyi* BB170 bacteria alone (*Figure 4.11*). It is difficult to compare two mutant strains, as mutation can have an effect on other metabolic systems within the bacteria such as expression of molecules involved in clustering such as lectins which could in turn affect luminescence and OD_{600}.

No clustering of *V. harveyi* was seen with mannose-or glucose functionalized dendrimers with the concentrations used for the cluster and microscopy assays. Mannose are known to bind mannose-specific type 1 adhesin of *E. coli* [24] and multivalent glucose polymers previously prepared by our group have been demonstrated to cluster *E. coli* and *V. harveyi* [3, 12, 13]. Clustering of bacteria with glycopolymers was observed for polymer concentrations of 0.04-0.06 mM for *E. coli* [12, 13] and 0.16 mM for *V. harveyi* [3]. GATG dendrimers functionalized with 27 mannose groups have previously been used to study binding affinity between Concanavalin A and carbohydrates [25].

With the hydrophilic nature of hydroxyl ligands it is expected that the terminal groups of the functionalised GATG dendrimers are accessible on the periphery in aqueous buffer. Estimated numbers of *V. harveyi* for OD_{600} = 1.0 used in the cluster assays were around ~10^9 CFU/mL [11]. Using a known dendrimer concentration, it is possible to calculate the number of dendrimer molecules per cell used in the cluster assay. For dendrimer concentration of 0.5 mg/mL, the numbers of carbohydrate dendrimers were 3 x 10^{16} for the G1 and 3 x 10^{15} for the G3 dendrimers; giving calculated dendrimer/bacteria ratios of ~3 x10^7 and ~3 x 10^6 dendrimers for the G1 and G3 respectively. With this large amount of dendrimers per bacteria, it is possible that the dendrimers were coating the bacteria surface through lectin binding but were not interacting with multiple cells. Due to time limits only one dendrimer concentration was used for the clustering assay (0.5 mg/mL final concentration of dendrimer). The concentration of carbohydrate moieties in these experiments were 0.9 -1 mM,

while the glucose concentration used for the glyco-polymers clustering of *E. coli* and *V. harveyi* were significantly lower: 0.04-0.06 mM [12, 13] and 0.16 mM [3]. If dendrimers were coating the bacteria surface instead of bridging several bacteria and binding to bacteria together, no clustering effect would have been seen. The clustering assay thus should be repeated with lower concentrations of dendrimers.

To evaluate the possibility of *Vibrio* to use the dendrimer as a carbon source, the bacteria could be grown in the presence of the repeating unit, composed of the gallic acid and triethylene glycol, in the absence of the added carbon source, casamino acids. The characterization of dendrimer after incubation with bacteria through NMR, TLC, DLS and GPC could help determine if the dendrimer have been biodegraded in any way.

4.5 CONCLUSIONS

Diol-dendrimers were designed to quench the QS signal AI-2 by binding to the boric acid necessary to from the active QS molecule. Unfortunately, none of the dendrimers were able to significantly inhibit luminescence in neither of the *V. harveyi* mutants MM32 nor BB170 at diol concentrations similar to those reported with linear polymers [3]. However carbohydrate dendrimers and high concentrations of G1-tetraol and G3-diol showed dose-dependent decreases in luminescence after 4h, while dose-dependent increase of luminescence was observed at later time points. The reason for this possible dual behaviour with

MM32 or the lack of quenching with BB170 is not clear. It is possible that the increased growth of *V. harveyi* in the presence of hydroxyl-dendrimer could explain the increase in luminescence apparent at later time points. Gram negative bacteria of *Pseudomonas* species have been shown to degrade polyethylene glycol chains, it is not known whether *Vibrio* species are capable of degrading GATG and ethylene-glycol chains through extracellular proteases in a nutrient-poor medium. More experiments are needed to understand the increase in growth observed with diol-dendrimers.

No clustering was seen for any of the diol-dendrimers, despite the effect on aggregation known of the linear glucose polymers. The dendrimer and glucose concentration used were higher than previously reported, and with a dendrimer/bacteria ratio of $10^{6-}10^{7}$ it may have been that the non-charged dendrimers were binding to single bacteria, in such a way, an individual cell may not have been able to aggregate and cluster, as was previously observed with linear polymers. It is possible that experiments with lower concentration of functional groups could show the induced clustering in *Vibrio*.

4.6 REFERENCES

[1] Miller, S.T., Xavier, K.B., Campagna, S.R., Taga, M.E., Semmelhack, M.F., Bassler, B.L., and Hughson, F.M. (**2004**). *"Salmonella typhimurium recognizes a chemically distinct form of the bacterial quorum-sensing signal AI-2."* Mol Cell 15(5): 677-87.

[2] Bosch, L.I., Fyles, T.M., and James, T.D. (**2004**). *"Binary and ternary phenylboronic acid complexes with saccharides and Lewis bases."* Tetrahedron 60(49): 11175-11190.

[3] Xue, X., Pasparakis, G., Halliday, N., Winzer, K., Howdle, S.M., Cramphorn, C.J., Cameron, N.R., Gardner, P.M., Davis, B.G., Fernandez-Trillo, F., and Alexander, C. (**2011**). *"Synthetic polymers for simultaneous bacterial sequestration and quorum sense interference."* Angew Chem Int Ed Engl 50(42): 9852-6.

[4] Nizet, V. and Esko, J.D., *Chapter 39 Bacterial and Viral Infections*, in *Essentials of Glycobiology*, A. Varki, et al., Editors. 2009, Cold Spring Harbor Laboratory Press: Cold Spring Harbor (NY).

[5] Sharon, N. (**2006**). *"Carbohydrates as future anti-adhesion drugs for infectious diseases."* Biochim Biophys Acta 1760(4): 527-37.

[6] Kunz, C., Rudloff, S., Baier, W., Klein, N., and Strobel, S. (**2000**). *"Oligosaccharides in human milk: structural, functional, and metabolic aspects."* Annu Rev Nutr 20: 699-722.

[7] Pieters, R.J. (**2007**). *"Intervention with bacterial adhesion by multivalent carbohydrates."* Med Res Rev 27(6): 796-816.

[8] Greenberg, E.P., Hastings, J.W., and Ulitzur, S. (**1979**). *"Induction of luciferase synthesis in Beneckea harveyi by other marine bacteria."* Arch Microbiol 120(2): 87-91.

[9] Pappin, B., Kiefel, M.J., and Houston, T.A. (**2012**). Boron-Carbohydrate Interactions - Comprehensive studies on Glycobiology and Glycotechnology, INTECH Open Access Publisher.

[10] Lui, L.T., Xue, X., Sui, C., Brown, A., Pritchard, D.I., Halliday, N., Winzer, K., Howdle, S.M., Fernandez-Trillo, F., Krasnogor, N., and Alexander, C. (**2013**). *"Bacteria clustering by polymers induces the expression of quorum-sensing-controlled phenotypes."* Nat Chem 5(12): 1058-65.

[11] Louzao, I., Sui, C., Winzer, K., Fernandez-Trillo, F., and Alexander, C. (**2015**). *"Cationic polymer mediated bacterial clustering: Cell-adhesive properties of homo- and copolymers."* Eur J Pharm Biopharm 95(Pt A): 47-62.

[12] Pasparakis, G. and Alexander, C. (**2008**). *"Sweet talking double hydrophilic block copolymer vesicles."* Angew Chem Int Ed Engl 47(26): 4847-50.

[13] Pasparakis, G., Cockayne, A., and Alexander, C. (**2007**). *"Control of bacterial aggregation by thermoresponsive glycopolymers."* J Am Chem Soc 129(36): 11014-5.

[14] Bernardi, A., Jimenez-Barbero, J., Casnati, A., De Castro, C., Darbre, T., Fieschi, F., Finne, J., Funken, H., Jaeger, K.E., Lahmann, M., Lindhorst, T.K., Marradi, M., Messner, P., Molinaro, A., Murphy, P.V., Nativi, C., Oscarson, S., Penades, S., Peri, F.,

Pieters, R.J., Renaudet, O., Reymond, J.L., Richichi, B., Rojo, J., Sansone, F., Schaffer, C., Turnbull, W.B., Velasco-Torrijos, T., Vidal, S., Vincent, S., Wennekes, T., Zuilhof, H., and Imberty, A. (**2013**). *"Multivalent glycoconjugates as anti-pathogenic agents."* Chem Soc Rev 42(11): 4709-27.

[15] Vydryakova, G.A., Kirpichenko, T.V., and Lifant'eva, A.A. (**2008**). *"Formation of Aggregated Structures by Luminescence Bacteria in the Presence of Carbohydrates."* Microbiology 76(2): 246-248.

[16] Vydryakova, G.A. (**2006**). *"Carbohydrate Specificity of Lectins from Luminous Bacteria."* Appl Biochemi Micro 42(4): 364-368.

[17] Liu, P.C. and Lee, K.K. (**1999**). *"Cysteine protease is a major exotoxin of pathogenic luminous Vibrio harveyi in the tiger prawn, Penaeus monodon."* Lett Appl Microbiol 28(6): 428-30.

[18] Chiellini E., Corti A., D'Antone S., and Solaro R. (**2003**). *"Biodegradation of poly (vinyl alcohol) based materials."* Prog Polym Sci(28): 963-1041.

[19] Huang, Y.-L., Li, Q.-B., Deng, X., Lu, Y.-H., Liao, X.-K., Hong, M.-Y., and Wang, Y. (**2005**). *"Aerobic and anaerobic biodegradation of polyethylene glycols using sludge microbes."* Process Biochem 40(1): 207-211.

[20] Haines, J.R. and Alexander, M. (**1975**). *"Microbial Degradation of Polyethylene Glycols."* Appl Microbiol 29(5): 621-625.

[21] Francis, V., Subin, S.R., Bhat, S.G., and Thachil, E.T. (**2012**). *"Characterization of linear low-density polyethylene/poly(vinyl alcohol) blends and their biodegradability by Vibrio sp. isolated from marine benthic environment."* J. Appl. Polym. Sci. (124): 257-265.

[22] Nogales, J., Canales, A., Jimenez-Barbero, J., Serra, B., Pingarron, J.M., Garcia, J.L., and Diaz, E. (**2011**). *"Unravelling the gallic acid degradation pathway in bacteria: the gal cluster from Pseudomonas putida."* Mol Microbiol 79(2): 359-74.

[23] Li, A., Chen, J., Zhu, W., Jiang, T., Zhang, X., and Gu, Q. (**2007**). *"Antibacterial activity of gallic acid from the flowers of Rosa chinensis Jacq. against fish pathogens."* Aquaculture Res 38(10): 1110-1112.

[24] Nagahori, N. and Nishimura, S.-I. (**2000**). *"Tailored Glycopolymers: Controlling the Carbohydrate−Protein Interaction Based on Template Effect."* Biomacromolecules 2(1): 22-24.

[25] Munoz, E.M., Correa, J., Fernandez-Megia, E., and Riguera, R. (**2009**). *"Probing the relevance of lectin clustering for the reliable evaluation of multivalent carbohydrate recognition."* J Am Chem Soc 131(49): 17765-7.

5. Biological application studies of Phenylboronic-acid Dendrimers

5.1 INTRODUCTION

The first strategy for interference of quorum sensing, as described in chapter 4, aimed to interfere with the formation of the active S-THMF-borate complex by synthesizing dendrimers with diol-functionality and affinity for the borate in the bacteria medium. Another approach for the inhibition of AI-2 is to target the DPD directly by mimicking the boronic acid binding to DPD using boronic acids (*Figure 5.1*). By targeting the molecule itself instead of the boric acid, a successful quorum-quenching molecule could be a potential QS interference agent for any of the bacteria depending on the AI-2 system.

Ni and colleagues evaluated a library of boronic acid derivatives for the inhibition of luminescence in *V. harveyi* MM32 and found that the five candidates with the lowest IC_{50} were all phenylboronic acids [1]. Other important structure-activity observations were that all phenylboronic acids had minimal substitution except in the *para*-position and that boronic acids attached directly to sp^3 carbon or with additional ionizable functional groups, such as carboxylic acids, had lower inhibitory activity.

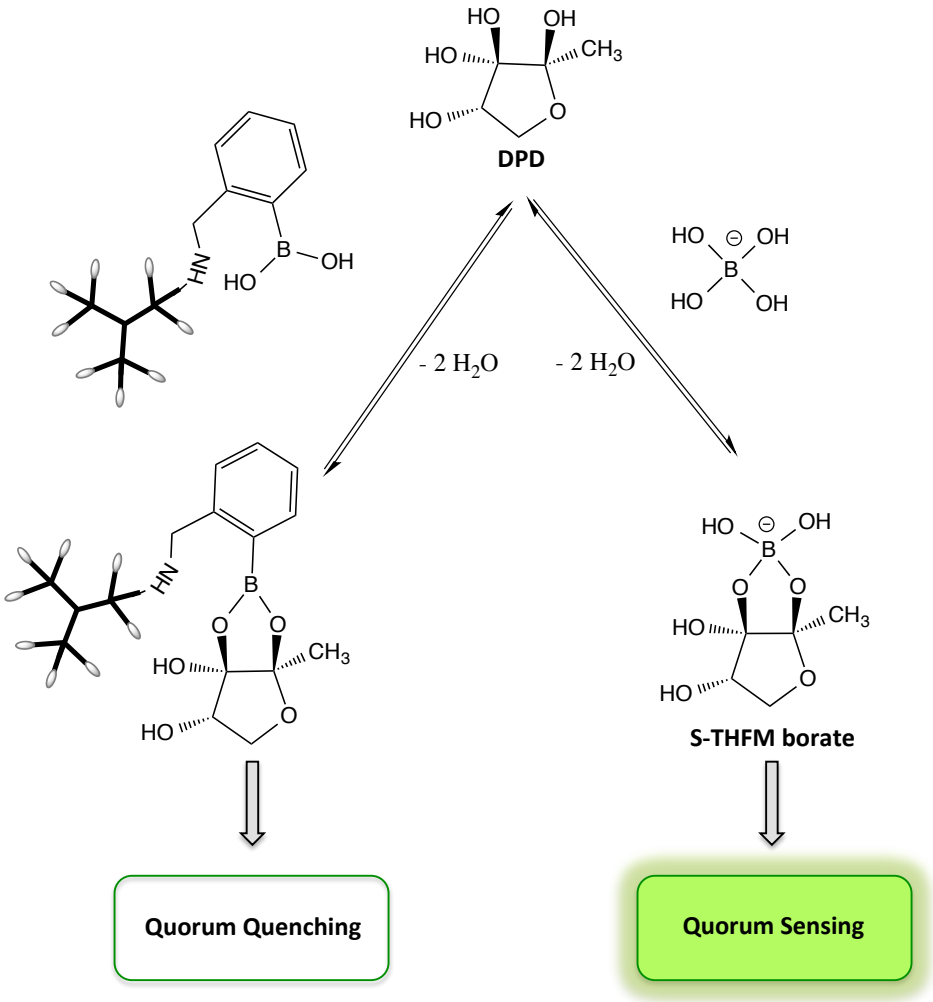

Figure 5.1 Strategy for the quorum quenching with phenylboronic-acid dendrimers. DPD complexes with boric acid to form S-THFM-borate, the QS molecule recognised by *V. harveyi*. This activates the QS cascade leading to luminescence. Dendrimers decorated with phenylboronic acid could bind to DPD, inhibiting the formation of the borate complex. Without the active QS molecule, the luminescence is not detectable.

In addition, boronic acid compounds have been shown to have antibacterial activity such as inhibition of penicillin binding proteins (PBPs), which are relevant for the synthesis of the cell wall [2, 3] and the deactivation of β-lactamase, an enzyme involved in bacterial antibiotic resistance [4-6]. PBPs are enzymes that catalyse the synthesis of the bacterial cell wall through reactions involved in the assembling of the peptidoglycan [7]. The enzymes are involved

in many different reactions but share the capacity to bind to the β-lactam rings present in relevant antibiotics. Bacteria that can produce β-lactamase enzymes can inactivate β-lactam antibiotics and thus will be resistant to their bactericidal effects. Boronic acids have been shown to be promising as β-lactamase inhibitors, binding to a serine residue present in the catalytic site of the enzyme [6]. Analysing the crystal structure of boronic acids derivatives in complexes with β-lactamase enabled the synthesis of boronic acid able to inhibit β-lactamase with inhibitory constants in the nano-molar range [8].

PBPs are classified in terms of high and low molecular weight. Inhibition of high molecular weight PBP leads to cell death while inhibition of low molecular weight PBP leads to changes in the crosslinking pattern of the cell wall [9]. Phenylboronic acids **39** (*Figure 5.2*) showed inhibition of low molecular weight PBP R39 from Gram-positive bacteria *Actinomadura*, a PBP sharing homology with *E. coli* [3]. On the other hand, boronic acid **40** (*Figure 5.2*) inhibited both high and low molecular weight PBPs from *Streptococcus pneumonia* and *Actinomadura* strains [2]. Peptide-boronic acids have also been shown to inhibit several different subtypes of PBPs [10].

In the work reported in this chapter, the possibility of phenylboronic-acid dendrimers to have an effect on bacterial growth and viability will be assessed by optical density and colony forming unit assays. The aim of this study was to decorate dendrimers with phenylboronic acids to quench the DPD and inhibit the formation of the active form in *V. harveyi*: S-THMF-borate. Accordingly,

the ability of phenylboronic acid-dendrimers to interfere with quorum sensing and bacterial growth were evaluated as described below.

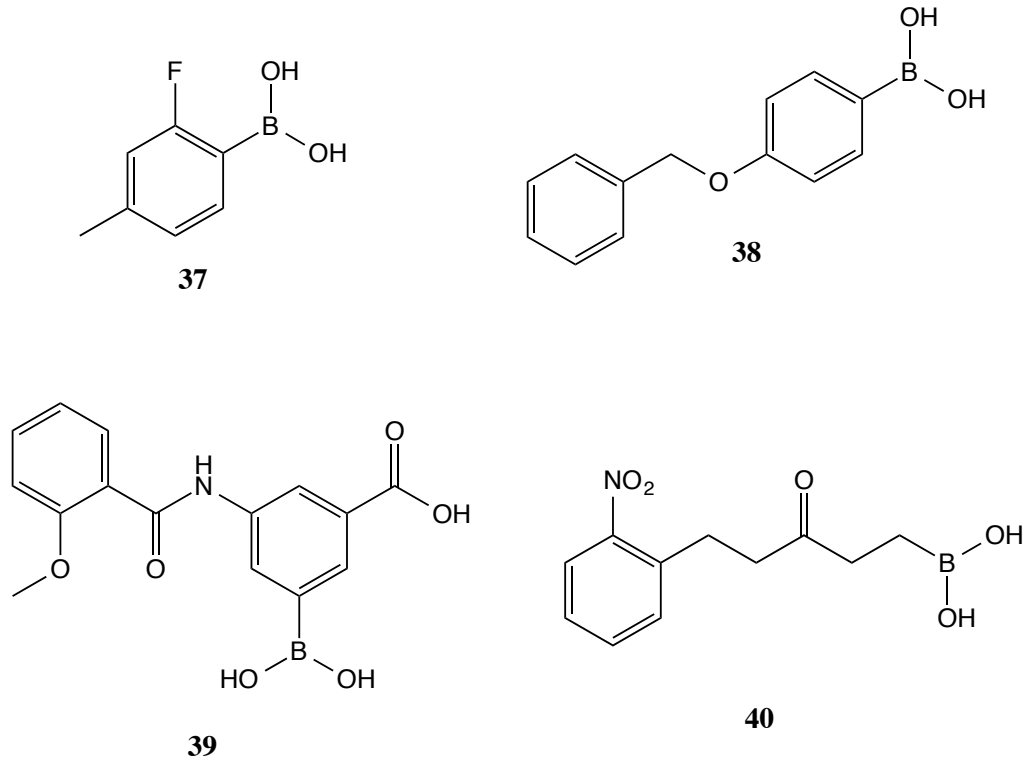

Figure 5.2 Examples of phenylboronic acids with antibacterial activity [1-3].

Structure of dendrimers investigated in this chapter:

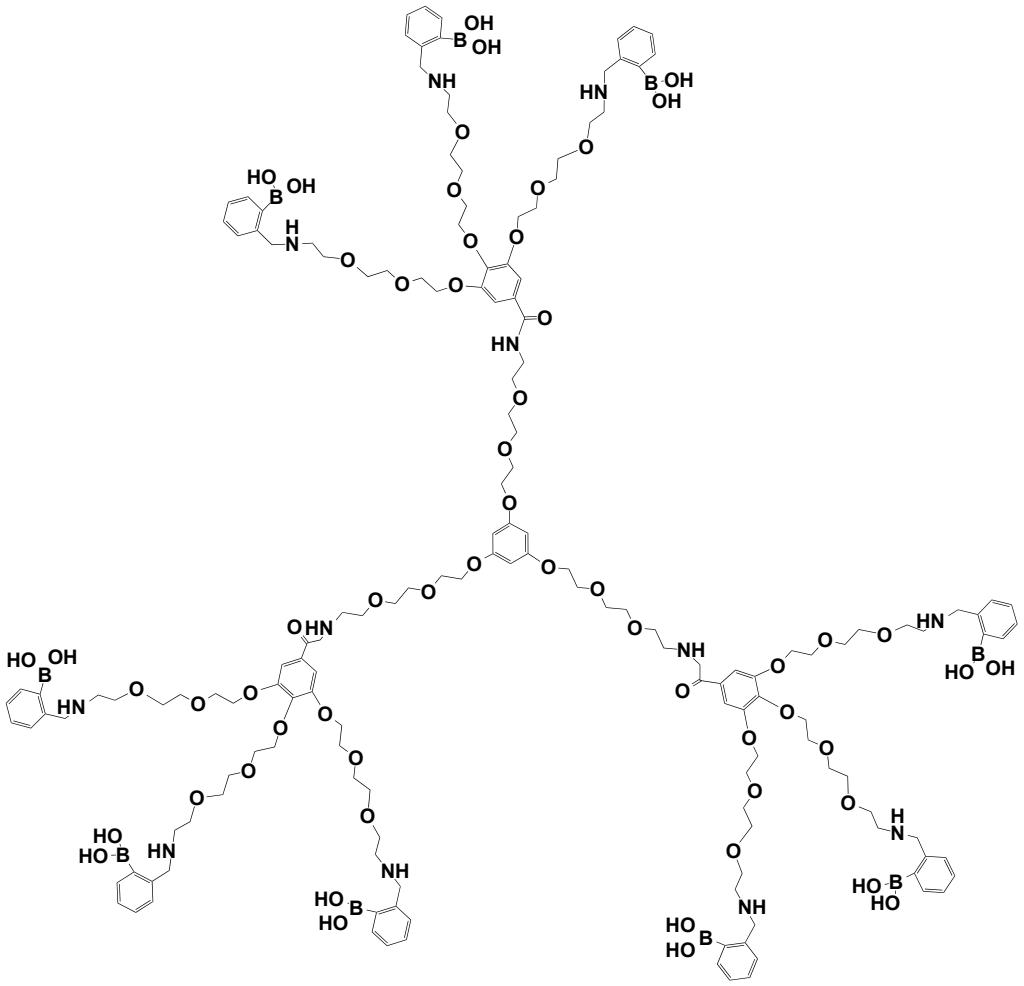

Figure 5.3 Structure of G1 GATG dendrimer functionalized with phenylboronic acid.

Boronic acid Dendrimers			
	B(OH)$_2$	Theoretical MW	Size
G1-B(OH)$_2$	9	3 390.01	2.7 nm
G3-B(OH)$_2$	81	32 735.04	6.0 nm

Table 5.1. Number of surface phenylboronic acids, calculated molecular weight and size (as determined by DLS at 25 °C (1 mg/mL) in a 150 mM LiCl solution.

5.2. EXPERIMENTS

The protocols for the assays are all described in Chapter 2. In brief; for the **luminescence assay (protocol 4**), overnight cultured bacteria were adjusted to OD = 1.0 and diluted 5000-fold in boron-depleted AB medium. Boric acid was added to the medium with final concentrations of 400 μM for experiments with *V.harveyi* MM32 and 22 μM for *V. harveyi* BB170. In the assay with MM32, DPD was added to media to a final concentration of 22 μM. Since MM32 is not able to produce DPD, in this way the limiting concentration for formation of S-THMF-borate induced luminescence was 22 μM for both bacterial strains. Dendrimer stock solutions were prepared in dH_2O with a concentration 10 times higher than final concentrations. Selected dendrimers (20 μL of stock solutions, 10 times more concentrated than final solution) were incubated with 180 μL of bacteria suspension (~10^4 CFU/mL) in a 96-well plate at 30 °C. The final volume in each well was 200 μL. Optical density at 600 nm and luminescence were measured every 30 min for at least 10 h. Graphs show the mean values of data obtained with error bars, based on the Standard Deviations (SD) from the mean. For MM32, the magnitude of the value for the luminescence in the presence of dendrimers was divided by the magnitude of the value for luminescence for bacteria alone for 4 h, 8 h, 12 h and 16 h in order to present the relative luminescence. For BB170, the time (in 30 min interval) to reach initial light production after decay phase (*Figure 4.8*) was presented as recovery time. Calculations for relative luminescence and recovery time were conducted for each individual sample. Graphs represent minimum, maximum and mean values.

For the **clustering assay** (**protocol 5**) overnight cultured bacterial suspensions were diluted to OD_{600} = 1.0 in PBS, the bacteria solution passed through a 5 μm filter and incubated with or without dendrimers (final dendrimer concentrations 0.25 mg/mL and 0.5 mg/mL). At different time points 300-1000 μL of the mixture was added to the water-filled counter cell and cluster size was measured. Graphs show mean values from triplicate experiments.

For the **CFU assay (protocol 7)**, bacteria were incubated with dendrimers as for the luminescence assay. At each time point, an aliquot was collected, diluted in PBS and plated on LB-agar plates. Plates were incubated overnight at 30 °C and colonies were counted the following day. Graphical data represent mean values and error bars, SD.

All samples were evaluated in triplicate and experiments were repeated at least twice, with the exception of the luminescence experiments with G1-$B(OH)_2$.

5.3 RESULTS

5.3.1 Luminescence of *V. harveyi* in the presence of Gn-B(OH)$_2$

GATG dendrimers functionalised with phenylboronic acids were synthesised to target DPD, preventing the formation of S-THMF borate. Dendrimers were evaluated in the *V. harveyi* MM32 and BB170 mutants, using the same conditions as described previously (**protocol 4**). The aim was to evaluate inhibition of the luminescence produced by bacteria in response to increasing concentrations of Gn-B(OH)$_2$.

The luminescence experiment with MM32 was first conducted using dendrimer concentrations of 0.25-1 mg/mL. At these concentrations G3-B(OH)$_2$ inhibited all luminescence while at the same time OD_{600} increased in a dose-dependent manner (*Figure 5.3*). However, after repeating experiments incubating dendrimers in AB medium in the absence of bacteria the increase in OD_{600} remained (*Figure 5.4*). Samples were then plated on LB agar plates to confirm that there was no contamination of other bacteria responsible for the increase in OD_{600} (*Figure 5.5*). MM32 was incubated with dendrimer in PBS to evaluate if the AB medium was the reason for the increase in OD. G3-B(OH)$_2$ in PBS medium did not cause any increase in optical density, however *V. harveyi* MM32 did not grow in this medium. This suggested that there were interactions of dendrimers with components in the AB medium, which subsequently caused aggregation. To confirm this point, dendrimers were incubated in AB medium for 24 h at different time points and the cluster sizes were measured via clustering assays. G3-B(OH)$_2$ in AB medium formed large

clusters in the absence of bacteria while *V. harveyi* did not aggregate in the presence of G3-B(OH)$_2$ in PBS medium *(Figure 5.6)*. This confirms the results that the increase in optical density was due to aggregation formed between boronic acid-dendrimers and the AB medium in the absence of bacteria.

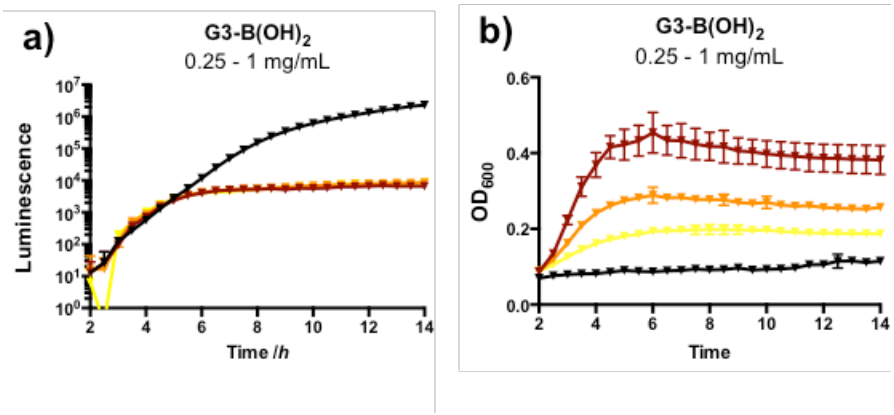

Figure 5.3 Luminescence (Relative Luminescence Units) of *V. harveyi* MM32 in the absence (black) and presence of G3-B(OH)$_2$ in AB medium. Luminescence (a) and optical density (b) at 600 nm (OD_{600}) are presented. Final dendrimer concentrations are 0.25 mg/mL (yellow), 0.5 mg/mL (orange) and 1 mg/mL (red).

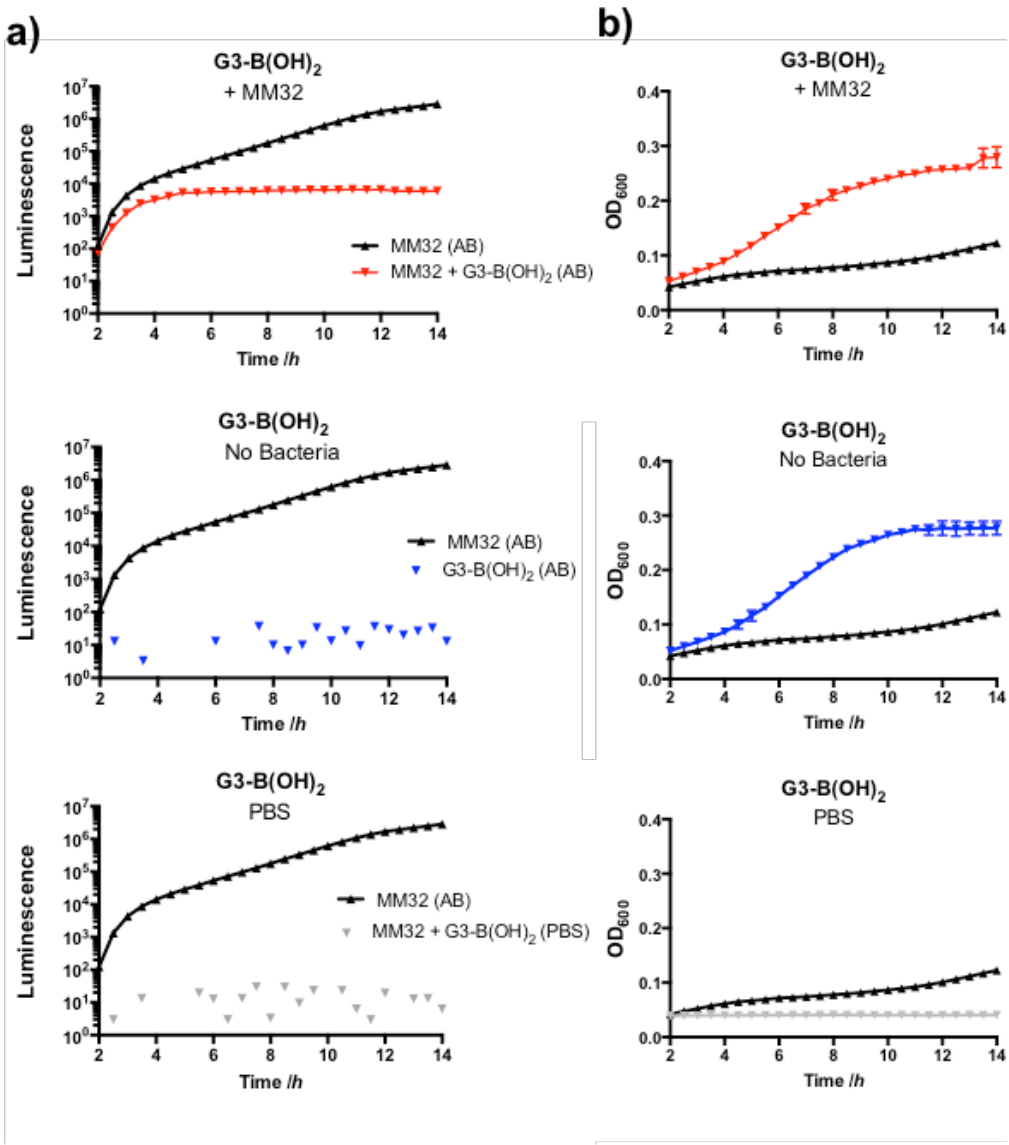

Figure 5.4 Luminescence (Relative Luminescence Units) (a) and optical density (b) at 600 nm (OD_{600}) of *V. harveyi* MM32 in AB medium (black). G3-$B(OH)_2$ in AB medium with (red) and without bacteria (blue). G3-$B(OH)_2$ with bacteria in PBS (grey) Final dendrimer concentration 0.25 mg/mL.

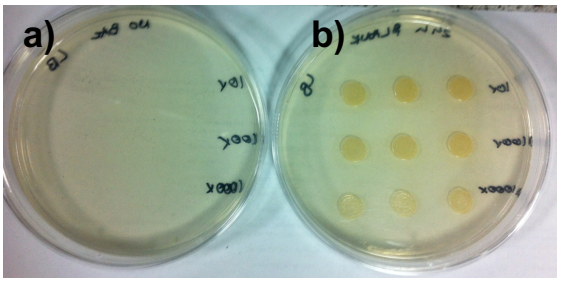

Figure 5.5 Aliquots plated from G3-$B(OH)_2$ (0.25 mg/mL) incubated in AB medium in the absence (a) and presence (b) of MM32.

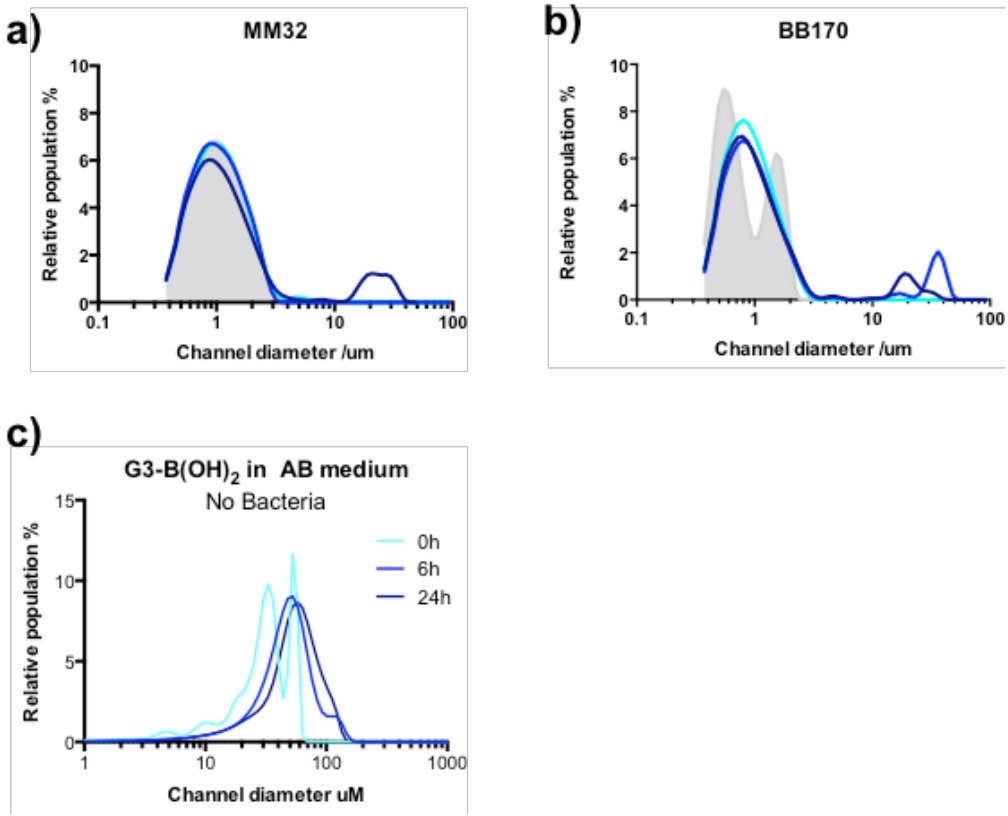

Figure 5.6 Size distribution of bacteria in the absence (grey) and presence of G3-$B(OH)_2$ in PBS after 5 min (light blue), 30 min (royal blue) and 60 min (dark blue) for (a) *V. harveyi* MM32 and (b) *V. harveyi* BB170 suspension (OD_{600} 1.0). Final concentrations of dendrimers: 0.25 mg/mL for MM32 and 0.5 mg/mL for BB170. (c) Size distribution of G3-$B(OH)_2$ in AB medium after 0 h (light blue), 6 h (royal blue) and 24 h (dark blue). Final concentrations of dendrimers: 0.25 mg/mL.

The AB medium contains $MgSO_4$, NaCl and casamino acids. After boron-depletion and adjustment of pH to 7.5 with KOH the additives (glycerol, L-arginine, K_2HPO_4 and boric acid) are added (*Figure 5.7a*) [11, 12]. In order to understand which component/s of the AB media could be involved in the aggregation with G3-$B(OH)_2$, OD_{600} was measured in the absence of one additive component at a time (*Figure 5.7b*). Removal of glycerol or L-arginine delayed the formation of aggregates, but only removal of K_2HPO_4 interrupted

aggregation all together suggesting that the presence of K_2HPO_4 was essential for the G3-$B(OH)_2$ aggregating.

Unfortunately, *V. harveyi* did not grow in the absence of K_2HPO_4 or in the alternative PBS medium tested, and these media could therefore not be used in further assay. G3-$B(OH)_2$ also caused aggregation in the absence of bacteria in LB medium (data not shown). Trials were made to find a medium with good bacterial growth and no dendrimer aggregation, however due to time limits no such medium was found. Using lower concentrations of G3-$B(OH)_2$ in AB medium it was possible to observe an increase in OD_{600} due to bacterial growth above that of $B(OH)_2$-AB medium aggregation. In this way the effect of dendrimers on optical density could be measured despite medium aggregation.

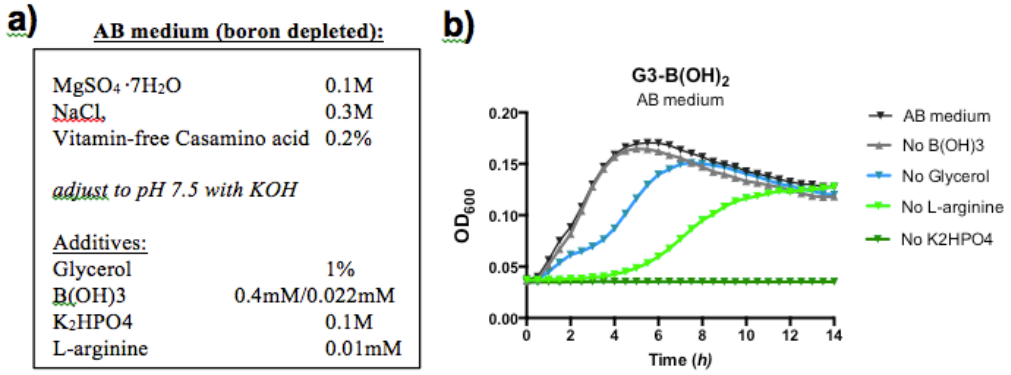

Figure 5.7 Components of AB medium with boric concentrations used in MM32/BB170 luminescence assay (b) and optical density (a) at 600 nm (OD_{600}) of G3-$B(OH)_2$ in AB medium (black) in the absence of $B(OH)_3$ (grey), glycerol (blue), L-arginine (light green) or K_2HPO_4 (dark green). Dendrimer concentration: 0.1 mg/mL.

Thus, MM32 was incubated with G3-$B(OH)_2$ at concentrations 0.02 -0.5 μg/mL following **protocol 4**. Luminescence and OD_{600} were recorded every 30 min (*Figure 5.9*). Relative luminescence after 4, 8, 12 and 16 h are presented in *Figure 5.10 and Appendix Figure A40.* G3-$B(OH)_2$ showed inhibition of concentration-dependent decrease of growth and luminescence with dendrimer concentration from 0.06 μg/mL (*Figure 5.9).* Since the G3 dendrimer contains 81 functional borate groups, the inhibitory concentrations were equivalent to a $B(OH)_2$ concentration of 0.16 μM (*Figure 5.10*). There was a dose-dependent decrease in relative luminescence at all 4 time points, with 50-60% inhibition of luminescence with $B(OH)_2$ concentrations of 0.31 μM.

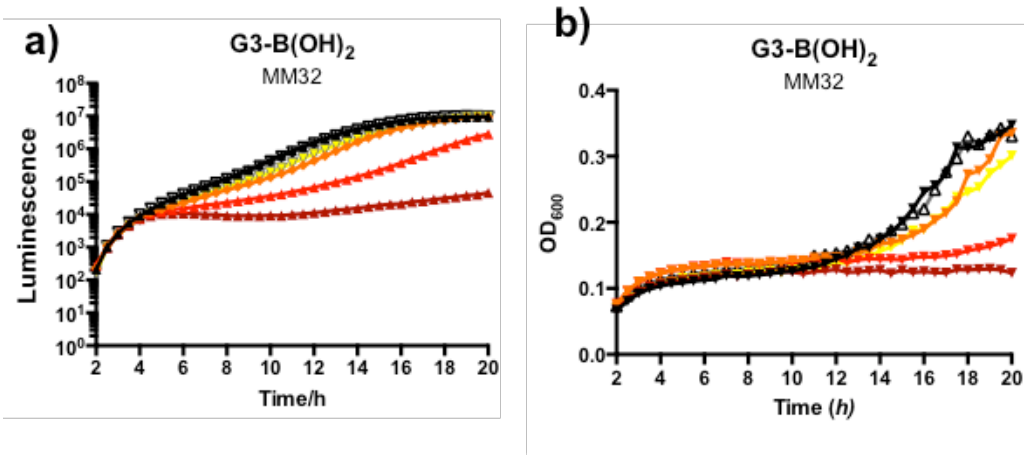

Figure 5.9 Luminescence (Relative Luminescence Units) of *V. harveyi* MM32 in the absence (black) and presence of G3-$B(OH)_2$ in AB medium. Luminescence (a) and optical density (b) at 600 nm (OD_{600}) are presented. Final dendrimer concentrations are 0.5 μg/mL (dark red), 0.25 μg/mL (red), 0.125 μg/mL (orange), 0.06 μg/mL (yellow) and 0.02 μg/mL (white). Presented are mean values from three sample replicates.

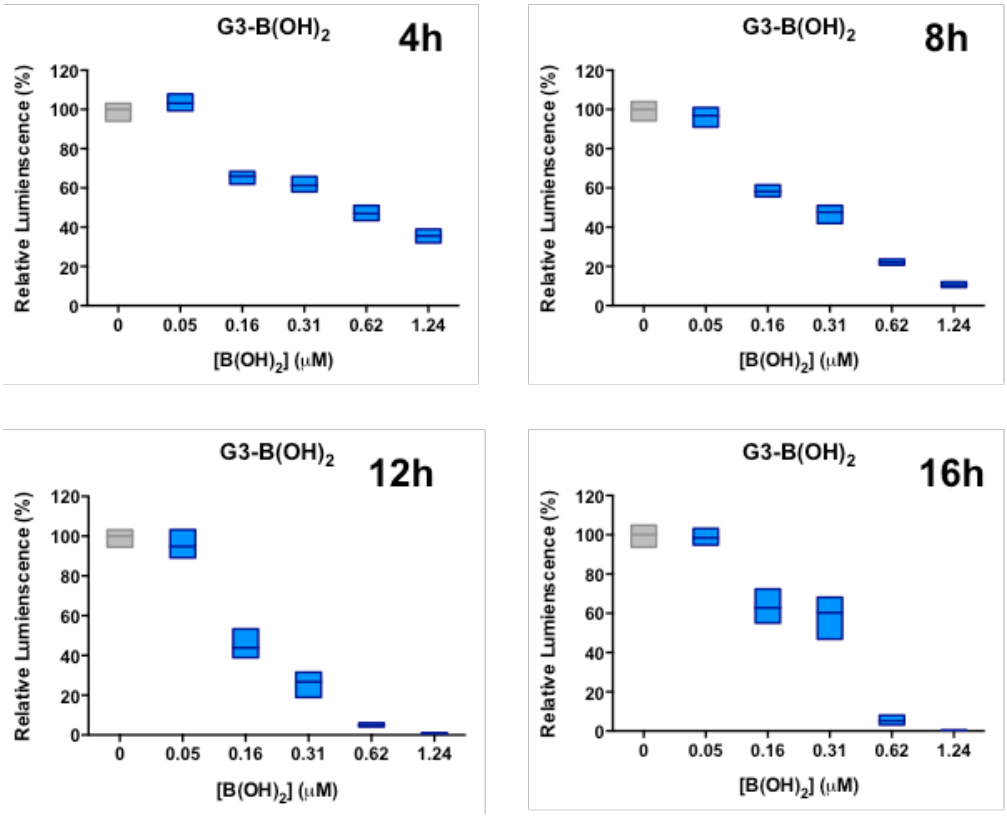

Figure 5.10 Effect of phenylboronic acid concentration on relative luminescence of MM32 in the presence of G3-$B(OH)_2$ in AB medium.

To see if the same effects on luminescence and optical density were observed with a bacterial strain able to produce its own DPD, luminescence and optical density were measured in the presence of dendrimers using the *V. harveyi* BB170 mutant. Quenching of quorum sensing in *V. harveyi* BB170 is observed as a shift to the right or a delay in the enhancement phase in the measured luminescence curve, and an increase in recovery time. (*Chapter 4, Figure 4.7*). BB170 was incubated with G3-$B(OH)_2$ at dendrimer concentrations of 0.06-5 μg/mL following **protocol 4.** The phenylboronic acid dendrimer of generation G1 was incubated with BB170 at dendrimer concentrations 0.06-1000 μg/mL. Luminescence and OD_{600} was recorded every 30 min (*Figure 5.12, Appendix*

Figure A41). The recovery times for G1 and G3 dendrimers are presented in *Figure 5.13*.

A similar effect as for MM32 was recorded when boronic acid-functionalized dendrimers were incubated with BB170, where both luminescence and OD_{600} decreased with dendrimer concentration There was a dose-dependent decrease in luminescence recovery time for both G1 and G3 dendrimers (*Figure 5.13*). For the generation three (G3), luminescence and OD_{600} decreased with dendrimer concentration from 0.06 μg/mL ($B(OH)_2$ concentration 0.16μM) (*Figures 5.11, 5.13*). In the case of G1, a dendrimer concentration of 25μg/mL was needed to see to detect decreasing luminescence (*Figures 5.12 and Appendix*), which corresponds to a $B(OH)_2$ concentration of 33 μM (*Figure 5.13*). The dendrimers in AB medium alone gave some increase in optical density, but not enough to account for the difference between bacteria in the absence and presence of dendrimers (*Figures 5.11-12*).

The G3 dendrimer showed inhibition of luminescence at sub-micromolar concentrations of boronic acid (0.16 – 0.31 μM), while a decrease in luminescence with corresponding G1 dendrimer was only observed with more than 100-fold more boronic acid (25-33 μM) (*Figures 5.13 and Appendix Figure A43*).

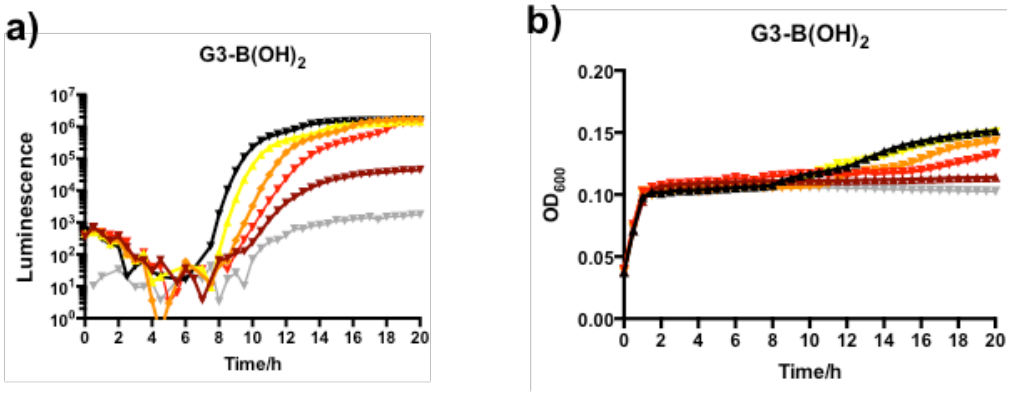

Figure 5.11 Luminescence (Relative Luminescence Units) of *V. harveyi* BB170 in the absence (black) and presence of G3-B(OH)$_2$ in AB medium. Luminescence (a) and optical density (b) at 600 nm (OD_{600}) are presented. Final dendrimer concentrations were 2.5 µg/mL (dark red), 0.5 µg/mL (red), 0.25 µg/mL (orange) and 0.06 µg/mL (yellow). G3-B(OH)$_2$ (5 µg/mL) in the absence of bacteria is presented in grey. Presented are mean values from three replicates.

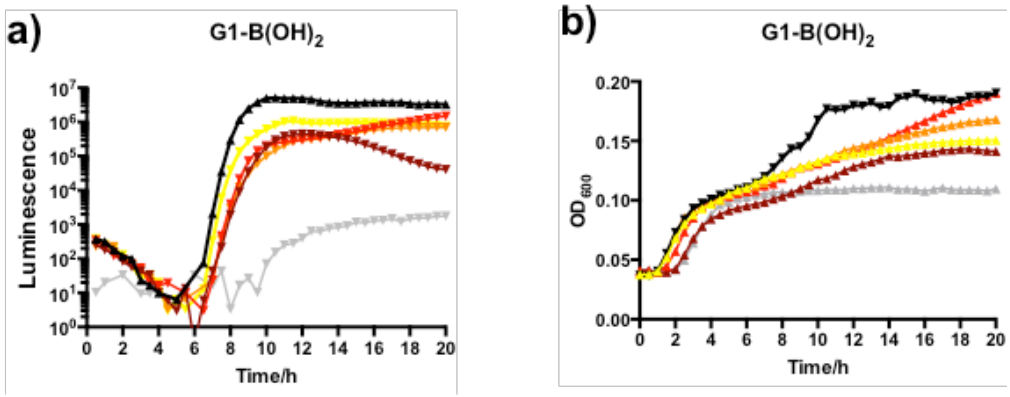

Figure 5.12 Luminescence (Relative Luminescence Units) of *V. harveyi* BB170 in the absence (black) and presence of G1-B(OH)$_2$ in AB medium. Presented are (a) luminescence and (b) optical density at 600 nm (OD_{600}). Final dendrimer concentrations were 1000 µg/mL (dark red), 500 µg/mL (red), 250 µg/mL (orange) and 25 µg/mL (yellow). G1-B(OH)$_2$ (1mg/mL) in the absence of bacteria is presented in grey. Presented are mean values from three replicates. *Some oscillation of the OD_{600} measurement was observed in this experiment; due to time limit the experiment could not be repeated again.

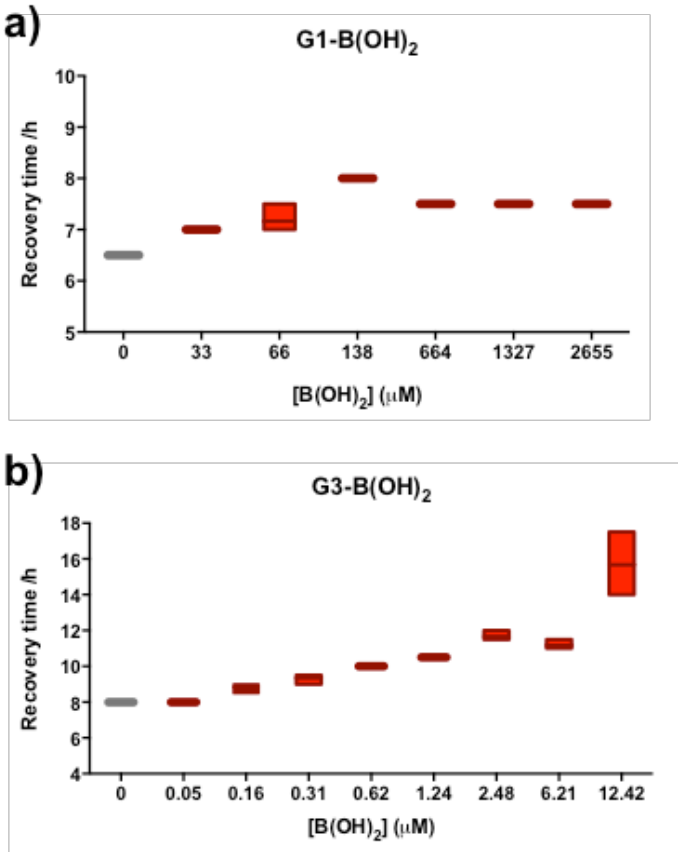

Figure 5.13 Recovery time in hours for BB170 in AB medium in the presence of different concentrations of G1-$B(OH)_2$ (a) and G3-$B(OH)_2$ (b).

5.3.2 Colony Forming Unit counts in the presence of Gn-$B(OH)_2$

In order to see if the decrease in growth observed by optical density was a consequence of reduced bacterial survival, the cell viability was tested by plate count assays after incubation with phenylboronic-acid dendrimers in AB medium and the more nutrient LB medium (**protocol 7**). At each time point, aliquots were collected, diluted and plated on LB-agar plates in triplicates and incubated overnight. The number of CFU for each condition was counted.

V. harveyi MM32 was incubated in the absence or presence of G3-$B(OH)_2$ dendrimers in AB-medium (**protocol 5**). *V. harveyi* BB170 was incubated with

G3-$B(OH)_2$ following the same protocol but AB-medium was exchanged for LB medium.

G3-$B(OH)_2$ showed a bacteriostatic effect on *V. harveyi* when incubated at 0.5 mg/mL in AB medium, with no difference in growth for bacteria incubated with dendrimer after 6, 8 or 24 h compared to time 0 h (*Figure 5.14*). This corresponds well with the optical density experiments, where no increase in OD_{600} was detected at concentrations above 0.5 μg/mL (*Figure 5.9*).

When *V. harveyi* BB170 was incubated with dendrimer in the more nutrient-rich LB medium, there was no difference in CFU between absence and presence of dendrimer at any of the time points. It should be noted that the cross-experiments with MM32 grown in LB medium and BB170 in AB medium were not able to be performed, and the comparison between the two conditions were done between two different bacteria mutants. However, it seems that in the case of the less nutrient-rich AB medium, *V. harveyi* growth was inhibited in the presence of G3-$B(OH)_2$ -dendrimers. The nutrient content of the medium can affect the potency of boronic acid growth inhibition, as reported by Bailey and colleagues [13].

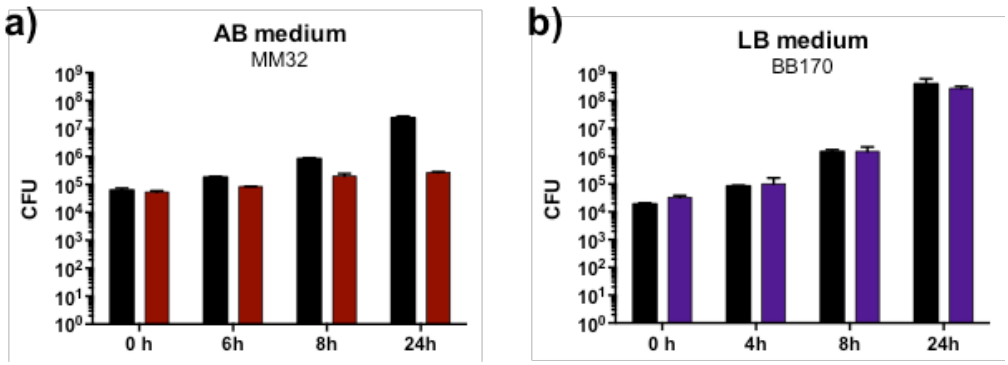

Figure 5.14 Colony Forming Unit (CFU) for *V. harveyi* in the absence (black) and presence (colour) of G3-$B(OH)_2$. MM32 in AB medium (a) and BB170 in LB medium (b) are presented. Final dendrimer concentration: 0.5 mg/mL.

5.4 DISCUSSION

Phenylboronic acids have been reported to have both inhibitory effects of AI-2 quorum sensing [1] and on bacterial growth [3, 13, 14]. Ni and colleagues identified several boronic-acids able to inhibit luminescence in *V. harveyi* MM32 (*Figure 5.1,* compounds **37** and **38**) [1]. The most active compounds were all phenylboronic acids with IC_{50} in the single micromolar range. None of these boronic acids showed significant inhibition of bacterial growth, as calculated by the bacterial cell doubling time, which was 80 min for all compounds tested at or above IC_{50} concentrations. The only exceptions were three phenylboronic acid compounds with a doubling time of 100 min (including compound **38**), a doubling time not significantly different from control (80 min).

Boronic acid compounds have been shown to have various antibacterial activities [14]. Phenylboronic acids have been identified to inhibit PBPs, the group of proteins to which β-lactam antibiotics binds irreversibly and which

are essential for bacterial cell wall synthesis [3]. The highest inhibitory effect was achieved with phenylboronic acid **39,** having a IC_{50} = 23μM against PBP related to Gram negative *E. coli,* and *Neisseria gonorrheae* [3].

Although boronic acid inhibition of PBPs in *Vibrio* has to our knowledge, not yet been studied, they are known to have PBPs, some of which share similarity with those in *E. coli* [15-17]. Waldor and colleagues reported the critical role of high molecular weight PBPs of *Vibrio cholera (V. cholera)* in cell wall biogenesis [18, 19], and the impaired growth and abnormal morphology in a *V. cholera* mutant lacking low molecular weight PBP [20].

Effect of medium nutrient content on the antibacterial effect of boron-containing compounds was reported by Bailey and colleagues [13]. In a low nutrient- medium, boron-containing compounds inhibited growth of *E. coli* while addition of mainly lysine and leucine amino acids increased turbidity. However, cell growth was still abnormal with decreased cell mass together with longer cells and morphological changes to bacterial cell walls.

The multivalent dendrimers with phenylboronic acids decreased quorum sensing and bacterial growth for *V. harveyi* at $B(OH)_2$ from concentrations as low as 0.16 μM for G3 and 33 μM for G1. These data suggest an activity of these dendrimers similar to that of phenylboronic acids previously reported by Ni and colleagues [1], although in this case the dendrimers decreased bacterial growth as well. The dendrimers could be decreasing quorum sensing by binding to DPD and blocking the formation of the active furanosyl boron ester.

Decrease in luminescence could also be a direct result of the inhibition of bacterial growth observed in the AB medium. Due to the aggregation formed in the AB medium in the presence of the dendrimer, it was difficult to distinguish any differences in OD_{600} at the earlier time points (before 10 h) due to the background absorbance of the aggregates. However, at later time points (after 10 h) were OD_{600} values were higher than that of the aggregates, the phenylboronic acids had a clear dose-dependent inhibition on bacterial growth. Decrease in growth will lead to lower levels of luminescence, and in many cases light output from *V. harveyi* is used as measurement of bacterial growth. G3 had a much higher effect on QS than the smaller dendrimer even when $B(OH)_2$ concentrations were normalised. If the decrease in quorum sensing is influenced by the decreased growth, the larger G3 dendrimer could have a larger bacteriostatic effect at lower concentrations than G1. The limiting of *V. harveyi* growth in the presence of phenylboronic acid dendrimers could be due to binding of the dendrimers to the penicillin-binding proteins of the cell wall, as described for other phenylboronic acids with antibacterial effects of other Gram-negative bacteria [3]. Whether binding of boronic-acid dendrimer to bacterial surface polysaccharides such as LPS could also have an effect on bacterial growth is not known and could be considered another possibility.

V. harveyi cells were able to recover from the G3-$B(OH)_2$-induced inhibition in growth seen in AB medium when grown in the more nutrient rich medium LB as determined by cell counts. The medium can affect the antibacterial effect of boronic acids [13]. However, cell counts via colony formation indicate viability, but not changes in cell mass or morphology. In addition, it was not possible to

conduct microscopy imaging to study if the boronic acid compounds induced abnormal behaviour in bacteria. It is possible that an antibacterial effect by boronic acids which inhibited growth in AB medium caused changes in cell morphology in the more LB medium, while the bacteria viability as measured by CFU was still unchanged (*Figure 5.14*). It should be noted that the G3-$B(OH)_2$ concentration in the CFU assay was 1000-fold higher than for the luminescence experiment, thus direct comparisons between the two experiments are difficult to make. A dendrimer concentration of 0.5 mg/mL were used in the CFU experiments for comparison between all dendrimers synthesised in this thesis. Due to time limitation it was not possible to perform the CFU assay with lower concentration of phenylboronic acid dendrimers.

Although the decrease in growth could be the reason the luminescence is decreased, it cannot be excluded that the phenylboronic acids dendrimers have a direct effect on the quenching of the quorum sensing as well. To fully understand the effect of the phenylboronic acid-dendrimers on growth and quorum sensing it is important to find a medium where no aggregation of dendrimer alone occurs while at the same time promotion of bacterial growth can act as a control. It is plausible that aggregation of medium in the presence of dendrimers could interfere with nutrient availability in the medium and bacterial growth.

To understand if the dendrimers have affinity for AI-2, the binding Alizarin Red, a red dye which has well-established ester formation with boronic acids, could be explored using the phenylboronic monomer and dendrimer in

competitive experiments with the QS signal in water. While OD_{600} is used to measure growth, plate counts are utilised to measure viability; thus it would be interesting to try lower concentrations of dendrimer in the colony-counting experiments to investigate Minimal Inhibitory Concentrations (MIC) of the phenylboronic acid monomer and dendrimers.

5.5 CONCLUSIONS

G1 and G3 phenylboronic acid dendrimers revealed an inhibitory effect on growth and luminescence, the dendrimer G3-$B(OH)_2$ inhibits quorum sensing and growth at $B(OH)_2$ concentrations as low as 0.16 μM.

The precipitation induced by this dendrimer in the presence of K_2HPO_4 and the lack of bacterial growth in the medium when it was absent, could be the reason for the decreased growth observed with Gn-$B(OH)_2$. However, it is also plausible that the phenylboronic functionality of the dendrimer is acting as a bacteriostatic agent interfering, for example, with PBPs or LPS of the bacterial cell wall.

More experiments need to be done to understand the reason for the decreasing growth and luminescence inhibition recorded in these preliminary experiments. As mentioned, it is important to find appropriate media to exclude the influence of K_2HPO_4 mediated aggregation induced by dendrimer boronic-acids. Furthermore, to find a MIC concentration and IC_{50} with colony counting or biomass weight experiments the use of phenylboronic acid monomer can give an idea of the concentration range of the growth inhibition. The affinity

for the phenylboronic acid dendrimer to DPD should be studied through competitive assays with boric acid and Alizarin Red.

5.6 REFERENCES

[1] Ni, N., Chou, H.T., Wang, J., Li, M., Lu, C.D., Tai, P.C., and Wang, B. (**2008**). *"Identification of boronic acids as antagonists of bacterial quorum sensing in Vibrio harveyi."* Biochem Biophys Res Commun 369(2): 590-4.

[2] Zervosen, A., Bouillez, A., Herman, A., Amoroso, A., Joris, B., Sauvage, E., Charlier, P., and Luxen, A. (**2012**). *"Synthesis and evaluation of boronic acids as inhibitors of Penicillin Binding Proteins of classes A, B and C."* Bioorg Med Chem 20(12): 3915-24.

[3] Inglis, S.R., Zervosen, A., Woon, E.C., Gerards, T., Teller, N., Fischer, D.S., Luxen, A., and Schofield, C.J. (**2009**). *"Synthesis and evaluation of 3-(dihydroxyboryl)benzoic acids as D,D-carboxypeptidase R39 inhibitors."* J Med Chem 52(19): 6097-106.

[4] Morandi, F., Caselli, E., Morandi, S., Focia, P.J., Blázquez, J., Shoichet, B.K., and Prati, F. (**2003**). *"Nanomolar Inhibitors of AmpC β-Lactamase."* J Am Chem Soc 125(3): 685-695.

[5] Caselli, E., Romagnoli, C., Vahabi, R., Taracila, M.A., Bonomo, R.A., and Prati, F. (**2015**). *"Click Chemistry in Lead Optimization of Boronic Acids as beta-Lactamase Inhibitors."* J Med Chem 58(14): 5445-58.

[6] Weston, G.S., Blazquez, J., Baquero, F., and Shoichet, B.K. (**1998**). *"Structure-based enhancement of boronic acid-based inhibitors of AmpC beta-lactamase."* J Med Chem 41(23): 4577-86.

[7] Sauvage, E., Kerff, F., Terrak, M., Ayala, J.A., and Charlier, P. (**2008**). *"The penicillin-binding proteins: structure and role in peptidoglycan biosynthesis."* FEMS Microbiol Rev 32(2): 234-58.

[8] Morandi, S., Morandi, F., Caselli, E., Shoichet, B.K., and Prati, F. (**2008**). *"Structure-based optimization of cephalothin-analogue boronic acids as beta-lactamase inhibitors."* Bioorg Med Chem 16(3): 1195-205.

[9] Gordon, E., Mouz, N., Duee, E., and Dideberg, O. (**2000**). *"The crystal structure of the penicillin-binding protein 2x from Streptococcus pneumoniae and its acyl-enzyme form: implication in drug resistance."* J Mol Biol 299(2): 477-85.

[10] Pechenov, A., Stefanova, M.E., Nicholas, R.A., Peddi, S., and Gutheil, W.G. (**2003**). *"Potential transition state analogue inhibitors for the penicillin-binding proteins."* Biochemistry 42(2): 579-88.

[11] Greenberg, E.P., Hastings, J.W., and Ulitzur, S. (**1979**). *"Induction of luciferase synthesis in Beneckea harveyi by other marine bacteria."* Arch Microbiol 120(2): 87-91.

[12] Miller, S.T., Xavier, K.B., Campagna, S.R., Taga, M.E., Semmelhack, M.F., Bassler, B.L., and Hughson, F.M. (**2004**). *"Salmonella typhimurium recognizes a chemically distinct form of the bacterial quorum-sensing signal AI-2."* Mol Cell 15(5): 677-87.

[13] Bailey, P.J., Cousins, G., Snow, G.A., and White, A.J. (**1980**). *"Boron-containing antibacterial agents: effects on growth and morphology of bacteria under various culture conditions."* Antimicrob Agents Chemother 17(4): 549-53.

[14] Trippier, P.C. and McGuigan, C. (**2010**). *"Boronic acids in medicinal chemistry: anticancer, antibacterial and antiviral applications."* MedChemComm 1(3): 183-198.

[15] Sengupta, T.K., Chatterjee, A.N., and Das, J. (**1990**). *"Penicillin binding proteins of Vibrio cholerae."* Biochem Biophys Res Commun 171(3): 1175-1181.

[16] Sengupta, T.K., Chaudhuri, K., Majumdar, S., Lohia, A., Chatterjee, A.N., and Das, J. (**1992**). *"Interaction of Vibrio cholerae cells with beta-lactam antibiotics: emergence of resistant cells at a high frequency."* Antimicrob Agents and Chemother 36(4): 788-795.

[17] Teo, J.W., Suwanto, A., and Poh, C.L. (**2000**). *"Novel beta-lactamase genes from two environmental isolates of Vibrio harveyi."* Antimicrob Agents Chemother 44(5): 1309-14.

[18] Dorr, T., Lam, H., Alvarez, L., Cava, F., Davis, B.M., and Waldor, M.K. (**2014**). *"A novel peptidoglycan binding protein crucial for PBP1A-mediated cell wall biogenesis in Vibrio cholerae."* PLoS Genet 10(6): e1004433.

[19] Dörr, T., Möll, A., Chao, M.C., Cava, F., Lam, H., Davis, B.M., and Waldor, M.K. (**2014**). *"Differential Requirement for PBP1a and PBP1b in In Vivo and In Vitro Fitness of Vibrio cholerae."* Infect Immun 82(5): 2115-2124.

[20] Moll, A., Dorr, T., Alvarez, L., Davis, B.M., Cava, F., and Waldor, M.K. (**2015**). *"A D, D-carboxypeptidase is required for Vibrio cholerae halotolerance."* Environ Microbiol 17(2): 527-40.

6. Cationic Dendrimers: aggregation and evaluation of bacterial response

6.1 INTRODUCTION

Cationic polymers have been extensively investigated as potential mimics of antimicrobial peptides, small cationic amphiphiles have an important function in the innate immune system [1-3]. Polycations can bind to the bacterial membrane through electrostatic interactions, causing aggregation of bacteria but due to the interaction with the membrane, can also work as bactericides by cell lysis [4]. Cationic macromolecules increase cell membrane permeability through introduction of nano pores that destabilizes the membrane or causing membrane thinning, both, which can ultimately cause cell lysis [4, 5]. Amphiphilic polymers with amide side chains have been shown to have antibacterial activity against methicillin resistant *S. aureus*, vanomycin resistant *Enterococci* and to disrupt established biofilms formed by *Acinetobacter baumannii* [6]. These polymers have been postulated to act by destabilizing the bacterial cell membrane through membrane depolarization, increasing membrane permeability, thereby decreasing bacterial burden as shown in mice models with chronic *Acinetobacter baumannii* burnt skin infection [6]. Our group has previously showed the clustering effect of cationic polymers with both Gram-positive and Gram-negative bacteria, due to the electrostatic interaction between positively charged polymer and the negatively charged bacterial cell membrane [7, 8]. As mentioned earlier in this thesis,

dendrimers are very amenable materials to interface with biology [9, 10] and since this adhesion is heavily affected by the spatial arrangement of the ligands, it is not surprising that a considerable effort has been placed in using dendrimers in anti-adhesion [10, 11]. This makes them excellent platforms to study interactions with bacteria membranes. In addition, the globular structure of these materials enables investigation of dendrimer architecture on bacterial interaction and clustering.

The presence of terminal azides in GATG dendrimers and their derivatives introduces great flexibility in their peripheral decoration, and not surprisingly, the functionalized dendrimers have found application in the study of receptor-ligand interactions [12, 13] and cell internalization [14], to interfere with protein-protein interactions [15] and amyloid formation [16], or as imaging agents [17]. Moreover, the terminal azides of GATG dendrimers can be easily reduced to afford cationic materials that have been applied in gene delivery [18, 19].

The diffusion of nutrients and signal molecules can be drastically changed inside bacterial clusters. Our group recently reported that polymer-induced aggregation induces expression of QS controlled phenotypes in both human pathogens *E. coli, P. aeruginosa* and in model bacteria *V. harveyi* [8]. Limited diffusion of signal molecules within the cluster leads to high local concentrations of QS molecules and activation of phenotypes controlled by QS, such as luminescence in *V. harveyi (Figure 5.1).*

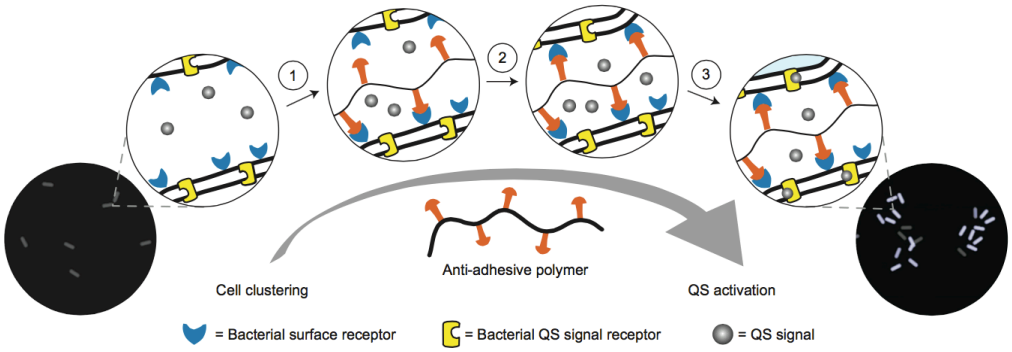

Figure 6.1 QS activation by polymer-induced bacteria clustering in *V. harveyi*. 1. Polymer binds to bacteria through various interactions. 2. Polymer interacts with several bacteria thereby forming aggregates. 3. Limited signal diffusion within the clusters lead to high local concentrations of QS and activation of luminescence. Figure taken from reference [8].

In this chapter the ability of cationic GATG dendrimer to cluster bacteria is evaluated. Using *V. harveyi* as a model organism the cluster effect on quorum sensing signalling is also studied. The combination of cationic charge and hydrophobic character in these antimicrobial dendrimers gives them interesting membrane properties, including increasing cell membrane permeability that can result in bactericidal activity.

Structure of dendrimers investigated in this chapter:

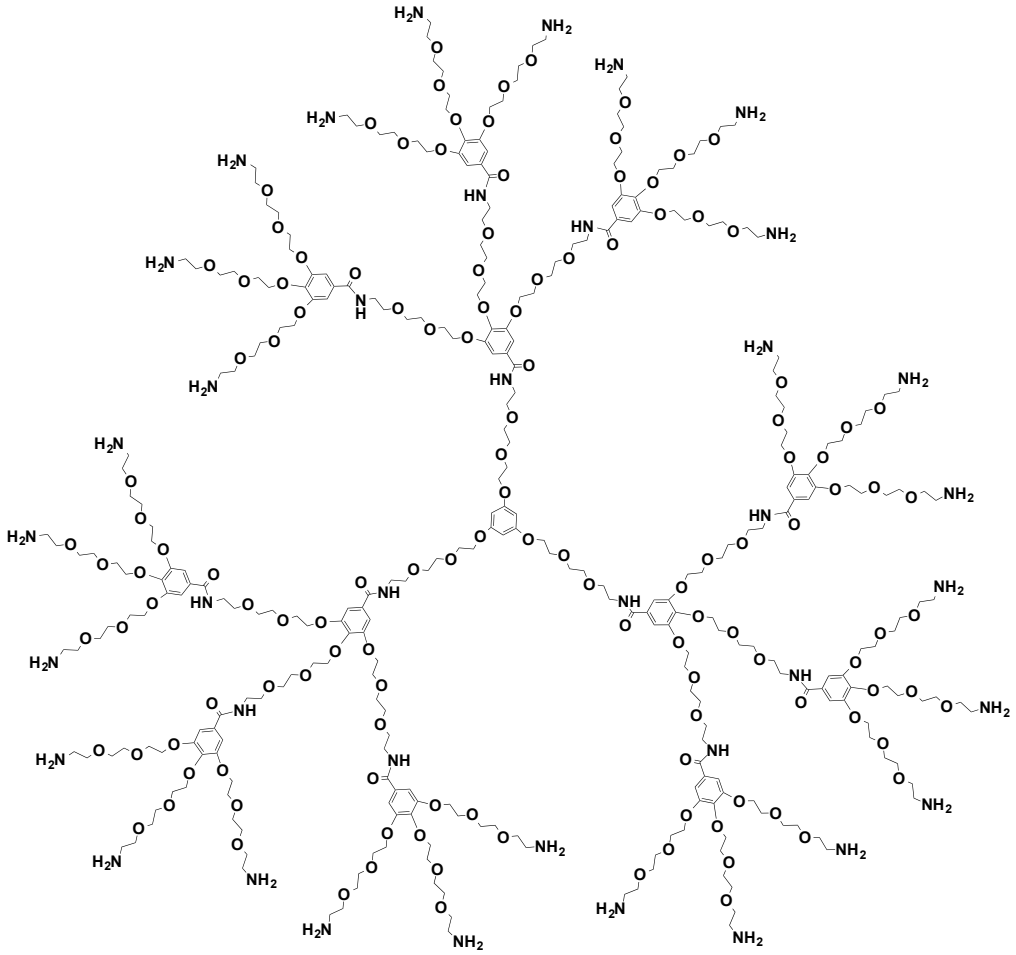

Figure 6.2 Structure of GATG dendrimer G2-NH_2.

Cationic Dendrimers			
	Amines	Theoretical MW	Size (nm)
G1-NH_2	9	2 389	n/a
G1-NH_2	27	7 765	3.62 ± 0.42
G3-NH_2	81	23 891	5.68 ± 0.39

Table 6.1 Number of surface amines, calculated molecular weight and size (as determined by DLS at 25 °C with hydrochloride amino dendrimers (1.5 mg/mL) in a 10 mM NaH_2PO_4 10% HCl 0.1M solution.

6.2 EXPERIMENTS

Fluorescent labelling of G3-NH_2

Stock solutions of MCCA (7.9 mg/mL in dry DCM), 1-ethyl-3-(3-dimethylaminopropyl)carbodiimide hydrochloride (EDC.HCl) (6.9 mg/mL in dry DCM) and NHS (8.3 mg/mL in dry MeOH) were prepared. 20 μL of those stock solutions (2.5 equiv.) were placed in a round-bottomed flask. 100 equiv. of Et_3N (3.6 mL) were added. 7.1 mg of dendrimer were dissolved in 600 μL of dry MeOH. The dendrimer solution was added slowly to the previous mixture under stirring. The mixture was stirred overnight. The solvent was removed under a nitrogen flow, re-dissolved in dH_2O and dialysed against dH_2O for 48 h (14 kDa MWCO). The labelling was confirmed by monitoring by spectrofluorimetry (λ_{ex} 330 nm, λ_{em} 402 nm).

The protocols for the assays are all described in Chapter 2. In brief; for the **luminescence assay (protocol 4**), overnight cultured bacteria were adjusted to OD = 1.0 and diluted 5000-fold in boron-depleted AB medium. Boric acid was added to the medium with final concentrations of 400 μM for experiments with *V. harveyi* MM32 and 22 μM for *V. harveyi* BB170. In the assay with MM32, DPD was added to medium to a final concentration of 22 μM. Since MM32 is not able to produce DPD, in this way the limiting concentration for formation of S-THMF-borate induced luminescence is 22 μM for both bacterial strains. Dendrimer stock solutions were prepared in dH_2O with a concentration 10 times higher than final concentration. Selected dendrimers (20 μL of stock solutions, 10X more concentrated than final solution) was incubated with 180

μL of bacteria suspension (~10^4 CFU/mL) in a 96-well plate at 30 °C. The final volume in each well was 200 μL. Optical density at 600 nm and luminescence were measured every 30 min for at least 10 h. Graphs show the mean values of data obtained with error bars, based on the Standard Deviations (SD) from the mean. For MM32, the magnitude of the value for the luminescence in the presence of dendrimers was divided by the magnitude of the value for luminescence for bacteria alone for 4 h, 8 h, 12 h and 16 h in order to present the relative luminescence. For BB170, the time (in 30 min interval) to reach initial light production after decay phase (*Figure 4.7*) was presented as recovery time. Calculations for relative luminescence and recovery time were conducted for each individual sample. Graphical data represent minimum, maximum and mean values.

For the **clustering assay** (**protocol 5**) overnight cultured bacterial suspensions were diluted to OD_{600} = 1.0 in PBS, passed through a 5 μm filter and incubated with or without dendrimers (final dendrimer concentrations 0.25 mg/mL and 0.5 mg/mL). At different time points 300-1000 μL of the mixture was added to the water-filled counter cell and cluster size was measured. Graphs represent mean values from triplicate experiments.

For the **membrane permeability** assay with Flow cytometer **(Protocol 8)** samples were incubated with dendrimer following the aggregation protocol (OD = 1.0 in PBS) or the luminescence protocol (OD =1.0, diluted 5000-fold in in AB-medium). 90 μL bacteria were incubated with 10 μL dendrimer (from stock solutions at concentration 10X more than final concentration for 1h in

room temperature in PBS for the aggregation experiment or 30°C for 10h in AB-medium for luminescence protocol. Bacteria-dendrimer suspension was centrifuged and re-suspended in 0.85% NaCl. 1μL of mixture of SYTO9 and propidium iodine was added to each sample, and incubated in the dark for 10 min prior to experiment.

All samples were done in triplicate and experiment was repeated at least twice.

6.3 RESULTS

Three generations of cationic dendrimers (Gn-NH2) were synthesized through modification of a previously published route [19-21]. Synthesis and characterisation of dendrimers are described in Chapter 3.

6.3.1 Cluster size analysis of *V. harveyi* by Gn-NH_2

Linear cationic polymers will readily form polymer-bacteria clusters due to electrostatic interaction with the negatively charged bacteria and the positively charged polymers [7, 8, 22]. The number of peripheral primary amines on the dendrimers increases 3-fold for each growing generation, with 9 amines on the surface of G1, 27 for G2 and 81 amines for G3, increasing the cationic charges for each generation. The ability of dendrimers to cluster *V. harveyi* was measured with clustering assays similar to those previously described [7]. *V. harveyi* BB170 cells were suspended in PBS pH 7.4 at OD_{600} = 1.0 and were incubated with cationic dendrimers of generation G1, G2 and G3 at final amine

concentration of 1.64 mM (0.5 mg/mL of dendrimer) (*Figure 6.4*). Dendrimer concentration was normalized, so that the concentration of amines was kept constant throughout the different dendrimer generations in order to compare the effect on bacteria based on concentrations of cationic centres. Dendrimers were compared with linear polymer poly(N-[3-(dimethylamino)propyl]methacrylamide) (P1), previously synthesised in our group with degrees of polymerization of (DP) 46 and 99, using the same overall amine concentration (1.64 mM).

Dendrimers of the smallest generation (G1) did not form bacteria clusters, and the mean size of the "clusters" did not differ from that of bacteria alone (around 1 μm). As the generation was increased (hence the multivalency and dendrimer size), a significant increase in mean aggregation size compared to control and G1 was observed (*Figure 6.3*). The largest aggregates were formed in the presence of G3, with clusters measuring more than twice those with G2 (5 μm for G3, 2 μm for G2 *Figure 6.3*). This effect was also observed in *V. harveyi* MM32, a different strain, although the overall aggregation size for all samples was increased compared to control *(Appendix Figure A44)*.

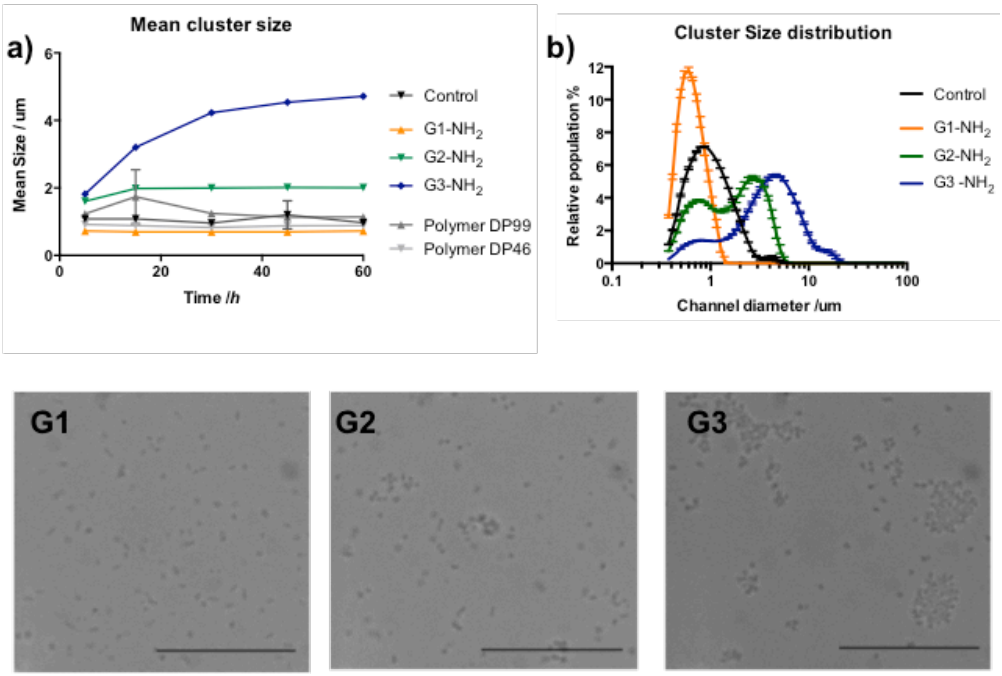

Figure 6.3 Cationic dendrimers increase in aggregation of *V. harveyi* for cationic dendrimers G1-G3 **a)** Mean cluster size of *V. harveyi* BB170 OD600 1.0 in the absence (black) and presence of G1 (orange), G2 (green) and G3 (blue) compared with linear polymer P1 DP 46 (light grey) and P1 DP99 (dark grey). **b)** Size distribution of *V. harveyi*'s clusters in the absence (black) and presence of G1 (orange), G2 (green) and G3 (blue). **c)** Aggregation as observed by optical microscopy (100X magnification) (BB170) The black bar represents 30 μm. Amine concentration 1.64 mM for each of the dendrimers in all above experiments.

The ability of these dendrimers to cluster bacteria was compared to poly(N-[3-(dimethylamino)propyl]methacrylamide) (P1). Under these conditions (PBS at pH 7.4) the linear polymers gave almost no increase in aggregation compared to *V. harveyi* BB170 alone regardless of the degree of polymerization used. A slight increase in clustering was observed when the MM32 strain was treated with these polymers *(Appendix Figure A44)*. In all cases, G3 dendrimer showed a better clustering ability than any of the polymers previously reported, even though the number of amines of G3 (81) was slightly smaller than the largest of P1 [8].

The generation-dependent increase in cluster size was also observed in the cluster size distribution of dendrimer-bacteria suspension (*Figure 6.4b*). Bacteria-G3 suspensions showed that only a modest part of the sample population was in the size of single cell populations, while the majority of the population was in the size range above 1 μm. In the case of G2 a large fraction of the relative cluster population is in a cluster size larger than control and a higher percentage of the population is in the size of a single bacteria when compared to that of G3. Optical microscopy of samples collected after 60 min confirmed the presence of clusters of bacteria for G2 and G3 dendrimers and the increase in cluster size with larger generation for both *V. harveyi* BB170 and MM32 strains (*Figure 6.4c and Appendix Figure A45*).

In order to verify that the dendrimers were co-located with the bacteria in the clusters, G3-NH_2 was labelled with 7-methoxy coumarin-3- carboxylic acid (MCCA), a blue dye, and incubated with *V. harveyi* BB170 stained with SYTO-9, a green dye permeable to microbial membranes (*Figures 6.5-6.6)*. Co-localization was apparent by comparing green (bacteria) and magenta (MCCA labelled G3-NH_2) channels in confocal laser scanning microscopy (*Figure 6.5*). The Z-stack analysis showed that the MCCA labelled G3-NH_2 was present throughout the levels of the cluster. The high density of white fluorescence within the clusters indicates co-localisation of both dyes suggesting that this cationic GATG dendrimer was able to bind to the bacterial membrane [7].

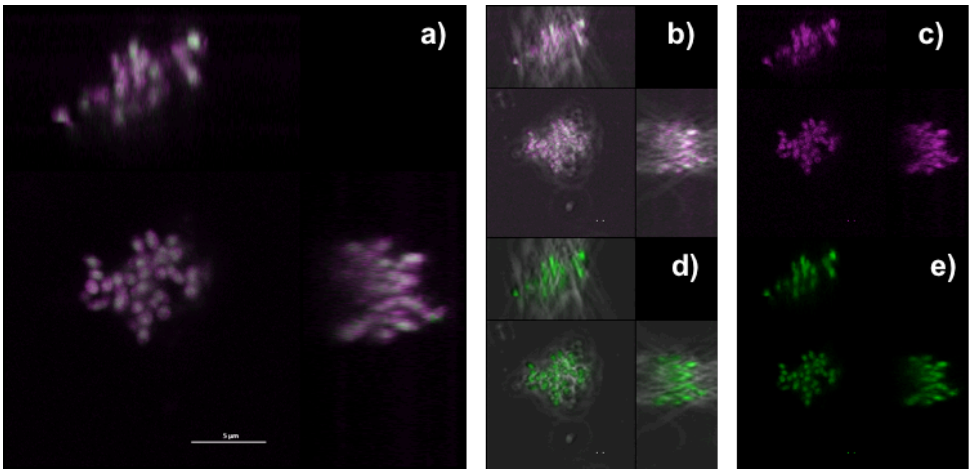

Figure 6.4 Confocal Laser Scanning Micrographs of *V. harveyi* BB170 (green) in the presence of MCCA labelled G3-NH_2 (magenta). Ortho projections from the overlaid magenta and green channels (white) including Z-stacks without (a) and with (b) trans- mission micrograph. Ortho projections for the magenta channel (c) and green channel with (d) and without (e) transmission micrograph.

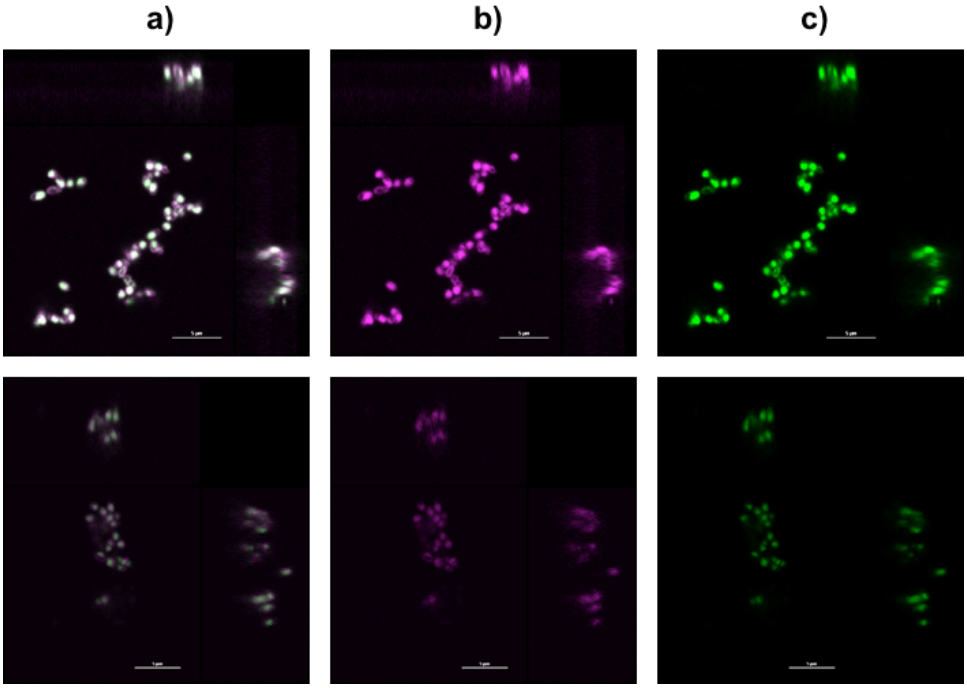

Figure 6.5 *V. harveyi* clusters (stained with green SYTO9) in the presence of MCCA- labelled G3-NH_2 (magenta). Ortho projections from the overlaid magenta and green channels (white) including Z-stacks with transmission micrograph(a). Ortho projections for the magenta channel (b) and green channel with (c) with transmission micrograph.

6.3.2 Luminescence of *V. harveyi* in the presence of Gn-NH_2

Once the ability of the cationic dendrimers G1-G3 to cluster *V. harveyi* was established, the potential of these new materials to induce the expression of QS controlled phenotypes was evaluated.

6.3.2.1. Luminescence of MM32 in the presence of Gn-NH_2

Based on previous work with cationic polymers [8, 22] it was decided to investigate the ability of these dendrimers to modulate the expression of quorum sense controlled luminescence in *V. harveyi*. When *V. harveyi* MM32 was incubated with the cationic dendrimer an increase in the production of light was observed, more evident when light emission was normalized against control (relative luminescence) (*Figures 6.6-6.7*). At 12 h time point the emitted light was dose-dependent, while at the earlier time points (4 h, 8 h) the lower NH_2 -concentrations had a larger effect on bacterial luminescence. Monitoring of optical density at 600 nm (OD_{600}) during the luminescence experiments showed that all three Gn-NH were able to delay growth in *V. harveyi,* suggesting that the higher concentrations reduced the bacterial number and fewer bacteria could produce light. At later time points the cationic dendrimer increased luminescence despite the delayed growth.

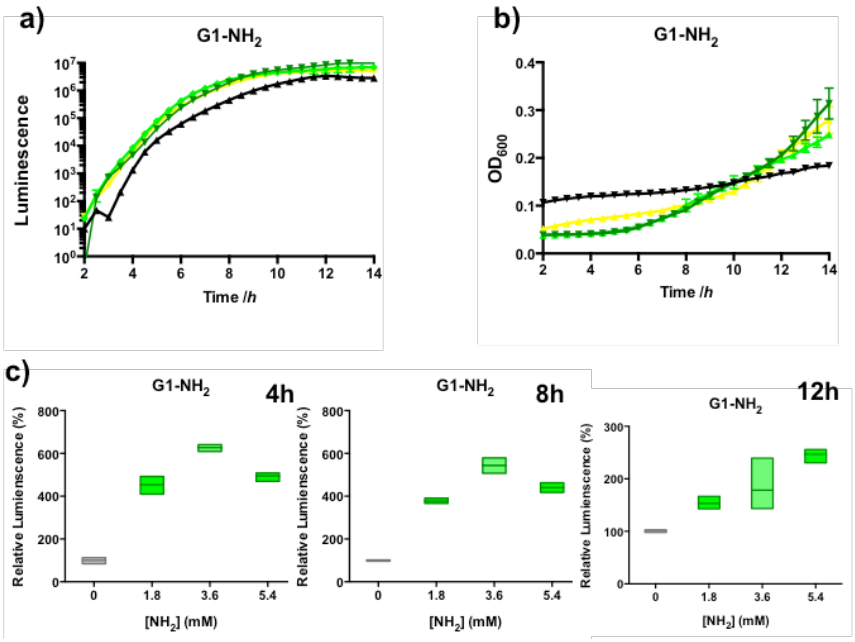

Figure 6.6 Luminescence (Relative Luminescence Units) (a) and optical density at 600nm (b) of *V. harveyi* MM32 in the absence (black) and presence of G1-NH_2 dendrimers with [NH_2] = 1.8 mM (yellow), 3.6 mM (light green) and 5.4 mM (dark green). (c) Relative luminescence after 4 h, 8 h and 12 h.

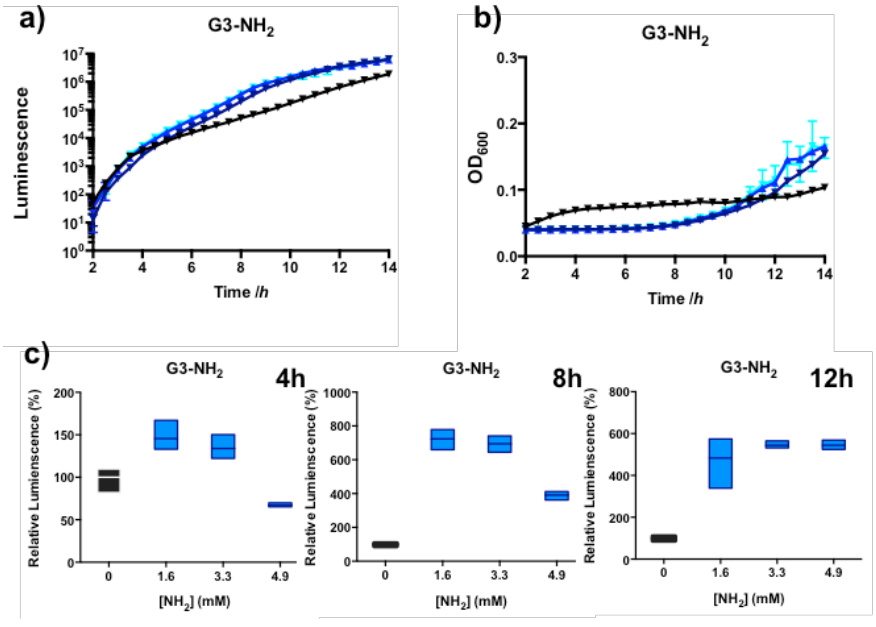

Figure 6.7 Luminescence (Relative Luminescence Units) (a) and optical density at 600nm (b) of *V. harveyi* MM32 in the absence (black) and presence of G3-NH_2 dendrimers with [NH_2] =1.6 mM (light blue), 3.3 mM (royal blue) and 4.9 mM (dark blue). (c) Relative luminescence after 4 h, 8 h and 12 h with the different [NH_2] concentrations.

When *V. harveyi* MM32 was incubated with cationic dendrimers a generation-dependent effect on emitted light could also be observed, more evident when observing the relative luminescence to control (*Figure 6.8*). At this NH_2-concentration (0.33 mM) the Gn-NH_2 dendrimers had no significant antibacterial effect on *V. harveyi* MM32 *(Figure 6.8c)*.

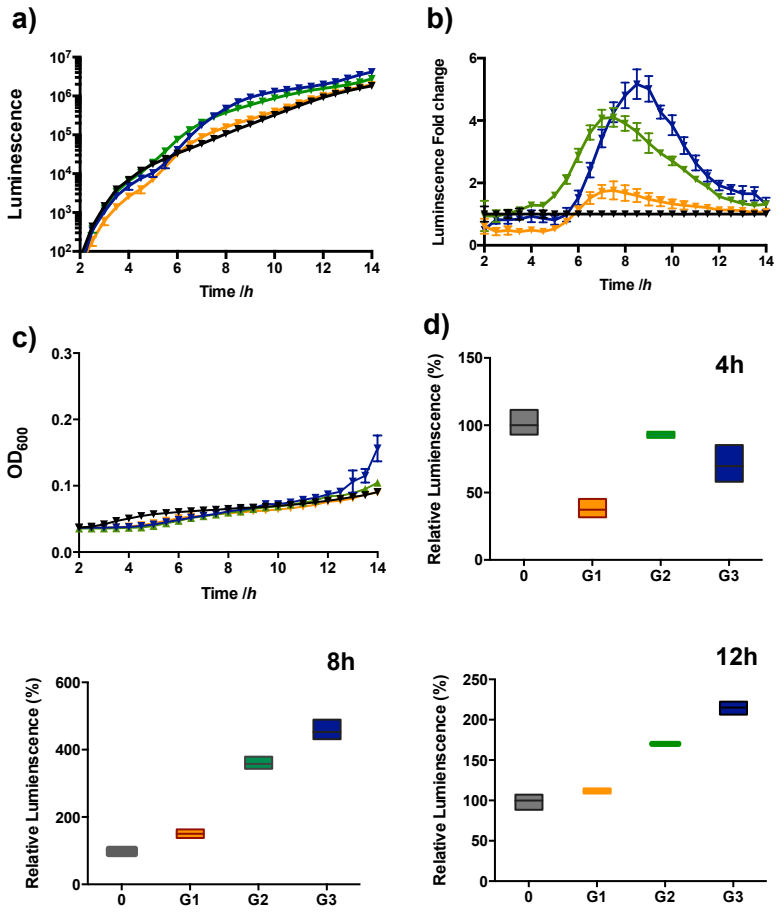

Figure 6.8 Luminescence (Relative Luminescence Units) of *V. harveyi* MM32 in the absence (black) and presence of G-NH_2 dendrimers of generation G1 (orange), G2 (green) and G3 (blue). Luminescence (a), fold change (b), optical density at 600nm (OD_{600}) (c) and relative luminescence after 4 h (d), 8 h (e) and 12 h (f) are presented. Final concentrations for all dendrimers [NH_2] = 0.33 mM.

6.3.2.2. Luminescence of BB170 in the presence of Gn-NH_2

When the production of light in BB170 was evaluated in the presence of the dendrimers, a significant change in the emission profiles could be observed (*Figures 6.9-6.11*). This was more evident when light production was normalised to the luminescence produced in the absence of the dendrimers (*Figures 6.9b, 6.10b, 6.11b*). In all cases, dendrimers promoted an enhancement in light production (normalised luminescence fold change >1), in a similar fashion to previously repeated experiments with linear polymers in our group, confirming the increase in QS controlled phenotype with bacterial sequestering [8]. For all three dendrimers, a dose dependent effect was observed across the concentrations evaluated. This increase was more apparent when the time taken by bacteria to recover the initial levels of luminescence (~3 x 10^3, *Figures 6.9-6.11*) was evaluated. Under normal conditions, *V. harveyi* switches off light production following dilution into the assay broth and taking almost 9 h for *V. harveyi* to reach a population density that could produce similar levels of luminescence than the initial. In the presence of G1-NH_2 however, this level of luminescence could be reached in as little as 5 h for the highest concentration tested (*Figure 6.9c*). A similar effect could be observed for the other generations (*Figure 6.10-6.11*).

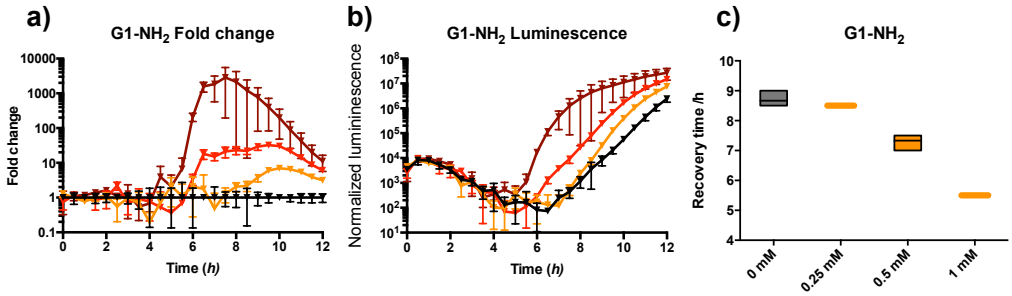

Figure 6.9 Luminescence (Relative Luminescence Units) of *V. harveyi* BB170 in the absence (black) and presence of G1- NH_2: [NH_2] = 0.25 mM (orange), 0.5 mM (red) and 1 mM (dark red). Fold increase of luminescence (a), normalised luminescence (b) and recovery time (c).

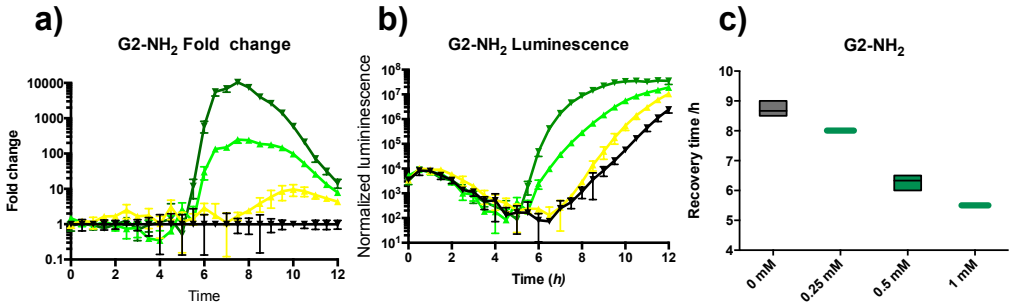

Figure 6.10 Luminescence (Relative Luminescence Units) of *V. harveyi* BB170 in the absence (black) and presence of G2-NH_2: [NH_2] = 0.25 mM (yellow), 0.5 mM (light green) and 1 mM (dark green). Fold increase of luminescence (a), normalised luminescence (b) and recovery time (c).

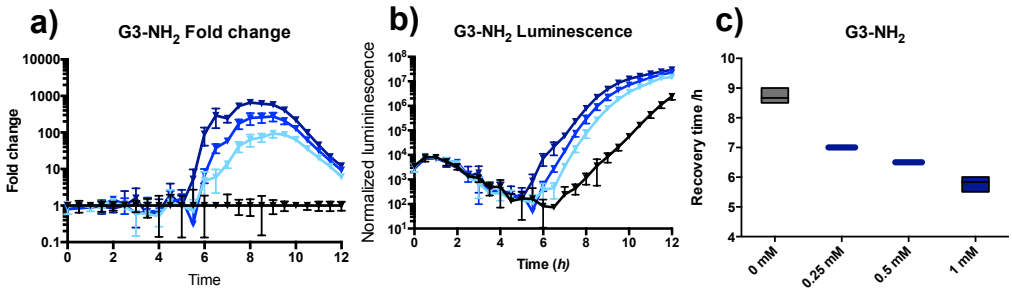

Figure 6.11 Luminescence (Relative Luminescence Units) of *V. harveyi* BB170 in the absence (black) and presence of G3-NH_2: [NH_2] = 0.25 mM (light blue), 0.5 mM (blue) and 1 mM (dark blue). Fold increase of luminescence (a), normalised luminescence (b) and recovery time (c).

When the same concentration of amines (e.g. 0.5 mM, *Figure 6.13*) was evaluated across the different dendrimers used, a clear generation effect could be observed (*Figures 6.12-6.15*). G3 had the highest effect on light production, and the effect of this dendrimer on the recovery time was up to 6 times greater than that of G1, the dendrimer of the smallest size (*Figure 6.13*).

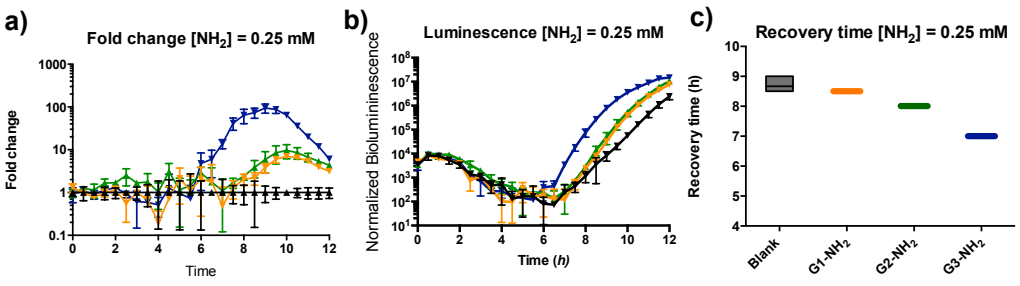

Figure 6.12 Representative generation dependent reduction (3 experiments) in the recovery time for Gn-NH_2 at 0.25 mM for G1 (orange), G2 (green) and G3 (blue).

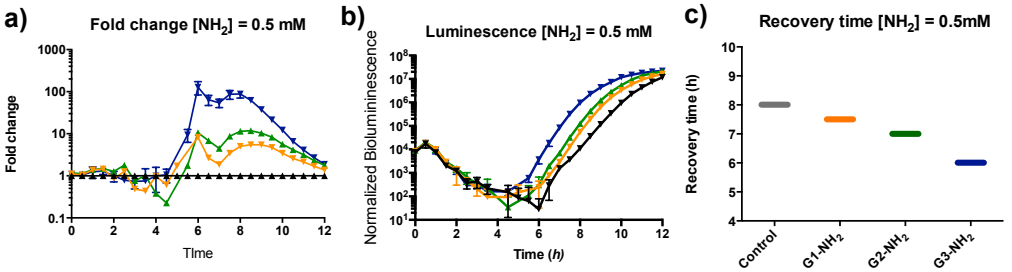

Figure 6.13 Representative generation dependent reduction (3 experiments) in the recovery time for Gn-NH_2 at 0.5 mM for G1 (orange), G2 (green) and G3 (blue).

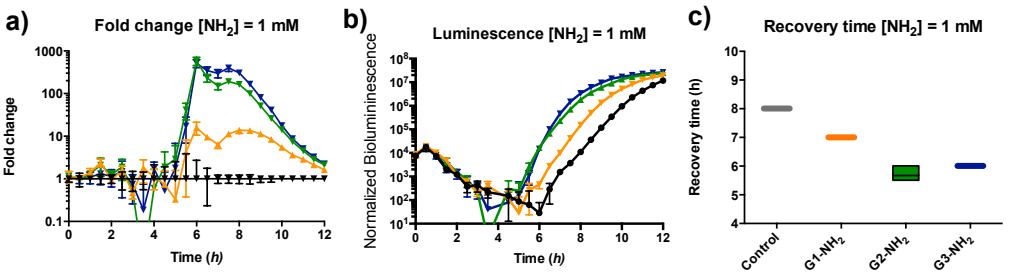

Figure 6.14 Representative generation dependent reduction (3 experiments) in the recovery time for Gn-NH_2 at 1 mM for G1 (orange), G2 (green) and G3 (blue).

Monitoring of optical density at 600 nm (OD_{600}) during the luminescence experiments showed that all three Gn-NH were able to delay growth in *V. harveyi* (*Figure 6.15*), suggesting that *V. harveyi* were achieving similar levels of light production at even lower densities of bacteria. Again this effect was dose-dependent, with higher concentrations of dendrimers showing the lowest recovery times.

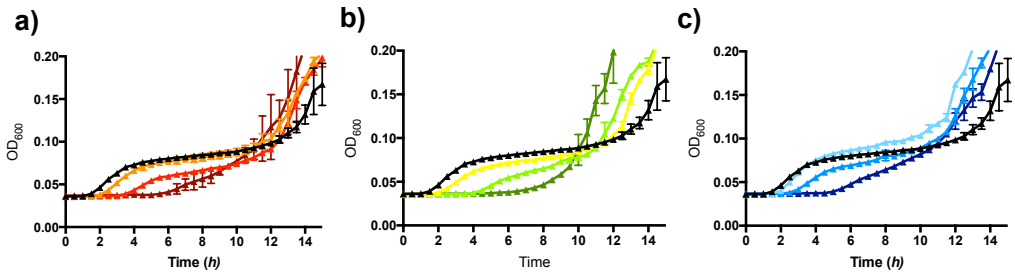

Figure 6.15 OD_{600} of *V. harveyi* BB170 in the absence (black) and presence of G1-NH_2 (a): [NH_2] = 0.25mM (orange), 0.5mM (red) and 1mM (dark red); G2-NH_2 (b): [NH_2] = 0.25 mM (yellow), 0.5 mM (light green) and 1 mM (dark green); and G3-NH_2 (c): [NH_2] = 0.25 mM (light blue), 0.5 mM (blue) and 1m M (dark blue).

6.3.3 Cell Membrane Permeability of *V. harveyi* in the presence of Gn-NH_2

Due to the cationic nature of the GATG dendrimers, it was decided to investigate if these dendrimers were able to induce membrane permeability and as such have potential antimicrobial activity. Incubation of *V. harveyi* (under the aggregation assay conditions) with a mixture of SYTO-9 and propidium iodide (PI), a red stain for cells with their membranes damaged, revealed that as the generation of dendrimers increased, an increase in the amount of bacteria that were stained red was also observed (*Figures 6.16-6.17)* While no increase in membrane permeability was observed for G1-NH_2, over 50% of the bacteria

were stained red in the presence of G2-NH_2 and up to 85% in the case of G3-NH_2.

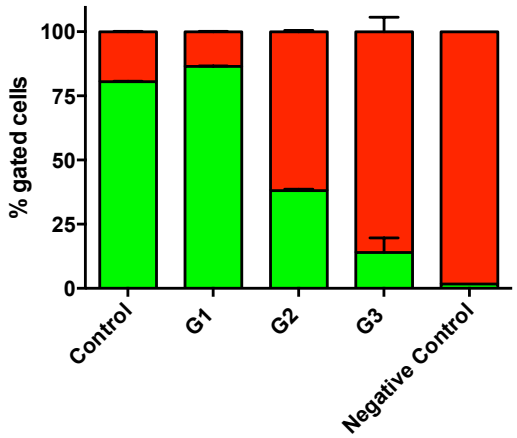

Figure 6.16 Normalized population of *V. harveyi* BB170 presented as the percentage of green (non-permeable/viable) and red (high permeability/dead) cells as measured by flow cytometry. *V. harveyi* was incubated in the absence (control) and presence of Gn-NH_2 for 1 h at room temperature. Bacteria were treated with *i*-PrOH as a negative control. Initial OD_{600} = 1, [NH_2] = 1.64 mM in PBS at pH 7.4.

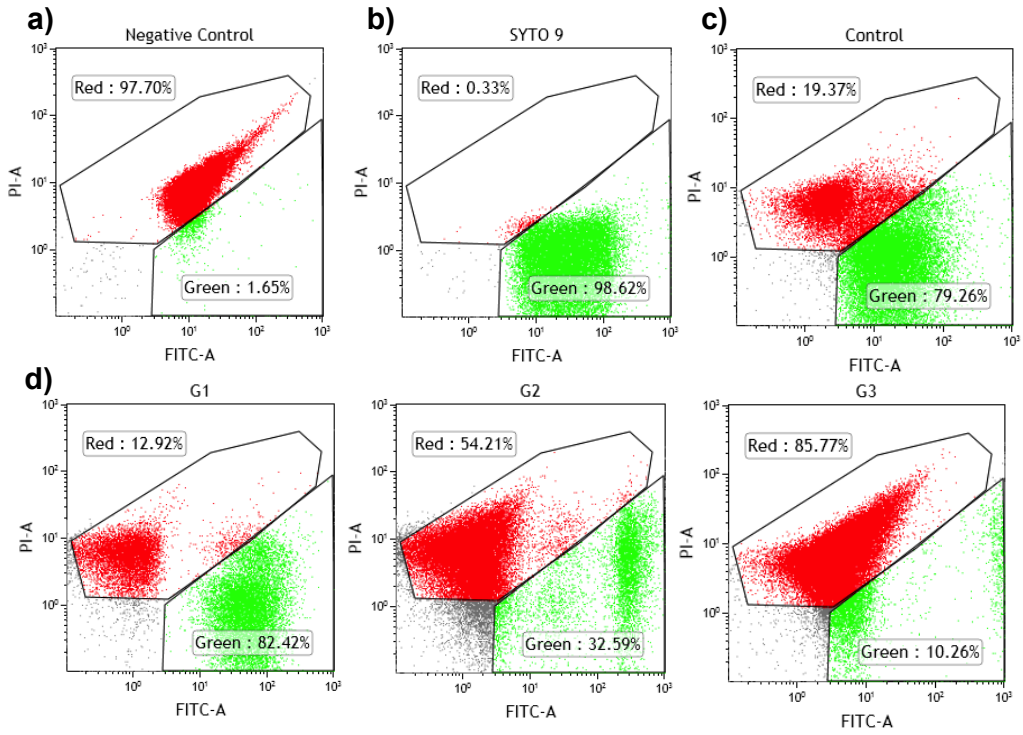

Figure 6.17 Flow cytometry of *V. harveyi* BB170 stained with propidium iodine (PI, red staining) (a) and SYTO-9 (green staining). Red fluorescence was recorded on the PI channel (PI-A, y -axis) and green fluorescence on the FITC channel (FITC x-axis). Gated population of *V. harveyi* BB170 based on calibration with a) bacteria treated with *i*-PrOH as negative control and stained with PI and SYTO-9 and b) non-treated bacteria stained with only SYTO-9 staining as positive control. c) Gated population of *V. harveyi* stained with PI and SYTO-9 in the absence (control) and d) presence of Gn-NH_2 dendrimers for 1 h at room temperature. Initial OD = 1.0, [NH_2] = 1.64 mM in PBS at pH 7.4. Values account for percentage of total number of counted cells.

Membrane permeability assays were performed under the luminescence assay conditions. Similar to the membrane permeability implicated during the aggregation experiments, GATG dendrimers were able to increase permeability of the membrane in a generation and concentration dependent matter (*Figure 6.18*). Gated populations as determined by flow cytometry are presented in *Appendix Figures A48-A50.*

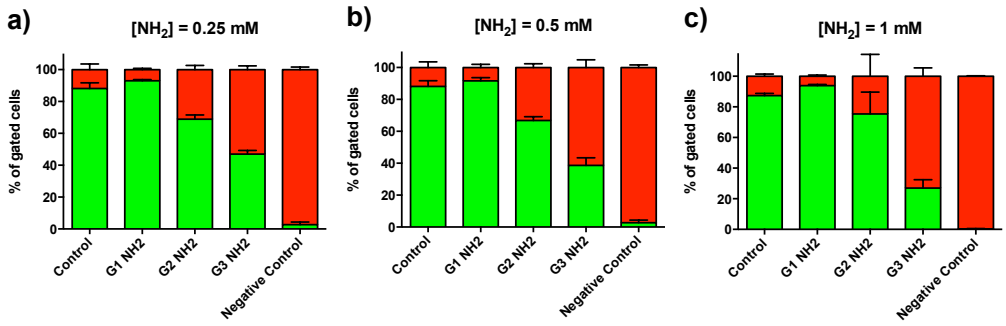

Figure 6.18 Normalized population of *V. harveyi* BB170 presented as the percentage of green (non-permeable/viable) and red (high permeability/dead) cells. *V. harveyi* was incubated in the absence (control) and presence of Gn-NH_2. Bacteria were treated with *i*-PrOH as a negative control. Initial OD_{600} = 1. Bacteria diluted 5000 fold in AB medium for prior to incubation with Gn-NH_2. Final [NH_2] = 0.25 mM (a), 0.5 mM (b) and 1 mM (c).

Discrepancies between single cell and multiple cell conformation can be gauged by looking at the Side-Scatter Area versus the Side-Scattered Height by flow cytometry (*Appendix Figure A46*). The Gn-NH_2 dendrimers increased the percentage of bacterial cells in multiple cell conformations in a generation-dependent matter supporting the findings of generation-dependent increase in bacterial clustering (*Appendix Figure A47*).

6.4 DISCUSSION

Previous work in our group has shown that linear cationic polymers form polymer-bacteria cluster by electrostatic interactions [7, 8]. In this study, the use of aminodendrimers, in which the size and number of terminal groups can be accurately controlled by design, were used to modulate systematically the antimicrobial and quorum sensing properties of polycations. As with previous experiment *V. harveyi*, was used as a model organism.

When *V. harveyi* BB170 was incubated with GATG dendrimers, a clear generation dependent cluster formation could be observed. The excellent ability of GATG dendrimers to cluster allowed for these experiments to be performed in PBS, conditions under which none of the linear polymers tested previously (poly(N-[3-dimethylamino)propyl]methacrylamide) of DP46 and DP99 were able to induce any clustering of *V. harveyi* (*Figure 6.3*) [7]. Inspection of the size distributions (*Figure 6.3b*) suggested that as the multivalency of the dendrimer increased, the number of free bacteria (population centred at 1 μm) was reduced. A similar effect could be observed when these clusters were inspected under the microscope (*Figure 6.3c*), with aggregates of increasing size forming with increasing dendrimer generation. Interestingly the average size for the bacteria in the presence of G1-NH_2 was smaller (~0.6 μm) than that of *V. harveyi* in the absence of the dendrimers (~0.9 μm). However, these measured bacterial sizes are relative to the calibrants used (i.e. polystyrene beads) and do not represent the size expected for *V. harveyi* (~1.5 μm). Despite this discrepancy, these values do inform of relative changes in size. Taking into account the size of these dendrimers (less than 3 nm for G1-NH_2, *Table 6.1*), it is quite possible that G1-NH_2 did not have the required size and multivalency to efficiently bridge between multiple bacteria and none or few small clusters are formed. Size distributions in the presence of G1-NH_2 were narrower (0.25-1.05 μm) than in its absence (0.30-3.0 μm) suggesting that G1-NH_2 would probably still bind to the surface of *V. harveyi*, modify its surface properties and colloidal stability, and potentially prevent the natural tendency of the microbes to aggregate. A similar reduction in size could be observed as well for the population of smaller size when *V.*

harveyi was incubated with G2-NH_2 (~0.75 μm) and G3-NH_2 (~0.65 μm), suggesting that these cationic dendrimers were able to bind to *V. harveyi* and, depending on their size and multivalency, induce the formation of bacterial clusters. It is remarkable that despite the relative small difference in size between different dendrimer generations (~3 nm) (*Table 6.1*), and the relative small size of dendrimers when compared with bacteria (1 μm), there was a significant difference in dendrimer-bacteria clustering size between the generations.

Based on the effect of linear cationic polymers on QS-induced phenotypes [8] it was decided to investigate the ability of these dendrimers to modulate the expression of QS-controlled luminescence in *V. harveyi*. When *V. harveyi* BB170 was incubated with this dendrimer, a significant increase in the production of light was observed, an increase that was proportional to the amount of dendrimer added. Comparison of the recovery time at different concentrations of dendrimers showed that the effect of these dendrimers on luminescence was also generation dependent with shorter recovery times for the largest dendrimers. Such a significant increase in luminescence for the even the smallest dendrimer was remarkable, considering the poor ability of G1-NH_2 to cluster bacteria. The amine concentrations for all generations were the same in the experiment, yet the dendrimers of higher generations had an increased effect on the QS controlled phenotype luminescence, with decreased recovery time for the highest generations. This is in agreement with previous work from our group where the clustering of cationic polymers increased QS phenotype expression and therefor shortened the recovery time [8]. Larger clusters would have a greater effect on the induction of luminescence as the local

concentration of AI-2 in the cluster increases with more bacteria present.

The enhancement of light production was even more notable when evaluated with the effect these GATG dendrimers had on *V. harveyi* growth. Monitoring of optical density at 600 nm (OD_{600}) during the luminescence experiments showed that all three Gn-NH_2 were able to delay growth in *V. harveyi (Figures 6.6-6.7* and *6.13),* suggesting that *V. harveyi* were achieving similar levels of light production at even lower densities of bacteria. In the case of MM32, luminescence was lower for the higher NH_2 concentrations at early time points (4 h and 8 h, *Figures 6.6-6.8*), suggesting the delay in growth was affecting luminescence output. For MM32 at later time point and for BB170 the effect on luminescence was dose-dependent, with higher concentrations of dendrimers showing the lowest recovery times.

From these luminescence assays, GATG dendrimers were having opposing effects on the production of light. Thus, Gn-NH_2 showed bacteriostatic effect and was expected to reduce the amount of light produced based on the slower growth of *V. harveyi* in the presence of these dendrimers. On the other hand, these dendrimers were inducing clustering and thereby activating quorum sense controlled light production [8]. Moreover, membrane permeability assays showed that these dendrimers were increasing membrane permeability (*Figures 6.16* and *6.18*). Again, cationic GATG dendrimers were able to increase membrane permeability in a generation and concentration dependent fashion, but the effect for G1-NH_2 was negligible, with no apparent difference in membrane permeability to the control at any of the concentrations tested. One possibility is that the increased permeability caused by the higher generation

dendrimers could facilitate the diffusion of the quorum sensing autoinducers inside the periplasm thus enhancing light production from bacteria. The generation-dependent increased membrane permeability suggests that cationic dendrimers could have a generation-dependent bactericidal effect, in a manner similar to that previously reported for ammonium functionalized carobosilane dendrimers [23, 24].

6.5 CONCLUSIONS

In summary, this study has shown that cationic GATG dendrimers induce clustering in *V. harveyi* in a generation dependent manner and that this clustering ability is greater than that of poly(N-[3-(dimethylamino)propyl]methacrylamide) (P1), a cationic linear polymer previously used in bacterial aggregation assays [7, 8]. Similarly, cationic GATG dendrimers induced the expression of QS controlled luminescence in a generation dependent matter. Although the increase in size between generations is small (~3 nm) compared to the size of the bacteria (~1 μm), there is a significant increase in bacterial cluster size and luminescence. This highlights the suitability of the globular structure for bacterial clustering and the importance of considering the architecture of the polymeric material for optimal interaction with bacteria.

In addition, these cationic dendrimers can increase the membrane permeability of the bacteria. As a result, cationic GATG dendrimers induce the expression of quorum sense controlled luminescence, despite inhibiting the growth of

bacteria. These results highlight the potential of GATG dendritic materials as a platform to develop new antimicrobials that can target microbial viability and/or virulence (e.g. adhesion). The inhibition of growth and increased membrane permeability in combination with cell clustering may be promising antibacterial features of these cationic dendrimers.

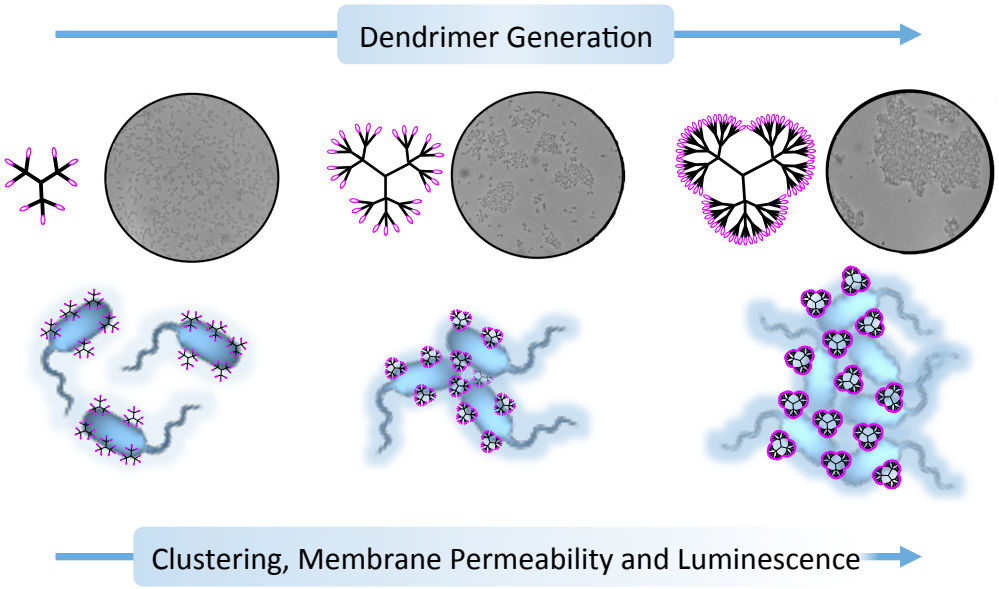

Figure 6.19 Interaction of GATG dendrimers with bacteria. Increasing generation (and multivalency) increases the ability of Gn-NH2 dendrimers to cluster bacteria. Cell clustering in *Vibrio harveyi* induces Quorum Sensing (QS) activation and expression of QS controlled phenotype luminescence. Increasing generation and multivalency increases the ability of Gn-NH_2 to cluster bacteria. Similarly, increasing generation increases membrane permeability and enhances quorum sensing controlled production of light. Dendrimers and bacteria are not to scale.

6.6 REFERENCES

[1] Timofeeva, L. and Kleshcheva, N. (**2011**). *"Antimicrobial polymers: mechanism of action, factors of activity, and applications."* Appl Microbiol Biotechnol 89(3): 475-92.

[2] Som, A., Vemparala, S., Ivanov, I., and Tew, G.N. (**2008**). *"Synthetic mimics of antimicrobial peptides."* Biopolymers 90(2): 83-93.

[3] Scott, R.W., DeGrado, W.F., and Tew, G.N. (**2008**). *"De Novo Designed Synthetic Mimics of Antimicrobial Peptides."* Curr Opin Biotechnol 19(6): 620-627.

[4] Jain, K., Kesharwani, P., Gupta, U., and Jain, N.K. (**2010**). *"Dendrimer toxicity: Let's meet the challenge."* Int J Pharm 394(1-2): 122-42.

[5] Sovadinova, I., Palermo, E.F., Huang, R., Thoma, L.M., and Kuroda, K. (**2011**). *"Mechanism of polymer-induced hemolysis: nanosized pore formation and osmotic lysis."* Biomacromolecules 12(1): 260-8.

[6] Uppu, D.S., Samaddar, S., Ghosh, C., Paramanandham, K., Shome, B.R., and Haldar, J. (**2016**). *"Amide side chain amphiphilic polymers disrupt surface established bacterial bio-films and protect mice from chronic Acinetobacter baumannii infection."* Biomaterials 74: 131-43.

[7] Louzao, I., Sui, C., Winzer, K., Fernandez-Trillo, F., and Alexander, C. (**2015**). *"Cationic polymer mediated bacterial clustering: Cell-adhesive properties of homo- and copolymers."* Eur J Pharm Biopharm 95(Pt A): 47-62.

[8] Lui, L.T., Xue, X., Sui, C., Brown, A., Pritchard, D.I., Halliday, N., Winzer, K., Howdle, S.M., Fernandez-Trillo, F., Krasnogor, N., and Alexander, C. (**2013**). *"Bacteria clustering by polymers induces the expression of quorum-sensing-controlled phenotypes."* Nat Chem 5(12): 1058-65.

[9] Svenson, S. and Tomalia, D.A. (**2005**). *"Dendrimers in biomedical applications--reflections on the field."* Adv Drug Deliv Rev 57(15): 2106-29.

[10] Mintzer, M.A., Dane, E.L., O'Toole, G.A., and Grinstaff, M.W. (**2012**). *"Exploiting dendrimer multivalency to combat emerging and re-emerging infectious diseases."* Mol Pharm 9(3): 342-54.

[11] Imberty, A., Chabre, Y.M., and Roy, R. (**2008**). *"Glycomimetics and glycodendrimers as high affinity microbial anti-adhesins."* Chemistry 14(25): 7490-9.

[12] Munoz, E.M., Correa, J., Fernandez-Megia, E., and Riguera, R. (**2009**). *"Probing the relevance of lectin clustering for the reliable evaluation of multivalent carbohydrate recognition."* J Am Chem Soc 131(49): 17765-7.

[13] Munoz, E.M., Correa, J., Riguera, R., and Fernandez-Megia, E. (**2013**). *"Real-time evaluation of binding mechanisms in multivalent interactions: a surface plasmon resonance kinetic approach."* J Am Chem Soc 135(16): 5966-9.

[14] Albertazzi, L., Fernandez-Villamarin, M., Riguera, R., and Fernandez-Megia, E. (**2012**). *"Peripheral functionalization of dendrimers regulates internalization and intracellular trafficking in living cells."* Bioconjug Chem 23(5): 1059-68.

[15] Domenech, R., Abian, O., Bocanegra, R., Correa, J., Sousa-Herves, A., Riguera, R., Mateu, M.G., Fernandez-Megia, E., Velazquez-Campoy, A., and Neira, J.L. (**2010**). *"Dendrimers as potential inhibitors of the dimerization of the capsid protein of HIV-1."* Biomacromolecules 11(8): 2069-78.

[16] Klajnert, B., Wasiak, T., Ionov, M., Fernandez-Villamarin, M., Sousa-Herves, A., Correa, J., Riguera, R., and Fernandez-Megia, E. (**2012**). *"Dendrimers reduce toxicity of Abeta 1-28 peptide during aggregation and accelerate fibril formation."* Nanomedicine 8(8): 1372-8.

[17] Fernandez-Trillo, F., Pacheco-Torres, J., Correa, J., Ballesteros, P., Lopez-Larrubia, P., Cerdan, S., Riguera, R., and Fernandez-Megia, E. (**2011**). *"Dendritic MRI contrast agents: an efficient prelabeling approach based on CuAAC."* Biomacromolecules 12(8): 2902-7.

[18] de la Fuente, M., Ravina, M., Sousa-Herves, A., Correa, J., Riguera, R., Fernandez-Megia, E., Sanchez, A., and Alonso, M.J. (**2012**). *"Exploring the efficiency of gallic acid-based dendrimers and their block copolymers with PEG as gene carriers."* Nanomedicine (Lond) 7(11): 1667-81.

[19] Ravina, M., de La Fuente, M., Correa, J., Sousa-Herves, A., Pinto, J., Fernandez-Megia, E., Riguera, R., Sanchez, A., and Alonso, M.J. (**2010**). *"Core− shell dendriplexes with sterically induced stoichiometry for gene delivery."* Macromolecules 43(17): 6953-6961.

[20] Amaral, S.P., Fernandez-Villamarin, M., Correa, J., Riguera, R., and Fernandez-Megia, E. (**2011**). *"Efficient multigram synthesis of the repeating unit of gallic acid-triethylene glycol dendrimers."* Org Lett 13(17): 4522-5.

[21] Fernandez-Megia, E., Correa, J., Rodríguez-Meizoso, I., and Riguera, R. (**2006**). *"A Click Approach to Unprotected Glycodendrimers†."* Macromolecules 39(6): 2113-2120.

[22] Xue, X., Pasparakis, G., Halliday, N., Winzer, K., Howdle, S.M., Cramphorn, C.J., Cameron, N.R., Gardner, P.M., Davis, B.G., Fernandez-Trillo, F., and Alexander, C. (**2011**). *"Synthetic polymers for simultaneous bacterial sequestration and quorum sense interference."* Angew Chem Int Ed Engl 50(42): 9852-6.

[23] Ortega, P., Copa-Patino, J.L., Munoz-Fernandez, M.A., Soliveri, J., Gomez, R., and de la Mata, F.J. (**2008**). *"Amine and ammonium functionalization of chloromethylsilane-ended dendrimers. Antimicrobial activity studies."* Org Biomol Chem 6(18): 3264-9.

[24] Rasines, B., Hernandez-Ros, J.M., de las Cuevas, N., Copa-Patino, J.L., Soliveri, J., Munoz-Fernandez, M.A., Gomez, R., and de la Mata, F.J. (**2009**). *"Water-stable ammonium-terminated carbosilane dendrimers as efficient antibacterial agents."* Dalton Trans(40): 8704-13.

7. Conclusions and Future work

7.1 CONCLUSIONS

The aim of this thesis was to use dendrimer as platform for development of novel antibacterial materials. Although dendrimers have been evaluated extensively before as antibacterial scaffolds [1, 2], only limited studies have explored their use as quorum sensing quenchers [3-5].

Cationic dendrimers have emerged as possible antibacterial agents due to their disruption of bacterial cell membranes [6-8]. The potent broad-spectrum antibacterial activity of cationic agents plays an important role in mammalian innate immunity. The cationic nature of antimicrobial peptides (AMPs) targets the bacterial membrane, introducing ion channels and aqueous pores that lead to cell lysis [9]. The anion character of the bacterial membrane induced by the presence of crucial components of the cell membrane structure is expected to result in lower risk of causing bacterial resistance to an electrostatic interaction compared to small molecule-receptor interactions due to the non-specific character of the interaction. However introduction of amino groups by D-alanine incorporation in the teichioc acid of Gram-positive cell walls can reduce the cell wall negative charge and repel cationic agents [9]. In Gram-negative bacteria, modification of LPS can also reduce overall negative charge, and in a similar manner reduce the activity of cationic materials [9]. Therefore, since cationic materials decrease bacterial viability, thus, even though targeting bacteria through electrostatic interactions could be less likely to increase

resistance, mutations of the bacterial genome might result in phenotypes with decreased anionic charge and increased resistance also to cationic antibacterial agents.

Glycodendrimers are promising anti-adhesive agents [10-12]. Since targeting lectins important for bacterial attachment to host cell does not act by killing the bacteria or arresting its growth, but through decreasing the virulence, it is very likely that resistance to such agents would evolve slower than against bactericidal materials. Although some reports of increased effects with higher generations have been reported, no clear trend for multivalency to all carbohydrate targets can be defined [1].

The effects of dendrimer architecture on clustering of bacteria have not been investigated, and often insufficient data have been obtained to determine a structure-activity relationship [1]. No one has to my knowledge reported the effect of dendrimer size and generation on bacterial clustering and QS signaling. The goals in this thesis were to synthesise ligands with hydroxyl moieties having affinity for the boronic acid present in media needed for the formation of the active AI-2 form in *V. harveyi* and also with the possibility to work as anti-adhesive agents. In order to do this it was necessary 1) to develop an efficient method for conjugation of diol ligands to GATG dendrimers of different size and multivalency (generations), 2) to synthesise dendrimers functionalized with phenylboronic acids for inhibiting the formation of STHMF-borate molecule, and 3) to synthesise cationic dendrimers for the potential as anti-adhesive macromolecules. The dendrimers containing

hydroxyl, phenylboronic acid, and cationic moieties were evaluated *in vitro*, using *V. harveyi* as model bacteria to study their effect on AI-2 quenching and bacterial aggregation.

Hydroxyl groups were expected to have affinity for the boronic acid needed for the formation of the active form of AI-2 (S-THMF-borate). Ligands with two hydroxyl groups (diols), four hydroxyl groups (tetraol) and double glucose- and mannose moieties were synthesised. The internal alkyne of the ligands enabled them to be conjugated to terminal azides of the biocompatible GATG dendrimers, with two functional groups per azide. The ligands were successfully conjugated to GATG dendrimers of generation G1 and G3, through a catalyst-free conjugation, resulting in monodisperse dendrimers with 18 and 162 functional groups in the periphery and a size of 3-10 nm.

A decrease in luminescence could be observed with bacterial mutant strain MM32 for the carbohydrate-dendrimers, at the early time points while the opposite effect was observed at later time point. The dendrimers with hydroxyl-groups were hypothesized to promote growth of *V. harveyi* under the conditions used in the assays, possibly disguising any effect on QS. The dendrimers functionalized with carbohydrates were expected to function as anti-adhesive agents and induce bacterial clustering of *V. harveyi* [13-15] thereby inhibit the bacteria to attach to host cell surfaces, needed to initiate the infection pathway. However at the high ratio of dendrimer per bacteria used in this study, no clustering was seen. The use of these GATG glycodendrimers as

anti-adhesives might thus be probed in the future using lower concentrations of G1 and G3 carbohydrate dendrimers.

The cationic dendrimers in this study were used to study the anti-adhesive effects of globular dendrimer of different sizes (generations) compared to cationic linear polymers previously studied in Nottingham [16, 17]. GATG dendrimers with 9, 27 and 81 primary amines, corresponding to generations G1-NH_2, G2-NH_2 and G3-NH_2 were obtained by quantitative reduction of terminal azides. The cationic GATG dendrimers induced clustering in *V. harveyi* in a generation dependent manner, and to a greater extent than that of poly(N-[3-(dimethylamino)propyl]methacrylamide) (P1), a cationic linear polymer previously used in these assays. Moreover, these cationic dendrimers increased the membrane permeability of the bacteria, again in a generation dependent matter. As a result, cationic GATG dendrimers induced the expression of quorum sense controlled luminescence, despite inhibiting the growth of *V. harveyi.*

Dendrimers functionalized with phenylboronic acids were synthesised to target directly the QS signal (S-THMF) in contrast to target of the AI-2 with diol-ligands binding to the boronic acids in the media. The synthesis strategy for PEGylated GATG dendrimers with phenylboronic acids were developed in the group in Santiago de Compostela for the formation of micelles (*Amaral S.P et. al. unpublished data*). A similar protocol was used to prepare dendrimers of generation G1 and G3 decorated with 9 and 81 phenylboronic acids in the periphery. Although the mechanism for the inhibition of growth and luminescence of *V. harveyi* in the presence of the phenylboronic acid

dendrimers is yet to be understood, the dendrimers shows an interesting antibacterial effect that could be explored further in future work.

In summary, 12 dendrimers with 6 different functionalities in the periphery have been synthesised. Cationic dendrimers induced generation-dependent clustering of *V. harveyi,* and an improved clustering compared a cationic linear polymer, thus demonstrating the importance of architecture and generation on the interaction with bacterial membranes. Inhibition of growth and increased membrane permeability in combination with bacteria clustering are potential antibacterial features of these cationic dendrimers. While dendrimers functionalized with hydroxyl groups unexpectedly increased the growth of *V. harveyi* possibly disguising a quorum quenching effect, the boronic acid had a bacteriostatic effect at low concentrations and could represent an interesting antibacterial strategy in the future.

The precise control over size and physicochemical properties makes dendrimers of interest for a range of studies into the interaction of polymeric materials with bacteria on a nano-scale. These versatile, multivalent material scaffolds may be useful to develop our understanding of how to design novel structures to optimize polymer-cell interactions for a number of biomedical applications, ranging from bacterial detection and binding to eukaryotic cell culture and delivery.

7.2 FUTURE WORK

The generation-dependent bacterial clustering effect of cationic dendrimers could be a result of both increased density of charges and the size of dendrimers. Future studies to understand the impact of dendrimer architecture could involve comparison of the larger dendrimer generations functionalized with a number of amines equal to that of a smaller dendrimer generation, thus evaluating the impact on bacterial clustering based on dendrimer size alone.

Dendrimers decorated with mannose and glucose have previously been reported to successfully interfere with bacterial adhesion through interactions with lectins [10, 18]. Although the GATG dendrimers in this study were not able to induce clustering of *V. harveyi* with the concentration used, future studies could evaluate the effect of dendrimer generation on bacterial clustering. Bacterial adhesion to a surface is generally described in two phases, an initial long-range interaction through for example electrostatic or hydrophobic interactions allowing the bacteria to approach the surface [19, 20]. The second, short-range interaction occurs via molecular-specific reactions between cell surface structures. These become effective when the cell and bacterial surface are in close contact and usually involve specific adhesins such as lectins. A potential new study could investigate the importance of electrostatic and lectin-based interactions using dendritic scaffolds, which enables excellent control over the ratio between the two functionalities.

Promising work using dendrimers to inhibit and disrupt biofilms have been reported [21, 22]. Applying the thermal AAC conditions on alkynated ligands

with other carbohydrates specific for various lectins (e.g. fucose) to functionalise GATG dendrimers could study the effect of generation and architecture on biofilm interference.

Synthesise of novel alkynated ligands with higher affinity for QS molecules, such as catechol moieties [13], could be carried out via conjugation to dendrimers using the AAC conditions developed here, and enable a study of the effects of dendrimer generation and multivalency on QS inhibition. The affinity of monomers for selected quorum sensing molecules could be usefully evaluated in assays such as Alizarin red for AI-2 binding, prior to development and functionalization of alkynated ligands.

The decrease in quorum sensing and bacterial growth of *V. harveyi* in the presence of phenylboronic acid-dendrimers was an interesting but unexpected finding and is not yet well understood. First and foremost, it is important to find a medium suitable for bacterial growth but in which spontaneous aggregation due to the dendrimers does not occur. For the effect of the phenylboronic acid-dendrimers on *V. harveyi* to be evaluated it is important to separate the quorum quenching and viability experiments. Binding studies of phenylboronic acid dendrimer to PBP's or saccharides of the bacterial cell wall was out of the scope of this thesis, but would be an interesting future study to understand the effect of the boronic acid on *V. harveyi* growth.

As previously mentioned in Chapter 3, a preliminary experiment showed solubility of QS signal of *P. aeruginosa* PQS, in the presence of phenyl-

boronic acid in $CHCl_3$, suggesting binding affinity of PQS to phenylboronic acid. However no medium for *P. aeruginosa* was found in which aggregation induced by phenylboronic acid alone was not observed. Further experiments to study the affinity of PQS to Gn-$B(OH)_2$ and a possible quorum quenching effect would be another application for the phenylboronic-acid dendrimers. Phenylboronic acid dendrimers with a PEG chain can form micelles with a boronic acid core (*Amaral S.P. et al. unpublished data*). If a high affinity for AI-2 or PQS could be confirmed, it would be interesting to explore the difference between terminal boronic acids, as the ones presented here, and nanoparticles with boronic acid in the core.

7.3 REFERENCES

[1] Mintzer, M.A., Dane, E.L., O'Toole, G.A., and Grinstaff, M.W. (**2012**). *"Exploiting dendrimer multivalency to combat emerging and re-emerging infectious diseases."* Mol Pharm 9(3): 342-54.

[2] Zhang, L., Pornpattananangku, D., Hu, C.M., and Huang, C.M. (**2010**). *"Development of nanoparticles for antimicrobial drug delivery."* Curr Med Chem 17(6): 585-94.

[3] Garner, A.L., Park, J., Zakhari, J.S., Lowery, C.A., Struss, A.K., Sawada, D., Kaufmann, G.F., and Janda, K.D. (**2011**). *"A multivalent probe for AI-2 quorum-sensing receptors."* J Am Chem Soc 133(40): 15934-7.

[4] Lowery, C.A., Abe, T., Park, J., Eubanks, L.M., Sawada, D., Kaufmann, G.F., and Janda, K.D. (**2009**). *"Revisiting AI-2 quorum sensing inhibitors: direct comparison of alkyl-DPD analogues and a natural product fimbrolide."* J Am Chem Soc 131(43): 15584-5.

[5] Xue, X.Y., Mao, X.G., Li, Z., Chen, Z., Zhou, Y., Hou, Z., Li, M.K., Meng, J.R., and Luo, X.X. (**2015**). *"A potent and selective antimicrobial poly(amidoamine) dendrimer conjugate with LED209 targeting QseC receptor to inhibit the virulence genes of gram negative bacteria."* Nanomedicine 11(2): 329-39.

[6] Chen, C.Z. and Cooper, S.L. (**2002a**). *"Interactions between dendrimer biocides and bacterial membranes."* Biomaterials 23(16): 3359-68.

[7] Ortega, P., Copa-Patino, J.L., Munoz-Fernandez, M.A., Soliveri, J., Gomez, R., and de la Mata, F.J. (**2008**). *"Amine and ammonium functionalization of chloromethylsilane-ended dendrimers. Antimicrobial activity studies."* Org Biomol Chem 6(18): 3264-9.

[8] Rasines, B., Hernandez-Ros, J.M., de las Cuevas, N., Copa-Patino, J.L., Soliveri, J., Munoz-Fernandez, M.A., Gomez, R., and de la Mata, F.J. (**2009**). *"Water-stable ammonium-terminated carbosilane dendrimers as efficient antibacterial agents."* Dalton Trans(40): 8704-13.

[9] Nizet, V. (**2006**). *"Antimicrobial peptide resistance mechanisms of human bacterial pathogens."* Curr Issues Mol Biol 8(1): 11-26.

[10] Imberty, A., Chabre, Y.M., and Roy, R. (**2008**). *"Glycomimetics and glycodendrimers as high affinity microbial anti-adhesins."* Chemistry 14(25): 7490-9.

[11] Touaibia, M. and Roy, R. (**2007**). *"Glycodendrimers as anti-adhesion drugs against type 1 fimbriated E. coli uropathogenic infections."* Mini Rev Med Chem 7(12): 1270-83.

[12] Salminen, A., Loimaranta, V., Joosten, J.A., Khan, A.S., Hacker, J., Pieters, R.J., and Finne, J. (**2007**). *"Inhibition of P-fimbriated Escherichia coli adhesion by multivalent galabiose derivatives studied by a live-bacteria application of surface plasmon resonance."* J Antimicrob Chemother 60(3): 495-501.

[13] Xue, X., Pasparakis, G., Halliday, N., Winzer, K., Howdle, S.M., Cramphorn, C.J., Cameron, N.R., Gardner, P.M., Davis, B.G., Fernandez-Trillo, F., and Alexander, C. (**2011**). *"Synthetic polymers for simultaneous bacterial sequestration and quorum sense interference."* Angew Chem Int Ed Engl 50(42): 9852-6.

[14] Pasparakis, G. and Alexander, C. (**2008**). *"Sweet talking double hydrophilic block copolymer vesicles."* Angew Chem Int Ed Engl 47(26): 4847-50.

[15] Pasparakis, G., Cockayne, A., and Alexander, C. (**2007**). *"Control of bacterial aggregation by thermoresponsive glycopolymers."* J Am Chem Soc 129(36): 11014-5.

[16] Lui, L.T., Xue, X., Sui, C., Brown, A., Pritchard, D.I., Halliday, N., Winzer, K., Howdle, S.M., Fernandez-Trillo, F., Krasnogor, N., and Alexander, C. (**2013**). *"Bacteria clustering by polymers induces the expression of quorum-sensing-controlled phenotypes."* Nat Chem 5(12): 1058-65.

[17] Louzao, I., Sui, C., Winzer, K., Fernandez-Trillo, F., and Alexander, C. (**2015**). *"Cationic polymer mediated bacterial clustering: Cell-adhesive properties of homo- and copolymers."* Eur J Pharm Biopharm 95(Pt A): 47-62.

[18] Pieters, R.J. (**2007**). *"Intervention with bacterial adhesion by multivalent carbohydrates."* Med Res Rev 27(6): 796-816.

[19] Katsikogianni, M. and Missirlis, Y.F. (**2004**). *"Concise review of mechanisms of bacterial adhesion to biomaterials and of techniques used in estimating bacteria-material interactions."* Eur Cell Mater 8: 37-57.

[20] An, Y.H. and Friedman, R.J. (**1998**). *"Concise review of mechanisms of bacterial adhesion to biomaterial surfaces."* J Biomed Mater Res 43(3): 338-48.

[21] Johansson, E.M., Crusz, S.A., Kolomiets, E., Buts, L., Kadam, R.U., Cacciarini, M., Bartels, K.M., Diggle, S.P., Camara, M., Williams, P., Loris, R., Nativi, C., Rosenau, F., Jaeger, K.E., Darbre, T., and Reymond, J.L. (**2008**). *"Inhibition and dispersion of Pseudomonas aeruginosa biofilms by glycopeptide dendrimers targeting the fucose-specific lectin LecB."* Chem Biol 15(12): 1249-57.

[22] Kadam, R.U., Bergmann, M., Hurley, M., Garg, D., Cacciarini, M., Swiderska, M.A., Nativi, C., Sattler, M., Smyth, A.R., Williams, P., Camara, M., Stocker, A., Darbre, T., and Reymond, J.L. (**2011**). *"A glycopeptide dendrimer inhibitor of the galactose-specific lectin LecA and of Pseudomonas aeruginosa biofilms."* Angew Chem Int Ed Engl 50(45): 10631-5.

APPENDIX

Active Carbonate Alkyne Characterisation (2)

NMR

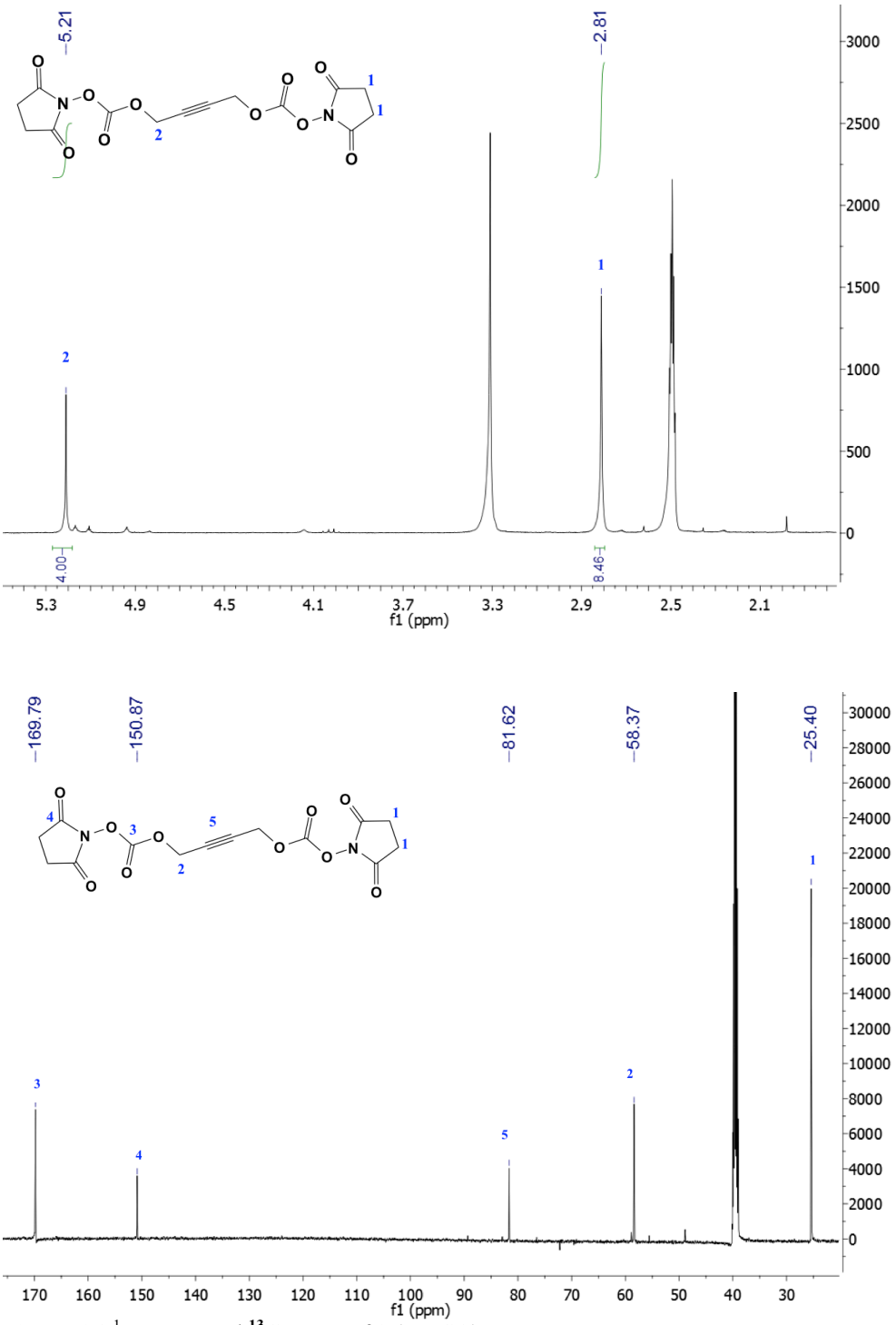

Figure A1 ^{1}H-NMR and ^{13}C-NMR of **2** (DMSO).

Mass Spectrometry

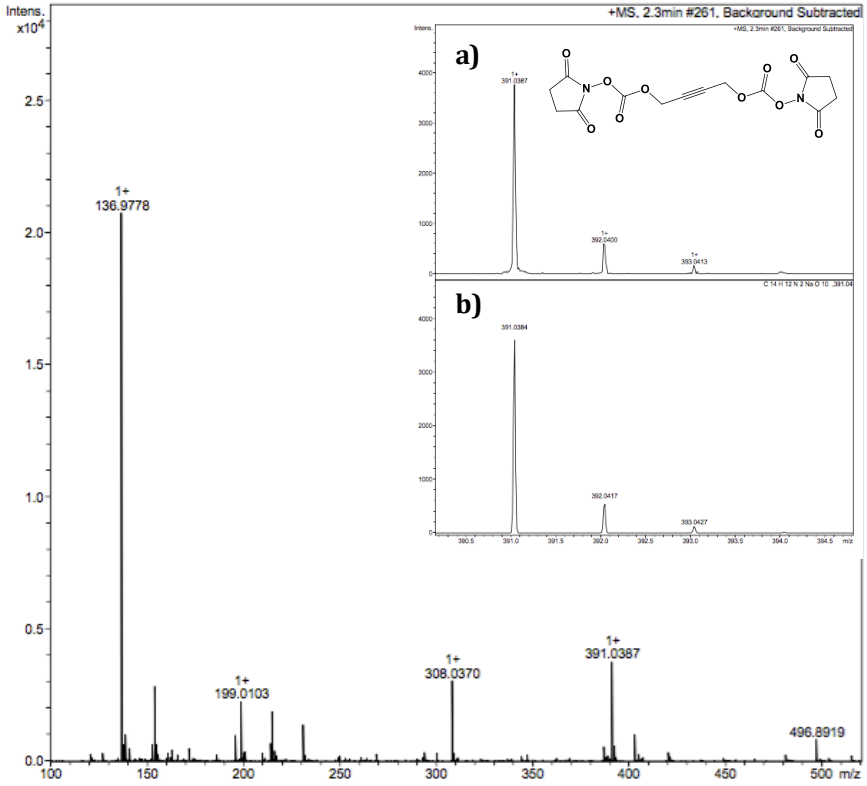

Figure A2 Mass spectrometry of **2**. Predicted (a) and measured mass (b).

Tetraol Ligand Characterisation (4)

NMR

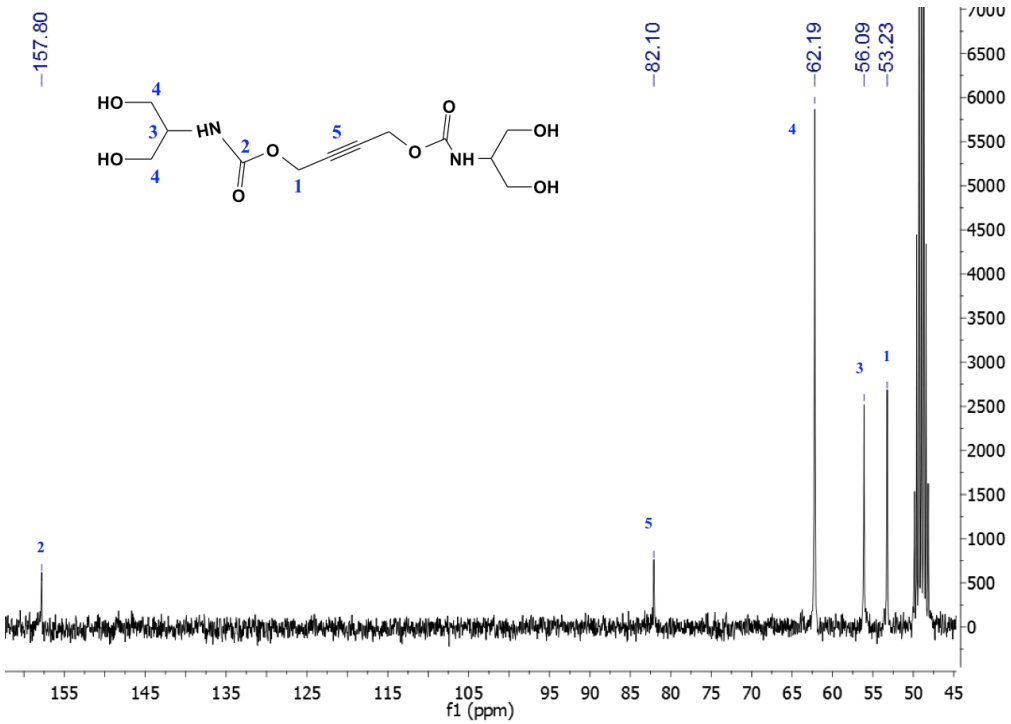

Figure A3 ^{13}C-NMR of tetraol ligand **4** (CD_3OD).

Infrared

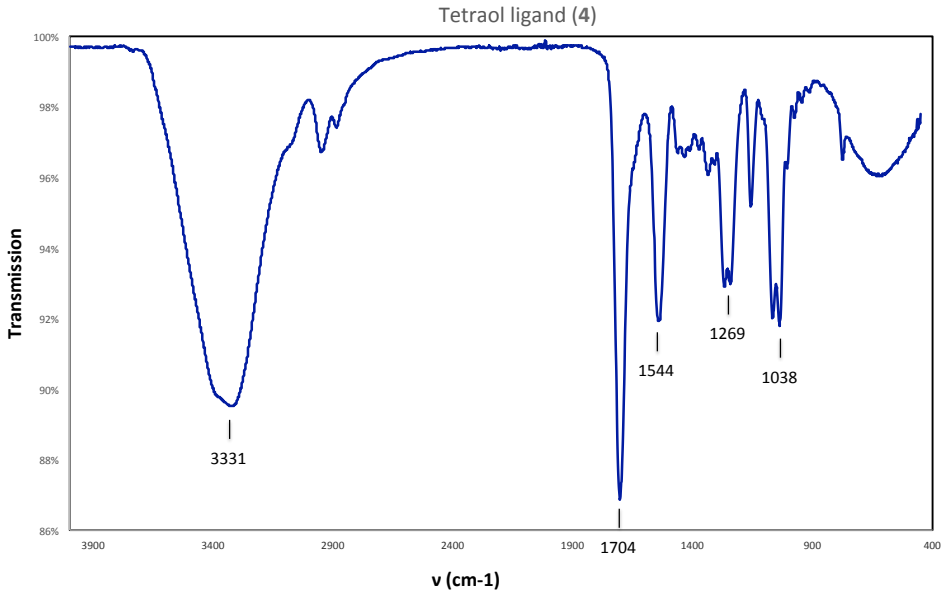

Figure A4 Infrared Spectra of tetraol ligand **4** (MeOH).

Mass Spectrometry

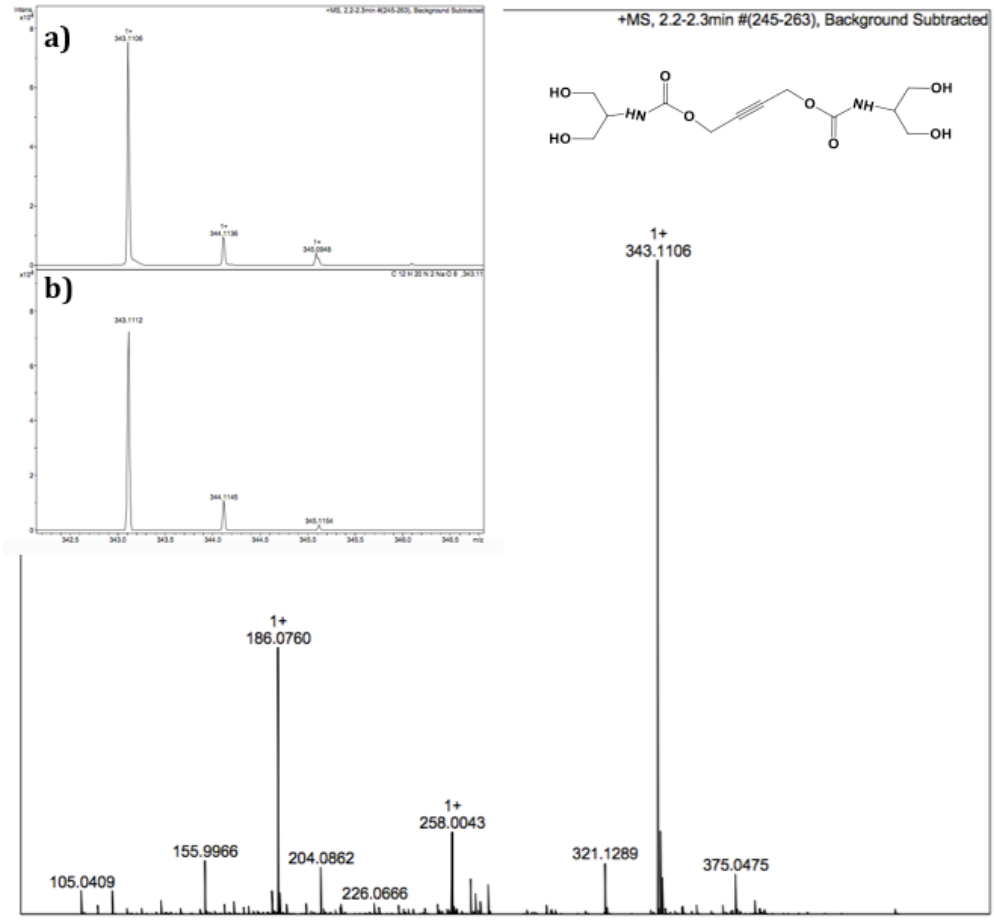

Figure A5 Masspec of tetraol ligand **4**. Predicted (a) and measured exact mass (b).

Diol Ligand Characterisation (7)

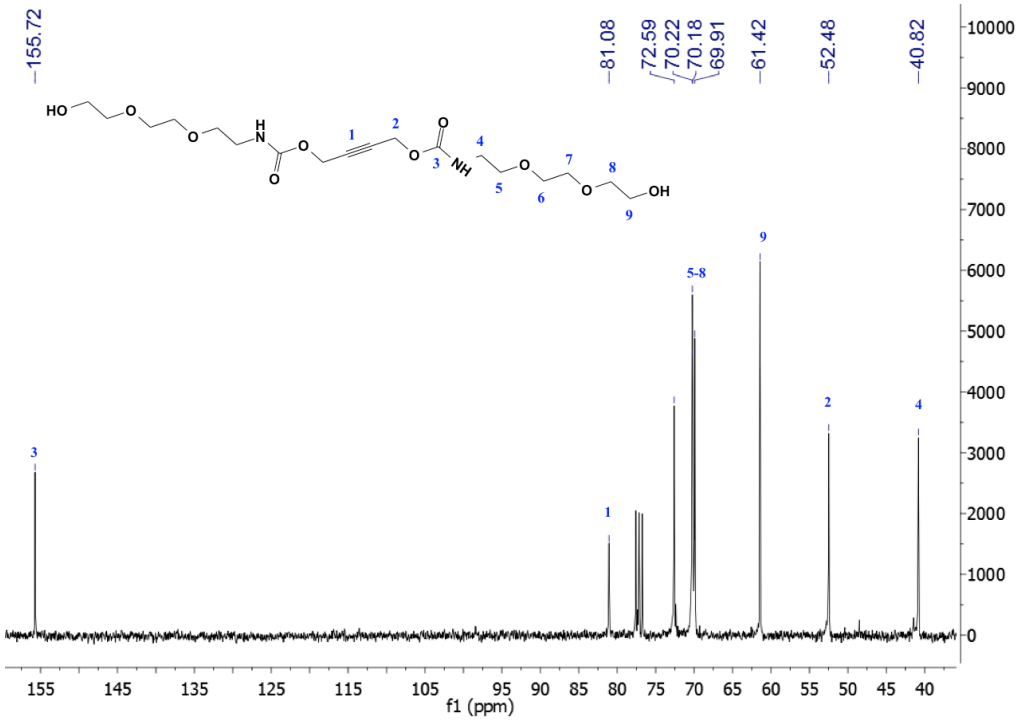

Figure A6 ^{13}C-NMR of diol ligand **7** ($CDCl_3$).

Infrared

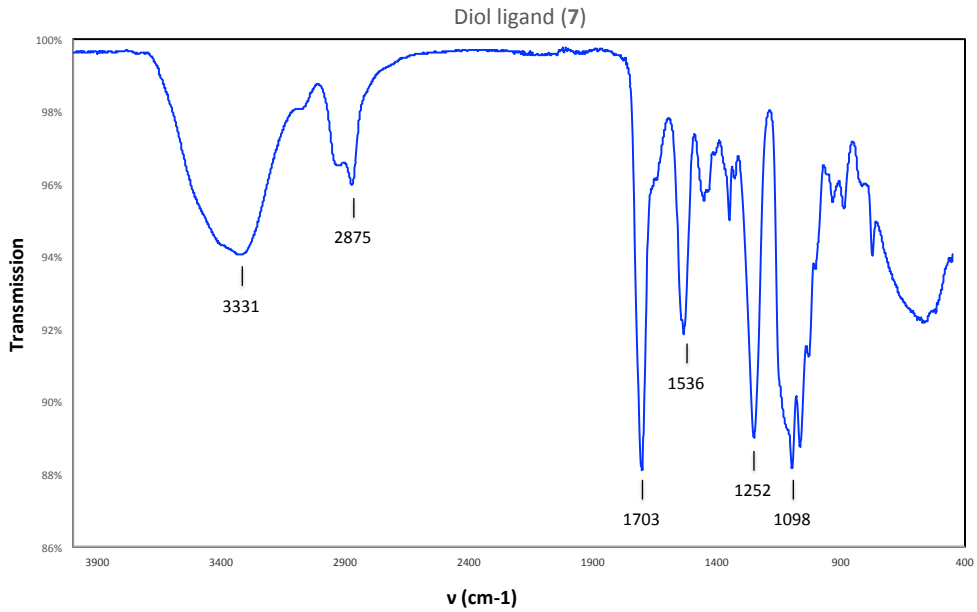

Figure A7 Infrared spectra of diol ligand **7** (MeOH).

Mass Spectrometry

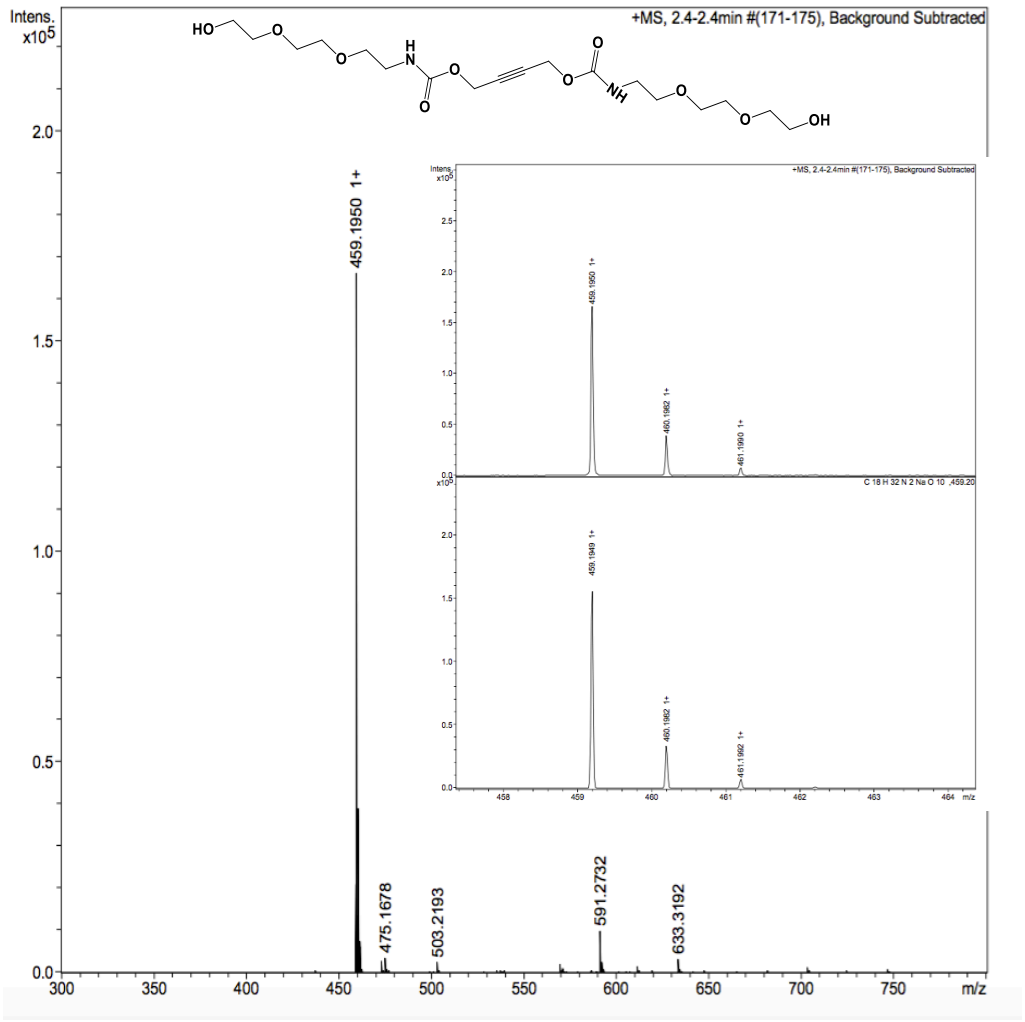

Figure A8 Masspec of diol ligand **7**. Predicted (a) and measured exact mass (b).

Optimization of Glucose/Mannose Ligands

Several protocols for the synthesis of the sugar ligands with internal alkynes were evaluated. The initial strategy was to directly conjugate protected sugar-trichloroacetimidates to 2-butyne-1,4-diol to get ligands like compound **19**.

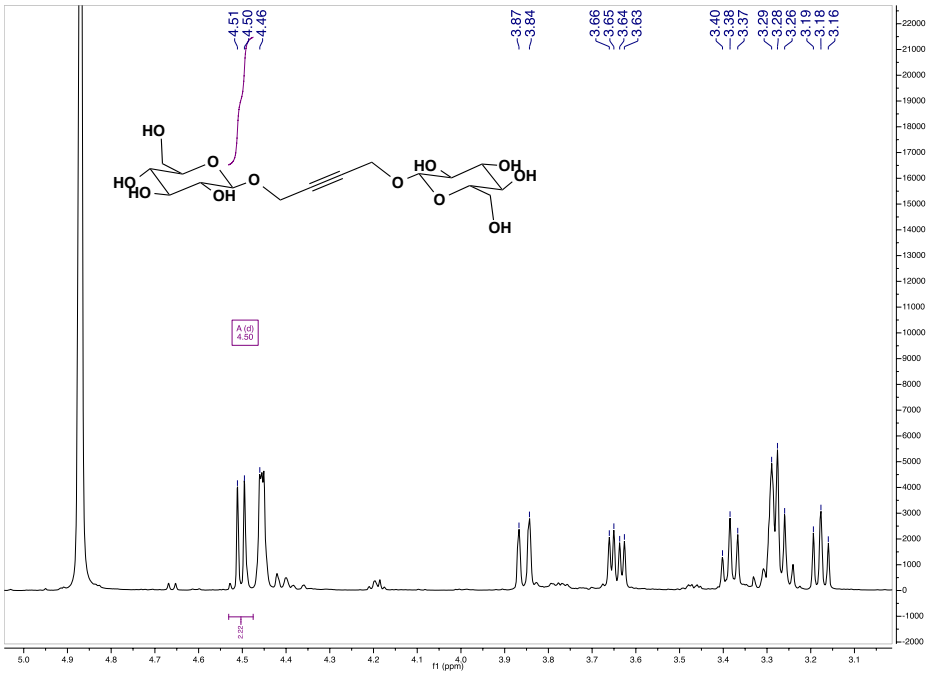

Figure A9 ^{1}H-NMR of compound **19** in D_2O. J-coupling constant 7.9Hz.

Since the product was found to be unstable, under the reaction conditions, an alkyne with carbamate groups (**20**) was synthesised and several conditions for Schmidt's glycosylation were evaluated.

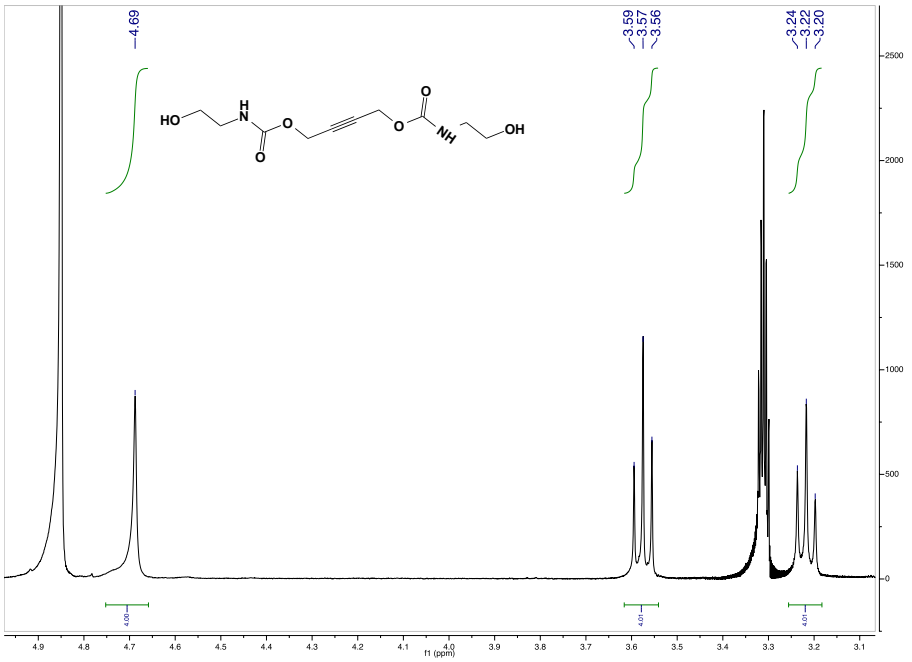

Figure A10 ^{1}H-NMR of compound **20** in CD_3OD.

Lewis acid	Conc.	Temp	Reaction Time	Purification	Result
BF_3*OEt_2	22%	**0 °C**	22h	1. DCM + 5% MeOH (15 min) 2. DCM + 5 %MeOH (25 min)	
BF_3*OEt_2	10%	**0 °C**	3h	1. DCM + 5 % MeOH 2. Hexane/Acetone 1:1	
BF_3*OEt_2	5 %	**-20 °C**	3h	n/a	
BF_3*OEt_2	22%	**0 °C**	23h	1. DCM + 5 % MeOH 2. Hexane/Acetone 1:1	
PPTS	2-20%	**0 °C**	16h	n/a	
$Zn(OTf)_2$	20%	**0 °C**	16h	n/a	
TMSOTf	20%	**0 °C**	16h	Hexane/Acetone 1:1 Unstabel compounds. Not product.	

Table A1. Synthesis strategy for protected sugar ligand **21** changing Lewis acid, concentration, temperature, purification and reaction time

Synthesis of Glucose/Mannose Ligands

Conditions for Schmidt's glycosylation with diol ligand **7**.

Lewis acid	Conc.	Temp	Reaction Time	Purification	Result
TMSOTf	2 %	**0 °C**	24h		Slow reaction, No Product
BF_3*OEt_2	22%	**0 °C**	22h	Hexande/Acetone	80 % impure product
BF_3*OEt_2	40%	**0 °C for 1h then r.t.**	5 h	Hexande/Aceton	
BF_3*OEt_2	40%	**0 °C for 1h then r.t.**	5 h	Hexande/EtOAc	Glucose ligand 76 % Mannose ligand 48 %

Table A2. Synthesis strategy for protected glucose **11** and protected mannose ligand **17** changing Lewis acid, concentration, purification and reaction time.

Glucose Ligands Characterisation

NMR

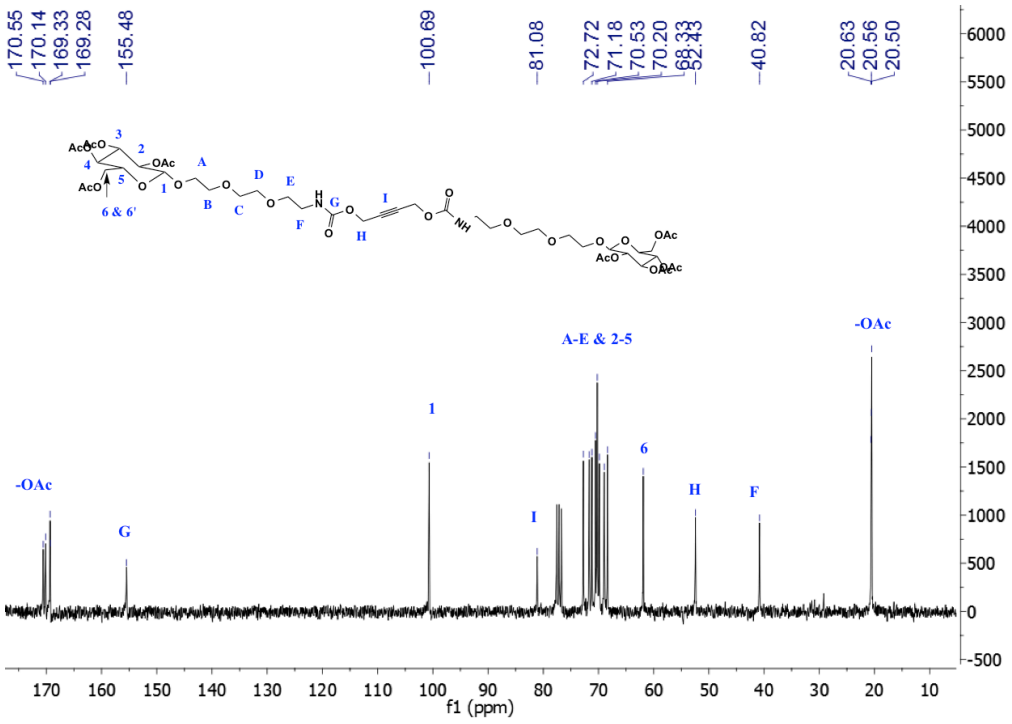

Figure A11 ^{13}C-NMR of protected glucose ligand **11** ($CDCl_3$).

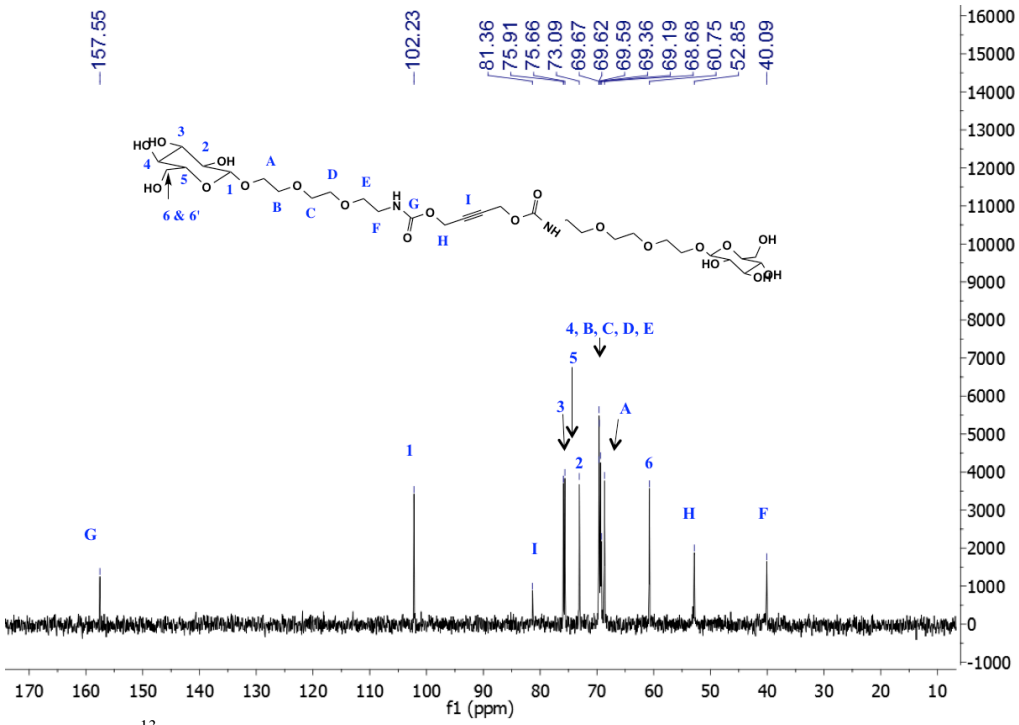

Figure A12 ^{13}C-NMR of glucose ligand **12** (D_2O)

Infrared

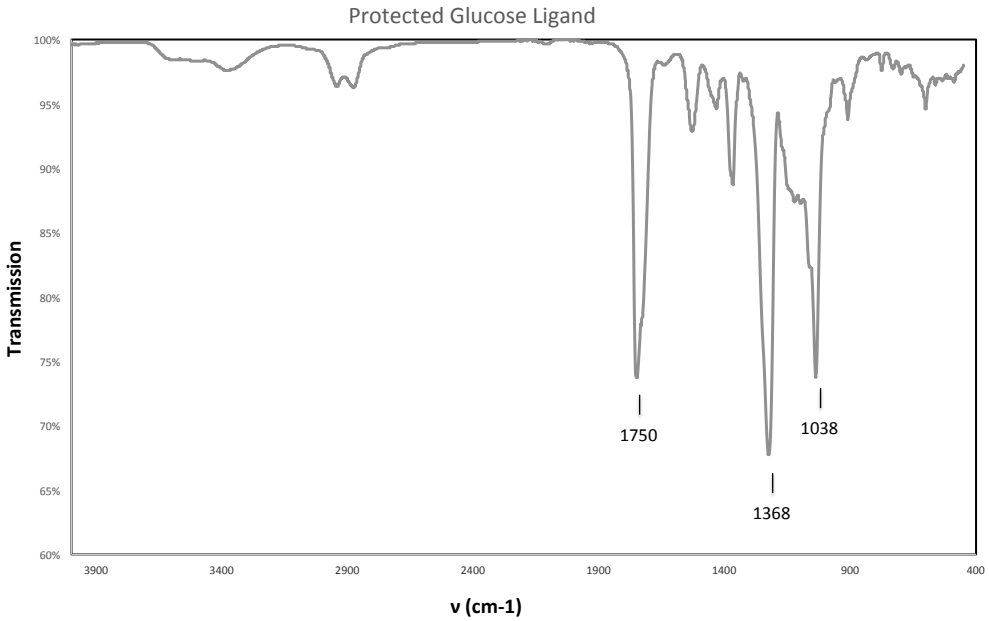

Figure A13 Infrared spectra of protected glucose ligand **11** ($CHCl_3$).

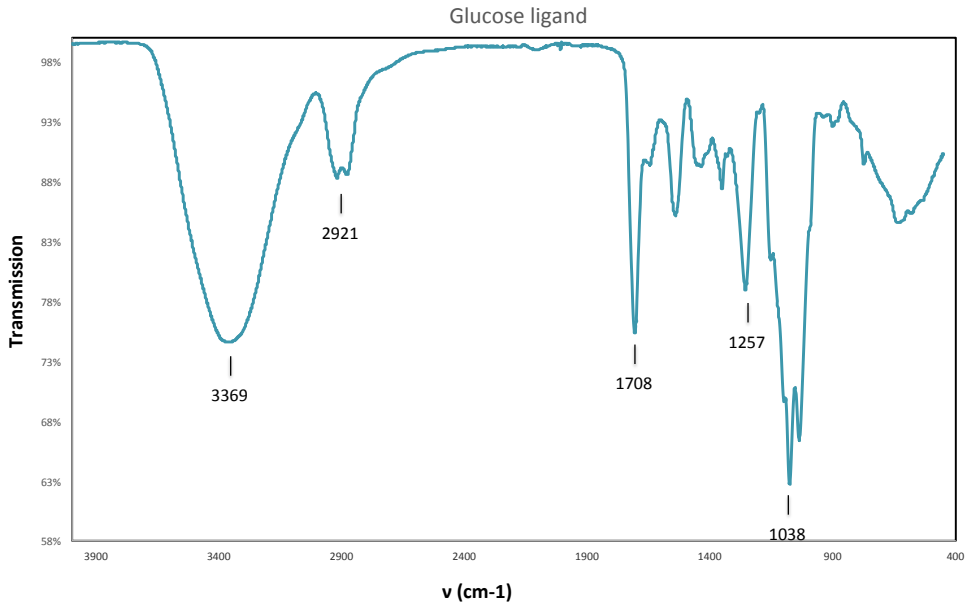

Figure A14 Infrared spectra of glucose ligand **12** (MeOH).

Mass Spectrometry

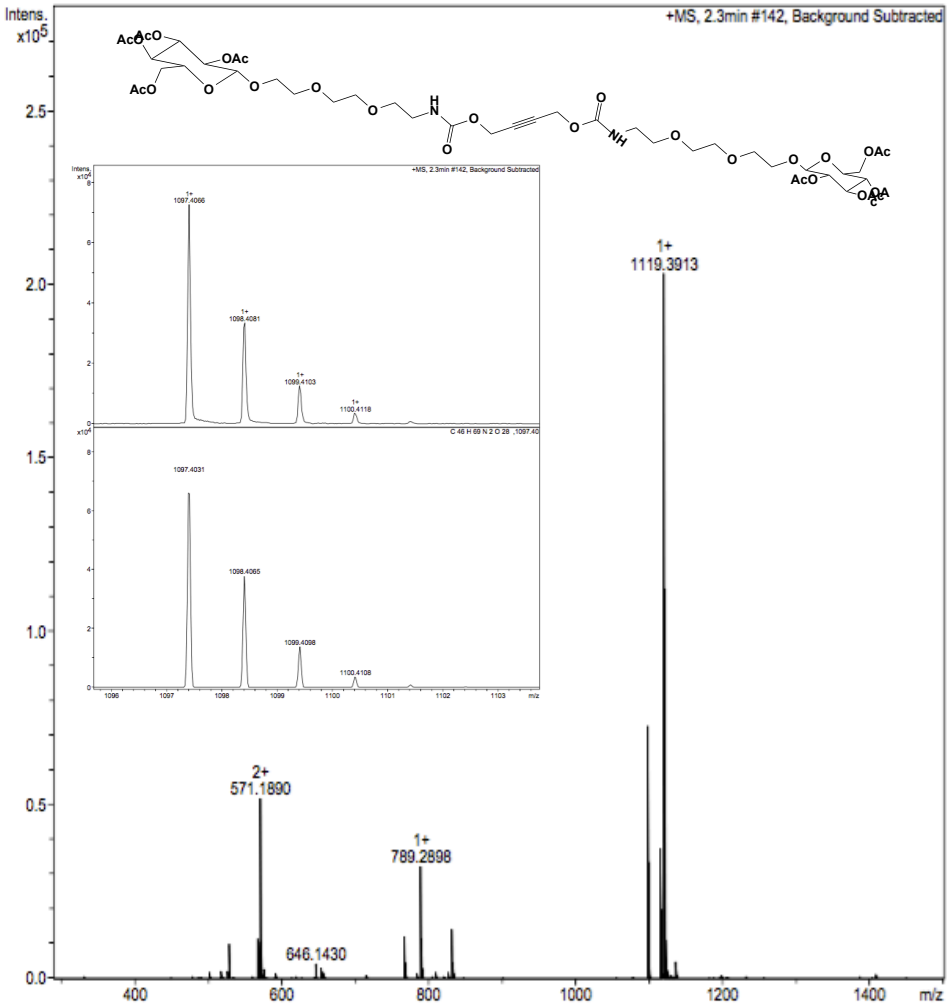

Figure A15 Mass spectrometry spectra of protected glucose ligand **11**. Predicted (a) and measured exact mass (b).

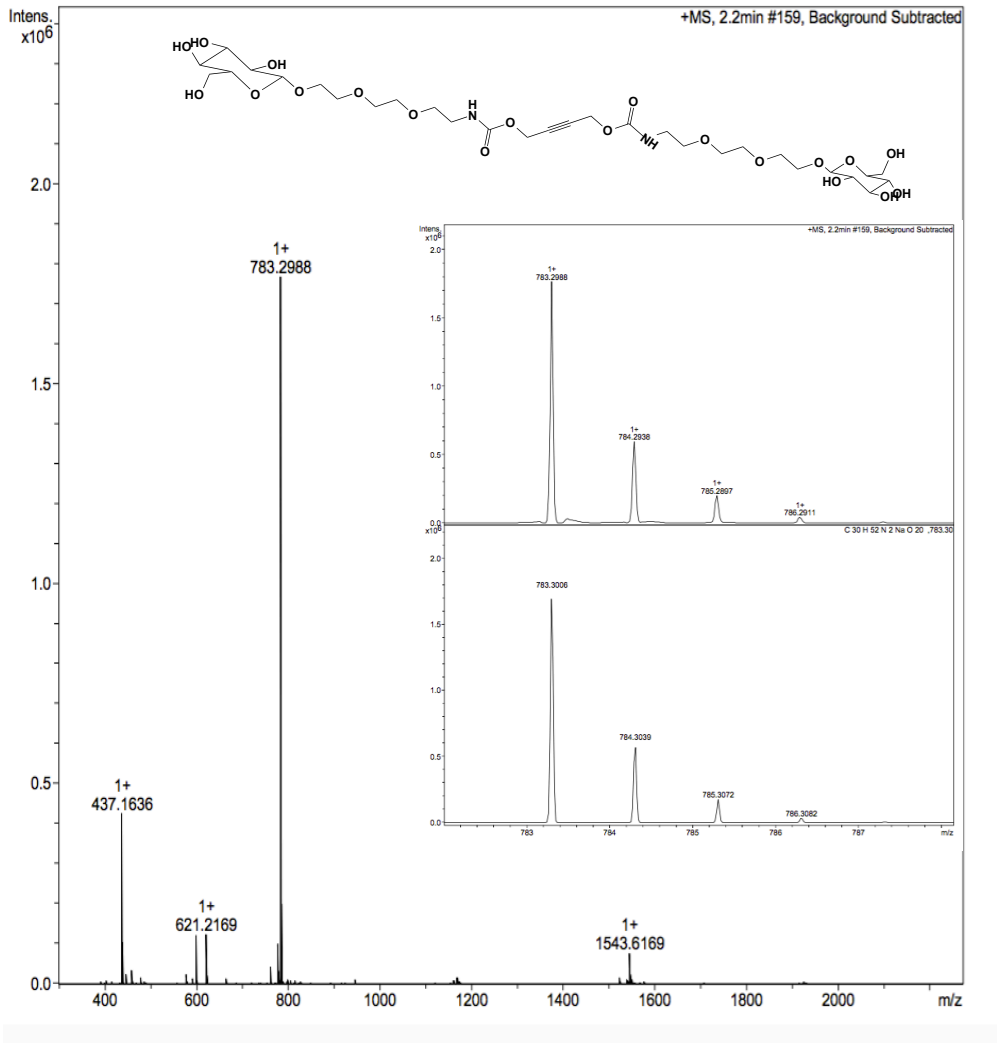

Figure A16 Mass spectrometry spectra of glucose ligand **12**. Predicted (a) and measured mass (b).

Mannose Ligand Characterisation

NMR

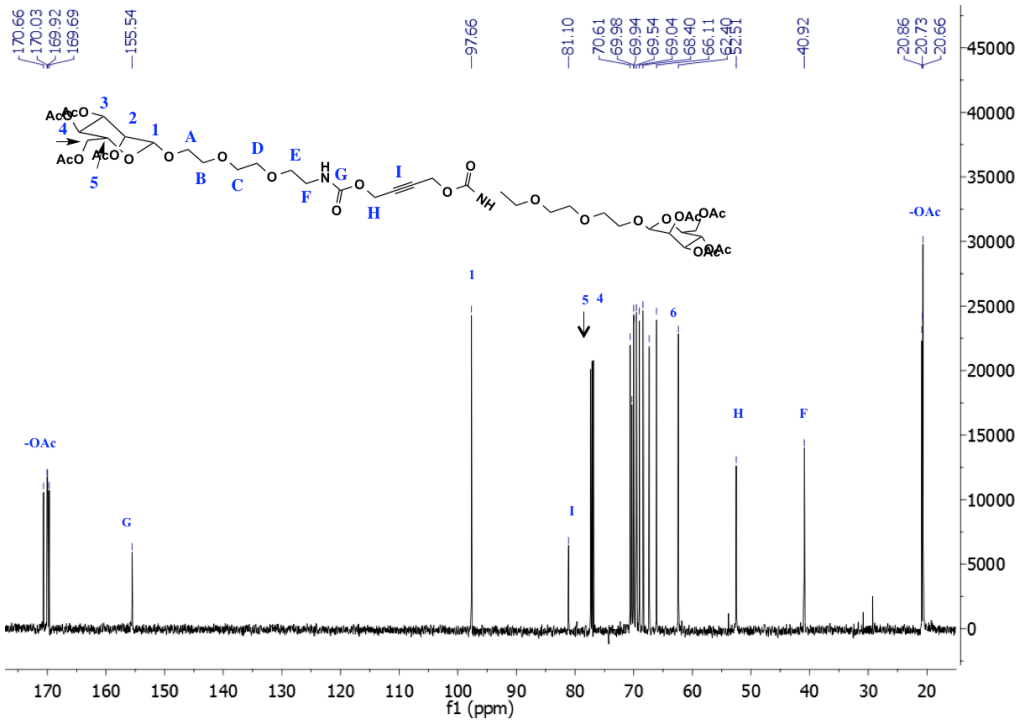

Figure A17 ^{13}C-NMR of protected mannose ligand **18** ($CDCl_3$).

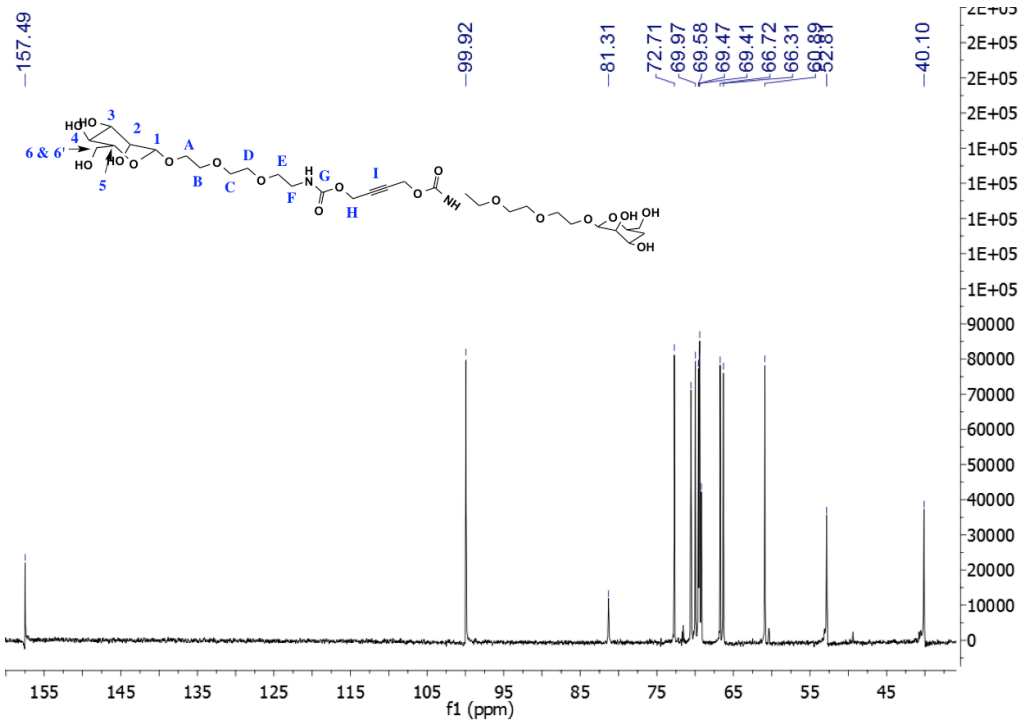

Figure A18 ^{13}C-NMR of mannose ligand **19** ($CDCl_3$).

Infrared

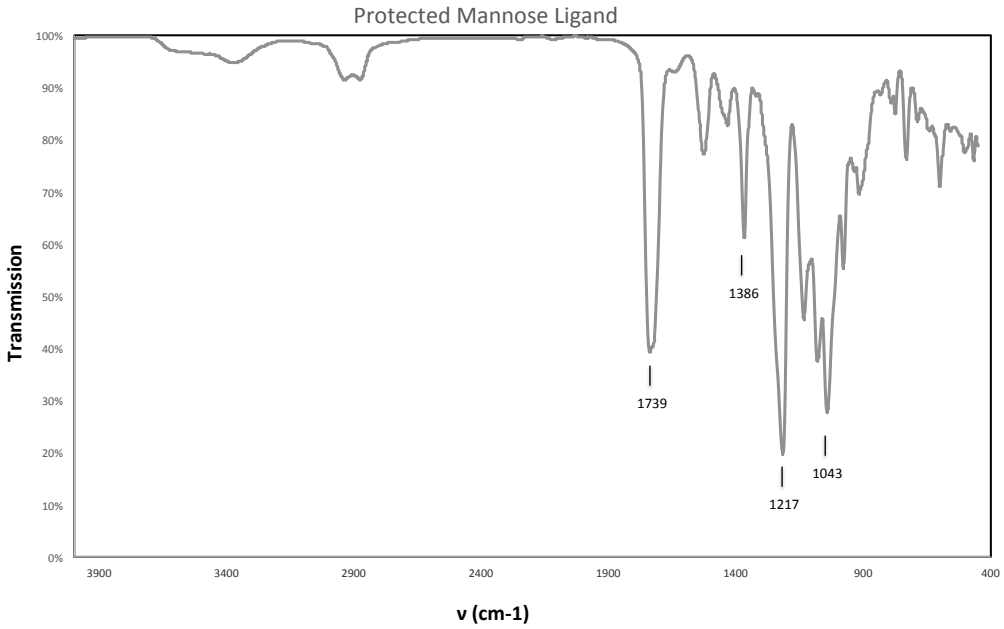

Figure A19 Infrared spectra of protected mannose ligand **18** ($CHCl_3$).

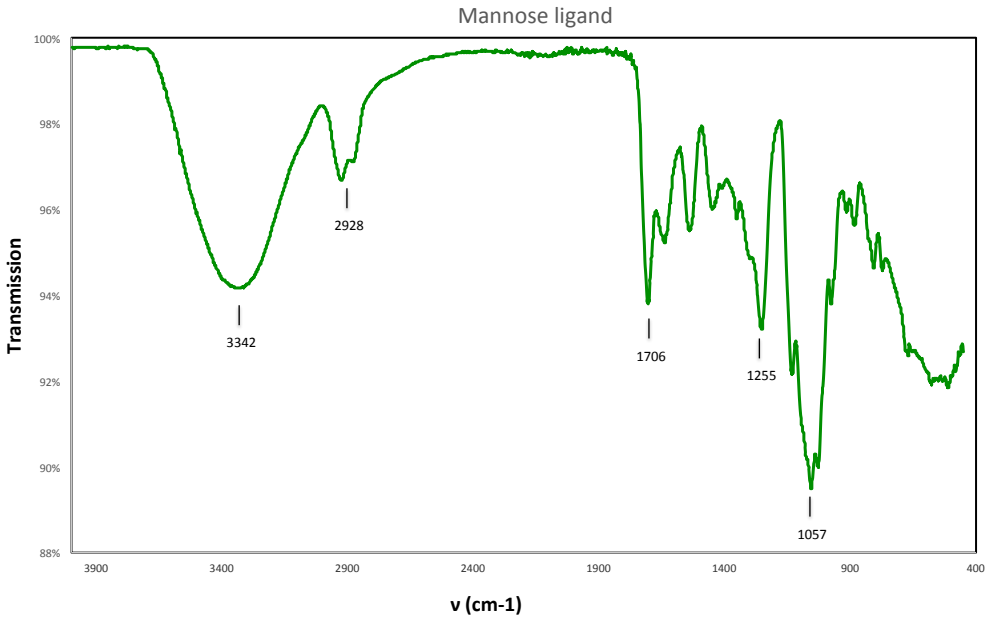

Figure A20 Infrared spectra of mannose ligand **19** (MeOH).

Mass Spectrometry

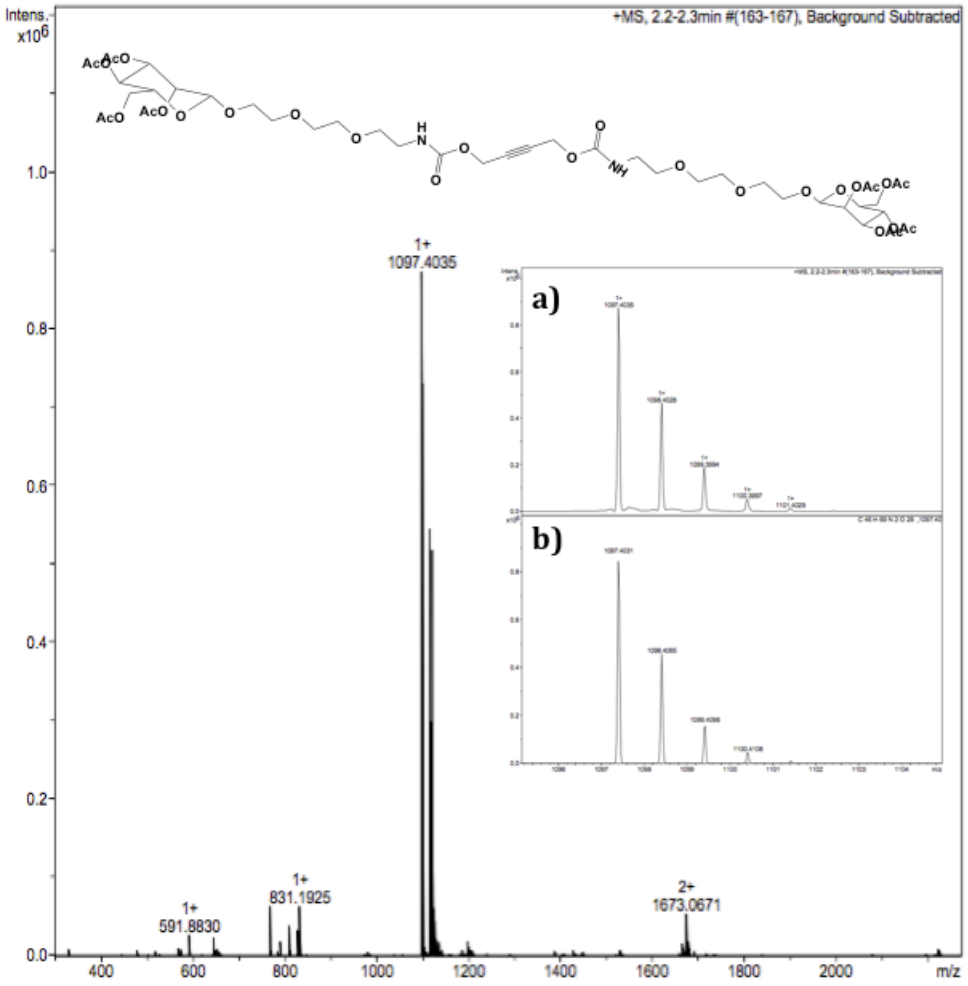

Figure A21 Mass spectrometry spectra of protected mannose ligand **18**. Predicted (a) and measured exact mass (b).

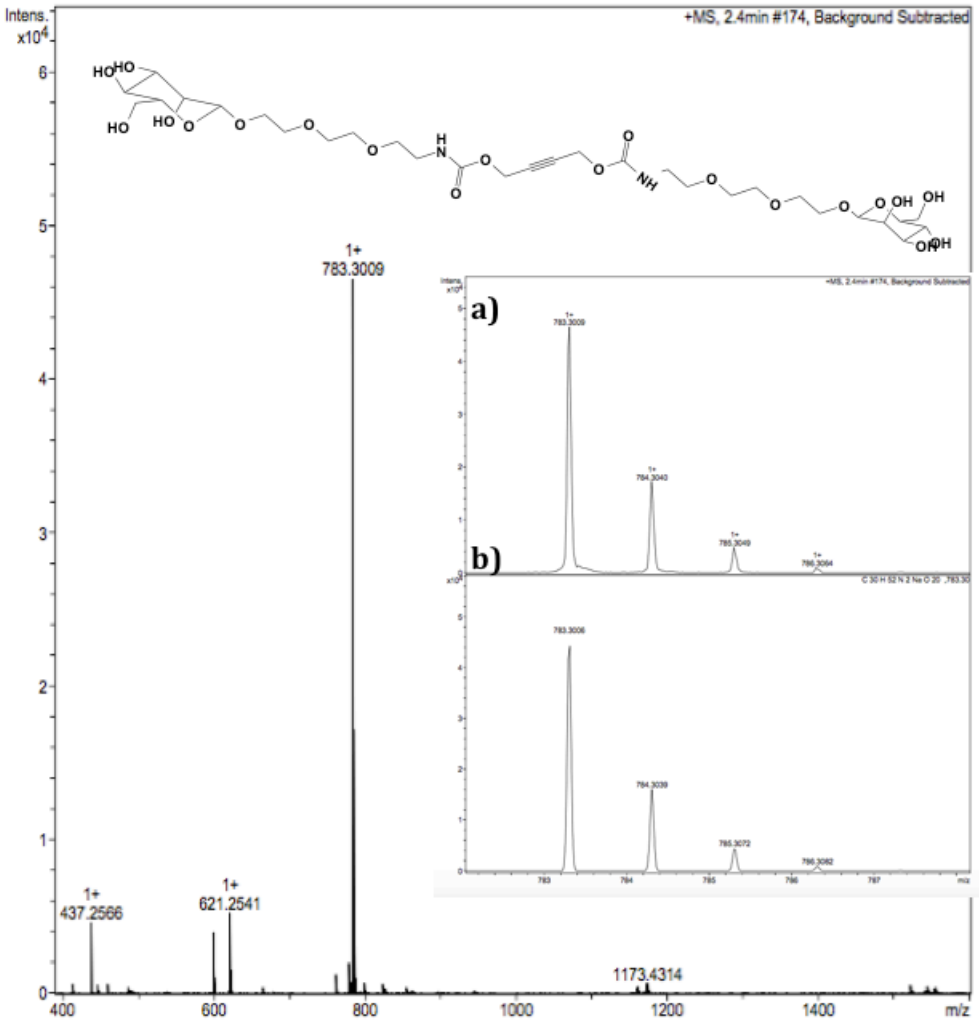

Figure A22 Mass spectrometry spectra of mannose ligand **19**. Predicted (a) and measured exact mass (b).

Microwave-assisted synthesis of dendrimers through Azide-alkyne cycloaddition.

Synthesis of new core (**22**)

The new core **22** was synthesised in a two-step reaction. 2,4,6-tris(bromomethyl)mesitylene (**35**) was synthesised in a one-step process following known conditions [1].

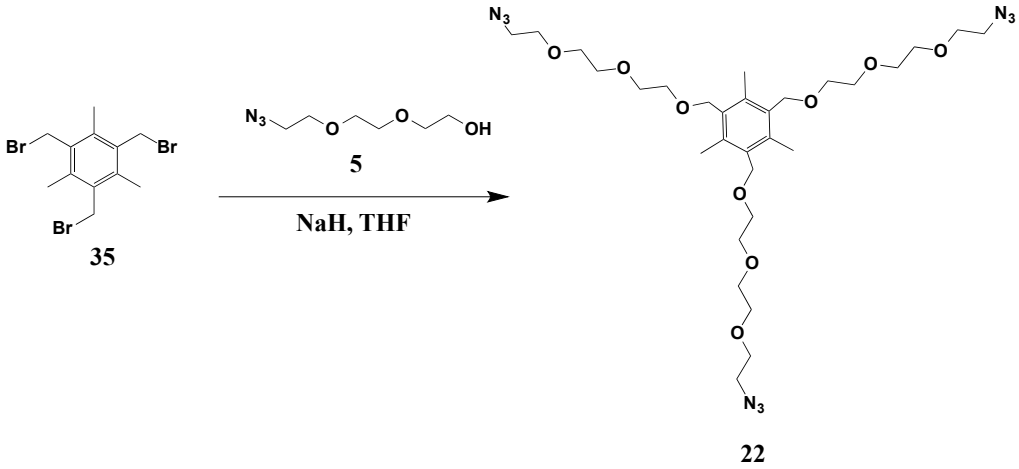

Figure A23 Chemical synthesis of core **22** for microwave-assisted AAC dendrimers

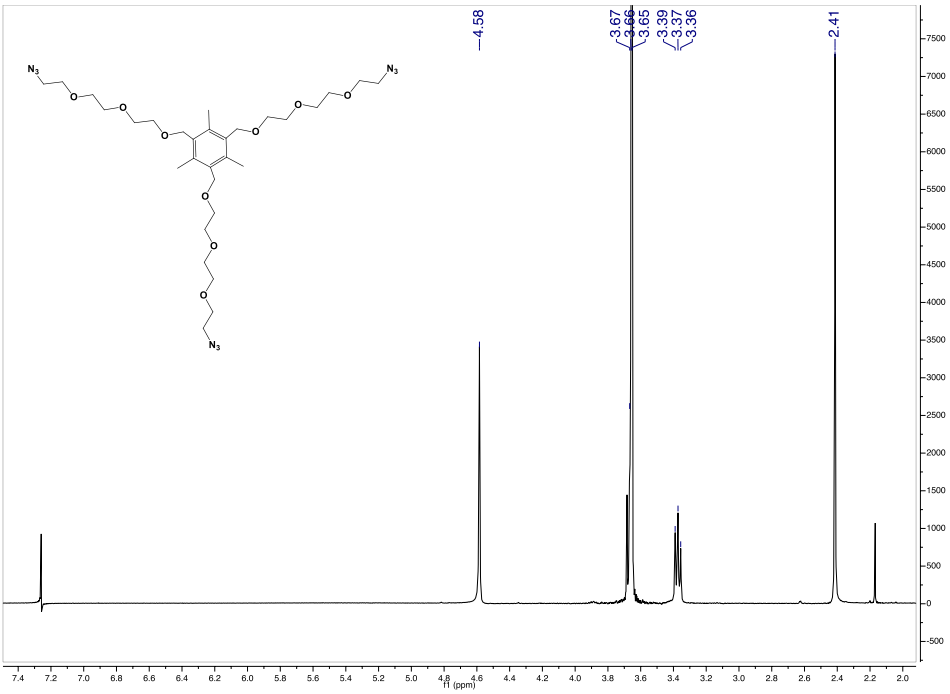

Figure A24 ^{1}H-NMR of core **22** ($CDCl_3$)

Synthesis of repeating unit for microwave-assisted AAC

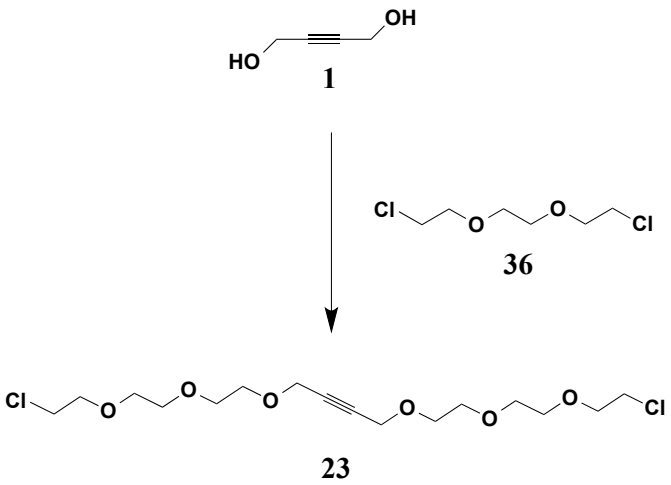

Figure A25 Chemical strategy for repeating unit **23** for microwave-assisted AAC synthesis of dendrimers.

Reactants	Solvent	Temperatur	Time	Nº of Fractions	Yield
NaH	THF,	60°C	27h	8	-
NaH (Dry)	THF	60°C	24h	6	-
NaH (Dry)	THF,	60°C	40h	4	<10%
NaOH, nBu_4NHSO_4 3 eq. of di-chlor	H_2O,	70°C	63h	4	16%
NaOH, nBu_4NHSO_4 5 eq. of di-chlor	H_2O	70°C	70h	4	Not pure (13 %)

Table A3. Synthesis strategy for synthesis of compound **23** changing Lewis reactants, solvent, and reaction time.

Microwave-assisted synthesis of dendrimers

The microwave-assisted AAC reaction (Figure 3.22) was done under fixed power settings, for a total of 10 h at 120 °C, but the reaction was not complete, (CH_2 alpha to the azide peak was still visible at 3.4ppm by ^{1}H-NMR) and a dark, oily product was obtained. Furthermore, multiple unwanted by-products and decomposition were noticed by TLC and ^{1}H-NMR. This result was the same using alternative core **34**, different solvents and temperatures. The repeating unit is not very reactive, with only the alpha oxygen pulling electrons from the alkyne to increase the reactivity for the click reaction. After 10 h at temperature as high as 120 °C, the reaction is still not complete, and because of the high temperature for so long, the small amount of solvent started to evaporate, leading dendrimer de-composition.

Dendrimers could be synthesised using a more reactive repeating unit, for example with a carbonyl group close to the internal alkyne, but as such esters are sensitive to water and can be hydrolysed, this type of dendrimer is not

suitable for our application with bacteria that requires stable water-soluble dendrimers.

Characterisation of AAC Functionalised GATG Dendrimers

NMR

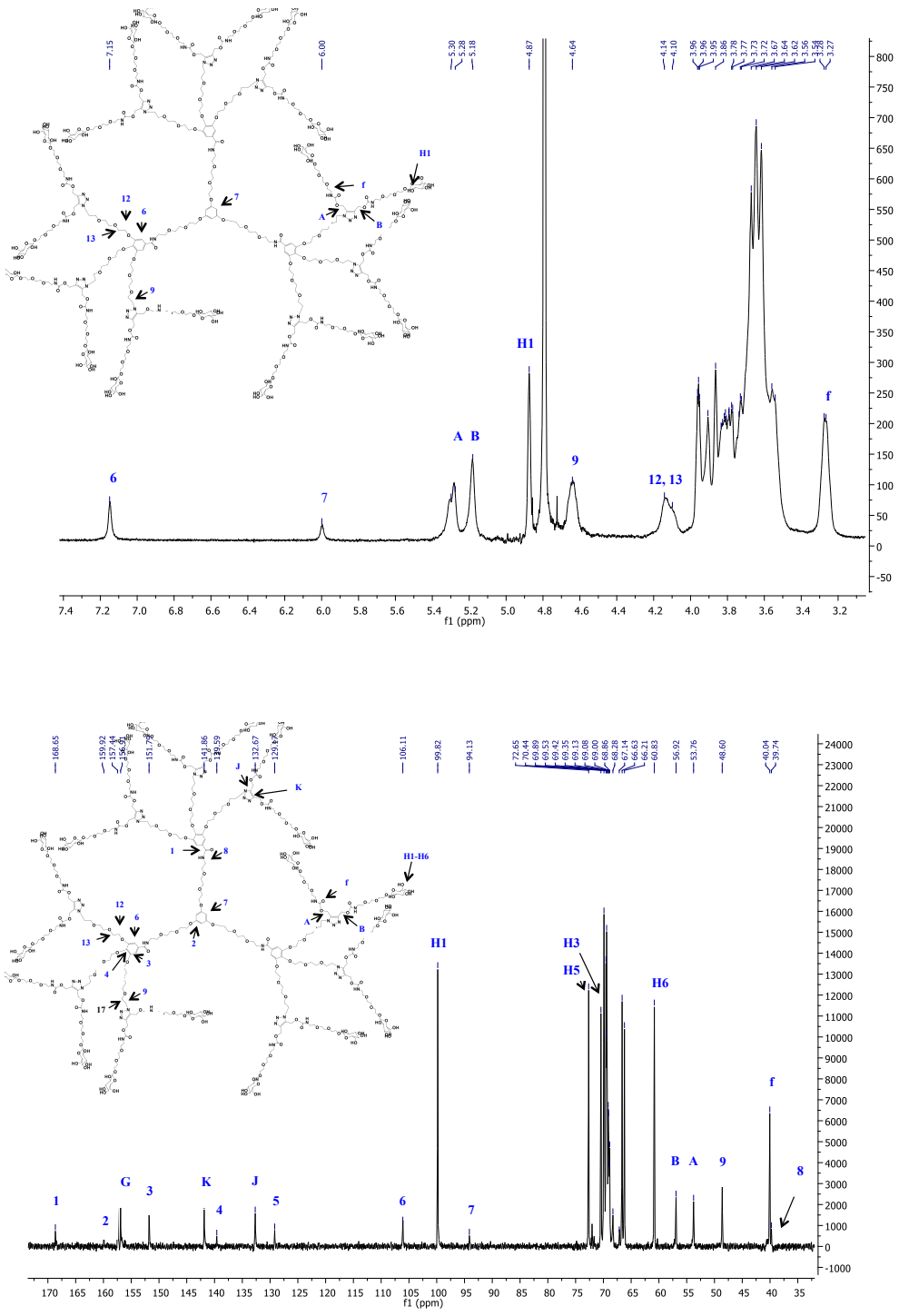

Figure A25 ^{1}H-NMR and ^{13}C-NMR of G1-mannose (D_2O).

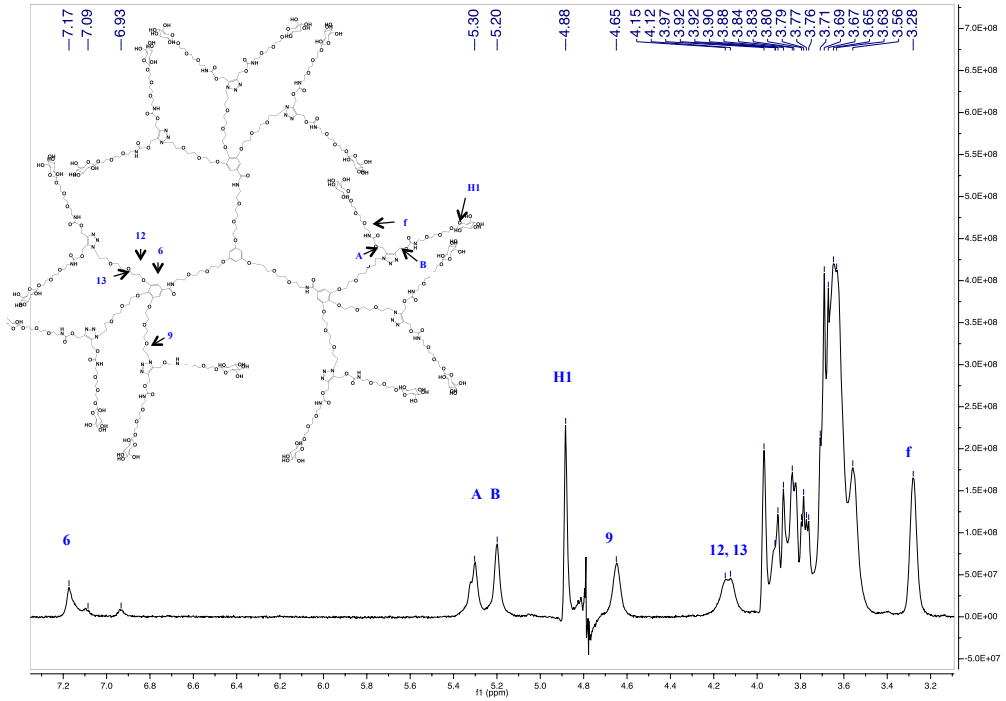

Figure A26 ^{1}H-NMR of G3-mannose (D_2O).

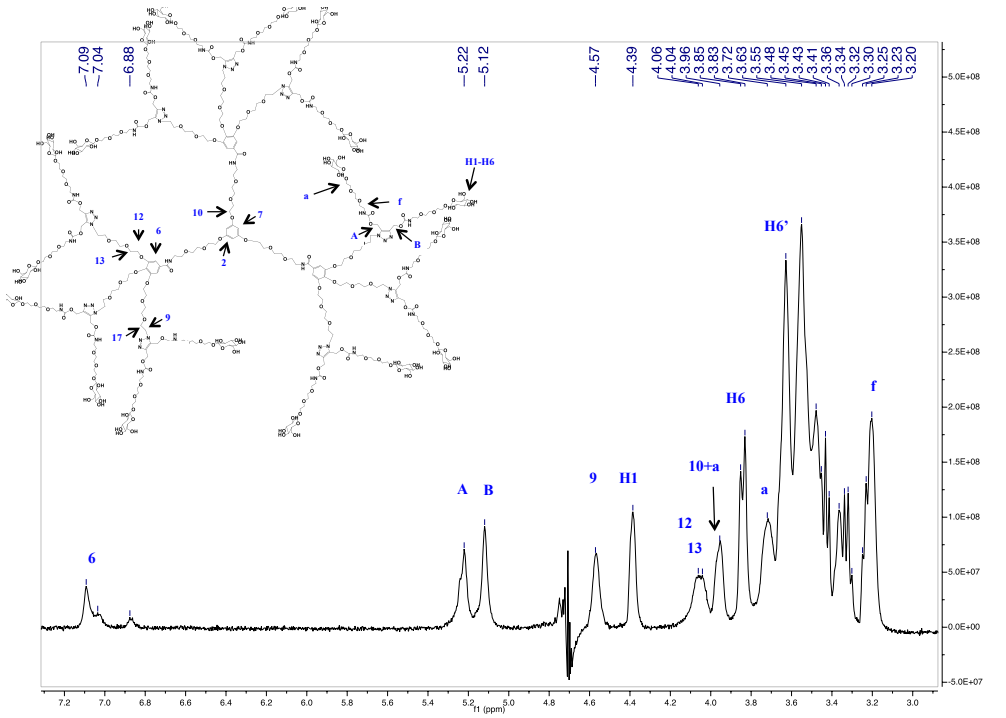

Figure A27 ^{1}H-NMR of G3-glucose (D_2O).

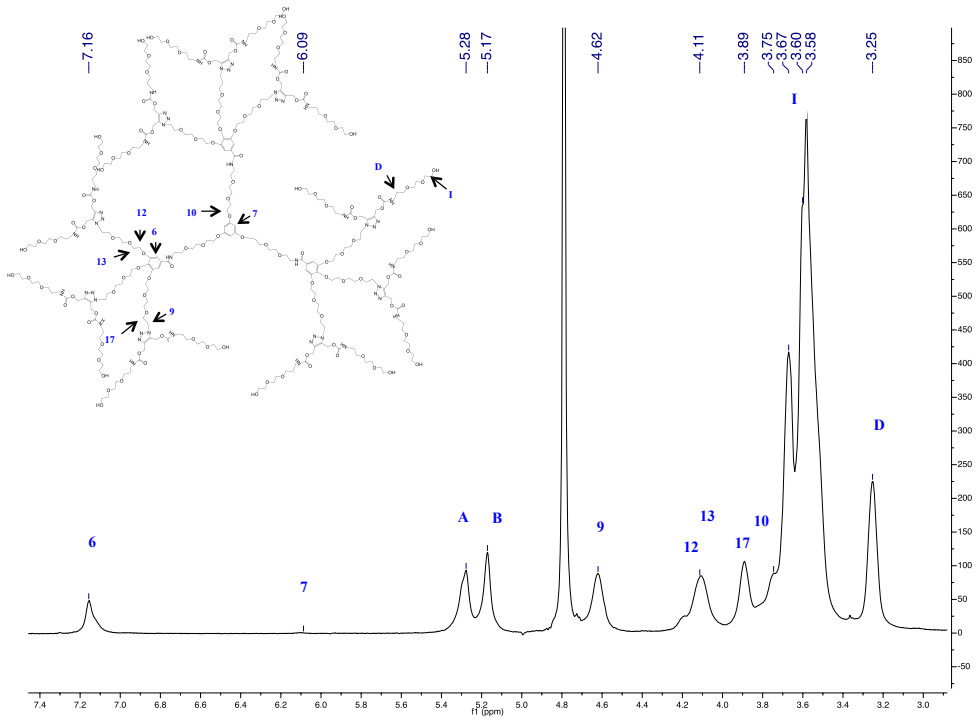

Figure A28 ^{1}H-NMR of G3-Diol (D_2O).

Infrared

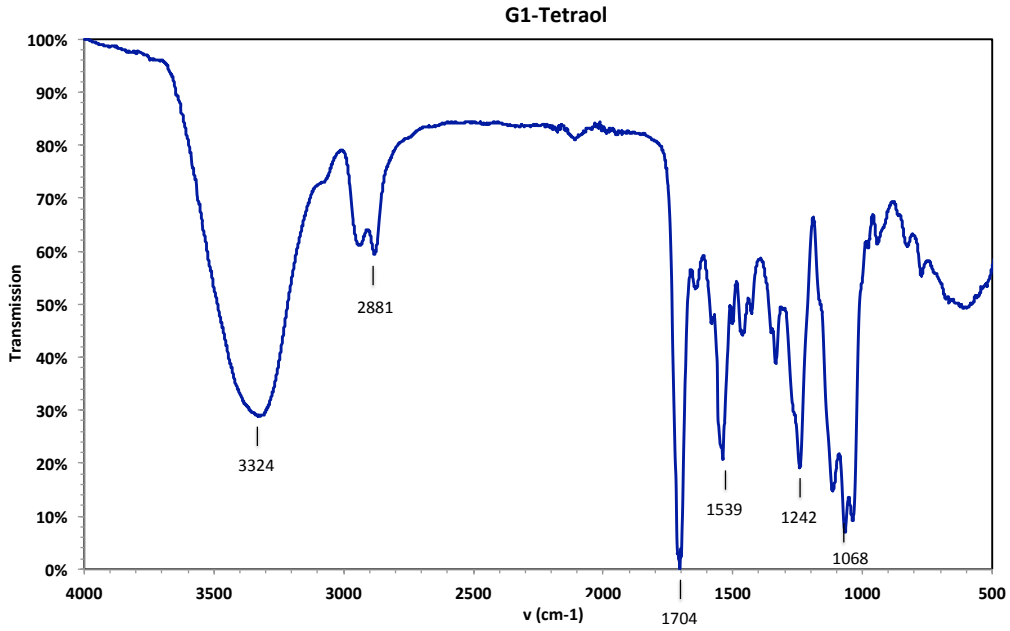

Figure A29 Infrared spectra of G1-Tetraol (MeOH).

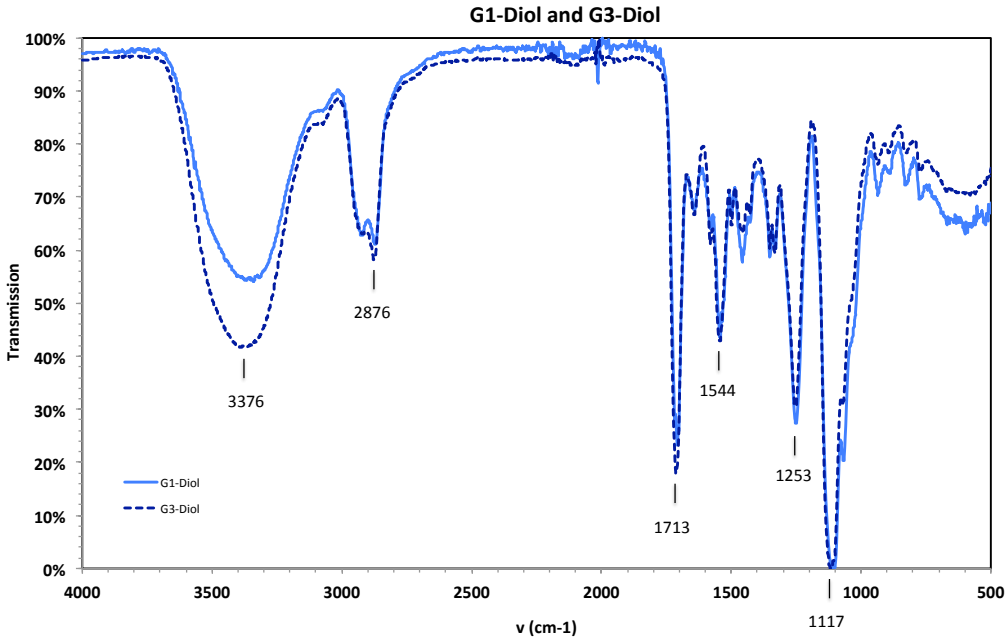

Figure A30 Infrared spectra of G1-Diol (solid line) and G3-Diol (dashed line) (MeOH).

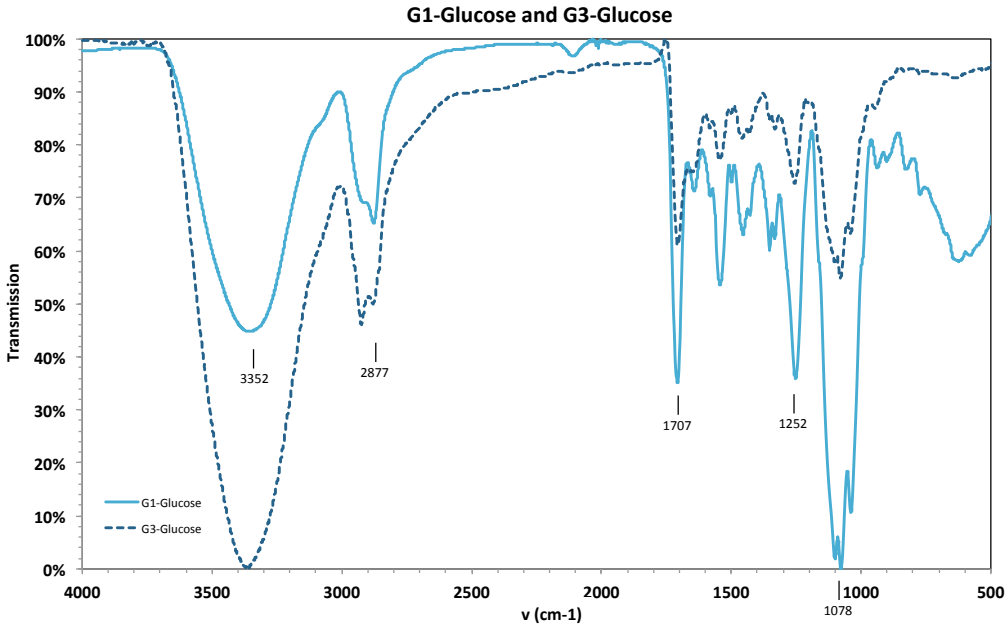

Figure A31 Infrared spectra of G1-Glucose and G3-Glucose (MeOH).

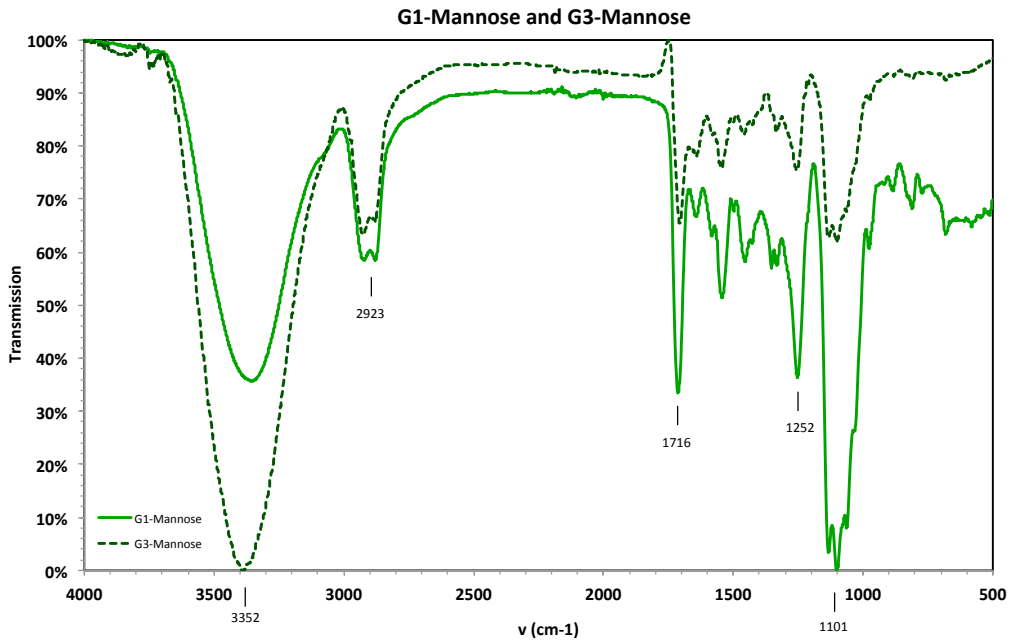

Figure A32 Infrared spectra of G1-Mannose and G3-Mannose (MeOH).

DLS

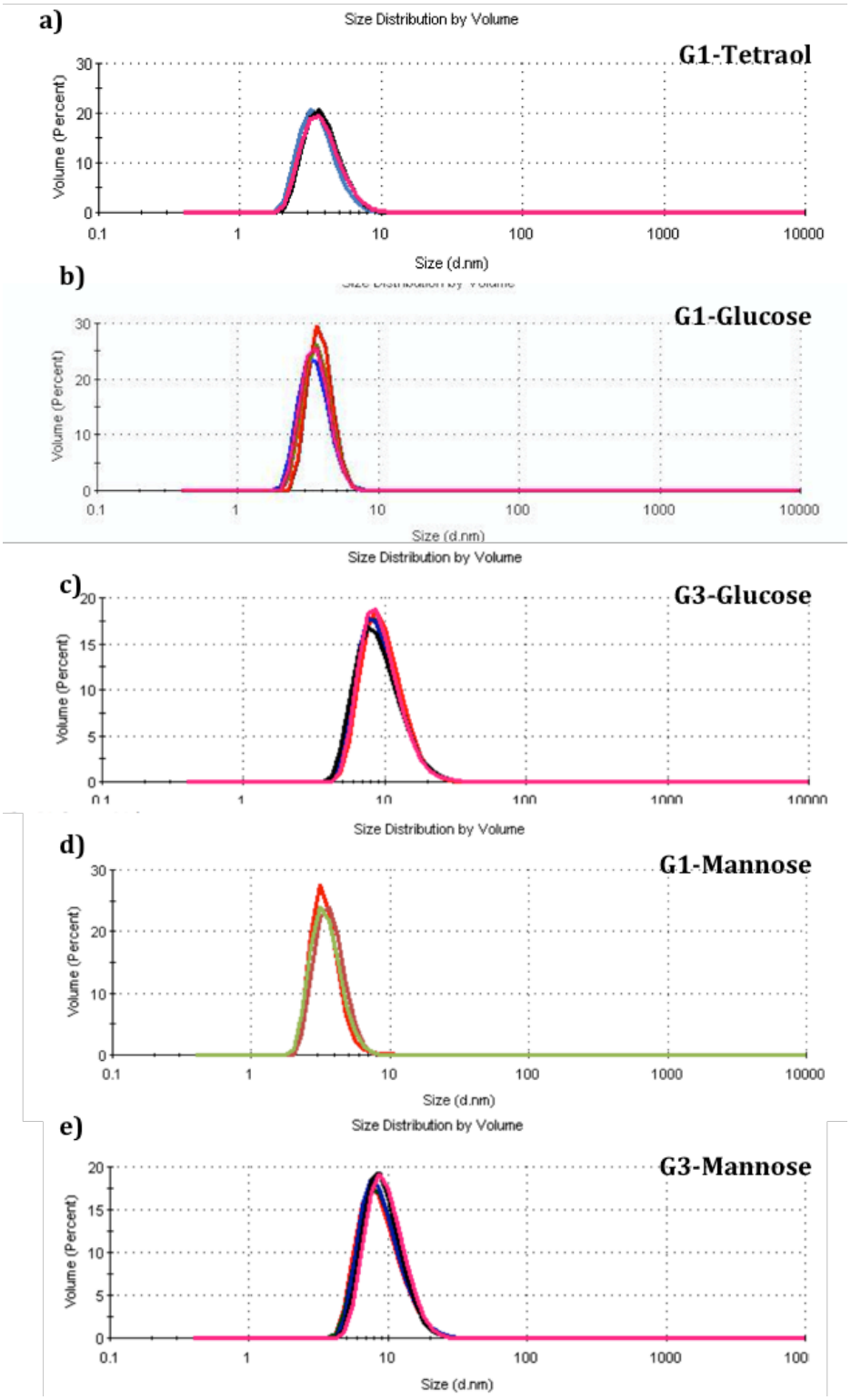

Figure A33 Size distribution by volume measured by Dynamic Light Scattering (DLS) for G1-Tetraol (a) G1-Glucose (b), G3-Glucose (c), G1-Mannose (d) and G3-Mannose (e). Samples at 1 mg/mL in 150 mmol LiCl. Shown are five measurements of each sample.

SEC

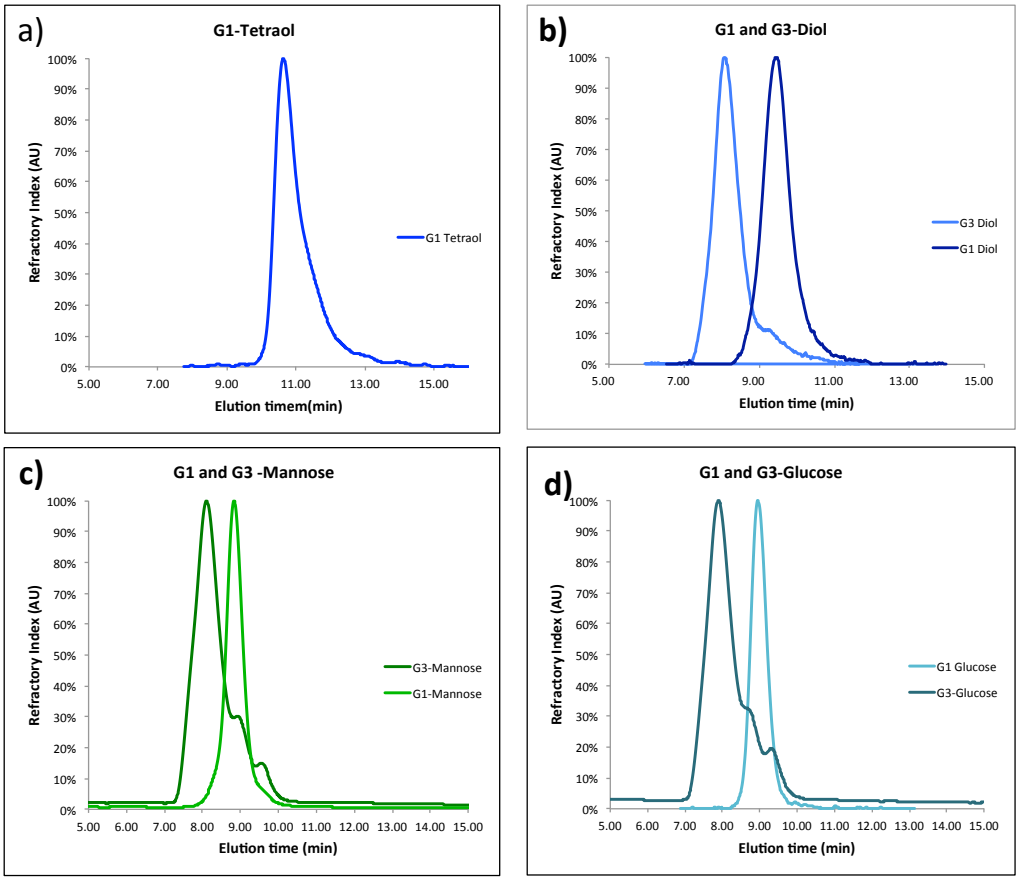

Figure A34 Size Exclusion Chromatography for GATG dendrimer G1-tetraol (a), G1 and G3-Diol (b), G1 and G3-Mannose (c) G1 and G3-Glucose (d) 150 mmol LiCl was used as an eluent at 1 mL/min and samples were filtered through 0.45 μm before injection.

Boronic acid- Dendrimer Characterisation

NMR

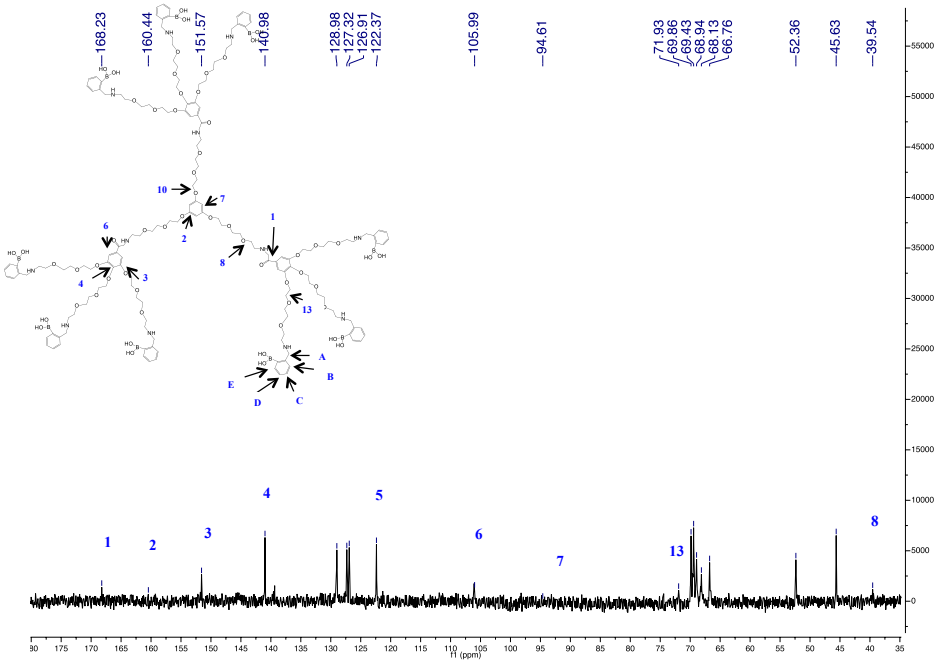

Figure A35 ^{13}C-NMR of G3-B(OH)$_2$ (D_2O).

Clustering of MM32 in the presence of diol-dendrimers

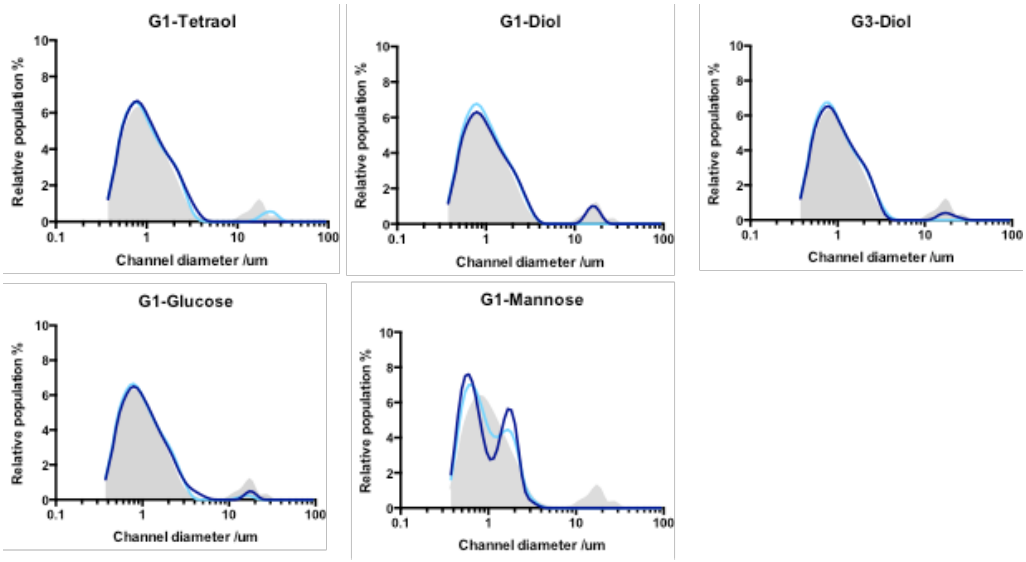

Figure A36 Size distribution of *V. harveyi* MM32 suspension (OD_{600}= 1.0) in the absence (grey) and presence of G1-tetraol after 5 min (light blue) and 60 min (dark blue). Dendrimer concentration 0.5 mg/mL. Plotted are mean values.

CFU of BB170 (LB-medium) in the presence of diol-dendrimers

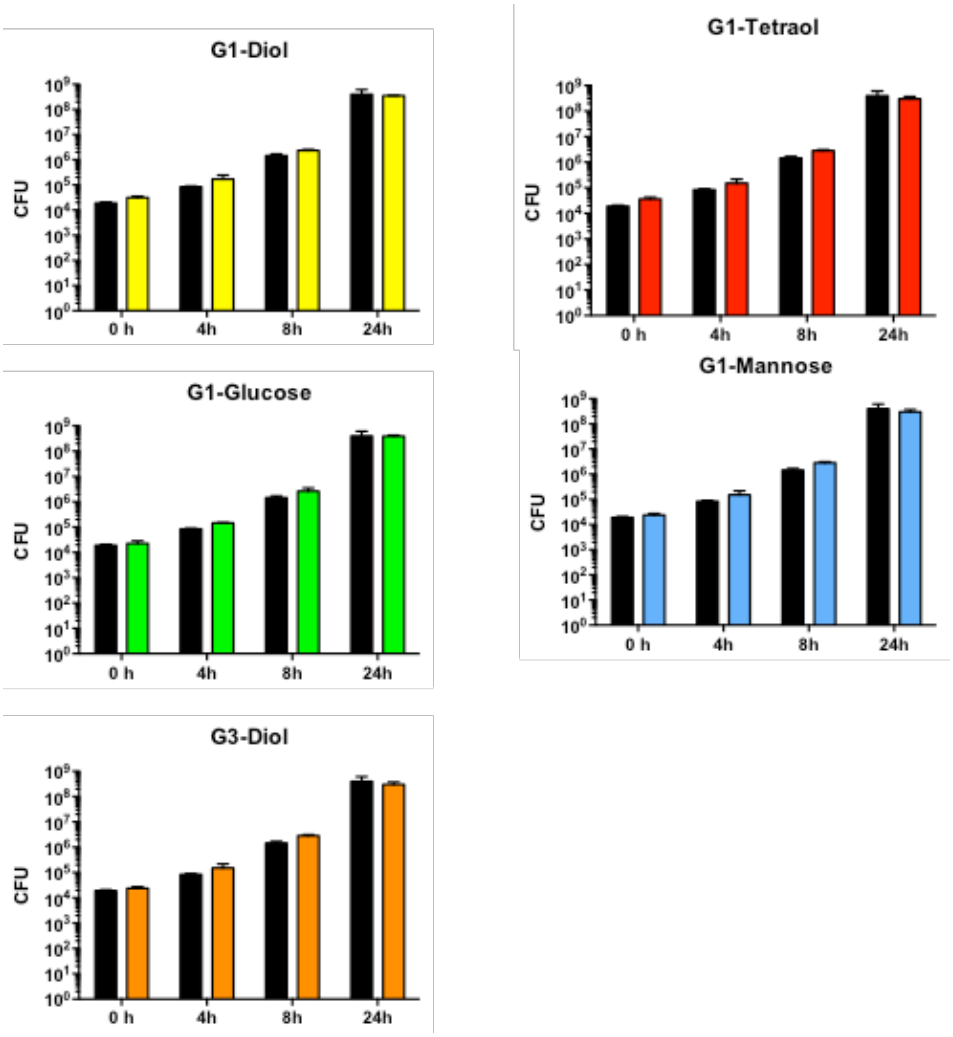

Figure A37 Colony Forming Unit (CFU) for *V. harveyi* BB170 in LB-medium in the absence (black) and presence (colour) of diol-dendrimers at time point 0, 8 and 24 h. Concentration of dendrimers 0.5 mg/mL.

Luminescence/OD of MM32 in the absence of DPD.

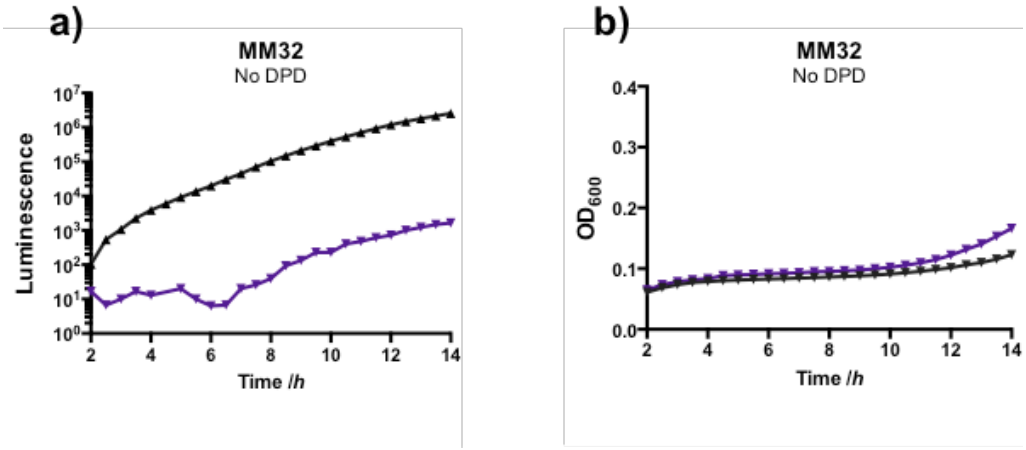

Figure A38 (a) luminescence and (b) optical density at 600nm (OD_{600}) of *V. harveyi* MM32 in AB medium with (black) and without DPD (purple).

Luminescence/OD of MM32 with G3-B(OH)$_2$ in the presence and antibiotics

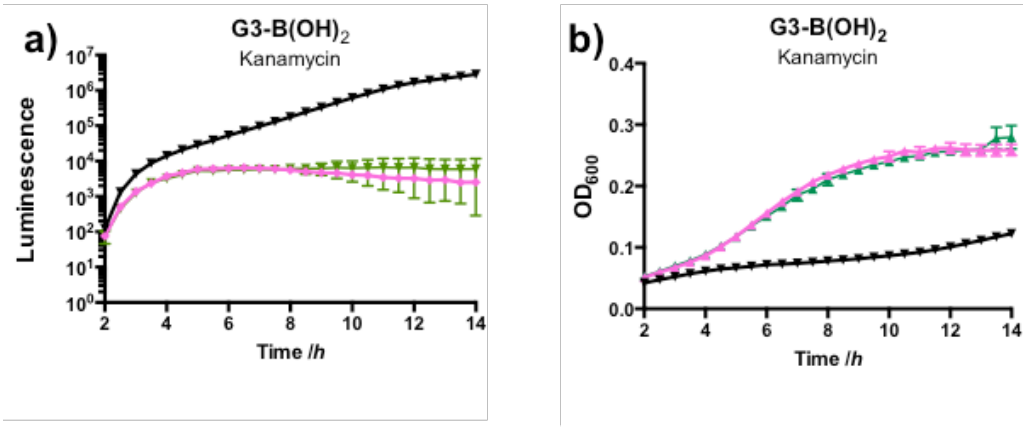

Figure A39 Luminescence (a) and optical density (b) at 600 nm (OD_{600}) of *V. harveyi* MM32 in AB medium (black). G3-B(OH)$_2$ in AB medium in the absence (green) and presence (pink) of 50 μg/mL kanamycin.

Relative luminescence of MM32 with G3-B(OH)$_2$

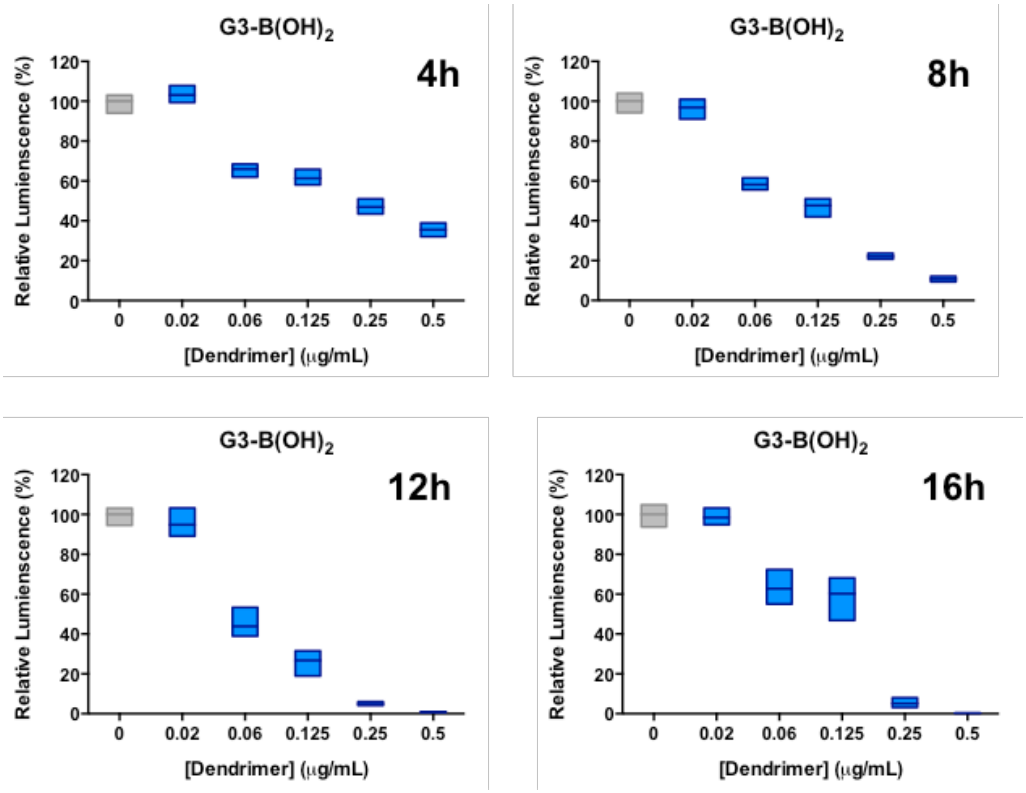

Figure A40 Relative luminescence of MM32 in the presence of G3-B(OH)$_2$ at 4, 8, 12 and 16 h.

Luminescence/OD of BB170 in presence of G3-B(OH)$_2$

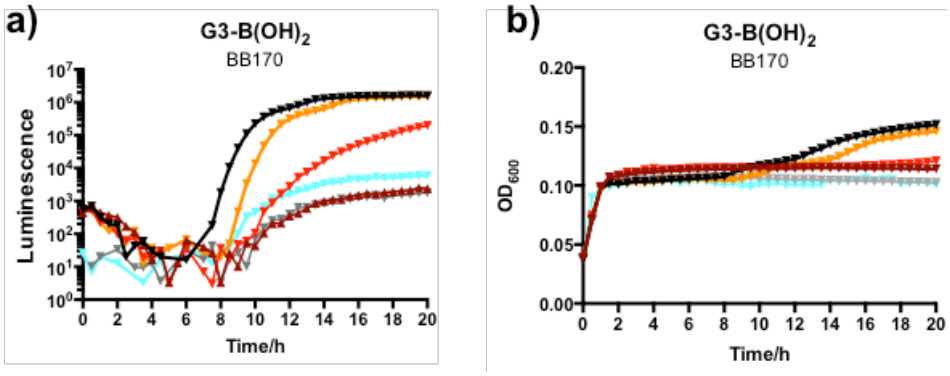

Figure A41 Luminescence of *V. harveyi* BB170 in the absence (black) and presence of G3-B(OH)$_2$. Presented are (a) luminescence and (b) optical density at 600 nm (OD_{600}). Final dendrimer concentrations were 5 µg/mL (dark red), 1 µg/mL (red) and 0.125 µg/mL (orange) G3-B(OH)$_2$ (5 µg/mL) in the absence of bacteria is presented in grey and AB medium alone blue. Presented are mean values from three replicates.

Luminescence/OD of BB170 in presence of G1-B(OH)$_2$

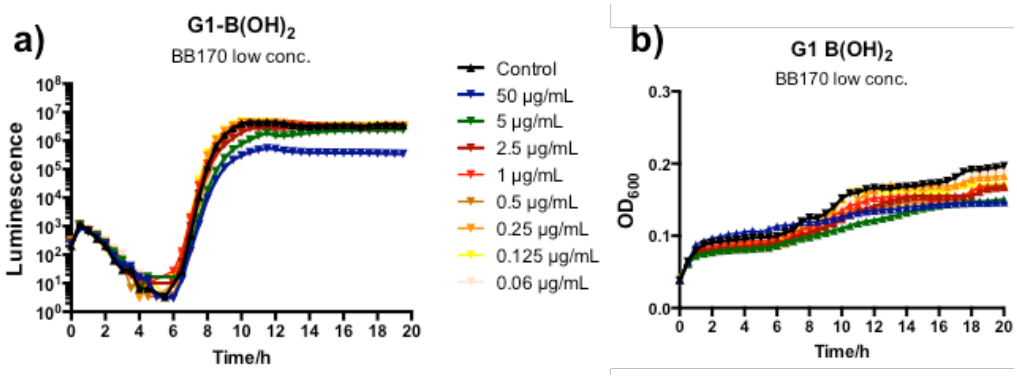

Figure A42 Luminescence of *V. harveyi* BB170 in the absence (black) and presence of G1-B(OH)$_2$. Presented are (a) luminescence and (b) optical density at 600 nm (OD_{600}). Final dendrimer concentrations were 50- 0.06 µg/mL.

Luminescence recovery time of BB170 in the presence of G-B(OH)$_2$ dendrimers (dendrimer concentration).

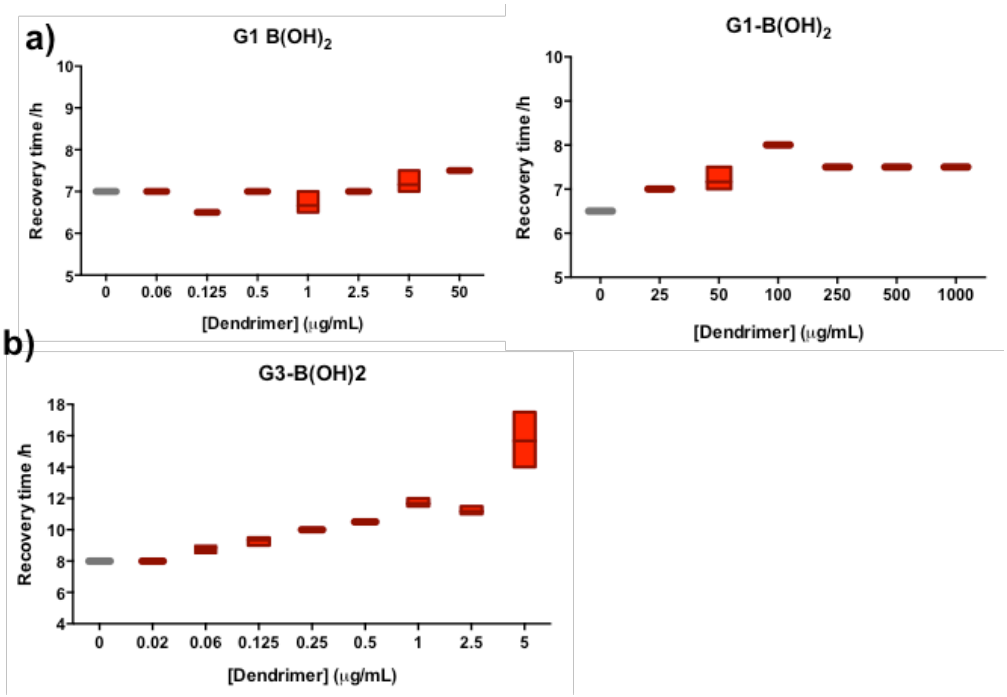

Figure A43 Recovery time in hours for BB170 luminescence in the presence boronic-acid dendrimers (a) G1-B(OH)$_2$ low concentration (left) and higher concentration (right) (b) G3-B(OH)$_2$.

Clustering of *V.harveyi* MM32 in the presence of Gn-NH_2 dendrimers

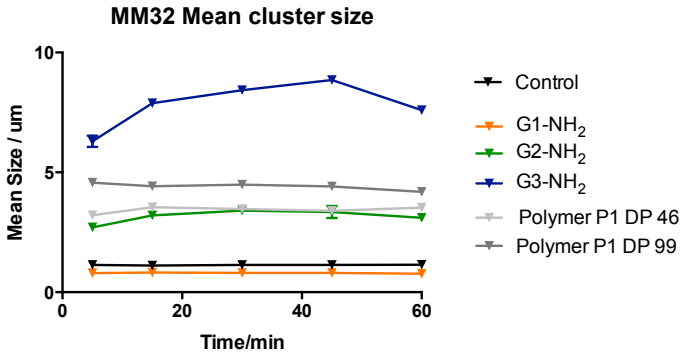

Figure A44 Mean Cluster size MM32 comparing Dendrimer with Polymer P1a DP46 and DP99 Mean cluster size of V. harveyi MM32 OD_{600}= 1.0 in the presence of cationic dendrimers generation G1 (orange), G2 (green) and G3 (blue) compared to bacteria alone (black) and P1 polymer DP46 (light grey) and DP 99 (dark grey). NH_2 concentration 1.64 mM for each of the dendrimers in all above experiments

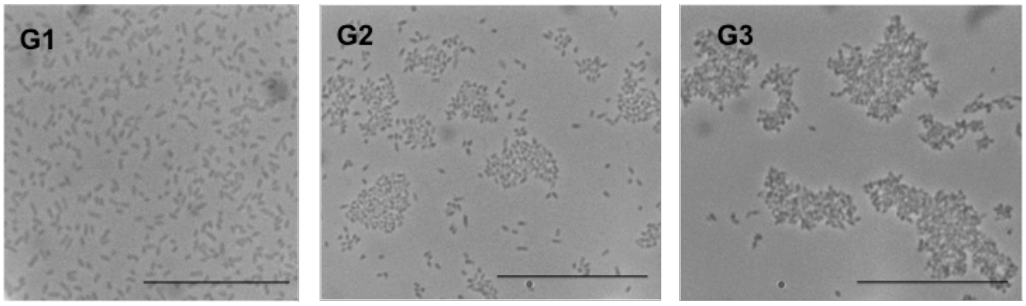

Figure A45 Increase in size by generation G1-NH_2, G2-NH_2 and G3-NH_2 of *V. harveyi* MM32 by optical microscopy. 100X magnification lens. Concentration of NH_2 = 1.64 mM. Black bar represents 30 μm.

Clustering of *V.harveyi* BB170 in the presence of Gn-NH_2 dendrimers

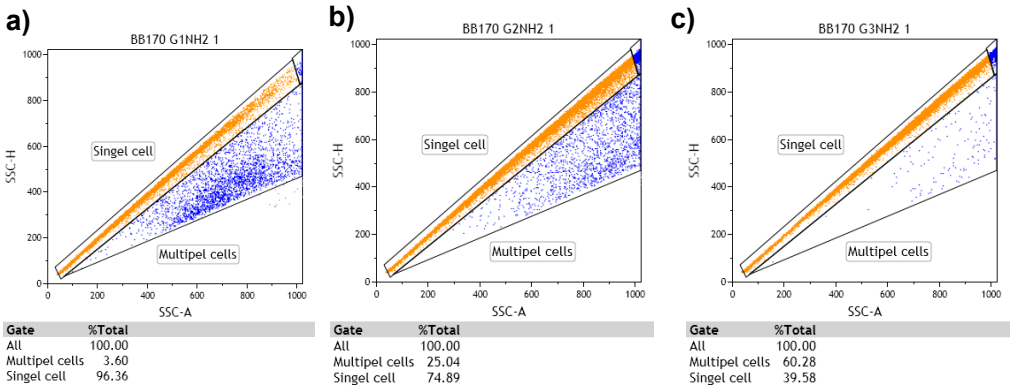

Figure A46 Gated *V.harveyi* BB170 bacteria in a single and multiple cell conformation after incubation in in PBS pH 7.4. Presented are bacterial cell conformation in the absence (control) and presences of with Gn-NH_2 of generation G1 (b), G2 (c) and G3 (d) for 1 h. Side-Scatter Area (SSC-A) vs Side-Scatter Heigh (SSC-H) are presented. [NH_2] = 1.64 mM.

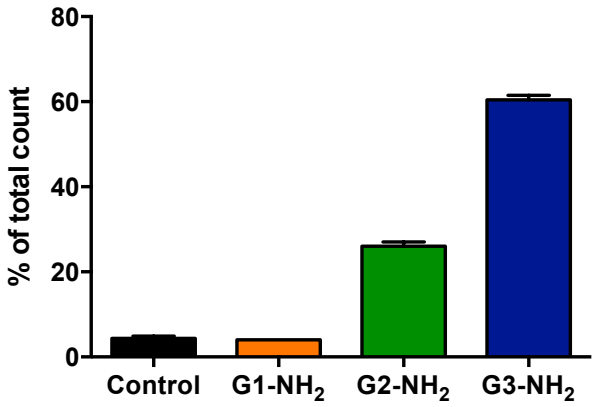

Figure A47 *V.harveyi* BB170 bacteria in a multicellular conformation after incubation with Gn-NH_2 for 1h in PBS pH 7.4

Cell Permeability of *V.harveyi* BB170 in the presence of Gn-NH_2 dendrimers under luminescence assay conditions

[NH_2] = 1 mM

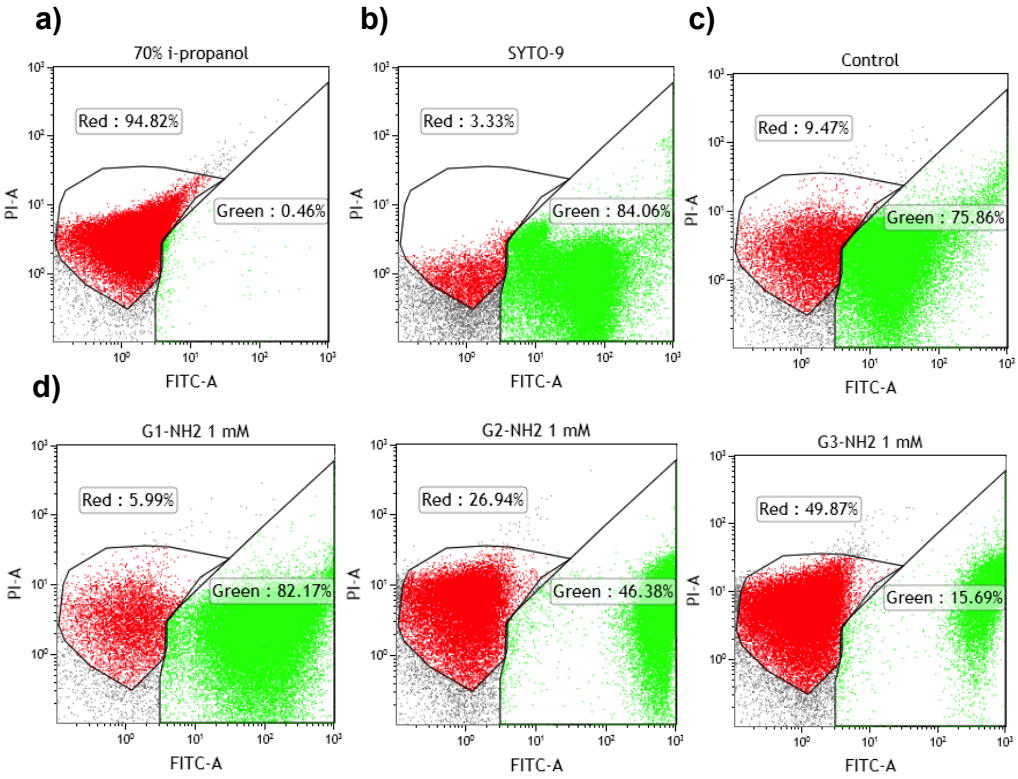

Figure A48 Gated population of *V.harveyi* based on calibration with propdoium iodine (PI-A) (a) and SYTO-9 (b) (FITC-A) staining. Gated population of *V.harveyi* in the absence (c) (control) and presence (d) of Gn-NH_2 dendrimers. Bacteria diluted 5000 fold in AB medium prior to incubation with Gn-NH_2. [NH_2] = 1 mM. Values account for percentage of total number of counted cells.

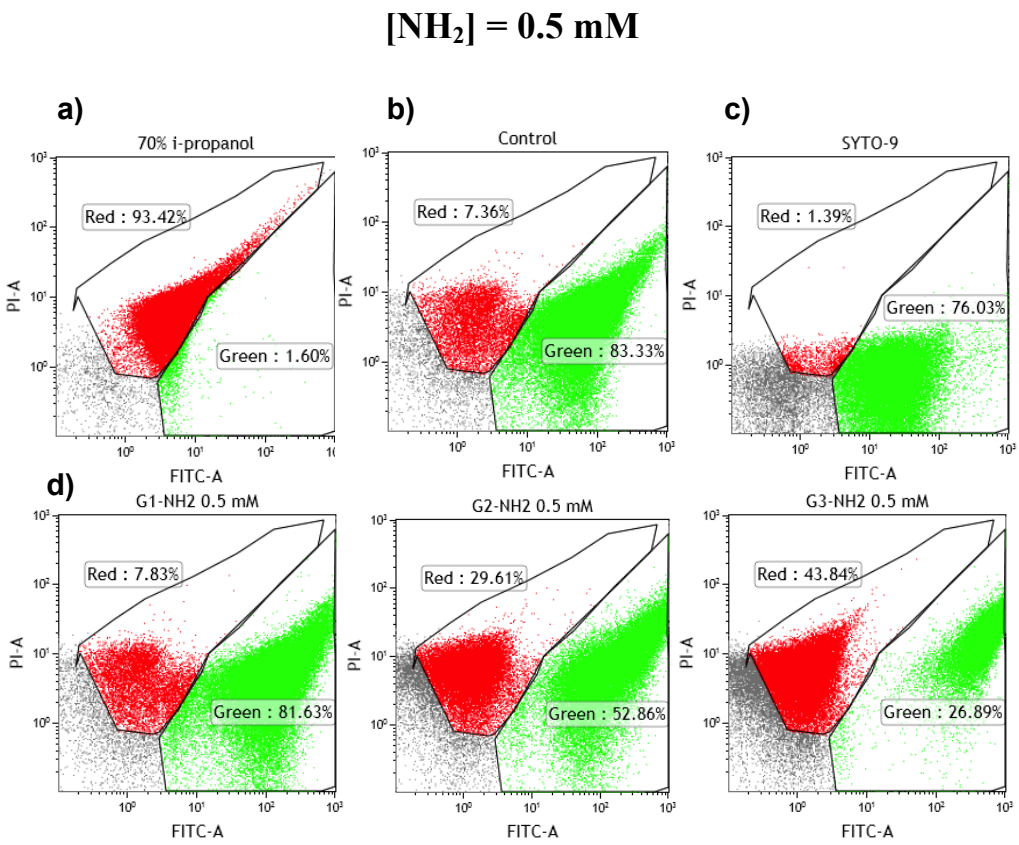

Figure A49 Gated population of *V.harveyi* based on calibration with propdoium iodine (PI-A) (a) and SYTO-9 (b) (FITC-A) staining. Gated population of *V.harveyi* in the absence (c) (control) and presence (d) of Gn-NH_2 dendrimers. Bacteria diluted 5000 fold in AB medium prior to incubation with Gn-NH_2. $[NH_2]$ = 1 mM. Values account for percentage of total number of counted cells

$[NH_2]$ = 0.25 mM

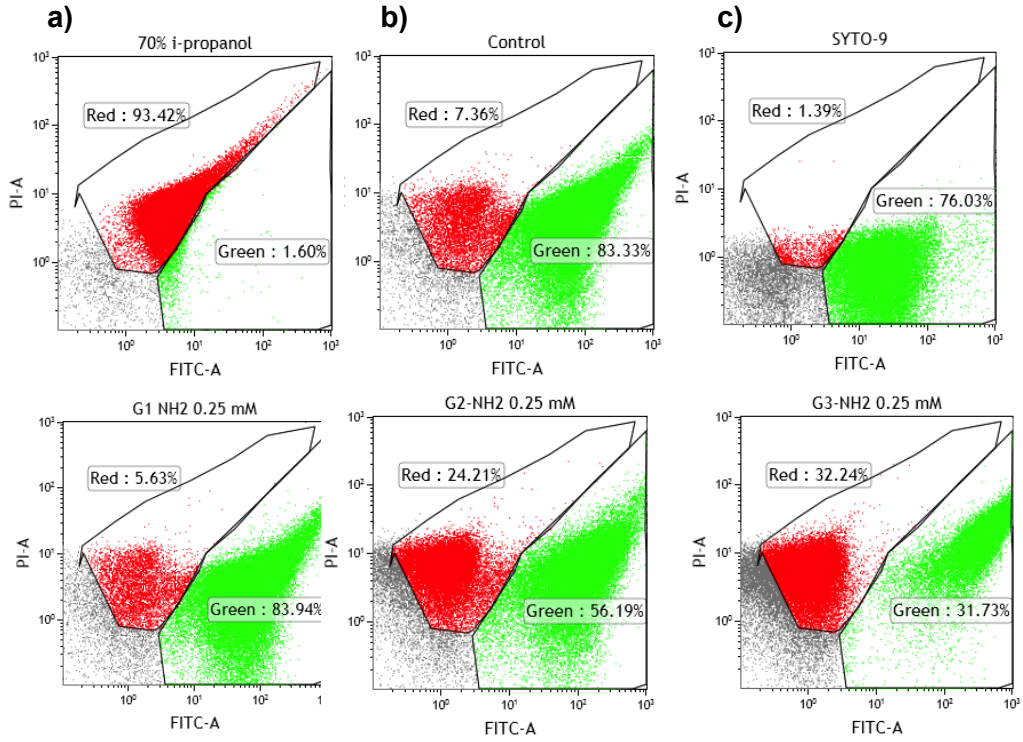

Figure A50 Gated population of *V.harveyi* based on calibration with propdoium iodine (PI-A) (a) and SYTO-9 (b) (FITC-A) staining. Gated population of *V.harveyi* in the absence (c) (control) and presence (d) of Gn-NH_2 dendrimers. Bacteria diluted 5000 fold in AB medium prior to incubation with Gn-NH_2. $[NH_2]$ = 0.25 mM. Values account for percentage of total number of counted cells.

CHEMICAL LIST

2-butyne-1,4-diol was purchased from Aldrich and was recrystallized in EtOAc PPh_3 was purchased from and Aldrich and was recrystallized in EtOH. All other chemicals were used without purification. All solvents were HPLC grade, purchased from Fisher Scientific except Hexane, which was purchased from Sigma Aldrich. Solvents were used without further purification unless otherwise described.

1,8-Diazabicyclo[5.4.0]undec-7-ene (DBU)	Sigma-Aldrich
2-(2-(2-chloroethoxy)ethoxy)ethan-1-ol	Sigma-Aldrich
2-formylphenylboronic acid	Sigma-Aldrich
BF_3*OEt_2	Sigma-Aldrich
BnNH2 (Benzylamine)	Fluka
chloroethoxy)ethoxyethanol	Sigma-Aldrich
D-Glucose pentaacetate	Sigma-Aldrich
D-Mannose	Sigma-Aldrich
DMAP (dimethylamine pyridine)	Fluka
EDC*HCl	Sigma-Aldrich
HOBt	Sigma-Aldrich
LiCl	Sigma-Aldrich
MeONaAc2O (acetic anhydride)	Sigma-Aldrich
NaBH4	Sigma-Aldrich
NaH	Sigma-Aldrich
nBu_4NHSO_4	Sigma-Aldrich
N, N' –Disuccinyl carbonate (DSC)	Sigma-Aldrich
PdC (10%)	Sigma-Aldrich

Serinol	Sigma-Aldrich
Triethylamine	Sigma-Aldrich

Biology (Nottingham)

Agar	Sigma-Aldrich
$B(OH)_4$	Sigma-Aldrich
Casamino acid	Sigma-Aldrich
Glycerol	Sigma-Aldrich
K_2HPO_4	Sigma-Aldrich
Kanamycin	Sigma-Aldrich
KOH	Sigma-Aldrich
L-Arginine	Sigma-Aldrich
$MgSO_4$ * $7H_2O$	Sigma-Aldrich
NaCl	Sigma-Aldrich
Tryptone	Sigma-Aldrich
Yeast extracts	Sigma-Aldrich

LB medium (10g/L NaCl, 5 g/L yeast extract/10g/Tryptone)

LB agar (LB medium + 15 g/L agar)

APPENDIX REFERENCES

[1] Kaur, N., Singh, N., Cairns, D., and Callan, J.F. (2009). *"A multifunctional tripodal fluorescent probe: "off-on" detection of sodium as well as two-input AND molecular logic behavior."* Org Lett 11(11): 2229-32.